

**Integration of paleolimnological and contemporary hydroecological analyses to
decipher effects of multiple stressors on water-rich northern landscapes**

by

Lauren Ashley MacDonald

A thesis
presented to the University of Waterloo
in fulfilment of the
thesis requirement for the degree of
Doctor of Philosophy
in
Biology

Waterloo, Ontario, Canada, 2015

© Lauren Ashley MacDonald 2015

Author's Declaration

This thesis consists of material all of which I authored or co-authored: see Statement of Contributions included in the thesis. This is a true copy of the thesis, including any required final revisions, as accepted by my examiners.

I understand that my thesis may be made electronically available to the public.

Statement of Contributions

Chapter 2: MacDonald LA, Turner KW, Balasubramaniam AM, Wolfe BB, Hall RI, Sweetman JN. 2012. Tracking hydrological responses of a thermokarst lake in the Old Crow Flats (Yukon Territory, Canada) to recent climate variability using aerial photographs and paleolimnological methods. *Hydrological Processes*, 26: 117-129.

Idea and planning: Kevin Turner, Lauren MacDonald, Brent Wolfe and Roland Hall

Field work: Kevin Turner, Ann Balasubramaniam and Lauren MacDonald

Laboratory analyses: Lauren MacDonald except water chemistry analyses which were submitted to NLET (Environment Canada's National Laboratory for Environmental Testing; Burlington ON) and chronological analyses by Johan Wiklund

Data analysis: Lauren MacDonald

Figures: Lauren MacDonald and Kevin Turner

Writing: Lauren MacDonald with comments and contributions to text in subsequent drafts by Brent Wolfe, Roland Hall, Kevin Turner and Jon Sweetman

Chapter 3: MacDonald LA, Farquharson N, Hall RI, Wolfe BB, Macrae ML, Sweetman JN. 2014. Avian-driven modification of seasonal carbon cycling at a tundra pond in the Hudson Bay Lowlands (northern Manitoba, Canada). *Arctic, Antarctic and Alpine Research*, 46: 206-217 (*special issue on Environmental Change in the Hudson and James Bay Region, Canada*).

Idea and planning: Lauren MacDonald, Jon Sweetman, Brent Wolfe, Roland Hall and Merrin Macrae

Field work: Lauren MacDonald, Nicole Farquharson, Brent Wolfe, Roland Hall, Jon Sweetman and Merrin Macrae

Laboratory analyses: Lauren MacDonald except water chemistry analyses which were submitted to NLET (Environment Canada's National Laboratory for Environmental Testing; Burlington ON) and the University of Waterloo Biogeochemistry Lab, and isotope analyses which were submitted to the University of Waterloo Environmental Isotope Laboratory

Data analysis: Lauren MacDonald

Figures: Lauren MacDonald and Nicole Farquharson (map)

Writing: Lauren MacDonald with comments and contributions to text in subsequent drafts by Brent Wolfe, Roland Hall, Merrin Macrae and Jon Sweetman

Chapter 4: MacDonald LA, Farquharson N, Merritt G, Fooks S, Medeiros AS, Hall RI, Wolfe BB, Macrae ML, Sweetman JN. 2015. Limnological regime shifts caused by climate warming and Lesser Snow Goose population expansion in the western Hudson Bay Lowlands (Manitoba, Canada). *Ecology and Evolution*, 5(4): 921-939.

Idea and planning: Lauren MacDonald, Jon Sweetman, Brent Wolfe and Roland Hall

Field work: Lauren MacDonald, Nicole Farquharson, Brent Wolfe, Roland Hall, Jon Sweetman and Merrin Macrae

Laboratory analyses: Lauren MacDonald except water chemistry analyses which were submitted to NLET (Environment Canada's National Laboratory for Environmental Testing; Burlington ON) and the University of Waterloo Biogeochemistry Lab, isotope analyses which were submitted to the University of Waterloo Environmental Isotope Laboratory and chronological analyses by Johan Wiklund. In addition, Lauren MacDonald supervised two

undergrad theses (Gillian Merritt and Sam Fooks) who provided diatom counts for two of the sediment cores.

Data analysis: Lauren MacDonald and Andrew Medeiros (breakpoint analysis)

Figures: Lauren MacDonald and Nicole Farquharson (map)

Writing: Lauren MacDonald with comments and contributions to text in subsequent drafts by Brent Wolfe, Roland Hall, Andrew Medeiros, Merrin Macrae and Jon Sweetman

Chapter 5: MacDonald LA, Wiklund JA, Elmes MC, Wolfe BB, Hall RI. In Review at Science of the Total Environment. Paleolimnological assessment of riverine and atmospheric pathways and sources of metal deposition in a floodplain lake (Slave River Delta, Northwest Territories, Canada)

Idea and planning: Roland Hall and Brent Wolfe

Field work: Roland Hall, Brent Wolfe, Johan Wiklund, Matthew Elmes

Laboratory analyses: Johan Wiklund and Matthew Elmes. Sediment samples were submitted for heavy metal analysis to ALS Canada Ltd. (Edmonton Alberta).

Data analysis: Lauren MacDonald

Figures: Lauren MacDonald and Pam Schaus (map)

Writing: Lauren MacDonald with comments and contributions to text in subsequent drafts by Brent Wolfe, Roland Hall and Johan Wiklund

Abstract

Northern freshwater ecosystems provide important habitat and resources which support abundant wildlife and waterfowl populations and the traditional lifestyle of many First Nation communities. However, concerns have been mounting regarding the effects of multiple stressors, including climate change and other human-related activities in these regions. In order to understand the consequences of stressors, information on both present and past conditions is needed. This thesis addresses knowledge gaps by using a combination of contemporary and paleolimnological methods to characterize lake and pond responses to different stressors in three northern landscapes. A paleolimnological record in combination with aerial images was used to investigate causes of lake-level changes at a lake in the Old Crow Flats (OCF). Contemporary measurements were used to identify how hydrological and limnological conditions of coastal ponds in Wapusk National Park (WNP) differ seasonally and with disturbance from Lesser Snow Geese (LSG). Paleolimnological studies were also used in this landscape to determine how hydroecological conditions have changed during the past few centuries in response to climate warming and LSG population expansion. At a lake in the Slave River Delta (SRD), paleolimnological studies of hydrology and contaminant deposition were used to establish baseline concentrations and assess if temporal changes have occurred in response to northern industrial development. Together, these studies provide a detailed record of environmental changes in response to stressors at three large northern freshwater landscapes.

Recent studies using remote sensing analysis of lake-rich thermokarst landscapes have documented evidence of declining lake surface area in response to recent warming. However, images alone cannot identify whether these declines are due to increasing

frequency of lake drainage events associated with accelerated thermokarst activity or to increasing evaporation in response to longer ice-free season duration. In Chapter 2, the potential of combining aerial photograph time series with paleolimnological analyses to track changes in hydrological conditions of a thermokarst lake in the OCF and to identify their causes was explored. Images showed water level in lake OCF 48 declined markedly sometime between 1972 and 2001. In a sediment core from OCF 48, complacent stratigraphic profiles of several physical, geochemical and biological parameters from ~1874-1967 indicated hydrolimnological conditions were relatively stable. From ~1967-1989, declines in organic matter content, organic carbon isotope values and pigment concentrations were interpreted to reflect an increase in supply of minerogenic sediment, and subsequent decline in aquatic productivity caused by increased thermo-erosion of shoreline soils. Lake expansion was likely caused by increased summer rainfall, as recorded by increased cellulose-inferred lake-water oxygen isotope compositions. Stratigraphic trends defining the lake expansion phase terminated at ~1989, which likely marks the year when the lake drained. Above-average precipitation during the previous year probably raised the lake-level and promoted further thermo-erosion of the shoreline soils that caused the lake to drain. These are meteorological conditions that have led to other recent lake-drainage events in the OCF. Thus, the decline in lake-level evident in the aerial photograph from 2001 is unlikely to have been caused by evaporation, but rather is a remnant of a drainage event that took place more than a decade earlier. After drainage, the lake began to refill, and most paleolimnological parameters approached levels that are similar to those during the stable phase. These findings indicated that combined use of aerial images and paleolimnological

methods offers much promise for identifying the hydrological consequences of recent climatic variations on thermokarst lakes.

The past ~40 years have seen a geometric increase (5-7% per year) in the Lesser Snow Goose (LSG) population (*Chen caerulescens caerulescens*) and marked spatial expansion of the area they inhabit within the coastal fen ecotype of WNP (Hudson Bay Lowlands, northern Canada), raising concerns and uncertainty about the environmental effects of their activities (grubbing of vegetation, soil disturbance, deposition of feces) on the abundant shallow tundra ponds. In Chapter 3, conventional limnological measurements as well as water and carbon (C) isotope tracers were used to explore similarities and differences in seasonal patterns of hydrological, limnological and biogeochemical conditions of 15 shallow coastal fen ponds that currently have minimal (if any) disturbance from the LSG population with one pond (WAP 20) that is subject to substantial LSG activity. Carbon isotope measurements reveal that C cycling at WAP 20 (LSG disturbed site) is markedly different compared to the other ponds, whereas only small differences were observed in hydrological conditions and concentrations of major nutrients and chlorophyll *a* of pond water. A mid-summer decrease in C isotope composition of dissolved inorganic carbon (DIC) occurred at WAP 20, likely as a consequence of high pond-water pH and intense C demand by aquatic productivity. These conditions appear to have promoted ‘chemically-enhanced CO₂ invasion’, which causes strong kinetic C isotope fractionation. High C demand at WAP 20 is also suggested by mid-summer ¹³C-enrichment in particulate organic matter. In contrast, the ponds with little to no LSG activity exhibited expected seasonal C isotope behaviour (i.e., ¹³C-enrichment of DIC) under conditions of increasing productivity when C is in relatively low demand. Small differences in nutrient concentrations may be due to rapid

uptake by the benthic mat at WAP 20. Data from the low disturbance ponds also provide baseline information for future studies assessing potential effects of LSG.

Shallow lakes are dominant features in Subarctic and Arctic landscapes and are responsive to multiple stressors, which can lead to rapid changes in limnological regimes with consequences for aquatic resources. In Chapter 4, this theme was addressed in the coastal tundra region of WNP. Integration of limnological and paleolimnological analyses document profound responses of productivity, nutrient cycling and aquatic habitat to warming at three ponds ('WAP 12', 'WAP 20', 'WAP 21'), and to LSG disturbance at the two ponds located in an active nesting area (WAP 20, WAP 21). Based on multi-parameter analysis of ^{210}Pb -dated sediment records from all three ponds, a regime shift occurred between 1875 and 1900 CE marked by a transition from low productivity, turbid, and nutrient-poor conditions of the Little Ice Age to conditions of higher productivity, lower nitrogen availability, and the development of benthic biofilm habitat as a result of climate warming. Beginning in the mid-1970s, sediment records from WAP 20 and WAP 21 reveal a second regime shift characterized by accelerated productivity and increased nitrogen availability. Coupled with three years of limnological data, results suggest that increased productivity at WAP 20 and WAP 21 led to atmospheric CO_2 invasion to meet algal photosynthetic demand. This limnological regime shift is attributed to an increase in the supply of catchment-derived nutrients from the arrival of LSG and their subsequent disturbance to the landscape. Collectively, findings discriminate the consequences of warming and LSG disturbance on tundra ponds from which we identify a suite of sensitive limnological and paleolimnological measures that can be utilized to inform aquatic ecosystem monitoring.

Growth of natural resource development in northern Canada has raised concerns that activities pollute downstream aquatic ecosystems, but insufficient knowledge of pre-industrial baseline conditions continues to undermine ability of monitoring programs to distinguish industrial-derived contaminants from those supplied by natural processes. In Chapter 5, a novel paleolimnological approach was used to define pre-development baseline concentrations of 13 priority pollutant metals and vanadium and assess temporal changes, pathways and sources of these metals at a flood-prone lake in the SRD (NWT, Canada) located ~500 km north of Alberta's oil sands development and ~140 km south of a former gold mine at Yellowknife, NWT. Results identify that metal concentrations, normalized to lithium concentration, were not elevated in sediments deposited during intervals of high flood frequency or low flood frequency since onset of oil sands development (post-1967) relative to the 1920-1967 baseline established at the study lake. When compared to a baseline for the lower Athabasca River, several metal-Li relations (Cd, Cr, Ni, Zn, V) in post-1967 sediments delivered by floodwaters appear to plot along a different trajectory, suggesting that the Peace and Slave River watersheds are important natural sources of metal deposition at the SRD. However, analysis revealed unusually high concentrations of As deposited during the 1950s, an interval of very low flood frequency, which corresponded with emission history of the Giant Mine gold smelter indicating a legacy of far-field atmospheric pollution. Our study demonstrates the potential for paleolimnological characterization of baseline conditions and detection of pollution in floodplain ecosystems, but that knowledge of paleohydrological conditions is important for accurate interpretations. Through the integration of paleolimnological and contemporary hydroecological analyses this thesis was able to decipher the effects of multiple stressors on water-rich northern landscapes.

Acknowledgements

I have received financial support throughout my graduate program for which I am grateful from NSERC, the Garfield Weston Foundation, OGS, the Davis Memorial Scholarship Program, the Golder Associates Graduate Scholarship Program and the University of Waterloo. My research has been financially supported by the Government of Canada International Polar Year Program, the NSERC Northern Research Chair Program, the NSERC Discovery Grant Program, the NSERC Discovery Frontiers Program (ADAPT), the Polar Continental Shelf Program of Natural Resources Canada, Parks Canada, the Churchill Northern Studies Centre, the Northern Scientific Training Program of Aboriginal Affairs and Northern Development Canada and the Government of the Northwest Territories Cumulative Impacts Monitoring Program.

I would like to thank the University of Waterloo Environmental Isotope Laboratory, the National Laboratory for Environmental Testing, Xiaowa Wang, the Macrae Lab and Johan Wiklund for running samples included in this thesis. I would also like to thank the anonymous reviewers who provided helpful suggestions to improve the manuscripts included in this thesis.

I would like to thank the local communities and agencies where I have conducted fieldwork for this thesis for providing the logistical support and the involvement needed to make a research project successful. Thank you to all of the bear monitors I have had over the years, I appreciate you looking out for me and always lending a helping hand. I would like to thank the Churchill Northern Studies Centre and everyone who works there. You have made many years of fieldwork logistically easy and enjoyable. In particular, I want to thank

LeeAnn Fishback. I have greatly appreciated your guidance, support and suggestions for research and life.

I would also like to thank the following people who have made the completion of this thesis possible:

Brent and Roland - thank you for the opportunity of completing this thesis, opportunities to conduct fieldwork in fun and exciting locations and opportunities to present my research at conferences. I have appreciated all of the knowledge you have taught me, the help you have given me and the patience and many edits you have provided throughout the years. Roland, thank you for thinking I had promise and taking a chance on sending an undergrad to Old Crow. Brent and Roland, thank you for helping me get teaching jobs and always being understanding of the associated demands. You have been great mentors to me.

Merrin – thank you for all of the help and support you have given me over the years. I have appreciated your willingness to answer all of my questions, help work through my ideas, review all of my work and the suggestions you have provided for research and life. Thank you for being a great role model to me and for women in science.

Jon Sweetman – thank you for all of your support and help setting up my projects. I have enjoyed working together and have great memories from fieldwork. I have appreciated your ideas and the fact that you have always made time to help me and review my work.

To the MBD/NHL/whatever the new name is group - I feel very fortunate to have worked with such great people, and would like to thank past and present members for always being willing to talk about ideas, for passing on knowledge and resources and for all of the great memories. Thank you to Nicole Farquharson, Hilary White, Kevin Turner, Katie Thomas, Ann Balasubramaniam, Meghan Feeney, Nick Sidhu, Kaleigh Eichel, Erin Light,

Jerry White and Matt Elmes who have helped with fieldwork for this thesis. I have also been very fortunate to make some of my best friends through this group. Thank you for always being there.

To my family - thank you for the constant support and understanding that I have needed while completing this thesis. You have provided me the ability to get an education without the worries and stress that many other students face and I would not be finishing a PhD without your help. Thank you for being silent when I needed to work and for providing distractions when I needed a break. Mom and Emily, thank you for always listening and for trying to learn a few science words. Dad, thank you for all of the airport pickups and drop-offs and chauffeuring field equipment and samples around. Ben, thank you for being the best listener, lab assistant and for spending many nights and weekends doing school related things with me. I am also very grateful that you took care of everything during terms where teaching, taing, helping undergrads and finishing this thesis seemed like a good idea.

Table of Contents

Author's Declaration.....	ii
Statement of Contributions.....	iii
Abstract.....	vi
Acknowledgements.....	xi
Table of Contents.....	xiv
List of Figures.....	xvii
List of Tables.....	xxii
Chapter 1: Introduction.....	1
1.1 General Introduction.....	1
1.2 Research Approach.....	6
1.3 Thesis Description and Contributions of Others.....	13
1.4 Figures.....	20
Chapter 2: Tracking hydrological responses of a thermokarst lake in the Old Crow Flats (Yukon Territory, Canada) to recent climate variability using aerial photographs and paleolimnological methods.....	24
2.1 Introduction.....	24
2.2 Site Description.....	27
2.3 Methods.....	28
2.4 Results and Interpretation.....	34
2.5 Discussion.....	39
2.6 Conclusions.....	44
2.7 Acknowledgements.....	45
2.8 Figures.....	46
2.9 Tables.....	54

Chapter 3: Avian-driven modification of seasonal carbon cycling at a tundra pond in the Hudson Bay Lowlands (northern Manitoba, Canada).....	55
3.1 Introduction.....	55
3.2 Study Area.....	59
3.3 Methods.....	61
3.4 Results.....	65
3.5 Discussion.....	73
3.6 Concluding Remarks.....	82
3.7 Acknowledgements.....	83
3.8 Figures.....	85
3.9 Tables.....	92
Chapter 4: Limnological regime shifts caused by climate warming and Lesser Snow Goose population expansion in the western Hudson Bay Lowlands (Manitoba, Canada).....	93
4.1 Introduction.....	93
4.2 Materials and Methods.....	95
4.3 Results and Interpretation.....	101
4.4 Discussion.....	112
4.5 Acknowledgements.....	118
4.6 Figures.....	119
4.7 Tables.....	127
Chapter 5: Paleolimnological assessment of riverine and atmospheric pathways and sources of metal deposition in a floodplain lake (Slave River Delta, Northwest Territories, Canada).....	129
5.1 Introduction.....	129
5.2 Methods.....	132
5.3 Results.....	135
5.4 Discussion.....	139

5.5 Conclusions.....	145
5.6 Acknowledgements.....	146
5.7 Figures.....	147
Chapter 6: Synthesis and Recommendations.....	156
6.1 Synthesis of Key Contributions.....	156
6.2 Recommendations for Ongoing and Future Studies.....	170
6.3 Figures.....	178
6.4 Tables.....	183
Copyright Permissions.....	184
References.....	186
Appendix A.....	205
Appendix B.....	212
Appendix C.....	215
Appendix D.....	225

List of Figures

- Figure 1.1:** Location of the Old Crow Flats (OCF), Yukon Territory, Canada. Details of the sediment coring site (OCF 48) shown with SPOT satellite image from July, 2007. Labels 6, 19 and 22 are locations of photographs from Figure 2.2 (Chapter 2). From MacDonald et al. (2012).....20
- Figure 1.2:** Location of Wapusk National Park (Manitoba, Canada) and the distribution of the 16 ponds studied in Chapter 3. Sampled pond ‘20’ (referred to as WAP 20 in the text) is situated in an area of high disturbance by Lesser Snow Geese. Grey regions in the four panels on the map depict the geographic limits of the LSG population distribution (data provided by Parks Canada, 2010). From MacDonald et al. (2014).....21
- Figure 1.3:** Location of Wapusk National Park (Manitoba, Canada) and the three study ponds (WAP 20, WAP 21 and WAP 12) used in Chapter 4. WAP 20 and WAP 21 are situated in an area of high disturbance by Lesser Snow Geese since ~1979, whereas WAP 12 is located outside of this area as of 2008. Grey regions depict the geographic limits of the LSG distribution at four time periods (data from Parks Canada, 2010). From MacDonald et al. (2015).....22
- Figure 1.4:** Maps and photo showing the Slave River Delta (Northwest Territories, Canada) and the study lake (SD2). The Slave River Delta is located downstream of the Alberta oil sands development and downwind of Giant Mine, a former gold mine near Yellowknife, NWT23
- Figure 2.1:** Location of the Old Crow Flats (OCF), Yukon Territory, Canada. Details of the sediment coring site (OCF 48) shown with SPOT satellite image from July, 2007. Labels 6, 19 and 22 are locations of photographs from Figure 2.....46
- Figure 2.2:** Photographs showing examples of lakes in the OCF that have experienced water-level decline. Locations of sites are shown on Figure 1: a) OCF 6, b) OCF 22, c) OCF 19 and d) OCF 48.....47
- Figure 2.3:** Water isotope results for OCF 48 from samples obtained during 2007-2009. Also shown is the Global Meteoric Water Line (GMWL; Craig, 1961) and the Local Evaporation Line (LEL) derived from isotopic and meteorological data from 2007 (Turner et al., 2010). δ_P is the average annual isotopic composition of precipitation, δ_{SSL} is the steady-state composition for a terminal basin where evaporation = inflow and δ^* is the limiting isotopic composition of a lake approaching desiccation.....48
- Figure 2.4:** Historical images of lake OCF 48 from a) 1951, b) 1972, c) 2001 and d) 2007.....49
- Figure 2.5:** ^{210}Pb and ^{214}Bi activity and depth-age profiles for OCF 48 KB2 sediment core. Error bars represent two standard deviations.....50

Figure 2.6: Summary of key paleolimnological indicators for OCF 48 KB2, plotted versus time derived from the ^{210}Pb analysis. Raw cellulose-inferred lake water $\delta^{18}\text{O}$ ($\delta^{18}\text{O}_{\text{lw}}$) values are plotted along with a three-point running mean.....51

Figure 2.7: Precipitation data based on Environment Canada’s Old Crow data (daily since 1951). Left plot: Annual precipitation from 1952 to 2010. Each year represents June 1 of the previous year to May 31 of the labelled year. White bars represent snow and grey bars represent rain. The numbers plotted on the left side of the bars represent the numbers of days of data missing. Right plot: Monthly precipitation from January 1987 to December 1990 plotted with the long-term monthly average (1951-2007).....52

Figure 2.8: Expected sedimentary organic matter content (%) profiles from paleolimnological analysis of lakes experiencing surface area changes from (a) accelerated thermokarst expansion-drainage cycles and from (b) increased evaporation.....53

Figure 3.1: Location of Wapusk National Park (Manitoba, Canada) and the distribution of the 16 ponds sampled for this study. Sampled pond ‘20’ (referred to as WAP 20 in the text, 58.6700° N, 93.4437° W) is situated in an area of high disturbance by lesser snow geese (LSG). Gray regions in the four panels on the map depict the geographic limits of the LSG population distribution (data provided by Parks Canada, 2010).....85

Figure 3.2: Top photographs depict ponds from the coastal fen ecotype of Wapusk National Park with low disturbance from the LSG population (panels a and b). Bottom photographs are from pond WAP 20 (panels c and d), which has evidence of high disturbance from the LSG population. Graph in panel (e) was taken from data available in Abraham et al. (2005b) on the Mid-Winter Index of Lesser Snow Geese and Ross’s geese from 1950-2003. The solid line is a 3-year running average.....86

Figure 3.3: Comparison of average monthly (a) temperature and (b) precipitation at Churchill, Manitoba (1971-2000) (Environment Canada, 2010).....87

Figure 3.4: $\delta^{18}\text{O}$ - $\delta^2\text{H}$ graph showing the seasonal trajectory of median water isotope compositions for the LDCF ponds (grey squares, dashed line) and WAP 20 (black triangles, solid line) with respect to the Global Meteoric Water Line (GMWL; Craig, 1961) and the Local Evaporation Line for the Churchill region as reported in Wolfe et al. (2011).....88

Figure 3.5: Principal components analysis (PCA) ordination biplot to compare limnological and biogeochemical conditions in WAP 20 (triangles) and the LDCF ponds (small circles) from the three sample periods in 2010. Vectors with solid lines represent active variables in the PCA, whereas vectors with dashed lines represent variables added passively. Lines connect sample scores for WAP 20 (triangles and solid line) and the median for the 15 LDCF ponds (squares, dashed lined) to assess seasonal patterns of change in the limnological variables with and without extensive LSG activity, respectively.....89

Figure 3.6: Boxplots depicting seasonal changes in (a) TKN concentration, (b) DOC concentration, (c) Chlorophyll *a* concentration, (d) TP concentration, (e) DIC concentration,

(f) pH, (g) $\delta^{13}\text{C}_{\text{DIC}}$, (h) $\delta^{13}\text{C}_{\text{POM}}$, (i) $\Delta^{13}\text{C}_{\text{DIC-POM}}$ and (j) CO_2 saturation. The boxes identify the 25th percentile, median value and 75th percentiles for the low disturbance coastal fen (LDCF) ponds. The whisker bars represent the 10th and 90th percentile, the solid black circles represent the maximum and minimum values observed for the LDCF ponds, and asterisks represent outliers. Black squares represent the mean seasonal value for the LDCF ponds. Black triangles joined by the solid line represent the values for WAP 20.....90

Figure 4.1: Location of Wapusk National Park (Manitoba, Canada) and the three study ponds (WAP 20, WAP 21 and WAP 12). WAP 20 and WAP 21 are situated in an area of high disturbance by LSG since ~1979, whereas WAP 12 is located outside of this area as of 2008. Grey regions depict the geographic limits of the LSG distribution at four time periods (based on data provided by Parks Canada in 2010).....119

Figure 4.2: Photographs a), b) and c) depict LSG disturbance in and adjacent to ponds WAP 20 and WAP 21. Photograph d) is from WAP 12 and depicts a pond with low disturbance from the LSG population. Graph in panel e) is an estimate of LSG population rise (Abraham et al., 2005b pg. 843). The solid line is a 3-year running average.....120

Figure 4.3: Left panels present scatterplots showing activity profiles for the radioisotopes and depth-age profiles for a) WAP 20, b) WAP 21 and c) WAP 12 sediment cores. Right panels present sedimentation rates. Error bars represent standard deviations.....121

Figure 4.4: Stratigraphic profiles of selected paleolimnological variables for WAP 20. The vertical axis presents the age of the sediment core, as estimated from the ^{210}Pb analysis. The average fitted breakpoint date of physical and geochemical variables is shown by a dashed line with the relative error indicated with a gray bar. The breakpoints were also applied to diatom and pigment profiles.....122

Figure 4.5: Stratigraphic profiles of selected paleolimnological variables for WAP 21. The vertical axis presents the age of the sediment core, as estimated from the ^{210}Pb analysis. The average fitted breakpoint date of physical and geochemical variables is shown by a dashed line with the relative error indicated with a gray bar. The breakpoints were also applied to diatom and pigment profiles.....123

Figure 4.6: Stratigraphic profiles of selected paleolimnological variables for WAP 12. The vertical axis presents the age of the sediment core, as estimated from the ^{210}Pb analysis. The average fitted breakpoint date of physical and geochemical variables is shown by a dashed line with the relative error indicated with a gray bar. The breakpoints were also applied to diatom and pigment profiles.....124

Figure 4.7: Line plots depicting average seasonal values for selected limnological parameters of ponds WAP 20, WAP 21 and WAP 12 based on findings of MacDonald et al. (2014). Values represent the average of samples collected in early June 2010-2012, late July 2010-2012 and mid-September 2010-2012. Values for WAP 12 July do not include July 2010 as the pond desiccated, and thus, samples could not be collected.....125

Figure 4.8: Depiction of the evolution of pond limnology, nutrient behaviour, and aquatic community in response to the different drivers of change. The solid horizontal line represents the limnological regime shift that all ponds experienced in response to climate warming and the dashed horizontal line represents the limnological regime shift that only the LSG disturbed ponds (WAP 20 and WAP 21) experienced.....126

Figure 5.1: Maps and photo showing the Slave River Delta (Northwest Territories, Canada) and the study lake (SD2). The Slave River Delta is located downstream of the Alberta oil sands development and downwind of Giant Mine, a former gold mine near Yellowknife, NWT.....147

Figure 5.2: Schematic diagram showing the Three-Step approach to assess metal pollution (e.g., zinc) from analyses of pre-development sediments supplied by floodwaters to flood-prone lakes. In the first step, we characterize baseline metal concentrations in river sediment by analyzing metal concentrations in pre-development lake sediments deposited by floodwaters. To do this, we develop linear relations for pre-development lake sediment metal concentrations relative to Li concentration, as is commonly done to normalize for grain-size effects because metals adsorb preferentially to clay-sized sediment and fluctuations in energy of river flow generate grain-size variations (Loring, 1991; Kersten and Smedes, 2002). And, we establish 95% prediction intervals (PIs) about this relation to define the natural range of variation. Second, we evaluate post-development sediment metal concentrations in flood-supplied stratigraphic samples against the pre-development baseline generated in Step 1. If >2.5% of post-development monitoring samples fall above the upper 95% PI, this identifies they have received an additional source of the metal, possibly due to pollution (Loring, 1991; Kersten and Smedes, 2002). Third, we re-express these data as time-series plots of residuals about the metal-Li relation to assess temporal trends of both past and ongoing monitoring data relative to the baseline (residual = 0), so that individual sample results can be evaluated for pollution immediately upon data acquisition.148

Figure 5.3: Stratigraphic profiles for the ratio of organic carbon-to-nitrogen concentration (C/N) and concentrations of 13 priority pollutant metals, vanadium and lithium. Grey horizontal shading indicates intervals of high flood frequency based on the C/N ratio, whereas absence of shading indicates intervals of low flood frequency (Elmes et al., In Review).....150

Figure 5.4: Scatterplots showing regressions of metal concentrations versus lithium concentration. Linear regressions (solid lines) and 95% prediction intervals (dashed lines) based on sediments deposited pre-1967 during intervals of high flood frequency.....151

Figure 5.5: Time-series plots showing temporal patterns of change in residual metal concentrations from the Li-normalized pre-1967 baseline based on sediments deposited at lake SD2 during intervals of high flood frequency (horizontal solid line at 0). Dashed lines represent the widest 95% prediction interval from the pre-1967 high flood frequency data.....152

Figure 5.6: Left panel shows a scatterplot of arsenic concentration versus lithium concentration in sediments deposited in lake SD2 during intervals of low flood frequency pre-1950 and post-1960 (black circles). The linear regression (solid line) and 95% prediction intervals (dashed lines) are shown. Open circles are from the low flood frequency interval of the 1950s. Right panel shows a re-expression of these data as time-series plots of residuals about the As-Li relation to assess temporal patterns of arsenic pollution above the pre-1950 and post-1960 low flood frequency baseline (horizontal solid line at 0). Dashed lines represent the widest 95% prediction interval.....153

Figure 5.7: Scatterplots showing Li-normalized metal concentrations in sediment samples from lake SD2 deposited post-1967 during intervals of high flood frequency superimposed on pre-development (pre-1920s) baseline (solid lines) and 95% prediction intervals (dashed lines) constructed for the Athabasca Delta from analyses on sediment cores from lakes PAD23 and PAD31 (from Wiklund et al., 2014). Also shown are RAMP (Regional Aquatics Monitoring Program) data from surficial river sediment samples taken from downstream Athabasca River and Delta stations, as reported in Wiklund et al. (2014).....154

Figure 5.8: Comparison of As emissions from Giant Mine as supplied by the company and by Northwest Region, Environmental Protection Service and reported in Hocking et al. (1978), with the temporal pattern of change in residual As concentration in sediments from lakes SD2 and PAD18 (Wiklund et al., 2012). SD2 residual As concentrations were derived from the As-Li relation of low-frequency flood samples from pre-1950 and post-1960 (Figure 6). PAD18 residual As concentrations were derived from the pre-1900 As-organic matter samples. Vertical grey bars represent intervals of high flood frequency at SD2 that bracket the ~1950s.....155

Figure 6.1: Expected sedimentary organic matter content (%) profiles from paleolimnological analysis of lakes experiencing surface area changes from (a) accelerated thermokarst expansion-drainage cycles, and from (b) increased evaporation (from MacDonald et al. 2012).....178

Figure 6.2: Expected seasonal trajectory profiles for nutrients, carbon isotope composition of dissolved inorganic carbon and conductivity for lakes experiencing no disturbance from the LSG population (left side) and lakes that are influenced by LSG disturbed (right side). Dashed lines represent multiple scenarios that could result depending on the severity of LSG disturbance. Image made by Pieter Aukes.....179

Figure 6.3: Representation of three step approach to assess future pollution in SD2. Left panel shows the establishment of baseline conditions from pre-industrial high flood frequency samples. Centre panel shows the comparison of post-industrial data with the established baseline. Right panel shows the time series that can be used for ongoing risk assessments in the Slave River Delta. Dashed lines represent the 95% prediction intervals based on pre-industrial conditions (left and centre) and the linear extrapolation of the widest 95% prediction interval from pre-industrial conditions (right). Samples that plot within the 95% prediction intervals (centre and right panels) can be interpreted as being within the range of natural variability for the contaminant. In contrast, if >2.5% of post-industrial

samples plot above the upper 95% prediction interval, the metal concentration is elevated above baseline possibly due to pollution from human activities.....180

Figure 6.4: Photo showing a severely degraded pond, with largely absent vegetation and exposed soils used in the 2014-2015 LSG monitoring program by Parks Canada.....181

Figure 6.5: Map showing the locations of 15 new ponds used in the 2014-2015 LSG monitoring program by Parks Canada. Map was created by James Telford.....182

List of Tables

Table 2.1: Selected physical and chemical limnological characteristics of lake OCF 48. Values represent the average and standard deviation of samples collected on July 24 2007, July 30 2008 and July 30 2009 measurements.....	54
Table 3.1: Results of one-sample t-tests which compare the mean value of water chemistry variables from the LDCF ponds with the value obtained at WAP 20. Comparisons are presented for all three sampling episodes (June, July, September).....	92
Table 4.1: Analytical strategy for the sediment cores.....	127
Table 4.2: The most sensitive limnological and paleolimnological parameters for identifying regime shifts from climate warming and LSG population expansion based on this stud.....	128
Table 6.1: The most sensitive limnological parameters that have been recommended to Parks Canada for monitoring the ongoing effects of LSG disturbance in Wapusk National Park. These indicators can all be used to track lake water chemistry responses to Lesser Snow Goose disturbance.....	183
Table A1: Geochemical data from OCF 48.....	205
Table A2: Diatom data from OCF 48. Data reported from the top of core until years where there were too few diatoms to enumerate.....	210
Table A3: Pigment data from OCF 48. Pigment concentrations are reported in nMol/gOM.....	211
Table B1: Contemporary hydroecological data from WAP 20 and the 15 LDCF ponds from June 2010.....	212
Table B2: Contemporary hydroecological data from WAP 20 and the 15 LDCF ponds from July 2010.....	213
Table B3: Contemporary hydroecological data from WAP 20 and the 15 LDCF ponds from September 2010.....	214
Table C1: Geochemical data from WAP 20.....	215
Table C2: Biological data from WAP 20.....	216
Table C3: Geochemical data from WAP 21.....	217
Table C4: Biological data from WAP 21.....	220
Table C5: Geochemical data from WAP 12.....	221

Table C6: Biological data from WAP 12.....	223
Table C7: Average seasonal values (2010-2012) for limnological conditions from WAP 20, WAP 21 and WAP 12. Values for WAP 12 do not include July 2010 as the pond desiccated.....	224
Table D1: Metal concentrations (mg/kg) from SD2. 1= presence of condition or influence, 0 = absence of condition or influence.....	225-228
Table D2: 95% Prediction Interval concentrations (mg/kg) for metal-Li relations based on pre-1967 flood samples for use in future monitoring studies. PIL is the lower 95% prediction interval for the associated Li concentration, PIU is the upper 95% predication interval for the associated Li concentration.....	229-231
Table D3: Equation for metal-Li linear relation ($y=mx+b$) for future use in monitoring studies.....	232
Table D4: Reported detection limits from ALS Canada Ltd for metals analyzed from the core from SD2.....	233

Chapter 1: Introduction

1.1 General Introduction

Freshwater resources of Canada's North are subject to a wide array of environmental stressors despite their relatively isolated locations (Rouse et al., 1997; ACIA, 2005; Schindler and Smol, 2006; IPCC, 2007). During the past century, the circumpolar North has experienced some of the greatest regional climate warming on Earth (IPCC, 2007). Climate warming in the North will exert the greatest effects on limnological and biogeochemical conditions of wetland landscapes via alteration of hydrological processes, rather than simply temperature rise alone (Rouse et al., 1997; Prowse et al., 2006; Schindler and Smol, 2006). Climate warming may also have indirect effects on other aspects of northern wetlands such as expansion of vegetation (e.g., Tape et al., 2006) and changes in wildlife and waterfowl population sizes and distribution (e.g., Luoto et al., 2014). In addition to climate warming, many regions in the North are also facing effects of increased human presence due to growing northern industrial developments. Understanding the observed and predicted effects of multiple environmental stressors on northern environments is particularly important due to the dominance and significance of freshwater in many northern landscapes.

Small ponds and lakes of thermokarstic and deltaic origin occupy a significant portion of northern Canada. These landscapes are highly productive and are often considered northern 'oases' that provide important habitat and resources for abundant wildlife and waterfowl, and they support the traditional lifestyle of many indigenous communities. High-latitude wetlands also play an important role in the global carbon budget, by acting as both sinks and sources of carbon dioxide and methane (Griffis et al., 2000; Macrae et al., 2004; Walter et al., 2006; Laurion et al., 2010). However, climate warming and environmental

change in the Canadian North is predicted to continue to be much more pronounced than in temperate locations (ACIA, 2005), and these wetlands are particularly vulnerable to stressors due to their high surface area to volume ratios (Rouse et al., 1997; Prowse et al., 2006; Schindler and Smol, 2006). Additionally, freshwater ecosystems in the North remain amongst the least studied and most poorly understood ecosystems due to the paucity of long-term monitoring data (Smol, 2002), especially with regards to the biogeochemical and ecological conditions of lakes and ponds since the start of anthropogenic-induced changes.

One of the main overarching concerns in northern freshwater ecosystems is current and future water quantity and quality. In the Arctic and Subarctic, key drivers of hydroecological change in response to climate warming include variations in the amount and duration of snow and ice cover, thaw season evaporation-to-precipitation ratios, glacier melt and permafrost thaw, proportions of rain- and snow-fall and carbon cycling (Rouse et al., 1997; Prowse et al., 2006; Schindler and Smol, 2006). Recent studies have begun to examine the responses of freshwater ecosystems to these changes throughout the North including locations in Alaska (e.g., Yoshikawa and Hinzman, 2003; Hinkel et al., 2005; Riordan et al., 2006), Siberia (e.g., Smith et al., 2005), Nunavut (e.g., Smol and Douglas, 2007), Yukon Territory (e.g., Labrecque et al., 2009, Turner et al., 2010; Bouchard et al. 2013), Hudson Bay Lowlands (e.g., Bouchard et al., 2013; Rühland et al., 2013) and Northwest Territories (Brock et al., 2010). To date, studies have shown that Arctic thermokarst landscapes are becoming increasingly dynamic, with the rate of lake expansion increasing in some locations and lake-water levels declining in other regions (Yoshikawa and Hinzman, 2003; Smith et al., 2005; Riordan et al., 2006; Plug et al., 2008; Labrecque et al., 2009; Pohl et al., 2009). Studies in northern deltas have shown that climate change has resulted in increasing rates of

retrogressive thaw slumps (e.g., Lantz and Kokelj, 2008) and changes in flood frequency (Slave River Delta; Brock et al., 2010). Many ponds and lakes have also shown an increase in lake productivity, and a shift in water chemistry and diatom community composition in response to increased ice-free season duration and lake evaporation (e.g., Douglas et al., 1994; Rühland et al., 2003; Antoniadis et al., 2005; Rühland and Smol, 2005). Although, the majority of studies provide evidence to indicate that the Arctic is changing in response to climate warming, regions display different spatial and temporal responses (e.g., Douglas and Smol, 1999; Serreze et al., 2000; Smol et al., 2005; Rühland et al., 2013). Most existing data sets are not comprehensive enough, neither spatially nor temporally, to fully understand how hydroecological and biogeochemical conditions have responded and will continue to respond to climate change, especially in the context of multiple, interacting stressors.

Concerns are also mounting regarding the environmental consequences of changes in wildlife and waterfowl population size and geographic distributions. These population expansions can act as a stressor and alter the structure and function of Arctic freshwater ecosystems by causing eutrophication via changes in nutrient sources and cycling, and vegetation and available habitat (e.g., Sorvari et al. 2002; Bayley and Prather 2003; Beisner et al. 2003; Rühland et al. 2003; Gregory-Eves et al. 2004; Smol et al. 2005; Smol and Douglas 2007; Côté et al. 2010). To date, limnological and paleolimnological studies of the effects of waterfowl populations in the Arctic have found varying degrees of disturbance with most showing some degree of change in productivity and traditional nutrient concentration in lakes where waterfowl are present (e.g., Michelutti et al., 2009; 2010; Keatley et al., 2009; 2011; Côté et al., 2010; Sun et al., 2013). These studies have mainly relied on more conventional styles of limnological sampling where concentrations of major

nutrients (mainly N and P) in the water column are examined on a single sampling trip or where paleolimnological analyses include mainly ‘traditional’ proxies (e.g., organic matter content, diatom community composition). Yet little research has been conducted on how waterfowl may influence biogeochemical cycles, particularly carbon cycling, and how conditions may change seasonally. Additional supplies of nutrients from waterfowl disturbance have the potential to increase productivity and alter the role of lakes and ponds as sources or sinks of carbon. This information is especially important as northern freshwater ecosystems play a significant role in the global carbon cycle. Furthermore, few studies have comprehensively examined the dual effects of climate warming and waterfowl expansion, knowledge required to assess ecosystem integrity of northern wetlands.

Exacerbating these threats to northern freshwater ecosystems is the ever increasing industrial development in the North. Resource development in the North, especially mining and processing of metals and hydrocarbons, has increased rapidly during the past several decades, and it is predicted to continue to expand during the next decade (Schindler 2010; The Conference Board of Canada, 2013). Industrial developments have the potential to affect human and environmental health in northern regions via release of heavy metals, polycyclic aromatic compounds (PACs), radioactive materials and human wastes. For example, studies assessing pollution from the Alberta oil sands have documented evidence of heavy metal and PAC contamination within a 50-km radius of the bitumen-upgrader facilities (Timoney and Lee, 2009; Kelly et al., 2009; 2010). In the Northwest Territories, increased concentrations of heavy metals have been documented in close proximity to different mines. For example, elevated concentrations of As have been reported in Yellowknife due to nearby Giant Mine (e.g., Hutchinson et al., 1982; Bromstad, 2011; Galloway, 2012), and increased

concentrations of a variety of metals have been reported in the Nahanni watershed due to nearby North American Tungsten Mine (e.g., Thomas et al., 2013). In most cases, less is known about fluvial and atmospheric transport of these contaminants to more distant locations. Consequently, these site-specific results have left many communities with questions and concerns regarding the long-range transport of contaminants and the effects on local water quality. However, many of these northern freshwater ecosystems are also located in areas that have abundant natural deposits of metals and other contaminants (e.g., Hall et al., 2012; Wiklund et al., 2014). Unfortunately, monitoring programs are not often initiated until well after resource development has already begun, which complicates our ability to distinguish between the natural and anthropogenic sources of contaminants. This information is critical for fully understanding the effects of industrial development in the North and creating management plans which can effectively distinguish sources of contaminants.

In order to adequately anticipate future environmental (hydrological, limnological and biogeochemical) changes in northern freshwater ecosystems, information on both present and past environmental conditions is required. As identified above, there are research gaps that require new knowledge on both of these timescales to fully assess the effects of climate warming, waterfowl population expansion and industrial development in the North. To address these issues, this thesis focuses on three large northern freshwater landscapes (Old Crow Flats, Yukon; western Hudson Bay Lowlands, northern Manitoba; Slave River Delta, NWT) with the objectives:

- 1) To evaluate the potential of using multi-proxy paleolimnological analyses to refine understanding of hydrological and ecological changes in thermokarst lakes in the Old Crow Flats (Yukon Territory) beyond information provided by aerial

photographs, and to identify the hydrological processes responsible for the observed changes.

- 2) To identify how hydroecological conditions of coastal ponds in Wapusk National Park (western Hudson Bay Lowlands, Manitoba) differ seasonally and with disturbance from Lesser Snow Geese. And, to determine what processes control the observed changes in nutrient balance.
- 3) To determine how hydroecological conditions have changed in Wapusk National Park (western Hudson Bay Lowlands, Manitoba) during the past few centuries in response to multiple stressors (i.e., climate warming, LSG population expansion).
- 4) To establish baseline concentrations of metal deposition and assess if temporal changes have occurred at a flood-prone lake in the Slave River Delta, Northwest Territories in response to northern industrial development.

1.2 Research Approach

As identified above, insufficient knowledge of baseline conditions challenges our ability to effectively identify responses to different environmental disturbances.

Paleolimnological studies examine the physical, biological and chemical information recorded in lake sediments and they provide a continuous long-term record that can be used to identify environmental changes when long-term monitoring data is unavailable or insufficient (e.g., Smol, 2002). Paleolimnological analyses have been used successfully in northern lakes to determine the effects of past climatic changes on hydrology and limnology (e.g., Douglas and Smol, 1999; Smol et al, 2005; Sokal et al., 2008; Brock et al., 2010; Wolfe et al., 2011a), identify disturbances from waterfowl (Michelutti et al., 2009; 2010; Keatley et

al., 2011; Sun et al., 2013) and assess pollution from industrial sources (e.g., Hall et al., 2012; Wiklund et al., 2012; 2014; Kurek et al., 2013). These long-term data sets have proven to be useful in the locations used, but the approaches are also needed to determine the effects of stressors in other understudied regions. In addition, many of these studies have focussed on the more traditional indicators of environmental change such as studies of diatom community composition. Although useful, there are other methods that combine the use of contemporary hydroecological and paleolimnological data that also may be of value to reconstruct past conditions and examine the effects of different stressors. To address the knowledge gaps outlined above, this thesis uses innovative methods, which combine multi-proxy paleolimnological data with other contemporary sources of data to develop new understanding of the effects of different stressors in several northern freshwater ecosystems. These data will provide frameworks for natural resource managers to evaluate further changes against and anticipate future trajectories within the context of continued climate change and landscape disturbance. This thesis focuses on three large northern wetland landscapes where scientific research is needed and management issues are growing regarding deleterious effects of several stressors. In each location, the research was performed to address important scientific questions in partnership with local government organizations or community members with an aim to provide new information about the effects of landscape disturbances on freshwater ecosystems. It is hoped that the information will be used to guide future research, policy development and stewardship decisions.

Old Crow Flats, Yukon

The Old Crow Flats (OCF) is a large (5600 km²) wetland, situated ~55 km north of the village of Old Crow in northern Yukon Territory (Figure 1.1). The OCF is recognized as a Wetland of International Importance by the Ramsar Convention due to its cultural and ecological significance of providing habitat for wildlife and waterfowl, which support the local First Nation (Vuntut Gwitchin) community's traditional lifestyle. This low-relief landscape is dynamic due to active thermokarst processes and contains over 2700 shallow thermokarst lakes (Lauriol et al., 2002). In recent decades, local community members have begun to express concerns over changes in the landscape in response to climate warming. Community concerns include fluctuating lake and river levels, unpredictable weather patterns and expansion of shrub vegetation (ABEK Co-op, 2007). To address these concerns, a large multi-disciplinary project involving both the local community and researchers was begun, funded by the Government of Canada International Polar Year (Yeendoo Nanh Nakhweenjit K'atr'ahanahtyaa; Wolfe et al., 2011b).

Tree-ring studies in the OCF indicate increased temperatures during the past few decades when compared to the past 300 years (Porter et al., 2010) and remote sensing images and visual observations confirm fluctuating water levels (Wolfe and Turner, 2008; Labrecque et al., 2009). Contemporary, landscape-scale hydrological studies show that different lakes and areas of the OCF are dominated by different hydrologic controls (e.g., precipitation inputs or evaporation) largely due to variations in catchment features and vegetation cover (Turner et al., 2010; 2014). However, further research is required to determine natural variations of thermokarst activity and provide information to help distinguish the processes responsible for changes in water levels and limnological conditions, as needed to better

predict future trajectories. Lakes in this region may show declining water levels from draining due to increased precipitation and overflow, or from drying due to increased evaporation. Knowledge of the potential consequence of a warming climate on water levels is particularly important, as this will affect the community's ability to travel safely to traditional hunting and trapping grounds (Tetlich, 2007; Wolfe et al., 2011b). Chapter 2 examines the use of sediment cores from thermokarst lakes combined with aerial photographs to track hydrological responses (i.e., declining water levels) of lakes to climate warming.

Western Hudson Bay Lowlands, Manitoba

The western Hudson Bay Lowlands (HBL) is a large Subarctic wetland, which contains over 10,000 shallow ponds and thermokarst lakes (Figure 1.2; 1.3). This low relief landscape (<200m above sea level) extends approximately 475,000 km² between the latitudes of 51° and 65° North (Rouse, 1991; Griffis et al., 2000). The HBL is located in a 'hotspot' of climate warming and has experienced some of the greatest increases in summer temperature during the last 50 years (Chapin et al., 2005). In terms of hydrology and ecology, the HBL is a particularly dynamic, sensitive and diverse region, because it spans the boundary between discontinuous and continuous permafrost and the treeline (Rouse, 1991; Duguay and Lafleur, 2003). This feature makes it one of the most sensitive regions in northern Canada to permafrost thaw (Smith and Burgess, 2004). Permafrost that underlies the HBL impedes the infiltration of surface water, and consequently, water pools on the surface creating thousands of lakes, ponds and vast wetlands. The lakes and ponds are formed from a variety of processes including thermokarst activity and isostatic rebound. For the latter process, ponds are formed in low areas between beach ridges (Klinger and Short, 1996; Lambert et al.,

2001). Wapusk National Park (WNP; 11,475 km²) was established in 1996 to protect a representative section of the western HBL.

During the past ~40 years, rapid increases in the Lesser Snow Goose (LSG) population size and geographic range of their nesting and feeding grounds have resulted in substantial disturbance to the coastal landscape of WNP (e.g., Batt et al., 1997; Iacobelli and Jefferies, 1991; Handa et al., 2002; Jefferies et al., 2004; Abraham et al., 2005ab, Jefferies et al., 2006). Areas with the highest population density have experienced extensive grubbing and vegetation loss, increased lake turbidity and large deposits of goose feces. Other areas within the Coastal Fen ecotype remain relatively undisturbed. Climate models predict that there will be continued high rates of warming in the HBL, because decreases in the duration of sea-ice on Hudson Bay are forecast to cause earlier onset of spring melt, increase the duration of the ice-free period, and reduce extreme winter temperatures in adjacent landscapes (Gagnon and Gough, 2005). Large increases in mean annual air temperature are predicted by the 21st century, and the area is also forecast to experience increased precipitation and evaporation rates during the summer (Gagnon and Gough, 2005; Macrae et al., 2014). Previous studies on the ponds of the western HBL near Churchill, Manitoba and within WNP have indicated diverse hydrological conditions and responses to climate warming (Macrae et al., 2004; Light, 2011; Wolfe et al., 2011; Bouchard et al., 2013). These characteristics of the HBL make it especially crucial to understand the hydrolimnological and biogeochemical responses of aquatic ecosystems in this landscape to climate warming and waterfowl disturbance in order to predict how they will respond to future disturbances. Chapters 3 and 4 use the combination of contemporary and paleolimnological methods (including a newer method in Arctic lakes and ponds - carbon isotopes) to examine the

influence of LSG and climate warming on limnological conditions and carbon cycling of coastal fen ponds.

Slave River Delta, Northwest Territories

The Slave River Delta (SRD) is a large (400 km²) northern floodplain landscape located in the Northwest Territories (NWT) where the Slave River enters Great Slave Lake (Brock et al., 2007; Figure 1.4). The SRD provides important habitat for wildlife and waterfowl that help support the mainly First Nation community of Fort Resolution (English et al., 1997; Brock et al., 2010). The Slave River's flow originates from the Peace River (~2/3) and the Athabasca River and its tributaries (~1/3). The SRD is a dynamic landscape where ice-jam flooding can occur and the delta contains many shallow lakes spanning broad hydrological gradients (Brock et al., 2007). Previous work in the area has focused on the relative importance of different hydrological processes (i.e., flooding and evaporation) on the water balances and limnological conditions of lakes and has also identified previous intervals of both high and low flood frequency during the past century (Brock et al., 2007; 2010; Sokal et al., 2008) – research that was driven mainly by concerns over the potential effects of the WAC Bennett Dam on the Peace River (Wolfe et al. 2007). Knowledge of these hydroecological controls and changes over time is important for understanding and providing context for other landscape disturbances.

Recent studies assessing pollution from the Alberta oil sands have documented evidence of atmospheric deposition of heavy metal and PAC contamination within a 50-km radius of the bitumen-upgrader facilities and suggest that effects may extend even farther (Timoney and Lee, 2009; Kelly et al., 2009; 2010; Kurek et al., 2013). These published

findings, and ensuing media attention, have left many communities, including Fort Resolution which is located ~550 km downstream of the Alberta oil sands, with questions and concerns regarding the long-range transport of contaminants and the effects on local water quality and human health (Campbell and Spritzer 2007; Wesche 2007; 2009). This prompted the Slave River and Delta Partnership to assess community concerns regarding the potential effects of oil sands mining activities. However, the Northwest Territories are and have been an area of extensive mining. Therefore, the potential for additional sources of heavy metal contamination does exist. For example, arsenic (As) contamination has been reported near Yellowknife, NWT, since the 1950s due to gold smelting at nearby Giant Mine (e.g., Hocking et al., 1978). Unfortunately, current monitoring programs were initiated well after development began and were not designed to identify long-term trends in contaminant deposition. Additionally, in this region, metals can be derived from both anthropogenic and natural sources, as areas exist that are naturally metal-rich and rivers and their tributaries flow through these deposits. Therefore, to accurately identify industrially enhanced contaminant loads, knowledge of natural metal deposition is required. Chapter 5 establishes pre-industrial baseline concentrations of heavy metals and examines the relative roles of atmospheric and fluvial transport of metals to the SRD by taking into account past hydrological changes. This allows the accurate assessment of temporal changes in metal concentrations in response to different northern industrial developments while taking into account natural variability.

1.3 Thesis Description and Contributions of Others

In addition to this Introduction, the thesis contains four ‘data chapters’ that report results of original research in the format of journal articles, followed by a final chapter that provides a synthesis and recommendations for future studies, and appendices. Due to the collaborative and multi-disciplinary approach used to conduct research for this thesis, the manuscripts are multi-authored, for which I am the lead author. Below is the outline of the four different data chapters, their publication status and the contributions made by others.

Chapter 2: MacDonald LA, Turner KW, Balasubramaniam AM, Wolfe BB, Hall RI, Sweetman JN. 2012. Tracking hydrological responses of a thermokarst lake in the Old Crow Flats (Yukon Territory, Canada) to recent climate variability using aerial photographs and paleolimnological methods. *Hydrological Processes*, 26: 117-129.

Chapter 2 used the combination of aerial images and multi-proxy paleolimnological analyses to assess water level changes at a thermokarst lake in the OCF. To date, most research on changing water levels in thermokarst lakes has relied on remote sensing images. This has allowed large landscapes to be analyzed without the logistical constraints and costs of remote field work in the Arctic. However, these images only represent snapshots in time and can’t accurately distinguish the processes responsible for the water level changes (e.g., is a dried up lake basin due to lake drainage or evaporation). In addition, although much paleolimnological work has been done in the Arctic, less has been done on thermokarst lakes and it has remained uncertain if they can preserve coherent records of past changes, due to the shallow depth and dynamic sedimentary environment. This chapter builds on previous

studies by assessing the use of multi-proxy paleolimnological analyses from a thermokarst lake to refine understanding of hydrological changes apparent in aerial photographs and identify processes responsible for the observed water level decline. Findings from this chapter identified four hydrological phases, including a rapid drainage event, which are consistent with a thermokarst lake expansion-drainage cycle. The results illustrate the promise of the combined approach of aerial images and paleolimnological methods for identifying hydrological consequences of climate warming. Additionally, hypotheses on the expected stratigraphic profiles of paleolimnological proxies are presented for lakes that have experienced water level declines due to rapid drainage versus evaporative drawdown.

Idea and planning: Kevin Turner, Lauren MacDonald, Brent Wolfe and Roland Hall

Field work: Kevin Turner, Ann Balasubramaniam and Lauren MacDonald

Laboratory analyses: Lauren MacDonald except water chemistry analyses which were submitted to NLET (Environment Canada's National Laboratory for Environmental Testing; Burlington ON) and chronological analyses by Johan Wiklund

Data analysis: Lauren MacDonald

Figures: Lauren MacDonald and Kevin Turner

Writing: Lauren MacDonald with comments and contributions to text in subsequent drafts by Brent Wolfe, Roland Hall, Kevin Turner and Jon Sweetman

Chapter 3: MacDonald LA, Farquharson N, Hall RI, Wolfe BB, Macrae ML, Sweetman JN.

2014. Avian-driven modification of seasonal carbon cycling at a tundra pond in the Hudson

Bay Lowlands (northern Manitoba, Canada). *Arctic, Antarctic and Alpine Research*, 46: 206-217 (*special issue on Environmental Change in the Hudson and James Bay Region, Canada*).

Chapter 3 used contemporary assessments of conventional limnological measurements as well as carbon isotope tracers to compare seasonal changes in trophic status and carbon cycling between one highly LSG-disturbed pond and 15 ponds that did not have visual evidence of LSG disturbance in WNP. In the past, limnological studies in Arctic and Subarctic locations of waterfowl disturbance have focused on assessing changes of conventional limnological characteristics (mainly P and N concentrations) in the water column at one single point in time. Carbon isotope tracers have been used successfully in temperate locations to assess productivity and track carbon cycling but have yet to be used in the Arctic and may be particularly important here due to the large role Arctic wetlands have in carbon cycling. This chapter builds on previous studies by using carbon isotope tracers in addition to conventional limnological measurements to compare seasonal changes. Findings illustrate marked differences in seasonal carbon cycling between the LSG disturbed pond and the 15 low disturbance ponds, whereas only small differences in conventional water chemistry variables were observed. This is important information for future study designs by land managers in determining how LSG populations may alter pond ecosystems. Additionally, data from the low disturbance ponds also provide baseline information for further studies as the LSG population may eventually expand to this area.

Idea and planning: Lauren MacDonald, Jon Sweetman, Brent Wolfe, Roland Hall and Merrin Macrae

Field work: Lauren MacDonald, Nicole Farquharson, Brent Wolfe, Roland Hall, Jon Sweetman and Merrin Macrae

Laboratory analyses: Lauren MacDonald except water chemistry analyses which were submitted to NLET (Environment Canada's National Laboratory for Environmental Testing; Burlington ON) and the University of Waterloo Biogeochemistry Lab, and isotope analyses which were submitted to the University of Waterloo Environmental Isotope Laboratory

Data analysis: Lauren MacDonald

Figures: Lauren MacDonald and Nicole Farquharson (map)

Writing: Lauren MacDonald with comments and contributions to text in subsequent drafts by Brent Wolfe, Roland Hall, Merrin Macrae and Jon Sweetman

Chapter 4: MacDonald LA, Farquharson N, Merritt G, Fooks S, Medeiros AS, Hall RI, Wolfe BB, Macrae ML, Sweetman JN. 2015. Limnological regime shifts caused by climate warming and Lesser Snow Goose population expansion in the western Hudson Bay Lowlands (Manitoba, Canada). *Ecology and Evolution*, 5(4): 921-939.

Chapter 4 used the combination of contemporary and multi-proxy paleolimnological analyses to identify regime shifts in response to climate warming and the LSG population expansion in WNP. Many northern regions are under the influence of both climate warming and waterfowl expansions. However, few studies have extensively examined and discriminated the ecosystem responses due to each stressor. Prior limnological research in the WNP area, including Chapter 3 of this thesis, has largely focused on short-term investigations, but sediment records may also provide a useful long temporal perspective of

shifting limnological conditions in response to both of these stressors. Chapter 4 builds on the results of Chapter 3 by combining both contemporary measurements of conventional water chemistry and carbon isotope composition of dissolved inorganic carbon and particulate organic carbon with paleolimnological analyses of a suite of indicators, including carbon isotope composition of organic matter from three lakes in WNP. Analyses of sediment cores from the three lakes (two are ponds in areas actively disturbed by the LSG and one is in a non-disturbed area) allowed us to identify limnological regime shifts at all three ponds in response to climate changes, whereas limnological regime shifts from LSG disturbance were only noted at the two ponds located in active nesting areas. Findings from this chapter demonstrate the use of combined contemporary and paleolimnological studies in identifying regime shifts and provide a suite of pond responses and key indicators that most effectively define each limnological regime.

Idea and planning: Lauren MacDonald, Jon Sweetman, Brent Wolfe and Roland Hall

Field work: Lauren MacDonald, Nicole Farquharson, Brent Wolfe, Roland Hall, Jon Sweetman and Merrin Macrae

Laboratory analyses: Lauren MacDonald except water chemistry analyses which were submitted to NLET (Environment Canada's National Laboratory for Environmental Testing; Burlington ON) and the University of Waterloo Biogeochemistry Lab, isotope analyses which were submitted to the University of Waterloo Environmental Isotope Laboratory and chronological analyses by Johan Wiklund. In addition, Lauren MacDonald supervised two undergrad theses (Gillian Merritt and Sam Fooks) who provided diatom counts for two of the sediment cores.

Data analysis: Lauren MacDonald and Andrew Medeiros (breakpoint analysis)

Figures: Lauren MacDonald and Nicole Farquharson (map)

Writing: Lauren MacDonald with comments and contributions to text in subsequent drafts by Brent Wolfe, Roland Hall, Andrew Medeiros, Merrin Macrae and Jon Sweetman

Chapter 5: MacDonald LA, Wiklund JA, Elmes MC, Wolfe BB, Hall RI. In Review at Science of the Total Environment. Paleolimnological assessment of riverine and atmospheric pathways and sources of metal deposition in a floodplain lake (Slave River Delta, Northwest Territories, Canada)

Chapter 5 used a sediment record from a lake in the SRD with a known flood history and hydroecological conditions to reconstruct the deposition of heavy metals from fluvial and atmospheric processes. The local community had expressed concerns of pollution from downstream Alberta oil sands mining activities, however, other potential sources of contaminants exist such as gold mining activities in the NWT. Additionally, no pre-industrial monitoring data exists in this area, which makes it difficult if not impossible to distinguish contaminants supplied by industrial sources from those supplied by natural processes acting within the watershed. This makes knowledge of baseline pollutant concentrations even more critical for stressor studies in this area. In this chapter, methods developed by Wiklund et al. (2014) that took into account natural variations in grain size due to changes in hydrology were used to define pre-development baseline conditions of metal deposition for a lake in the SRD. Post-development concentrations were then compared against the baseline and assessed for industrial enhancement of metals from both the Alberta oil sands and Giant

Mine. Findings from this chapter illustrate that normalized metal concentrations were not elevated in post-oil sands stratigraphic samples compared to the baseline. However, there was enhancement of As in the ~1950s, the timing of which is consistent with atmospheric emissions from gold smelting at Giant Mine. Results demonstrate the potential for the use of floodplain lake sediments to develop baselines and assess pollution in contaminant studies, but that paleohydrological conditions need to be included for accurate results.

Idea and planning: Roland Hall and Brent Wolfe

Field work: Roland Hall, Brent Wolfe, Johan Wiklund, Matthew Elmes

Laboratory analyses: Johan Wiklund and Matthew Elmes. Sediment samples were submitted for heavy metal analysis to ALS Canada Ltd. (Edmonton Alberta).

Data analysis: Lauren MacDonald

Figures: Lauren MacDonald and Pam Schaus (map)

Writing: Lauren MacDonald with comments and contributions to text in subsequent drafts by Brent Wolfe, Roland Hall and Johan Wiklund

1.4 Figures

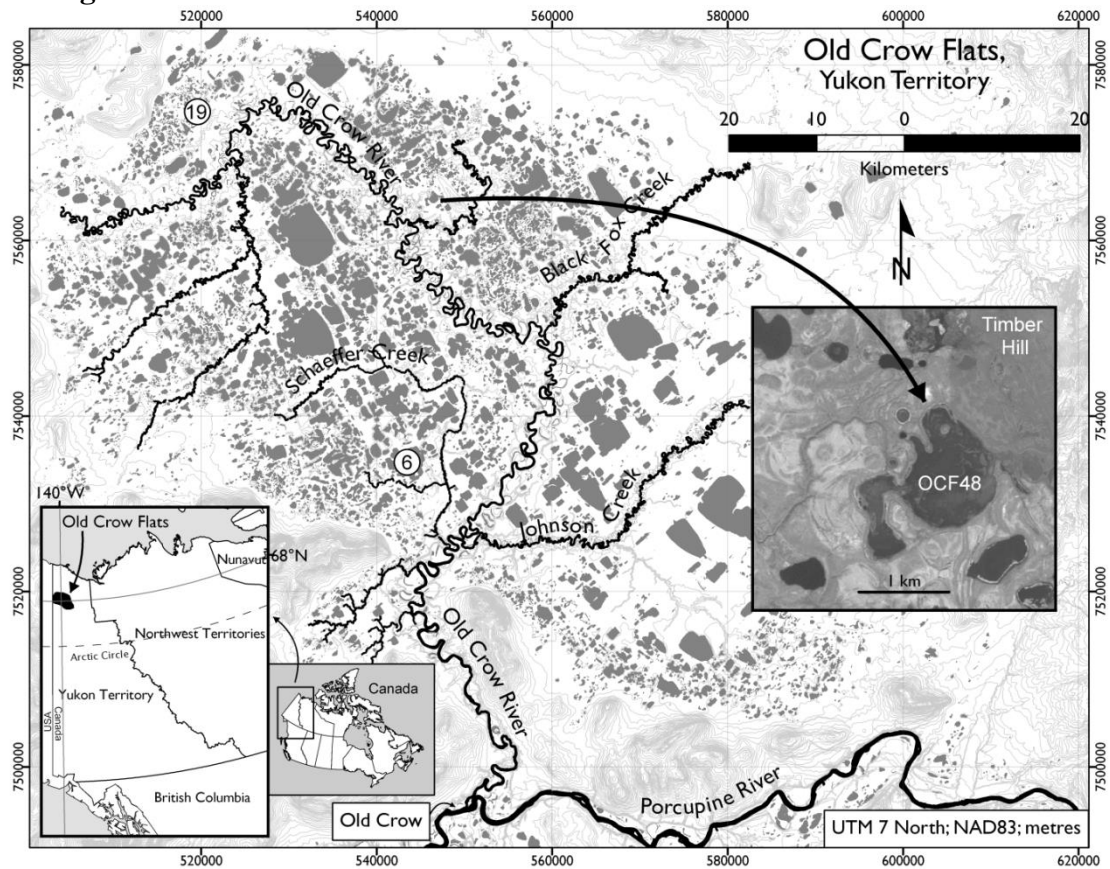


Figure 1.1: Location of the Old Crow Flats (OCF), Yukon Territory, Canada. Details of the sediment coring site (OCF 48) shown with SPOT satellite image from July, 2007. Labels 6, 19 and 22 are locations of photographs from Figure 2.2 (Chapter 2). From MacDonald et al. (2012).

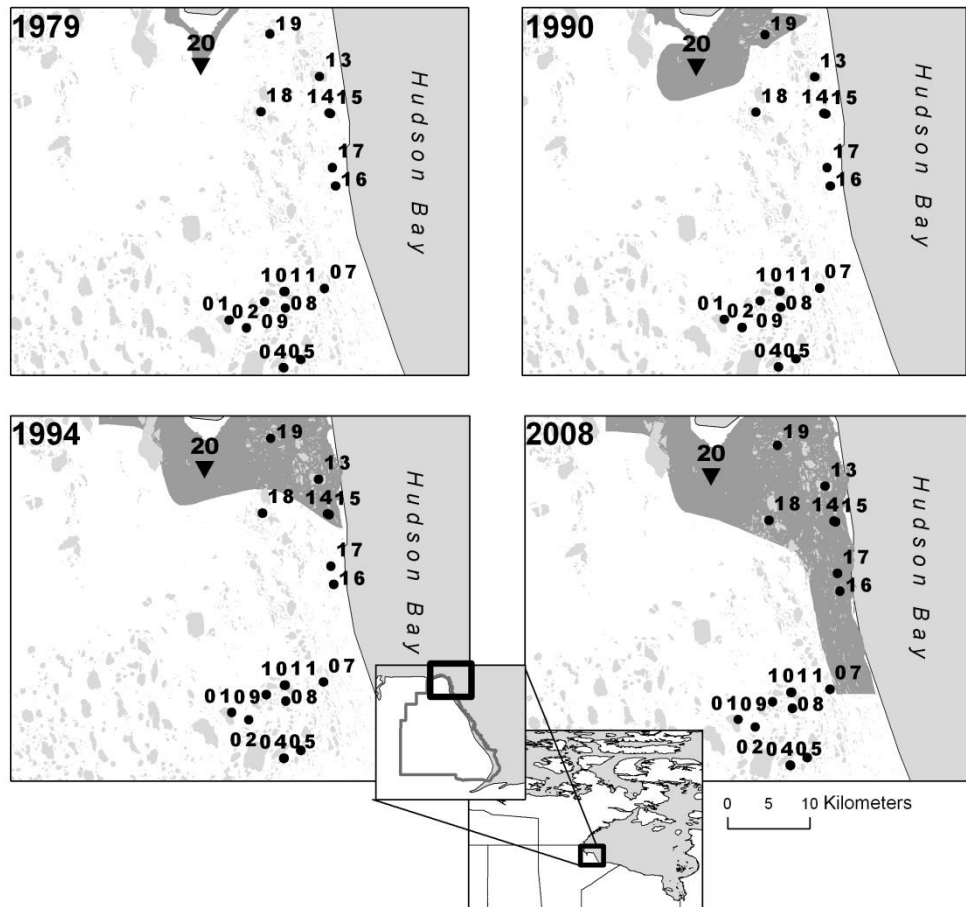


Figure 1.2: Location of Wapusk National Park (Manitoba, Canada) and the distribution of the 16 ponds studied in Chapter 3. Sampled pond ‘20’ (referred to as WAP 20 in the text) is situated in an area of high disturbance by Lesser Snow Geese. Grey regions in the four panels on the map depict the geographic limits of the LSG population distribution (data from Parks Canada, 2010). From MacDonald et al. (2014).

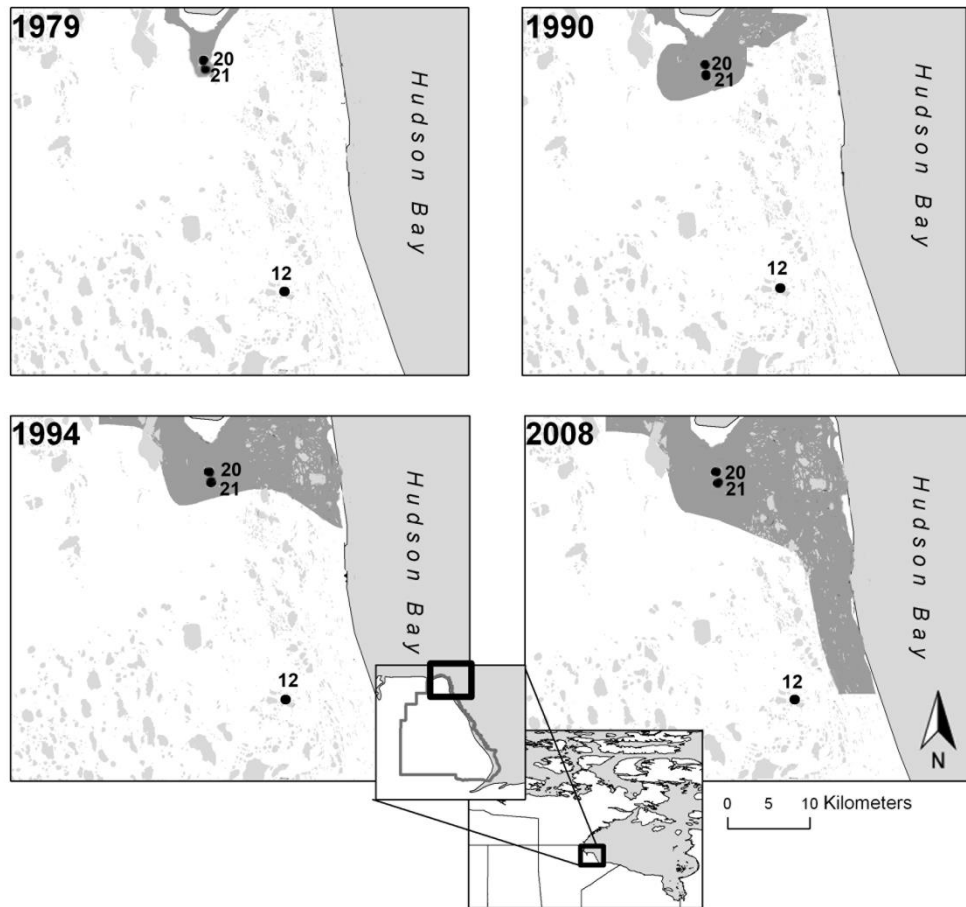


Figure 1.3: Location of Wapusk National Park (Manitoba, Canada) and the three study ponds (WAP 20, WAP 21 and WAP 12) used in Chapter 4. WAP 20 and WAP 21 are situated in an area of high disturbance by Lesser Snow Geese since ~1979, whereas WAP 12 is located outside of this area as of 2008. Grey regions depict the geographic limits of the LSG distribution at four time periods (data from Parks Canada, 2010). From MacDonald et al. (2015).

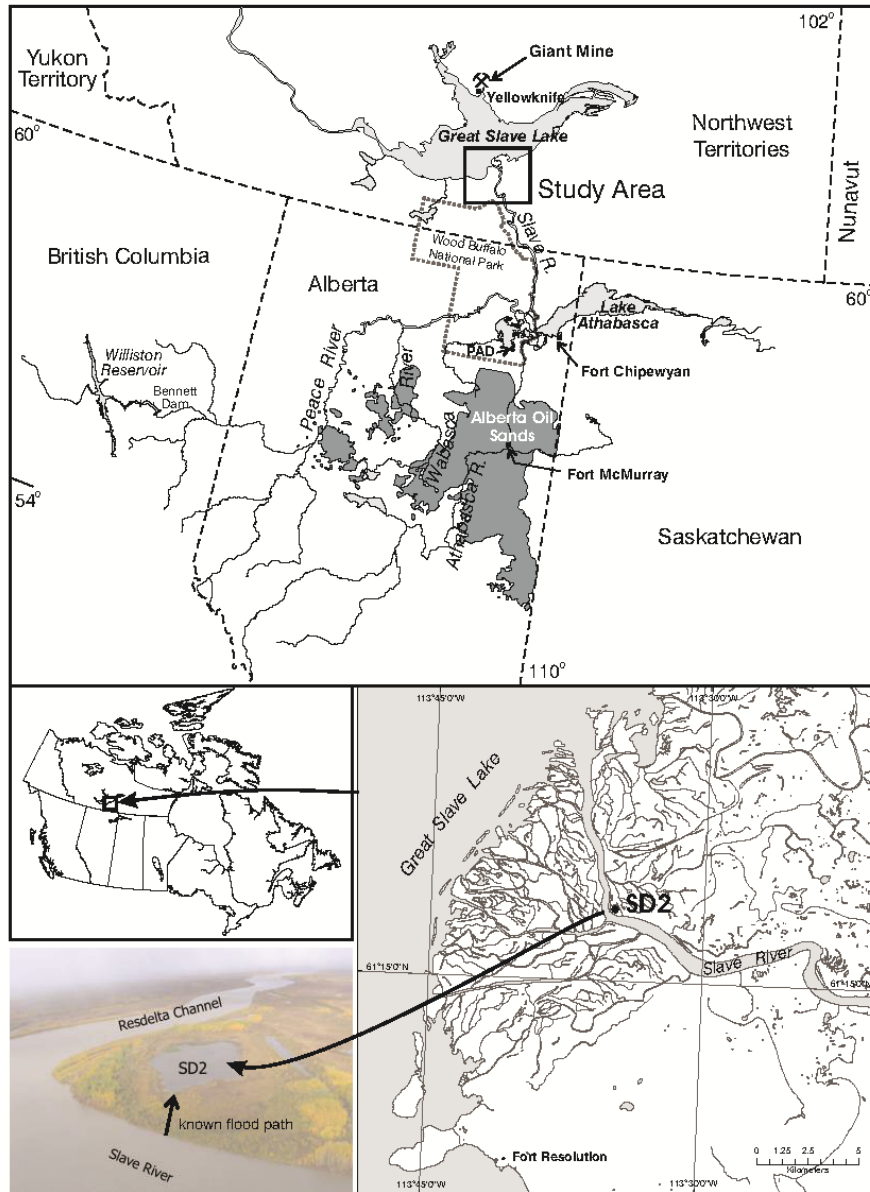


Figure 1.4: Maps and photo showing the Slave River Delta (Northwest Territories, Canada) and the study lake (SD2). The Slave River Delta is located downstream of the Alberta oil sands development and downwind of Giant Mine, a former gold mine near Yellowknife, NWT.

Chapter 2: Tracking hydrological responses of a thermokarst lake in the Old Crow Flats (Yukon Territory, Canada) to recent climate variability using aerial photographs and paleolimnological methods

2.1 Introduction

Lake-rich thermokarst landscapes are highly productive northern ‘oases’ that provide important habitat for abundant wildlife, but they are particularly vulnerable to climate change (Rouse et al., 1997; Rowland et al., 2010). Recent observations from remote sensing analysis suggest that thermokarst landscapes are becoming increasingly dynamic in response to climate change, with the rate of lake expansion increasing in some regions and lake-water levels declining in other regions (Yoshikawa and Hinzman, 2003; Smith et al., 2005; Riordan et al., 2006; Plug et al., 2008; Labrecque et al., 2009). However, remote sensing images are taken only periodically and, consequently, when used alone often cannot distinguish the processes responsible for the observed changes in surface area and water-level. For example, water-level declines may result from lake drainage events associated with accelerated thermokarst activity (Plug et al., 2008; Labrecque et al., 2009; Pohl et al., 2009) or from increasing evaporation in response to a longer ice-free season (Riordan et al., 2006). Identifying the processes responsible for water-level changes in these northern landscapes is important for natural resource stewardship since such changes will have ecological consequences that ultimately affect the local wildlife and traditional lifestyle of northern communities.

The Old Crow Flats (OCF) is a vast (5600-km²) thermokarst landscape that has been recognized as a Wetland of International Importance by the Ramsar Convention. Centered approximately 55 km north of the village of Old Crow in the northern Yukon Territory (Figure 2.1), the OCF comprises approximately 2700 shallow thermokarst lakes and provides

habitat for abundant wildlife including the Porcupine Caribou Herd, moose, muskrat and waterfowl. The thermokarst landscape and large populations of wildlife of the OCF support the traditional lifestyle of the Vuntut Gwitchin First Nation (VGFN). Results from a recent tree-ring study conducted in the OCF indicate that there has been marked warming over the last few decades that exceeds any other interval over the past ~300 years (Porter et al., 2010), a pattern consistent with shorter meteorological records in the area (Wolfe et al., 2011). This recent temperature increase corresponds with local observations of water-level declines in the OCF (Tetlich, 2007; Figure 2.2). VGFN land users are concerned that these ongoing hydrological changes will alter wildlife dynamics and the ability to travel safely to traditional hunting and trapping grounds (Wolfe et al., 2011). One such example is Zelma Lake, an accessible, culturally-important and large (12 km²) lake that rapidly drained in spring 2007. This drainage event was attributed to above-average precipitation during the preceding ten months, which led to the erosion of an outlet channel (Wolfe and Turner, 2008; Turner et al., 2010). Water-level declines in other basins in the OCF may also be due to rapid drainage; however, some of the declines could also potentially be caused by increasing evaporation. The timing and processes responsible for the observed changes in the OCF cannot be deciphered through use of remote sensing images alone.

Paleolimnological approaches have been widely used to detect the effects of past climatic changes on the hydrology and limnology of Arctic lakes, ponds and wetlands (e.g., Lotter et al., 1999; Douglas and Smol, 1999). Multi-proxy paleolimnological analyses provide continuous long-term records of hydrological conditions over time and help identify the timing, causes and limnological consequences of hydrological changes. In past studies of shallow lakes in northern landscapes, paleolimnological analyses have been used

successfully to determine changes in the extent of open-ice conditions, lake-water chemistry, river flooding and other hydrological processes (e.g., Douglas and Smol, 1999; Edwards et al., 2004; Wolfe et al., 2005; 2008a; 2008b; Sokal et al., 2010; Brock et al., 2010). However, paleolimnological techniques have not been widely used for thermokarst lakes, in part because these remote landscapes are difficult to access. Also, due to their shallow depth and active thermokarst processes, which can potentially complicate radiometric dating of sediment cores, it remains uncertain if thermokarst lakes preserve informative records of past hydrological conditions. If they do preserve informative, continuous paleohydrological records, sediment core studies of thermokarst lakes have the potential to fill temporal gaps between discrete remote sensing images, and enhance knowledge of long-term hydrological evolution of these lacustrine environments.

This study employs physical, geochemical and biological analyses of a sediment core from one thermokarst lake in the OCF for which a series of historical aerial- and satellite-images were available. The images indicate that water-level in the lake declined markedly sometime between 1972 and 2001. However, the timing of the water-level decline cannot be determined more precisely from these images. Also, it remains uncertain if the water-level decline resulted from a lake drainage event or if it was caused by increased net annual evaporation. Thus, this study aims to evaluate the potential of using multi-proxy paleolimnological analyses to refine understanding of the hydrological changes apparent in a time series of satellite images of a shallow thermokarst lake in the OCF and to identify the processes responsible for the observed water-level decline.

2.2 Site Description

The low relief, lake-rich landscape of the OCF occupies the former lakebed of Glacial Lake Old Crow, which drained catastrophically westward through the Upper Ramparts between 16,440 and 14,860 years BP (Zazula et al., 2004). Since then, the Old Crow River has been the main drainage channel exporting water from the OCF. It flows into the Porcupine River and continues westward where it meets the Yukon River. Throughout the Holocene, the OCF underwent significant physical changes including thermokarst lake formation and downcutting of river channels, which have left lakes of this headwater system perched high above rivers (Lauriol et al., 2002). Presently, lakes and wetlands cover ~40% of the OCF. The lakes are generally shallow (0.5-6 m depth) and vary considerably in surface area (1-3700 ha) (Labrecque et al., 2009). Using water isotope tracers, Turner et al. (2010) identified five distinctive hydrological lake types including snowmelt-dominated, rainfall-dominated, groundwater-influenced, evaporation-dominated and drained, which highlights the diversity in water-balance conditions of the lakes.

The study site (OCF 48; local name: “Hot spring Lake”) is a small (1.3 km²), shallow (0.68 m) lake located in the north-central part of the OCF adjacent to Timber Hill within Vuntut National Park (Figure 2.2; Table 2.1). Turner et al. (2010) identified that the lake oscillates between snowmelt- and rainfall-dominated hydrological lake categories, but also exhibits characteristics of groundwater-influenced basins. Water isotope monitoring during 2007-2009 indicates the lake undergoes minimal evaporative enrichment (mean $\delta^{18}\text{O} = -19.7\text{‰}$; mean $\delta^2\text{H} = -164\text{‰}$; Figure 2.3) relative to other lakes in the OCF (Turner et al., 2010). Shallow groundwater seepage into the lake, resulting from a locally steep hydraulic gradient, likely offsets the effects of evaporation. Local land-users have indicated to us that

“Hotspring Lake” receives groundwater inflow, which causes ice cover to melt relatively early in the spring, an observation that was also reported by Geldsetzer and van der Sanden (2010). Limnological characteristics reflect the input of ion-rich groundwater likely from the adjacent Timber Hill, which is an outcrop of micritic limestone from the Kayak Formation (Morrell and Dietrich, 1993). The lake is nutrient-rich, meso-eutrophic and alkaline (Table 2.1). Abundant macrophytes include *Potamogeton* and sedges (*Carex spp.*). The terrestrial portion of the lake’s ~7 km² catchment is dominated by black spruce (*Picea mariana*), and also includes deciduous shrubs, herbaceous and non-vascular species. Tall willow stands (*Salix spp.*) are densely established around shoreline areas of the lake. Groups of drowned willows are located throughout the lake, which provide evidence that the water level has undergone pronounced changes in the recent past, including an episode of water-level decline followed by a rise.

Meteorological conditions have been monitored at the Old Crow Airport since 1951 (Environment Canada, 2010). However, data for several years are missing or incomplete, particularly during the early part of the record. The available data provide a fairly continuous climate record since 1981. Average annual precipitation for years with complete data sets (n=23) is 262.4 mm (rain =161.8 mm, snow = 100.6 mm). The average monthly temperature in Old Crow varies greatly over the year (-31°C in January; 15°C in July).

2.3 Methods

Aerial Photographs

The aerial photographs of OCF 48 are from 13-15 July 1951, 8-9 July 1972 and 30 August 2001. A SPOT (Satellite Pour l'Observation de la Terre) image was acquired on 24

July 2007 (5 m pixel resolution). The spatial extent of OCF 48 at each time-stamp was digitized in ArcView to provide estimates of changes in lake surface area over time. These images were compared with the paleolimnological record to interpret past hydroecological changes.

Collection and Analysis of Lake Sediment Cores

Two sediment cores (KB1 (36.5 cm) and KB2 (40.0 cm)) were collected from approximately the centre of OCF 48 on September 6, 2008 using a Glew gravity corer (Glew, 1989) fitted with a Lucite tube (7.6-cm inside diameter). The corer was deployed from a helicopter with floats. Each core was sectioned into 0.5-cm intervals using a vertical extruder (Glew, 1988) upon return to the field base in the town of Old Crow, and samples were stored at 4°C until analysis. For both cores, weight loss on heating (90°C for 24 hours), loss-on-ignition (LOI; 550 °C for 1 hour) and loss-on-combustion (LOC; 950°C for 1 hour) was conducted on subsamples of $\sim 0.5 \pm 0.05$ g wet sediment at contiguous 0.5-cm intervals to determine water content, organic matter content and carbonate content, respectively (Dean, 1974; Heiri et al., 2001). The residue after the LOC step was used to calculate the mineral matter content. Results showed no substantial differences between the LOI profiles for the two cores and, thus, all subsequent analyses (radiometric dating, geochemical and biological analyses) were conducted on consecutive 0.5-cm sediment intervals from the longer KB2 core.

Core Chronology

The sediment core chronology was developed by analyzing at least every second 0.5-cm thick sediment sample from 0 to 14 cm depth, and every fourth sample for the remainder of the core (14-40 cm depth; all weights between 1-3 g dry mass), for activities of ^{210}Pb , ^{214}Bi and ^{137}Cs at the Waterloo Environmental Change Research Laboratory (WATER), University of Waterloo. For each sample, a measured mass of freeze-dried sediment was packed into 8 ml polypropylene tubes (SARSTEDT; product No. 55.524), sealed with 1-cm³ of epoxy resin (Devcon®; product No 14310) and allowed to equilibrate for at least 2 weeks before analysis. Activities of the radioisotopes were measured in an Ortec co-axial HPGe Digital Gamma Ray Spectrometer (Ortec # GWL-120-15) interfaced with Maestro 32 software (Version 5.32). Samples were run for at least two days. The Constant Rate of Supply (CRS) model (Appleby, 2001), which assumes a constant flux of ^{210}Pb but allows for varying sedimentation rates, was used to develop a sediment core chronology.

Geochemical Analyses

Bulk organic carbon and nitrogen elemental and isotope composition were measured on contiguous 0.5-cm thick subsamples following methods described by Wolfe et al. (2001). Sediment samples were rinsed with 10% hydrochloric acid to remove carbonates. Samples were then rinsed repeatedly with de-ionized water until a neutral pH was reached. Acid-washed samples were freeze-dried to remove moisture and a 500- μm sieve was used to remove coarse organic debris. Fine fraction samples (<500 μm) were then analyzed for organic carbon and nitrogen elemental and isotope composition using a continuous flow isotope ratio mass spectrometer (CF-IRMS) at the University of Waterloo Environmental

Isotope Laboratory. The stable carbon isotope ratio is reported as $\delta^{13}\text{C}_{\text{org}}$ values in per mil (‰) units relative to the Vienna – Peedee Belemnite (VPDB) standard and the nitrogen isotope ratio is expressed as $\delta^{15}\text{N}$ (‰) relative to atmospheric nitrogen (AIR). Based on sample repeats, the analytical uncertainty for elemental carbon and nitrogen was $\pm 0.044\%$ and $\pm 0.005\%$, respectively, while $\delta^{13}\text{C}_{\text{org}}$ and $\delta^{15}\text{N}$ values have an analytical uncertainty of $\pm 0.04\%$ and $\pm 0.05\%$, respectively. Carbon-to-nitrogen (C/N) ratios were calculated using percent dry weight organic carbon and nitrogen contents.

The acid-washed fine fraction (<500 μm) of the sediment subsamples was also used to reconstruct lake water oxygen isotope composition from measurements of cellulose oxygen isotope composition following standard methods (Wolfe et al., 2001; 2007). Solvent extraction, bleaching and alkaline hydrolysis were used to remove non-cellulose organic constituents, hydroxylamine leaching removed iron and manganese oxyhydroxides and heavy liquid density separation was used to concentrate the cellulose. The purified cellulose samples were then freeze-dried to remove moisture. Cellulose oxygen isotope composition was measured on continuous 0.5-cm intervals of the core with weights of $\sim 0.8 \pm 0.05$ mg using a CF-IRMS at the University of Waterloo Environmental Isotope Laboratory. Results are expressed as δ -values relative to the Vienna – Standard Mean Ocean Water (VSMOW) standard and normalized to $\delta^{18}\text{O}_{\text{SLAP}}$. Based on sample repeats, the analytical uncertainty for $\delta^{18}\text{O}_{\text{cell}}$ is $\pm 0.6\%$. Lake water oxygen isotope composition was reconstructed from cellulose oxygen isotope composition using a cellulose-water oxygen isotope fractionation factor of 1.028 (Wolfe et al., 2001).

Diatom Analyses

Subsamples ($\sim 0.3 \pm 0.05$ g) of consecutive 0.5-cm interval samples were treated with 10% hydrochloric acid to remove carbonates and rinsed repeatedly with de-ionized water until a neutral pH was reached. The subsamples were then digested with strong acids (50:50 concentrated sulphuric: nitric acids by volume) following standard methods (Battarbee et al., 2001) to digest organic material. Diatom slurries were rinsed repeatedly with de-ionized water until a neutral pH was reached. Samples of the diatom slurries were dispensed and dried onto circular coverslips, and then mounted onto microscope slides using Naphrax™. At least 300 diatom valves were identified and enumerated from each sample when possible (0-10.5 cm depth) at 1000x magnification under oil immersion using a Zeiss Axioskop II Plus compound light microscope fitted with differential interference contrast optics. Samples with less than 10 diatom valves per microscope slide transect were deemed uncountable, and, as a result the diatom stratigraphy is only available for the upper 10.5 cm core depth. Uncountable samples can be attributed to either poor preservation or dilution of diatoms by inorganic sediment. The diatoms were identified to the lowest taxonomic level possible using the keys of Krammer and Lange-Bertalot (1988, 1991a b, 1999) and Lavoie et al. (2008). Taxa were considered rare if they had less than 1% abundance in a sample and were not included in further analyses. Selected diatom taxa were classified into habitat preference groups based on ecological information in Wolfe et al. (2008a), Sokal et al. (2008) and Wiklund et al. (2010): (1) *Fragilaria pinnata* (Ehrenberg) is inferred to indicate turbid, low-light environments or shallow water that reduce epiphytic and planktonic habitats for other diatom taxa and (2) epiphytic diatom taxa were inferred to indicate greater water clarity and higher light environments. The epiphytic diatom species included *Achnanthes lanceolata* (Grunow), *A.*

minutissima (Kützing), *Amphora libyca* (Ehrenberg), *A. pediculus* (Kützing), *Cocconeis placentula* (Ehrenberg), *Cymbella cuspidata* (Kützing), *C. microcephala* (Grunow), *C. minuta* (Hilse ex Rabenhorst), *Encyonema lange-bertalotti* (Krammer) *Eolimna minima* (Grunow), *Gomphonema angustum* (Agardh), *G. parvulum* (Kützing), *G. gracile* (Ehrenberg), *Navicula cryptocephala* (Kützing), *N. cryptonella* (Lange-Bertalot), *N. pseudoangilica* (Lange-Bertalot), *N. pupula* (Kützing), *N. radiosa* (Kützing), *Nitzschia amphibia* (Grunow) and *N. palea* (Kützing).

Pigment Analyses

Subsamples ($\sim 0.4 \pm 0.05$ g) of every second 0.5-cm interval of sediment were prepared, extracted and analyzed for pigment concentrations following standard methods (Reuss et al., 2010) at the University of Waterloo WATER lab. Pigment concentrations were determined using a WATERS 2695 HPLC following the reverse phase high performance liquid chromatography procedure described by Mantoura and Lleywellyn (1983) and modified by Leavitt et al. (1989). Pigment concentrations (expressed as nMol per gram organic matter) were identified based on retention time and chromatograms compared to known standards (Jeffrey et al., 1997). Four pigments were chosen to inform paleoenvironmental reconstructions. These pigments are not easily degraded and are known to represent different algal classes: diadinoxanthin is an indicator of diatom abundance, lutein is an indicator of green algae abundance, β -carotene is an indicator of total algal abundance and canthaxanthin is an indicator of cyanobacteria abundance (Jeffrey et al., 1997).

2.4 Results and Interpretation

Aerial Photographs Record of Lake Surface Area Changes

The aerial photographs from 1951, 1972, 2001 and 2007 provide useful temporal context of discrete hydrological changes that can be compared to the paleolimnological record (Figure 2.4). Digitization of these images indicate that OCF 48 had a surface area of 1.90 km² in 1951, 1.64 km² in 1972, 0.63 km² in 2001 (including remnant ponds) and 1.31 km² in 2007. Based on these measurements, the surface area of OCF 48 was relatively stable between 1951 and 1972, declined between 1972 and 2001, and increased between 2001 and 2007. Thus, the images indicate that the lake underwent phases of variable water level, which includes a stable phase, followed by a decline in water level, and a refilling phase that did not recover to the pre-1972 levels.

Multi-proxy Paleolimnological Record

²¹⁰Pb activities fluctuated between 0.054 Bq g⁻¹ and 0.079 Bq g⁻¹ in the upper 5 cm of the core from OCF 48 (Figure 2.5). Below 5 cm sediment depth, the total ²¹⁰Pb activity profile declined from 0.079 Bq g⁻¹ to 0.037 Bq g⁻¹, with some variability and a slight increase to 0.048 Bq g⁻¹ at the bottom of the core (Figure 2.5). ²¹⁰Pb activity remained higher than ²¹⁴Bi activity throughout the core and consequently background (i.e., supported) ²¹⁰Pb activity was not reached. Therefore, the mean ²¹⁴Bi activity of the core (0.034 Bq g⁻¹) was used to estimate the supported ²¹⁰Pb levels. ¹³⁷Cs could not be used as an independent marker in this core because it did not provide a discernable peak. Radiometric dating of another lake in the OCF (OCF 29) with slower sedimentation rates shows that unsupported and supported ²¹⁰Pb values merge at an activity of 0.032 Bq g⁻¹. The ²¹⁰Pb-derived chronology at OCF 29

was confirmed with a sharp peak in ^{137}Cs occurring at the ^{210}Pb -estimated date of 1969, which is just after the expected peak fallout in 1963. The similarity in supported ^{210}Pb activity profiles from the two lakes and correspondence of water-level changes at OCF 48 depicted in the aerial image time series with estimated timing of comparable changes in several paleolimnological parameters (see below) provide evidence that the ^{210}Pb -methods resulted in a sufficiently reliable chronology. The CRS model for OCF 48 gave a basal date of 1874 (40 cm) and resulted in a mean sampling resolution of $3.35 \text{ years cm}^{-1}$ over the 40-cm core length.

Physical, geochemical and biological proxies show stratigraphic variations, which indicate that the lake has undergone marked hydroecological changes during the past ~135 years. This includes four distinct hydroecological phases that are consistent with the aerial and satellite images (Figure 2.6).

Phase 1 (~1874 to ~1967): Stable

During the earliest period of the sediment record (~1874 to ~1967), all paleolimnological parameters remained relatively constant. Values of organic matter (~13-15%), mineral matter (~80-84%) and carbonate content (~7-8%) varied only slightly. The sedimentation rate remained relatively consistent ($\sim 0.1 \text{ g cm}^{-2} \text{ year}^{-1}$) until ~1956 when it began to increase to $\sim 0.4 \text{ g cm}^{-2} \text{ year}^{-1}$. During this period, C_{org} (%) fluctuated around 7%, while N (%) fluctuated around 0.7%. The C/N ratio, which is often used to distinguish terrestrial versus aquatic sources of organic matter (Meyers and Teranes, 2001) was low throughout this period (~10) and remained low throughout the entire core suggesting that organic matter is mainly from aquatic primary production. Both $\delta^{13}\text{C}_{\text{org}}$ and $\delta^{15}\text{N}$ values

remained constant throughout this period and only varied slightly from ~-20‰ and ~-2.5‰, respectively. In general, pigment concentrations remained fairly constant during this phase and no clear changes or trends were apparent. Based on the three-point running mean, cellulose-inferred lake water $\delta^{18}\text{O}$ ($\delta^{18}\text{O}_{\text{lw}}$) values were low, ranging between -22.4‰ and -19.8‰, likely indicating that the lake was fed mainly by snowmelt and minimal evaporation occurred. Overall, these results indicate that hydrological and limnological conditions of OCF 48 were stable during this time period. This corresponds well with evidence from the first two aerial images (1951 and 1972) that display very little change in lake surface area and state.

Phase 2 (~1967 to ~1989): Expansion

Between ~1967 and 1989, there was a marked stratigraphic shift in most parameters. Sedimentation rates began to increase and peaked at ~1969 (~0.1 to 0.9 g cm⁻² year⁻¹). Marked declines occurred in sedimentary content of organic matter (~15 to 10%), organic carbon (~8 to 5%) and nitrogen (~0.7 to 0.4%). Also, pigment content declined sharply to non-detectable levels. Correspondingly, mineral matter content increased from ~82 to 85%. The C/N ratio remained constant overall (~10.3) throughout this period, $\delta^{13}\text{C}_{\text{org}}$ values declined (~-20‰ to -26‰), $\delta^{15}\text{N}$ values increased (~-2.5‰ to 4.0‰) and $\delta^{18}\text{O}_{\text{lw}}$ values remained consistently higher (mean = -19.7 ‰) than during Phase 1.

The stratigraphic records indicate marked limnological and hydrological changes occurred during Phase 2. The decline in organic matter, organic carbon and nitrogen and the concomitant increase in mineral matter are consistent with a response to increased minerogenic turbidity and a subsequent decline in available light and aquatic productivity. A

decline in productivity is also supported by decreased pigment concentrations and a decrease in $\delta^{13}\text{C}_{\text{org}}$ values. The latter is commonly used to reconstruct paleo-productivity because increasing algal demand on dissolved inorganic carbon (DIC) commonly leads to ^{13}C -enrichment of DIC and phytoplankton, which is often recorded in lake sediments by increases in $\delta^{13}\text{C}_{\text{org}}$ values (Meyers and Teranes, 2001; Meyers, 2003; Leng et al, 2005). Numerous factors and processes may cause changes in the $\delta^{15}\text{N}$ values in lake sediment records, including ^{15}N -enrichment caused by increasing productivity (see Talbot, 2001). However, the other paleolimnological data are inconsistent with this interpretation. Alternatively, the increase in $\delta^{15}\text{N}$ values may reflect an increase in the supply of ^{15}N -enriched nitrate derived from the leaching of soils along the margin of the lake (e.g., Wolfe et al., 1999). Based on these data, we suggest that the limnological changes inferred from the sediment record during Phase 2 were caused by lake expansion and erosion of shoreline sediments. The increase in $\delta^{18}\text{O}_{\text{lw}}$ values was most likely due to an increase in the supply of isotopically-enriched summer precipitation to the lake, which may have been a key driver of lake expansion. A small increase in evaporation, due to expansion in lake surface area, may also account for the rise in $\delta^{18}\text{O}_{\text{lw}}$ values. This hydrological phase was not captured in the aerial images.

Phase 3 (~1989): Drainage

In ~1989, stratigraphic trends from the expansion phase terminated abruptly. A rapid increase in sedimentation rate, values of $\delta^{18}\text{O}_{\text{lw}}$ and $\delta^{13}\text{C}_{\text{org}}$, concentrations of organic matter, organic carbon and nitrogen, and concentrations of the pigments diadinoxanthin, lutein and β -carotene occurred while mineral matter content, $\delta^{15}\text{N}$ and the C/N ratio declined.

These stratigraphic changes indicate an abrupt alteration in the hydrological and limnological conditions of OCF 48, which we attribute to the rapid drainage of the lake. Rapid loss of lake water via surface or subsurface drainage would lead to lower water levels and increased concentration of nutrients. Combined with greater light availability due to decreased shoreline erosion, these conditions would have promoted the rapid increase in lake productivity and sedimentation rate that is recorded in the physical, biological and geochemical profiles. A spike in the $\delta^{18}\text{O}_{\text{lw}}$ profile immediately after the drainage event may represent an abrupt increase in the proportion of summer rainfall contributing to the lake water balance. Stratigraphic evidence of lake drainage in ~1989 is consistent with aerial images that indicate a water level decline sometime between 1972 and 2001. Notably, $\delta^{18}\text{O}_{\text{lw}}$ values are substantially lower during 1972-2001 (-22.3‰ to -18.9‰) than the predicted value for a terminal basin at steady-state (~-12‰) under present-day climatic conditions (Turner et al., 2010). Thus, the lake-level decline captured in the 2001 image could not have been caused by evaporation.

Phase 4 (~1989 to 2008): Refilling

Stratigraphic analyses indicate that organic matter (~10 to 17%), carbonates (~7 to 15%), organic carbon (~4 to 8%), nitrogen (~0.4 to 0.9%) and $\delta^{13}\text{C}_{\text{org}}$ (~-25‰ to -23‰) all increased after the rapid drainage of OCF 48 in ~1989, whereas mineral matter content (~86 to 76%), C/N ratio (~10 to 9) and $\delta^{18}\text{O}_{\text{lw}}$ values (~-19‰ to -21‰) continued to decline gradually. The concentrations of all pigments continued to increase with β -carotene, lutein, and canthaxanthin reaching their highest recorded concentrations. *Fragilaria pinnata* dominated diatom assemblages throughout this entire phase, while epiphytic taxa contributed

~25-40%. Relative abundance of epiphytic taxa increased after 2004, a period when $\delta^{15}\text{N}$ values continued to decrease.

Increasing organic content, carbonate content, pigment concentrations and $\delta^{13}\text{C}_{\text{org}}$ values are all indicative of increasing lake productivity that we associate with a period of lake refilling. As erosion of shoreline sediments ceased, turbidity declined and the lake productivity increased. A reduction in leaching of ^{15}N -enriched nitrate in shoreline sediments may explain the decline in $\delta^{15}\text{N}$ values. As the lake continued to refill and become clearer and more productive, macrophytes likely began to grow, resulting in relatively high abundance of epiphytic diatom species. The trend towards lower $\delta^{18}\text{O}_{\text{w}}$ values that approach lake-water oxygen isotope values measured during 2007-2009 indicate an increasing proportion of the lake's input waters was provided by isotopically-depleted snowmelt relative to isotopically-enriched rainwater. These results are in agreement with the 2007 SPOT image that indicates increased water levels since the aerial image from 2001, and with present-day observations of clear water and abundant macrophytes.

2.5 Discussion

Thermokarst lakes undergo hydroecological successional changes and cycles in response to climate conditions. Early stages of thermokarst development include subsidence of ice-rich permafrost soils, formation of ice-wedge polygons and boundary trenches, and subsequent surface-water accumulation and coalescence of ponds (Mackay, 1992; Yoshikawa and Hinzman, 2003; Plug et al., 2008). Once larger water bodies are established, lake development and expansion continues as ice-rich bank material subsides in response to various processes including erosion from elevated water levels and waves, and thaw of

exposed surfaces during prolonged periods of warm air temperatures and exposure to sunlight. Thermokarst lakes may eventually drain following elevated water levels in response to increased precipitation or rapid snowmelt. Drainage outlets may, for example, form along thermo-contraction cracks that occur in ice-wedges connected to lower-lying areas (Mackay, 1988, 1992) or in response to erosion of ice-rich bank material within a narrow divide. The latter example requires a rapid increase in lake level, following prolonged intense precipitation, rapid snowmelt or blockage of other outlets (Mackay, 1988, 1992; Brewer et al., 1993; Marsh and Neumann, 2001; Hinkel et al., 2007; Wolfe and Turner, 2008; Marsh et al., 2009; Turner et al., 2010). Alternatively, subsurface drainage into the water table may also occur when the underlying talik completely penetrates the underlying permafrost and a negative vertical hydraulic gradient exists (Yoshikawa and Hinzman, 2003; Smith et al., 2005; Riordan et al., 2006).

Multi-proxy paleolimnological analysis of the sediment record from OCF 48 indicates that the lake has experienced four phases of hydroecological change over the past ~135 years that are consistent with thermokarst lake evolution described above and which includes a complete cycle characterized by stability, expansion, rapid drainage and gradual refilling. During Phase 1 (~1874-1967), physical, geochemical and biological indicators were complacent, indicating that the lake did not experience any substantial hydrological or limnological changes. During Phase 2 (~1967-1989), a decline in organic matter content (and the concomitant rise in mineral matter content), $\delta^{13}\text{C}_{\text{org}}$ and pigment concentrations, and increase in $\delta^{18}\text{O}_{\text{1w}}$ and $\delta^{15}\text{N}$ values are likely due to lake expansion that may have been initiated by recent climate warming (Porter et al., 2010) and above average summer precipitation. These stratigraphic trends terminate abruptly in ~1989 (Phase 3), which we

attribute to the sudden drainage of OCF 48. Phase 4 (~1989-2008) is characterized by increasing organic matter content, $\delta^{13}\text{C}_{\text{org}}$ values, pigment concentrations, decrease in $\delta^{15}\text{N}$ values, as well as the increased abundance of diatoms, which reflect an increasingly productive, clearer water, macrophyte-rich lake as the basin partially refilled. By 2008, the majority of parameters (organic and mineral matter content, sedimentation rate, C_{org} (%), N (%), $\delta^{13}\text{C}_{\text{org}}$, $\delta^{15}\text{N}$ and pigments) approach levels that are similar to the earlier stable phase. Rapid establishment of willow on the newly exposed lakebed may have provided for greater snowpack accumulation, and subsequently, increased supply of isotopically-depleted snowmelt to the lake during Phase 4.

Interpretations based on the multi-proxy paleolimnological record are largely consistent with the remote sensing images from 1951, 1972, 2001 and 2007. However, due to a large time gap between images, the lake expansion phase is only evident in the paleolimnological record. Also, aerial images alone indicate that a decline in lake-level occurred sometime between 1972 and 2001 but cannot identify if the water-level drop was sudden (drainage event) or gradual (increased evaporation). Paleolimnological analyses were able to refine the hydrological history apparent in the aerial photograph time series by more precisely identifying when lake-level decline occurred (~1989) and the cause (rapid drainage).

Meteorological records were examined to explore potential causes of the rapid drainage of OCF 48 that was identified in the paleolimnological analysis. Precipitation records from the Old Crow airport (Environment Canada, 2010; Figure 2.7) indicate high amounts of antecedent precipitation in the months prior to the inferred lake drainage. In particular, there was a very large amount of rainfall in August 1987, followed by above

average (1951-2007) precipitation until August 1988. Increased rain likely resulted in water levels rising to near maximum capacity at the time of lake freeze-up. We suggest that the combination of snowmelt and slightly above average spring rainfall (June 1989) caused water levels to rise above maximum capacity and an overland outlet channel was likely formed. Further erosion of the shoreline sediments and channel likely occurred as water flowed through, increasing the rate of water export and consequently resulting in the rapid drainage of OCF 48 in 1989. An outlet channel was not visible in satellite images or during field visits, possibly due to establishment of vegetation in the outlet channel. The pattern of above-average precipitation leading to rapid drainage has also been observed in the more recent drainage of Zelma Lake and lake OCF 56 in the region (Wolfe and Turner, 2008; Turner et al., 2010). Interestingly, other studies in the Arctic Coastal Plain (Brewer et al., 1993) and Northwest Territories near the Mackenzie Delta (Marsh and Neumann, 2001; Pohl et al., 2009) have reported rapid thermokarst lake drainage events in 1989, and also attributed these to high antecedent precipitation. Our results support the findings of other studies (Brewer et al., 1993; Marsh and Neumann, 2001; Plug et al., 2008; Labrecque et al., 2009), which suggest that precipitation is a key driver in thermokarst lake drainage-expansion cycles.

Given that precipitation appears to be an important driver of lake drainage events in the OCF, the precipitation record may provide information to hindcast when other lake drainage events are likely to have occurred. For example, the precipitation record (Figure 2.7) identifies that the following years experienced above-average (262 mm) annual precipitation prior to the start of the ice-free season (June 1): 1975 (349 mm), 1982 (344 mm), 1985 (314 mm), 1988 (325 mm), 1992 (277 mm), 1994-2001 (average = 306 mm), 2004 (334 mm) and 2007 (359 mm). In the OCF, we hypothesize that drainage events are

more likely to have occurred during these years or the years immediately following compared to years with average or below average antecedent precipitation. Ongoing paleolimnological studies are being employed to test this hypothesis. As many climate models predict a continued increase in precipitation in the Arctic (Kattsov et al., 2005; Prowse et al., 2006), identifying the hydrological response of thermokarst lakes in the OCF to previous years of elevated precipitation is important for predicting future scenarios.

While these results are exceptionally promising for furthering our understanding of the hydrological behaviour of thermokarst lakes in the OCF, our findings are from only one lake and uncertainty remains about the factors that promote water-level declines in other lakes in the OCF (e.g., Figure 2.2) and at the landscape level. However, based on the remarkably clear and coherent stratigraphic record from OCF 48, we can hypothesize on expected stratigraphic profiles for lakes that have experienced water-level declines due to rapid drainage versus evaporative drawdown (Figure 2.8). In scenario (a), increasing temperature, if accompanied by increasing precipitation, may accelerate natural thermokarst lake expansion-drainage cycles. In the case of sedimentary organic content, an initial phase of stable productivity would be followed by a rapid decrease in organic matter content as lake expansion initiates and increased supply of minerogenic sediment increases lake turbidity that reduces lake productivity. As expansion continues and episodes of elevated precipitation occur, water levels increase leading to rapid drainage and subsequent rapid increase in organic matter as the water column becomes clearer, nutrients concentrate and growth of macrophytes and phytoplankton increase. Alternatively, in scenario (b), increasing temperature and duration of the ice-free season (without pronounced increases in precipitation) may cause increasing evaporation and desiccation of lakes. Under these

conditions, a period of stable limnological conditions would be followed by a gradual increase in productivity due to evaporative concentration of nutrients, declining water volume and longer duration of the ice-free season. Other parameters may show similar patterns but trend directions may differ (e.g., profiles of mineral matter content will be a mirror image of the organic matter content profiles). Overall, we hypothesize that sediment records from lakes experiencing accelerated thermokarst expansion-drainage cycles would likely show more abrupt changes and rapid stratigraphic inflections compared to lakes experiencing evaporative drawdown – patterns that need to be tested at other locations.

2.6 Conclusions

Small, shallow thermokarst lakes have often been avoided for paleolimnological studies due to the dynamic sedimentary environment that may cause preservation problems, complicate radiometric dating and confound coherent paleohydrological reconstructions. Here, we show correspondence of changes in stratigraphic profiles of paleolimnological parameters with changes depicted in historical aerial images, which suggest that sediment cores contain reliable records of hydrological and limnological conditions. Importantly, parameters as simple to measure as LOI depict clear shifts in hydroecological conditions of our study lake. Overall, our study indicates that multi-proxy paleolimnological approaches can be employed to track past hydroecological changes and events in thermokarst lakes and that they are able to help identify the causes of past changes. OCF 48 experienced four well-defined phases during the past ~135 years; Phase 1: stable (~1874-1967), Phase 2: expansion (~1967-1989), Phase 3 (~1989): rapid drainage and Phase 4 (~1989-2008): refilling, that correspond with an aerial photograph time series but also reveal an additional phase not

apparent in the photographs (i.e., Phase 2). Examination of meteorological records suggest that high antecedent precipitation may have caused the lake to erode an outlet and drain rapidly, as has been observed more recently in the OCF (Wolfe and Turner, 2008; Turner et al., 2010). Ongoing paleolimnological research aims to further evaluate the nature of recent water-level declines observed in the OCF, knowledge that will help inform future predictions of lake hydrological conditions under different climate change scenarios.

2.7 Acknowledgements

We thank Trevor Lantz, Claude Duguay and Sylvain Labrecque for providing the satellite images. Funding for this study was provided by the Government of Canada International Polar Year Program, the Natural Sciences and Engineering Research Council of Canada (Northern Research Chair, and Discovery Grant / Northern Supplement Programs), the Polar Continental Shelf Program, the Indian and Northern Affairs Northern Scientific Training Program and Parks Canada Agency. We thank the Vuntut Gwitchin First Nation and the community of Old Crow for logistical support and contributions to this study. Two anonymous reviewers provided helpful comments that improved the paper.

2.8 Figures

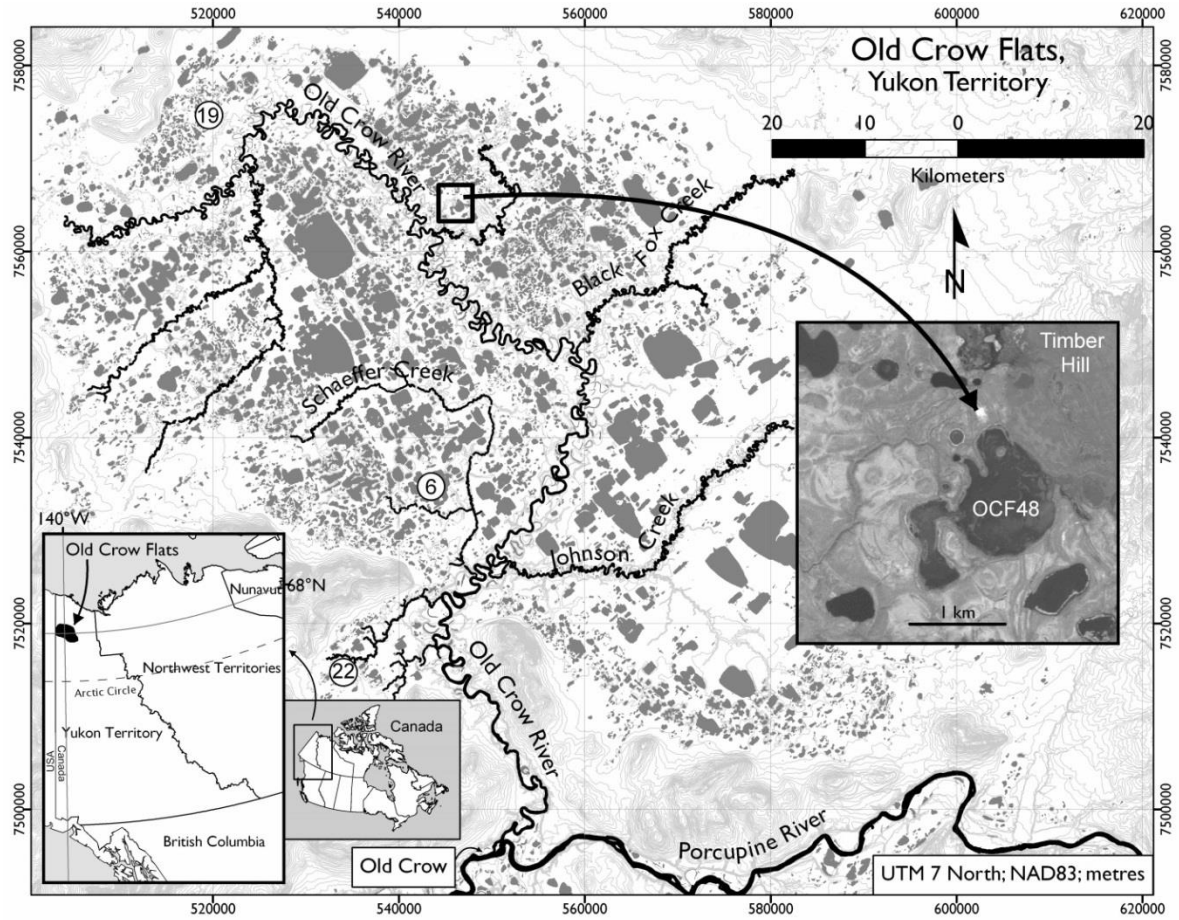


Figure 2.1: Location of the Old Crow Flats (OCF), Yukon Territory, Canada. Details of the sediment coring site (OCF 48) shown with SPOT satellite image from July, 2007. Labels 6, 19 and 22 are locations of photographs from Figure 2.

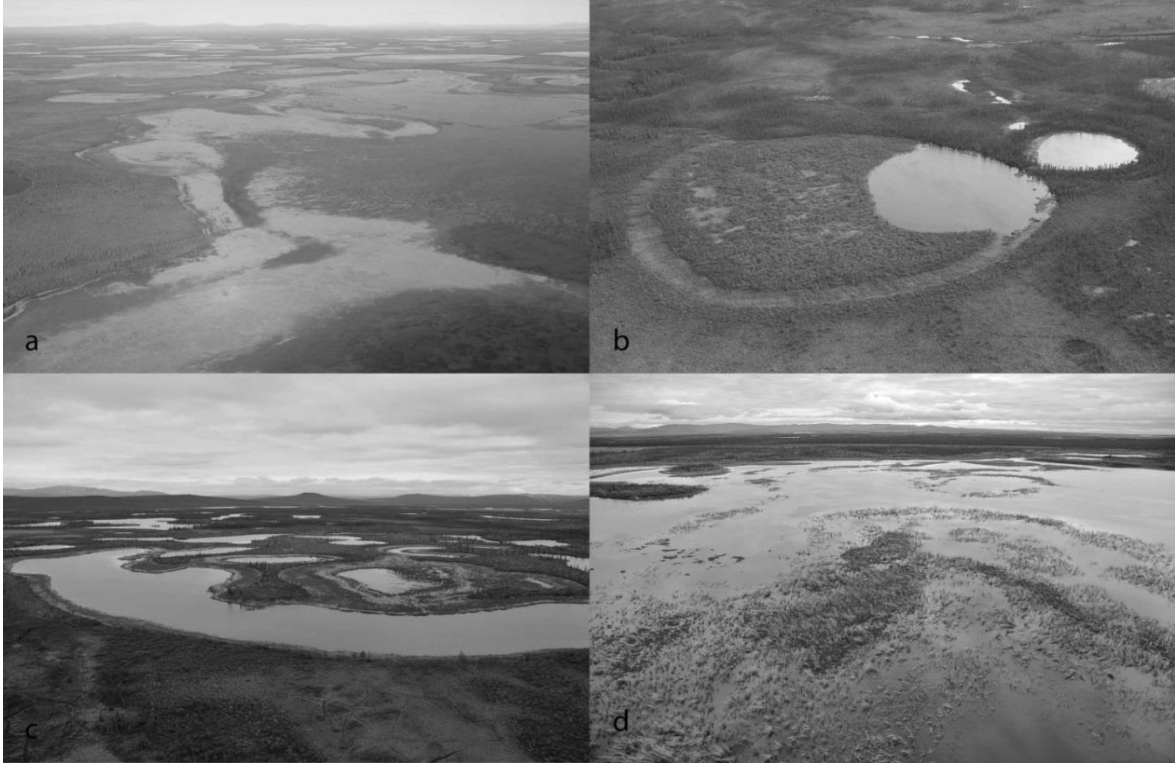


Figure 2.2: Photographs showing examples of lakes in the OCF that have experienced water-level decline. Locations of sites are shown on Figure 2.1: a) OCF 6, b) OCF 22, c) OCF 19 and d) OCF 48.

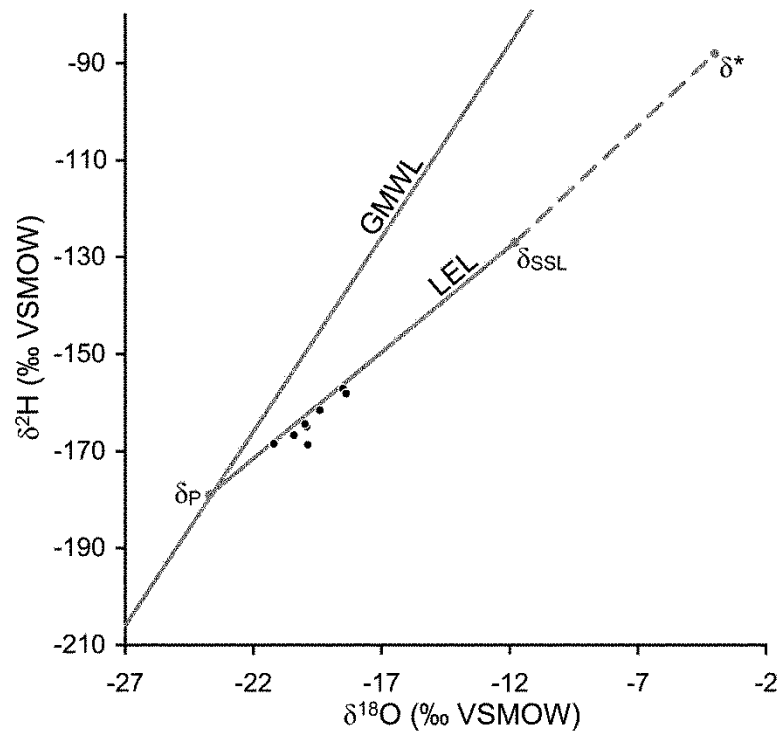


Figure 2.3: Water isotope results for OCF 48 from samples obtained during 2007-2009. Also shown is the Global Meteoric Water Line (GMWL; Craig, 1961) and the Local Evaporation Line (LEL) derived from isotopic and meteorological data from 2007 (Turner et al., 2010). δ_P is the average annual isotopic composition of precipitation, δ_{SSL} is the steady-state composition for a terminal basin where evaporation = inflow and δ^* is the limiting isotopic composition of a lake approaching desiccation.

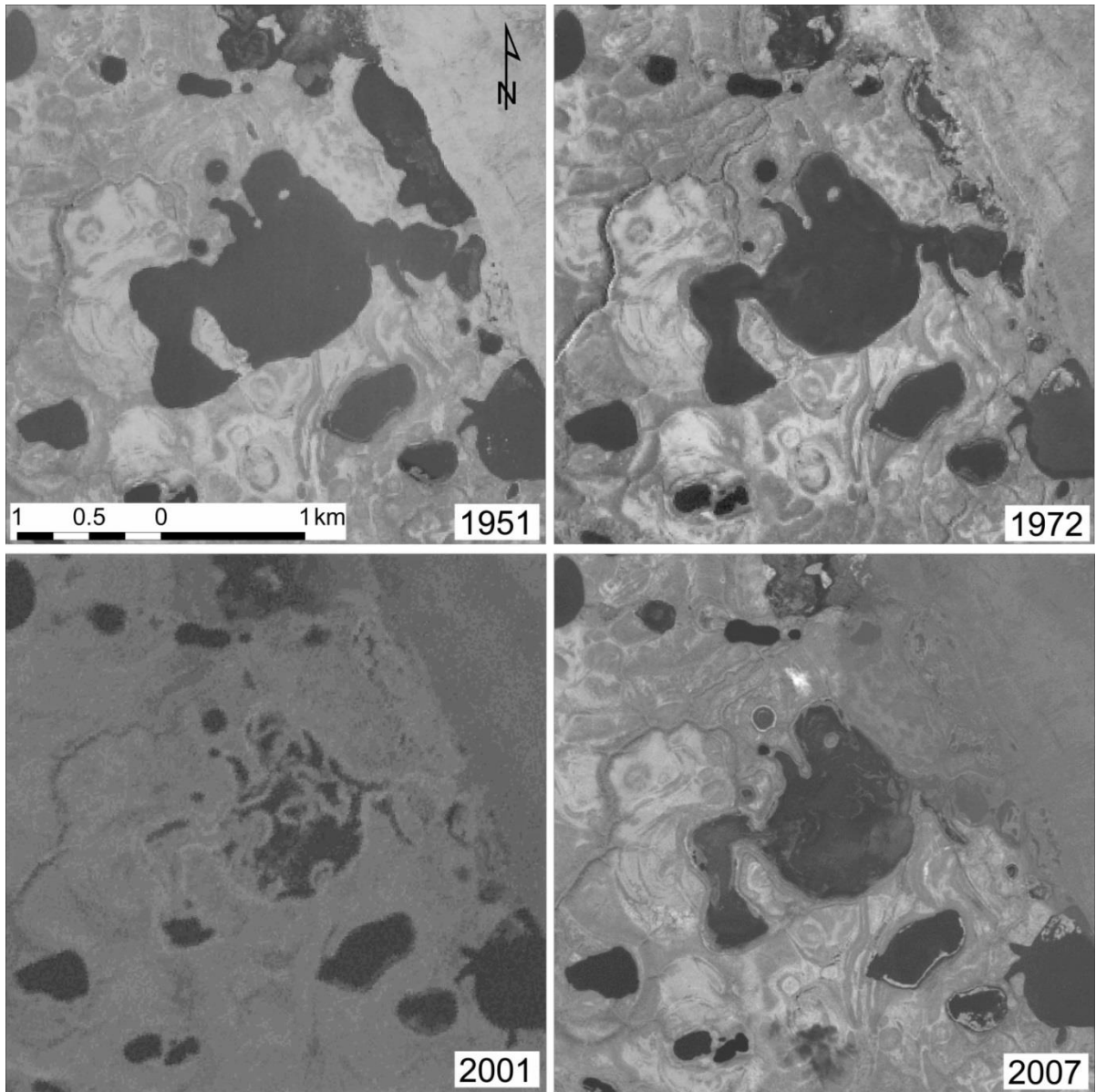


Figure 2.4: Historical images of lake OCF 48 from a) 1951, b) 1972, c) 2001 and d) 2007.

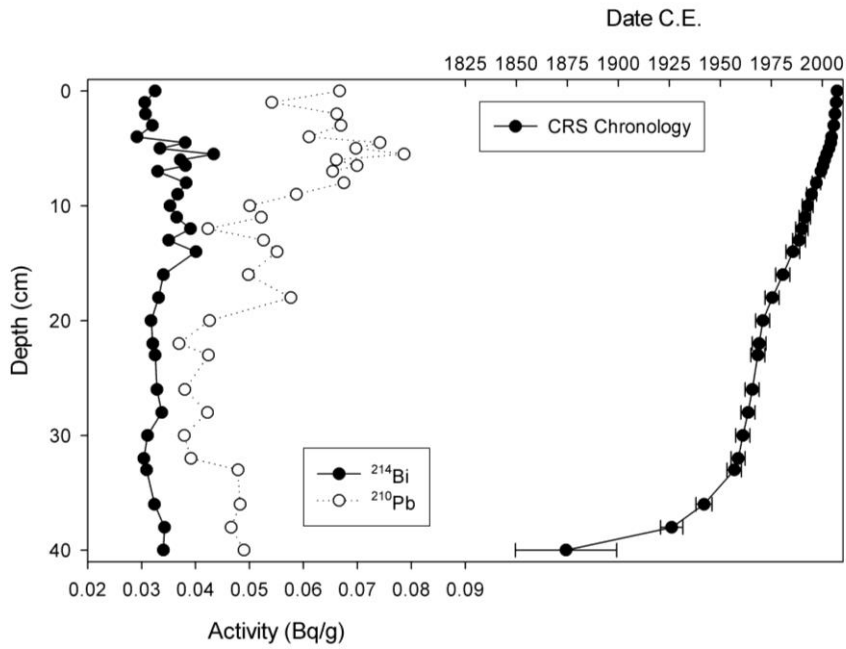


Figure 2.5: ^{210}Pb and ^{214}Bi activity and depth-age profiles for OCF 48 KB2 sediment core.

Error bars represent two standard deviations.

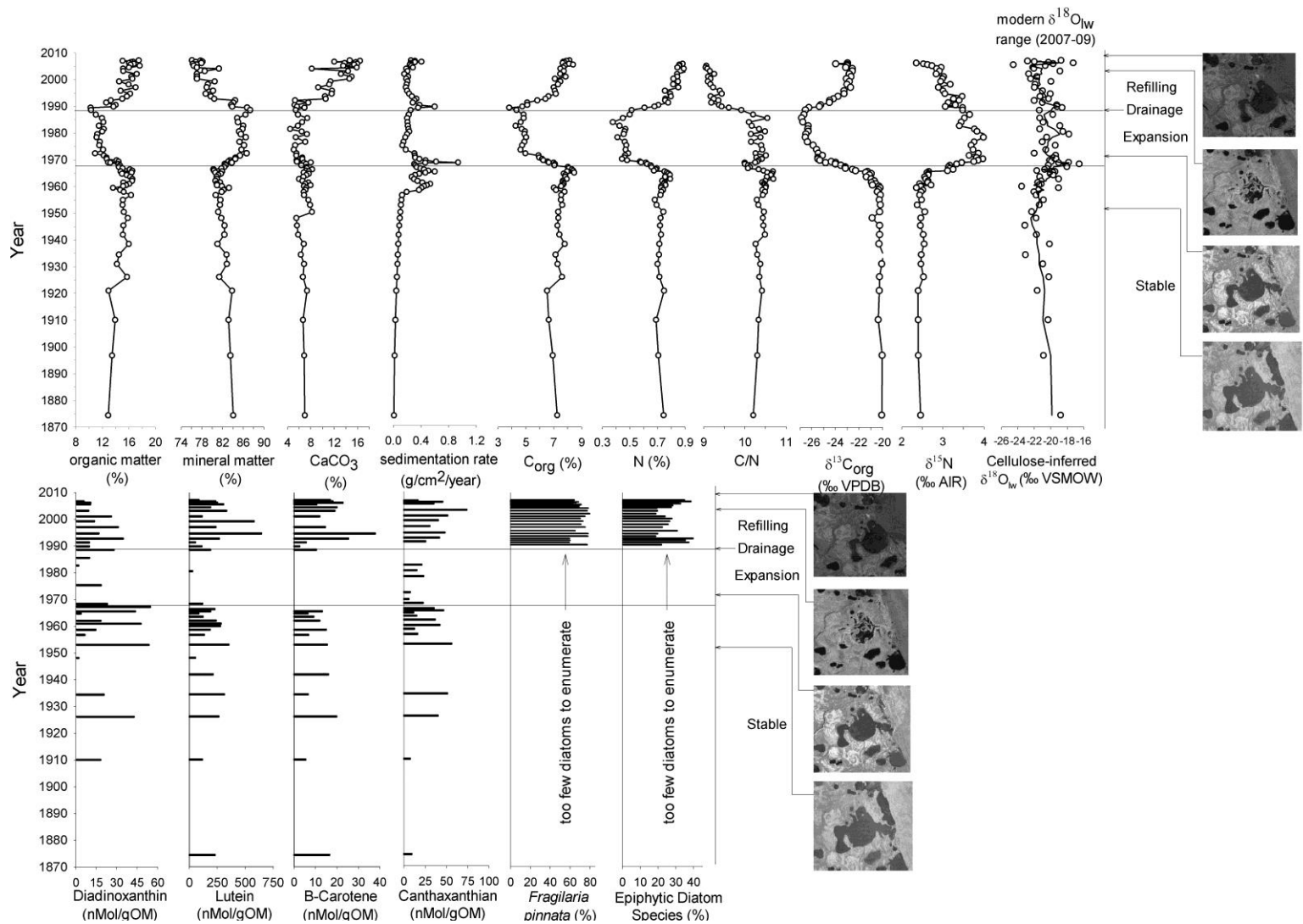


Figure 2.6: Summary of key paleolimnological indicators for OCF 48 KB2, plotted versus time derived from the ^{210}Pb analysis.

Raw cellulose-inferred lake water $\delta^{18}\text{O}$ ($\delta^{18}\text{O}_{\text{lw}}$) values are plotted along with a three-point running mean.

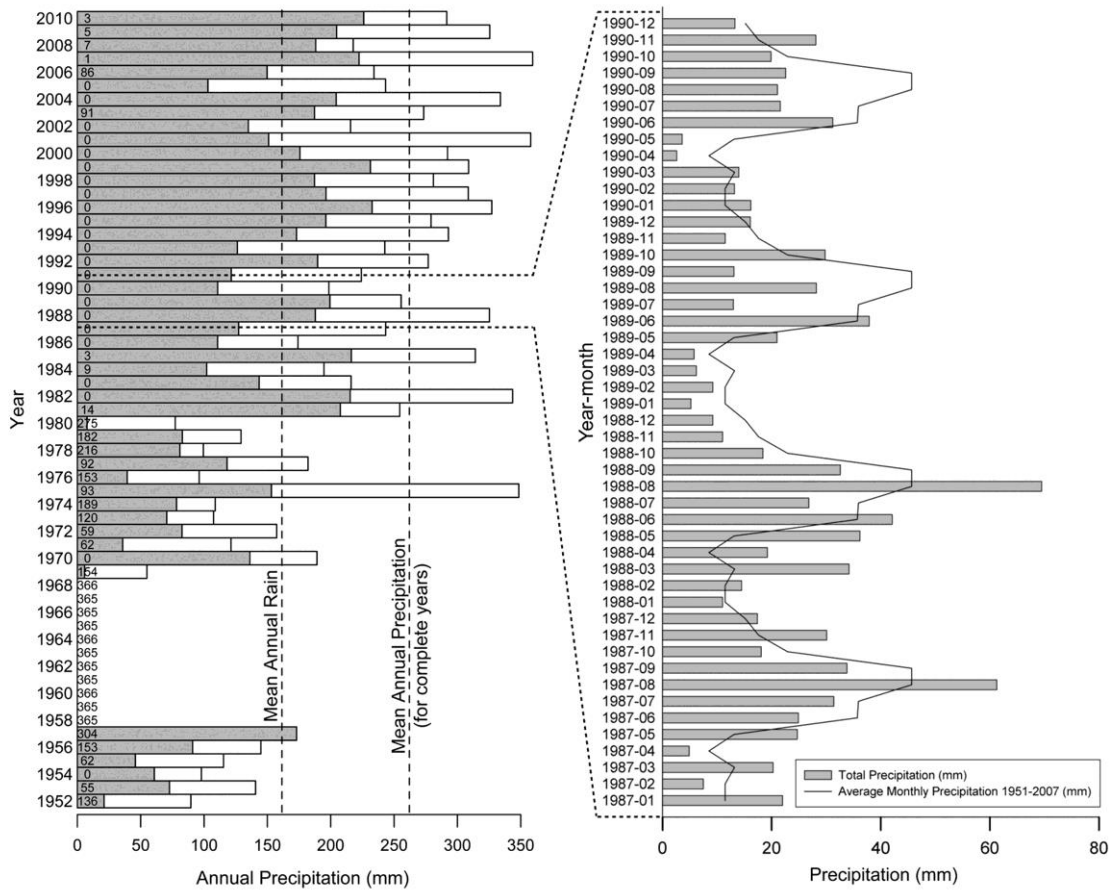


Figure 2.7: Precipitation data based on Environment Canada’s Old Crow data (daily since 1951). Left plot: Annual precipitation from 1952 to 2010. Each year represents June 1 of the previous year to May 31 of the labelled year. White bars represent snow and grey bars represent rain. The numbers plotted on the left side of the bars represent the numbers of days of data missing. Right plot: Monthly precipitation from January 1987 to December 1990 plotted with the long-term monthly average (1951-2007).

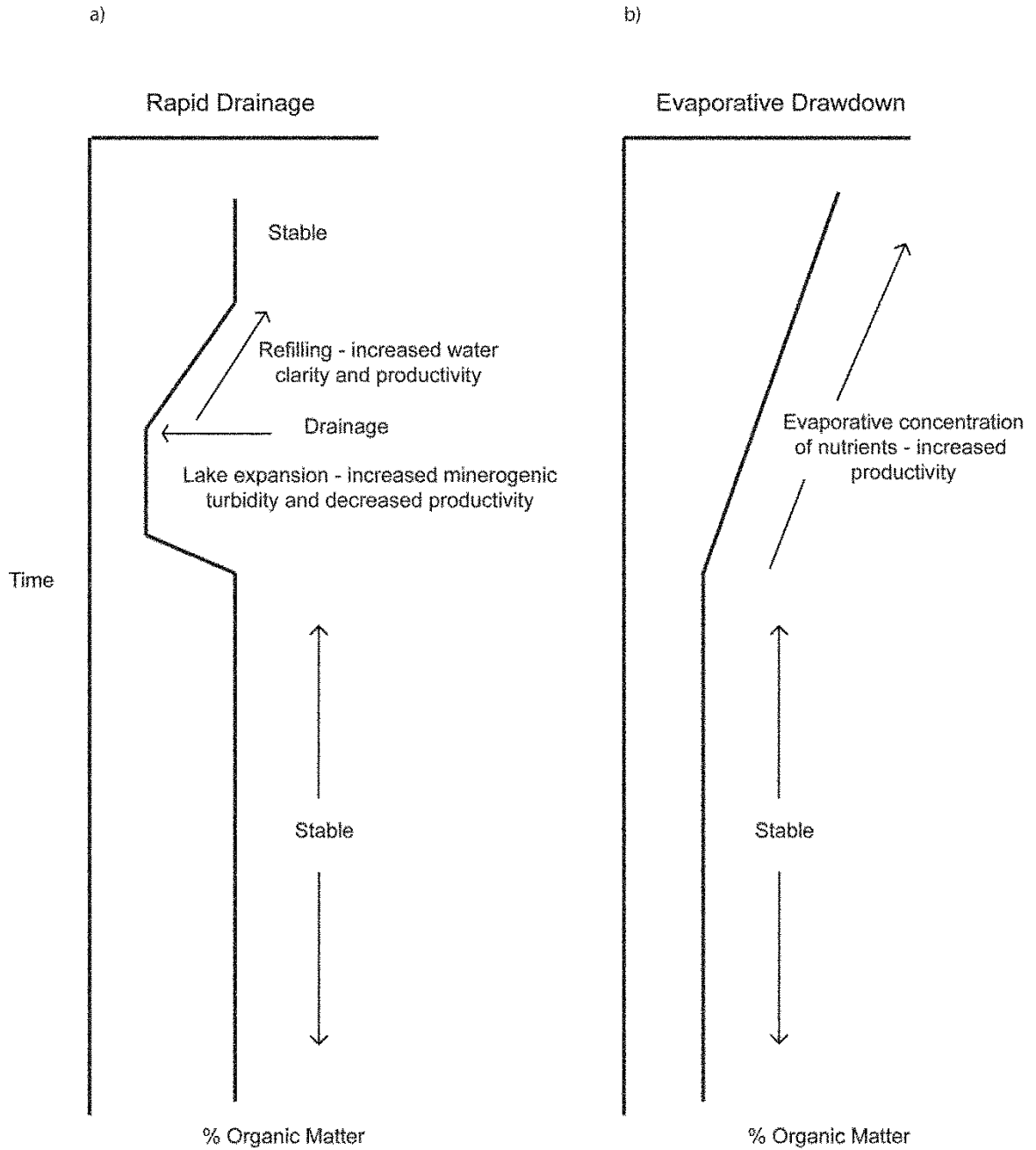


Figure 2.8: Expected sedimentary organic matter content (%) profiles from paleolimnological analysis of lakes experiencing surface area changes from (a) accelerated thermokarst expansion-drainage cycles and from (b) increased evaporation.

2.9 Tables

Table 2.1: Selected physical and chemical limnological characteristics of lake OCF 48.

Values represent the average and standard deviation of samples collected on July 24 2007, July 30 2008 and July 30 2009 measurements.

	SI Units	Average July (2007-2009)	Standard Dev
pH		9.27	0.44
Specific conductivity	µS/cm	170.67	17.90
Alkalinity	meq/L	1.82	0.23
Dissolved organic carbon	mg/L	8.20	1.48
Dissolved inorganic carbon	mg/L	18.60	4.08
Calcium	mg/L	14.17	3.14
Magnesium	mg/L	7.23	0.72
Potassium	mg/L	1.72	0.36
Silica	mg/L	2.97	2.41
Total nitrogen	mg/L	0.79	0.15
Total dissolved phosphorus	µg/L	30.80	14.05
Total phosphorus	µg/L	46.53	18.28
Chlorophyll <i>a</i>	µg/L	3.20	2.81
Average (point) depth	m	0.68	0.39

Chapter 3: Avian-driven modification of seasonal carbon cycling at a tundra pond in the Hudson Bay Lowlands (northern Manitoba, Canada)

3.1 Introduction

Shallow lakes and ponds are a dominant feature of tundra landscapes in the Arctic and Subarctic, and they provide important habitat and resources for abundant waterfowl populations. These relatively pristine freshwater ecosystems are particularly responsive to environmental stressors, because they possess small water volumes and high surface area to volume ratios (e.g., Rouse et al., 1997; Prowse et al., 2006; Schindler and Smol, 2006; Smol and Douglas 2007ab; Rowland et al., 2010). For over 20 years, concerns have been mounting about the environmental effects of increased waterfowl populations, and how changes in their geographic distribution may alter the structure and function of Arctic and Subarctic freshwater ecosystems. Consequences may include eutrophication, changes in nutrient cycling, and destruction of vegetation and available habitat (e.g., Handa et al., 2002; Gregory-Eaves et al., 2004; Lim et al., 2005; Van Geest et al., 2007; Côté et al., 2010; Sun et al., 2013).

Limnological and paleolimnological approaches have been utilized to assess the effects of fluctuations in waterfowl populations on Arctic and Subarctic lakes and ponds. For example, Côté et al. (2010) used measurements of several physical and chemical variables, including water-column concentrations of dissolved organic carbon (DOC), dissolved inorganic carbon (DIC), total phosphorus (TP) and total Kjeldahl nitrogen (TKN), to assess the influence of Greater Snow Goose (*Chen caerulescens atlantica*) activity on lakes and ponds on Bylot Island, Nunavut, Canada. Based on a single sampling episode during the summer (July-August), they found no significant difference in DOC and DIC concentrations in lakes and ponds with and without geese. Concentrations of TP were generally low (mean:

13.8 $\mu\text{g L}^{-1}$, range: 3.9-37.4 $\mu\text{g L}^{-1}$), and were significantly elevated in lakes with geese. Keatley et al. (2009) combined measurements of limnological variables (e.g., pH, concentration of P and N) with the analysis of diatoms in surface sediments of ponds on Devon Island (Nunavut, Canada) to determine that influence of seabirds (northern fulmars, *Fulmarus glacialis*) significantly elevated pH and concentrations of P and N and altered diatom community composition. Additional contemporary and paleolimnological studies, including work from Devon Island, Cape Vera and Cornwallis Island, have also found increases in productivity and nutrient concentrations in response to seabird populations (e.g., Michelutti et al., 2009; 2010; Keatley et al., 2011; Sun et al., 2013).

To date, limnological studies in Arctic locations have focused almost exclusively on assessing whether waterfowl population expansion modifies nutrient (mainly P and N) concentrations in the water column. Considerably less research has been conducted to assess the influence of waterfowl population expansion on C cycling. Moreover, previous studies of the influence of waterfowl on biogeochemical cycles and productivity of Arctic lakes have used conventional limnological measurements of C (e.g., concentrations of DOC and DIC; Côté et al., 2010), but as far as we are aware have yet to incorporate measurements of C isotope composition of dissolved and particulate fractions. Carbon isotopes have been used successfully in temperate lakes to assess productivity and track C cycling (e.g., Rau, 1978; Quay et al., 1986; Takahashi, 1990, Bade et al., 2004), and so may be useful to assess effects of waterfowl disturbance in Arctic and Subarctic ponds.

Most of the limnological studies that have examined the influence of waterfowl on Arctic lakes have relied on single, point-in-time water chemistry measurements. This is often a consequence of logistical constraints and high costs associated with sampling in remote

northern locations. For example, Côté et al. (2010) sampled lakes once (in July or August) to provide a ‘snapshot’ of the differences in limnological conditions between lakes with and without substantial waterfowl populations. And, Keatley et al. (2009) sampled sites once per year during July for three years, although not every site was sampled each year. An exception is a study by Mallory et al. (2006), which involved a nine-week sampling period to track changes in limnological conditions of a single pond in Nunavut located adjacent to an eider colony. They documented a decrease of pH and increase of P and N concentrations by the end of the ice-free season compared to lakes uninfluenced by the eider colony. Mallory et al. (2006) demonstrated that multiple limnological measurements over seasonal timescales may be important to quantify the influence of waterfowl populations on limnological conditions in some situations. Furthermore, findings illustrated that trends and differences may be missed by studies that rely on single, point-in-time sample collection.

Shallow lakes and ponds of Wapusk National Park (WNP; northeastern Manitoba, Canada) offer an opportunity to examine the influence of changes in waterfowl populations on the hydrolimnological and biogeochemical conditions in a Subarctic setting (Figure 3.1, 3.2). WNP, located in the Hudson Bay Lowlands (HBL), contains abundant shallow lakes and ponds and is internationally renowned for its biodiversity and vital habitat for polar bears (*Ursus maritimus*) and migratory birds. Coastal regions of WNP have experienced a rapid increase in the Lesser Snow Goose (LSG; *Chen caerulescens caerulescens*) population. A geometric increase of 5-7% per year has occurred since the 1960s (Batt, 1997; Jefferies et al., 2006), which has disturbed the landscape and caused substantial changes in vegetation and habitat (Figure 3.2). For example, extensive grubbing by the LSG population in the soil to obtain roots and shoots of plants for nutrition has denuded vegetation in areas of coastal salt

marshes and increased salinity and humidity in the soils (Figure 3.2; e.g., Srivastava and Jefferies, 1996; Parks Canada, 2000; Handa et al., 2002; Jefferies and Rockwell, 2002). As the LSG have moved farther inland, grubbing for nutrition, removal of grasses for manufacture of nests and substantial deposits of feces have been observed. As the number of geese has grown, the spatial extent of the limit of their breeding grounds has also increased markedly, from $<5 \text{ km}^2$ in 1969 to $>300 \text{ km}^2$ as of 2008 (Figure 3.1). These increases have been attributed to a combination of agricultural food subsidies in their wintering grounds, creation of conservation refuges along migration flyways and warmer nesting locations, all of which increased energy allocated to reproduction and survival rates (Batt, 1997; Abraham et al., 2005b; Jefferies et al., 2006). At present, little is known about the consequences of the increased LSG population on the hydrolimnological and biogeochemical conditions of the coastal ponds of WNP. This information is required to predict the potential effects of further expansion of waterfowl populations in WNP and inform effective ecosystem stewardship decisions.

In this paper, we present a pilot study that characterizes the water chemistry and biogeochemical conditions of 16 shallow ponds located in the coastal fen ecotype within WNP and assesses influences of Lesser Snow Goose activities on carbon cycling and trophic status. Fifteen ponds that span the coastal fen ecotype and that currently have only low (if any) disturbance from the LSG population were sampled to provide insight into the range of hydrolimnological variability for ponds unaffected by the LSG population expansion. Results are compared with analyses from pond WAP 20, which receives heavy use by LSG - its catchment is strongly disturbed by their activities during the breeding season (late May to late August; Jefferies et al., 2003). Our intent was to expand on methods employed in

previous limnological studies of waterfowl disturbance. We used conventional water chemistry (e.g., nutrients, ions and alkalinity), water isotope (e.g., $\delta^{18}\text{O}$ and $\delta^2\text{H}$) and C isotope (e.g., $\delta^{13}\text{C}_{\text{DIC}}$ and $\delta^{13}\text{C}_{\text{POM}}$) measurements to compare seasonal changes and patterns of hydrological, limnological and biogeochemical conditions between the 15 low disturbance ponds and one highly-disturbed pond. From these data, we explore potential hydrological, limnological and biogeochemical effects of disturbance by the LSG population on a tundra pond in WNP. Data from the low disturbance ponds also provide baseline information for future studies assessing potential effects of LSG.

3.2 Study Area

Wapusk National Park

WNP was established in 1996 to protect a representative section of the northwestern HBL. WNP is underlain by continuous permafrost in northern sections and discontinuous permafrost in the far south end of the park. Vegetation spans the transition between Arctic tundra and boreal forest (Parks Canada, 2000). Wetlands cover approximately 80% of the surface area of the park, with fens and bogs located along the coast and polygonal peat plateaus located farther inland (Parks Canada, 2008). In this study, we focus on ponds located within the coastal fen of WNP because it is the ecotype selected by LSG for their breeding grounds (Figure 3.1). The coastal fen region comprises approximately 11% of the park (Parks Canada, 2000). Within this area, vegetation includes mainly sedges (*Carex aquatilis*) and rushes (*Scorpidium scorpioides* and *Scirpus caespitosus*), and terrestrial plant cover is sparse. During the past ~40 years, the LSG population has expanded dramatically throughout the coastal fen ecotype in population size, density and geographic distribution

(Figures 3.1, 3.2). The LSG population typically arrives in the HBL in late May and begins the southward migration at the end of August (Jefferies et al., 2003). Terrestrial areas with the highest disturbance show evidence of substantial grubbing activity and vegetation loss, and contain abundant deposits of feces. However, based on our field observations, the influence of LSG in the mapped areas of Figure 3.1 is patchy and substantial areas remain relatively undisturbed.

Study Sites

The original intent of this study was to characterize seasonal hydrolimnological and biogeochemical behaviour in coastal fen ponds. However, following conversations with wildlife ecologists at the Churchill Northern Studies Centre (CNSC) and assessment of our data and field observations, we recognized an opportunity to explore differences in hydrolimnological and biogeochemical conditions between a highly LSG-disturbed pond (WAP 20) in our dataset and 15 other low disturbance ponds (note that WAP 3, 10, 11 and 12 were removed from the data set because they desiccated during mid-summer of the sampling year (2010); Figure 3.1). These ponds are all small (average area = 0.29 km²) and shallow (<0.5 m), and were selected under the assumption that they are representative of ponds within the coastal fen ecotype. Based on observations made during our field campaigns, ponds WAP 1-19 had little to no visual evidence of disturbance by geese within their catchments even though several are located within the mapped area of the LSG breeding grounds (Figure 3.1). Catchments of these ponds contained few deposits of feces and only small, if any, amounts of grubbing (hereafter termed low-disturbance coastal fen ponds, or LDCF ponds). In contrast, LSG have substantially disturbed the catchment of pond WAP 20

by depositing high densities of feces, establishing nests with eggs along the pond shoreline, and removing the terrestrial vegetation by grubbing (Figure 3.2c, d). WAP 20 is located in the area that has been longest disturbed by the LSG (e.g., Batt, 1997; Iacobelli and Jefferies, 1991; Abraham et al., 2005ab, Jefferies et al., 2006; Figure 3.1).

Climate

Meteorological conditions monitored at the Churchill airport show marked seasonal variations in temperature and precipitation (Figure 3.3; Environment Canada, 2010). Based on 1971-2000 climate normals, average annual temperature is -6.9°C and average annual precipitation is 431.6 mm (rain = 264.4 mm, snow = 167.2 mm). During the sampling season of 2010, temperature was similar to climate normals in May, June and August but slightly elevated in July and September. Rainfall was lower in June but markedly higher in late August (Figure 3.3). Snow accumulation during the preceding winter (2009-2010) was considerably lower than the climate normal.

3.3 Methods

To characterize seasonal variations in hydrology, water chemistry and C dynamics of the study ponds, surface water samples were collected at approximately 10- to 15-cm depth from all ponds on June 8 (soon after ice-off), July 31 (mid-summer) and September 23 (before ice-on) of 2010. The sampling dates were selected to encompass the early-ice free season (snow and ice melt), mid-summer (growth season) and autumn periods.

Isotope Hydrology

Pond-water samples for analysis of water isotope composition were stored in tightly-sealed 30-ml high density polyethylene bottles until analysis following standard methods (Epstein and Mayeda, 1953; Morrison et al., 2001) at the University of Waterloo Environmental Isotope Laboratory (UW-EIL). Isotopic compositions are reported as $\delta^{18}\text{O}$ (‰) and $\delta^2\text{H}$ (‰) relative to the Vienna Standard Mean Ocean Water (VSMOW) standard. $\delta^{18}\text{O}$ and $\delta^2\text{H}$ results are normalized to -55‰ and -428‰, respectively, for Standard Light Antarctic Precipitation (Coplen, 1996). The analytical uncertainty was $\pm 0.2\%$ and $\pm 2.0\%$ for $\delta^{18}\text{O}$ and $\delta^2\text{H}$, respectively.

Water Chemistry

Surface water samples and limnological measurements were collected from all the ponds during the three field visits. *In situ* measurements for pH were also conducted at approximately 10- to 15-cm depth using a YSI 600QS multi-meter. Following collection, all water samples were stored at 4°C until analysis. Immediately following collection, the pond water was passed through a screen (80- μm mesh) to remove large particles that can affect estimates of concentrations in the pond water. For determination of DIC and DOC, water was filtered within 12 hours of collection (cellulose acetate filters: 0.45- μm pore size, 47-mm diameter) and stored in the dark at 4°C until analysis at Environment Canada's National Laboratory for Environmental Testing (Burlington, Ontario) following their standard methods (Environment Canada, 1994). Samples for determination of TP and TKN were acidified (held at 0.02% H_2SO_4) and analyzed at the Biogeochemistry Lab at the University of Waterloo (TKN = Bran Luebbe, Method No. G-189-097; TKP = Bran Luebbe, Method

No. G-188-097; Seal Analytical, Seattle, USA). Chlorophyll *a* concentrations were determined by filtering measured volumes of water onto Whatman® GF/F filters at the CNSC, and the filters were stored frozen and in the dark until chlorophyll *a* concentration was determined using standard fluorometric techniques (Parsons and Strickland, 1963; SCOR/UNESCO, 1966) at the Aquatic Ecology Group Analytical Laboratory at the University of Waterloo.

Carbon Isotope Analyses

Water samples were collected from all ponds during the three field visits in 2010 for the analysis of C isotope composition of DIC ($\delta^{13}\text{C}_{\text{DIC}}$) using 125 ml glass serum bottles, with rubber stoppers and syringe needles that were used to expel excess air. Samples were stored at 4°C until analysis. Samples for the C isotope analysis of suspended particulate organic matter ($\delta^{13}\text{C}_{\text{POM}}$) were collected using multiple horizontal tows with a phytoplankton net (mesh size = 25 μm). Upon return to the field base (CNSC), samples were passed through a 63- μm mesh net to remove zooplankton and other large particles, filtered onto pre-ashed Whatman® quartz filters (0.45- μm pore size) and dried at 60°C for 24 hours in a drying oven. Filters were then exposed to 12 N HCl fumes in an air-tight vessel for 4 hours to remove carbonates, following the methods of Lorrain et al. (2003). Water samples were analyzed for $\delta^{13}\text{C}_{\text{DIC}}$ and acidified filters were analyzed for $\delta^{13}\text{C}_{\text{POM}}$ at the UW-EIL. Stable C isotope ratios are reported as $\delta^{13}\text{C}$ (‰) relative to the Vienna-PeeDee Belemnite (VPDB) standard. The analytical uncertainty was $\pm 0.05\text{‰}$ and $\pm 0.01\text{‰}$ for $\delta^{13}\text{C}_{\text{DIC}}$ and $\delta^{13}\text{C}_{\text{POM}}$, respectively. The C isotope fractionation factor was estimated from the difference between $\delta^{13}\text{C}_{\text{DIC}}$ and $\delta^{13}\text{C}_{\text{POM}}$ (i.e., $\Delta^{13}\text{C}_{\text{DIC-POM}}$; Fry 2006). To supplement C isotope measurements,

dissolved CO₂ concentration and saturation values in the ponds were calculated based on methods outlined by Stumm and Morgan (1981) and Macrae et al. (2004), which determines the ratio of pond dissolved CO₂ concentration to equilibrium pond CO₂ concentration. A partial pressure of atmospheric CO₂ of 393 ppm was used for calculations (representative value for 2010 conditions; M. Macrae and R. Bourbonniere, unpublished data). Values of CO₂ saturation <1 indicate waters are under-saturated in dissolved CO₂, whereas values >1 indicate waters are over-saturated in dissolved CO₂.

Numerical and Statistical Analyses

Principal components analysis (PCA) was used to explore patterns of variation in limnological and biogeochemical conditions among ponds over the course of the ice-free season. Only ponds that had a complete data set for all three sampling episodes were included in the PCA (i.e., ponds WAP 1 and 2 were not included in the PCA due to loss of the July $\delta^{13}\text{C}_{\text{DIC}}$ sample). The median value for the sample scores of the LDCF ponds was added in the ordination plot to assess the typical pattern of seasonal change for the undisturbed ponds. The values for CO₂ saturation were added passively to the PCA to avoid over-representation, as it was calculated based on other variables included in the PCA. The PCA was performed using CANOCO version 4.5 software (ter Braak and Šmilauer, 2002).

To further compare limnological and biogeochemical conditions between the highly disturbed WAP 20 and the LDCF ponds (WAP 1-19), the distribution of values for the LDCF ponds were compared using boxplots with values from WAP 20 for the three sampling periods. One-sample t-tests were used to determine if the mean value of each variable in the LDCF ponds differs from the value obtained at WAP 20. These tests were performed for

each of the three sampling periods using SPSS version 20, and alpha was set at 0.05.

Interquartile ranges (IQR) were also calculated using SPSS version 20 in order to provide information on the variability of data. Spearman Rank correlations were used to assess trends over time for pH and DIC.

3.4 Results

Isotope Hydrology

During the ice-free season of 2010, seasonal variations in pond water balances did not differ substantially between WAP 20 and the LDCF ponds based on water isotope values (Figure 3.4). Pond water isotope composition at WAP 20 plots in similar $\delta^{18}\text{O}$ - $\delta^2\text{H}$ space as the median values for the LDCF ponds during each of the corresponding three sampling periods in 2010 (June $\delta^{18}\text{O}$: -10.1‰ and -10.4‰, $\delta^2\text{H}$: -87.6‰ and -82.7‰; July $\delta^{18}\text{O}$: -6.2‰ and -6.2‰, $\delta^2\text{H}$: -66.7‰ and -67.1‰; September $\delta^{18}\text{O}$: -12.6‰ and -11.1‰, $\delta^2\text{H}$: -94.5‰ and -89.2‰; WAP 20 and LDCF, respectively). Pond waters were more isotopically-depleted in the spring and fall, compared to summer values, and mostly plotted above the Local Evaporation Line (LEL), likely owing to the influence of rainfall. During the summer, waters became more isotopically-enriched in the LDCF ponds and WAP 20 and exceeded δ_{SSL} , the terminal basin steady-state value, indicating marked mid-summer evaporation and pond-level drawdown. Substantial evaporation was noted throughout the coastal fen ecotype between June and July, and four ponds within our original study set (WAP 3, 10, 11 and 12) desiccated during this time.

Multivariate Analysis: Limnology and Carbon Isotope Measurements

Multivariate ordination by PCA was used to assess similarities and differences in seasonal patterns of variation in limnological conditions and C isotope biogeochemistry between WAP 20 and the LDCF ponds (Figure 3.5). The first two PCA axes explained 59.9% of the total variation in the measured limnological variables and C biogeochemistry. Axis 1 explained 34.8% and separated sample scores mainly based on seasonal changes in C biogeochemistry ($\delta^{13}\text{C}_{\text{DIC}}$, DIC concentration), pH and alkalinity. Axis 2 captured 25.1% of the variation and separated samples mainly based on variations in concentrations of nutrients (TP, TKN) and chlorophyll *a*. For the LDCF ponds, sample scores in June generally clustered in the lower left quadrant, associated with relatively high pH, low concentrations of DIC, DOC and TKN, and low values of alkalinity, CO_2 saturation and $\delta^{13}\text{C}_{\text{DIC}}$. In June, limnological conditions of LDCF ponds differed markedly from those at WAP 20, based on clear separation of the sample score for WAP 20 from the median of the sample scores for the LDCF ponds. The sample score for WAP 20 was positioned centrally within the ordination plot, representing more moderate values of all the variables relative to the LDCF ponds. In July, even greater limnological differences occurred between WAP 20 and the LDCF ponds. At this time, WAP 20 possessed higher concentrations of nutrients (TP, TKN), chlorophyll *a* and $\delta^{13}\text{C}_{\text{POM}}$ than all but one of the LDCF ponds (WAP 8, which had high [13.9 $\mu\text{g L}^{-1}$] chlorophyll *a* values compared to other ponds). The highest amount of variability among LDCF ponds occurred in July, as illustrated by the wide dispersal of sample scores along PCA axes 1 and 2. By September, differences in the distribution of limnological and biogeochemical variables between WAP 20 and the LDCF ponds lessened considerably, as indicated by the relatively close positioning of sample scores for most of

ponds (including WAP 20) towards the lower right quadrant. Sample scores during this time were associated with lower nutrient concentrations, pH and $\delta^{13}\text{C}_{\text{POM}}$, and higher DIC concentrations, alkalinity, CO_2 saturation and $\delta^{13}\text{C}_{\text{DIC}}$ compared to July. Overall, the position of the sample scores identified that both differences and similarities existed in the seasonal progression of limnological and biogeochemical conditions between WAP 20 and the LDCF ponds.

Univariate Analyses: Water-chemistry Variables

Use of boxplots (Figure 3.6) and one-sample t-tests (Table 3.1) allowed more detailed assessment of the similarities and differences in the values and seasonal patterns of variation in water chemistry variables between WAP 20 and the LDCF ponds. Generally, the boxplots illustrate that concentrations of TKN, TP, DOC (except September) and chlorophyll *a* at WAP 20 were within the range of values at the LDCF ponds (Figure 3.6a-d). However, two interesting patterns were observed. First, concentrations of TKN and DOC at WAP 20 were near the upper range of the LDCF ponds, but chlorophyll *a* concentrations at WAP 20 were not elevated. In fact, chlorophyll *a* was near the lower range for the LDCF ponds in June and September of 2010. Second, WAP 20 and the LDCF ponds had different seasonal patterns of variation in TP concentration. Additional details are presented below.

In June, the range of TKN concentrations in the LDCF ponds was relatively small (IQR: 0.4 mg L^{-1}) and the median concentration (0.54 mg L^{-1}) was low (Figure 3.6a). At WAP 20, TKN concentration was 1.01 mg L^{-1} , which approached the 90th percentile of the LDCF ponds and differs significantly from the mean of the LDCF ponds (Table 3.1). Between June and July, TKN concentration increased (median = 1.32 mg L^{-1}) in the LDCF

ponds and variability rose as shown by a larger interquartile range (0.8 mg L^{-1}). TKN concentration also rose at WAP 20 (2.28 mg L^{-1}), to a value slightly above the 75th percentile of the LDCF ponds. By September, TKN concentrations declined, the IQR remained similar (0.9 mg L^{-1}) and the concentration at WAP 20 (0.69 mg L^{-1}) was close to the median of the LDCF ponds (0.64 mg L^{-1}).

Seasonal patterns of DOC concentration were similar to the patterns for TKN concentration for both WAP 20 and the LDCF ponds, with lower concentrations in June followed by increased values in July and declines between July and September (Figure 3.6b). However, mean DOC concentrations for the LDCF ponds were significantly lower than the values at WAP 20 for all three sampling periods (Table 3.1; Fig. 6b). In June, both WAP 20 (11.0 mg L^{-1}) and the LDCF ponds (median: 6.0 mg L^{-1}) had low concentrations compared to the rest of the season. Variability of DOC concentrations among the LDCF ponds was small in June (IQR: 4.7 mg L^{-1}), and the concentration at WAP 20 was close to the 90th percentile of the LDCF ponds. Increased concentrations were observed for both WAP 20 (21.6 mg L^{-1}) and the LDCF ponds (median 11.1 mg L^{-1}) in July. Also in July, a larger range of concentrations was observed for the LDCF ponds (IQR: 6.4 mg L^{-1}), and the DOC concentration at WAP 20 again approached the 90th percentile of the LDCF ponds. In September, DOC concentrations declined to values similar to those in June (13.6 mg L^{-1} and 9.8 mg L^{-1} ; WAP 20 and LDCF medians, respectively). Additionally, the LDCF ponds had a narrower range of DOC concentrations in September (IQR: 1.8 mg L^{-1}), and the concentration at WAP 20 was slightly above the maximum value of the LDCF ponds.

In contrast to TKN and DOC, water-column concentrations of chlorophyll *a* were not elevated in WAP 20 compared to the LDCF ponds throughout the ice-free season (Figure 3.6,

part c). In June and September, chlorophyll *a* concentrations were low in the LDCF ponds (median: 1.9 $\mu\text{g L}^{-1}$ and 1.6 $\mu\text{g L}^{-1}$, respectively) and spanned a relatively narrow range (June IQR: 1.8 $\mu\text{g L}^{-1}$; September IQR: 2.2 $\mu\text{g L}^{-1}$). At these times, chlorophyll *a* concentrations at WAP 20 (1.1 $\mu\text{g L}^{-1}$ and 0.7 $\mu\text{g L}^{-1}$, respectively) were near the 10th percentile and significantly lower than the mean of the LDCF ponds (Table 3.1). Maximum chlorophyll *a* values occurred in July for both WAP 20 and the LDCF ponds, and the value at WAP 20 was close to the median value for the LDCF ponds (3.2 $\mu\text{g L}^{-1}$ and 3.0 $\mu\text{g L}^{-1}$, respectively), while the IQR remained similar (2.2 $\mu\text{g L}^{-1}$).

For the LDCF ponds, relatively low TP concentrations in June (median: 4.0 $\mu\text{g L}^{-1}$; IQR: 9.0 $\mu\text{g L}^{-1}$) were followed by an increase in July (median: 12.0 $\mu\text{g L}^{-1}$), with a marked increase in range (from <0.5 $\mu\text{g L}^{-1}$ to 69.0 $\mu\text{g L}^{-1}$; IQR: 18.0 $\mu\text{g L}^{-1}$; Figure 3.6, part d). In September, TP concentrations declined in the LDCF ponds (median: <0.5 $\mu\text{g L}^{-1}$) and there was a much narrower range of values (IQR: 0.0 $\mu\text{g L}^{-1}$). In contrast, TP concentration decreased from June to July (13.0 $\mu\text{g L}^{-1}$ and 10.0 $\mu\text{g L}^{-1}$, respectively) at WAP 20, corresponding to a decline from the 75th percentile of the LDCF ponds in June to the 25th percentile in July, and then declined more substantially between July and September (to <0.5 $\mu\text{g L}^{-1}$, a value similar to the median of the LDCF ponds). Although, seasonal patterns in TP differed, one-sample t-tests only indicate a significant difference in June between the mean of the LDCF ponds and the value for WAP 20 (Table 3.1).

Univariate Analysis: Variables Related to Carbon Isotope Behaviour

In contrast to broadly similar patterns of seasonal variation in pond-water concentrations of TKN, DOC and chlorophyll *a*, seasonal behaviour of variables associated

with C biogeochemistry differed markedly between WAP 20 and the median of the LDCF ponds. For example, seasonal trajectories of change in DIC concentration differed between WAP 20 and the LDCF ponds (Figure 3.6e). Although values at WAP 20 were within the range of the LDCF ponds for all three sampling periods, WAP 20 was the only pond where DIC concentrations did not increase between June and July, as demonstrated by a strong rise of DIC between June and July for the LDCF ponds ($r_s(28)=0.697$, $p = 1.870 \times 10^{-5}$). In June, WAP 20 had a higher DIC concentration than the 90th percentile of the LDCF ponds (WAP 20: 20.1 mg L⁻¹ and LDCF median: 13.2 mg L⁻¹; IQR: 6.9 mg L⁻¹) and this value is significantly different from mean of the LDCF ponds (Table 3.1). In July, the median DIC concentration in the LDCF ponds increased by ~7.8 mg L⁻¹ (range 3.6-15.6mg L⁻¹; IQR: 8.4 mg L⁻¹), whereas the DIC concentration remained relatively constant (19.8 mg L⁻¹) at WAP 20 and fell within the 25th and 50th percentile of values for the LDCF ponds. Between July and September, both the range (IQR: 6.7 mg L⁻¹) of DIC concentrations and the median value (21.3 mg L⁻¹) remained similar at the LDCF ponds. In contrast, DIC concentration increased at WAP 20 between July and September, to 25.8 mg L⁻¹, a value near the 75th percentile of the LDCF ponds.

From June to July, pH declined in all the LDCF ponds that are supported by a significant negative trend ($r_s(45) = -0.805$, $p=2.671 \times 10^{-11}$), but in July, pH was significantly higher in WAP 20 compared to the mean for the LDCF ponds (Figure 3.6; part f; Table 3.1). In June, both WAP 20 and the LDCF ponds possessed similar pH values (9.2 and 9.1; WAP 20 and LDCF median, respectively). Between June and July, pH declined only slightly at WAP 20 (9.2 to 9.0, respectively), whereas median pH declined more strongly in the LDCF ponds (9.2 to 8.5). In the LDCF ponds, the range of pH values in July declined to below the

25th percentile of the values measured in June. In the LDCF ponds, pH continued to decline between July and September (median 8.2), with the 75th percentile value in September falling below the 25th percentile from July. At WAP 20, pH declined to 8.4 in September, which was slightly above the 75th percentile of the LDCF ponds. The variability of pH in the LDCF ponds was similar in June, July, and September (IQR: 0.2, 0.2, and 0.3, respectively).

Measurements of the C isotope composition of DIC revealed unique seasonal C behaviour in WAP 20 compared to the LDCF ponds (Figure 3.6, part g). In June, the $\delta^{13}\text{C}_{\text{DIC}}$ value at WAP 20 was similar to the median value for the LDCF ponds (-3.9‰ and -4.0‰, respectively). At this time, the LDCF ponds spanned a relatively broad range of $\delta^{13}\text{C}_{\text{DIC}}$ values, (-7.6‰ to -0.3‰; IQR: 3.0‰). In July and September, there was a large divergence in the seasonal pattern of change in $\delta^{13}\text{C}_{\text{DIC}}$ between WAP 20 and the LDCF ponds, and the mean for the LDCF ponds differed significantly from the value at WAP 20 (Table 3.1). Median $\delta^{13}\text{C}_{\text{DIC}}$ values of the LDCF ponds increased throughout the ice-free season (July: -3.2‰ and September: -2.5‰). All but three of the LDCF ponds showed this pattern. Those three LDCF ponds showed only small decreases between June and July (0.4 to 1.1‰). In contrast, the $\delta^{13}\text{C}_{\text{DIC}}$ of WAP 20 decreased sharply between June and July (to -7.3‰). The $\delta^{13}\text{C}_{\text{DIC}}$ increased between July and September (to -6.1‰) as was observed in the LDCF ponds. In July, the interquartile range of $\delta^{13}\text{C}_{\text{DIC}}$ values in the LDCF ponds was more narrow (IQR: 2.0‰), but the overall range was large due to occurrence of ponds with more extreme minimum (WAP 13: -6.8‰) and maximum (WAP 9: 0.1‰) values. Despite the large range, the July $\delta^{13}\text{C}_{\text{DIC}}$ value for WAP 20 fell below the minimum value for the LDCF ponds. And, $\delta^{13}\text{C}_{\text{DIC}}$ at WAP 20 remained below the range of the LDCF ponds in September (IQR: 2.6‰).

Seasonal patterns for $\delta^{13}\text{C}_{\text{POM}}$ were similar at WAP 20 and the LDCF ponds, but larger changes occurred between sampling episodes for WAP 20. (Figure 3.6, part h). In June, $\delta^{13}\text{C}_{\text{POM}}$ at WAP 20 fell within the range of LDCF ponds (-23.5‰ and -25.4‰, respectively). Between June and July, $\delta^{13}\text{C}_{\text{POM}}$ increased by 3.3‰ to -20.3‰ in WAP 20. In contrast, the median value of the LDCF ponds increased only slightly. Also, the range of values for the LDCF ponds was wider in July (IQR: 3.4‰) than in June (IQR: 2.4‰), and $\delta^{13}\text{C}_{\text{POM}}$ at WAP 20 was near the 90th percentile of the LDCF ponds. The mean for the LDCF ponds was significantly lower than the value at WAP 20 in July (Table 3.1). In September, $\delta^{13}\text{C}_{\text{POM}}$ decreased substantially (to -32.1‰) in WAP 20, whereas the decline was more muted at the LDCF ponds (median: -27.0‰). In September, the range of $\delta^{13}\text{C}_{\text{POM}}$ values declined in the LDCF ponds (IQR: 1.8‰), and $\delta^{13}\text{C}_{\text{POM}}$ at WAP 20 fell well below the minimum value of the LDCF ponds.

The patterns of seasonal change in C isotope fractionation ($\Delta^{13}\text{C}_{\text{DIC-POM}}$; Figure 3.6i) also differed markedly between WAP 20 and the LDCF ponds. C isotope fractionation did not change appreciably for most of the LDCF ponds during the 2010 sampling season, as evidenced by the large amount of overlap among interquartile ranges in June, July and September, and the comparable amount of variation (3.0‰, 4.6‰ and 3.3‰, respectively) and median values (21.8‰, 23.5‰ and 24.0‰, respectively). In contrast, $\Delta^{13}\text{C}_{\text{DIC-POM}}$ declined significantly in July at WAP 20 (June: 19.7‰, July: 13.0‰ and September: 25.9‰; Table 3.1) to well below the minimum value in July at the LDCF ponds.

In June, all ponds were under-saturated for CO_2 with little variability (CO_2 saturation = 0.2 and 0.1 for WAP 20 and median LDCF ponds, respectively; IQR: 0.1; Figure 3.6j). In July, all of the LDCF ponds had increased values for CO_2 saturation and the majority (9 out

of 15) were supersaturated in CO₂ (median value 1.3). The range of values also increased (0.5 at WAP 13 to 5.7 at WAP 2; IQR: 0.8). In contrast, WAP 20 remained under-saturated in CO₂ in July and its value was significantly different from the mean of the LDCF ponds (Table 3.1) with a CO₂ saturation value (0.3) similar to that measured in June. In September, the majority (11 out of 15) of the LDCF ponds were supersaturated in CO₂ (median value 1.4; IQR: 1.4) and CO₂ saturation in WAP 20 increased to a value similar to the LDCF ponds (1.3).

3.5 Discussion

During the past ~40 years, WNP has witnessed a rapid increase in the LSG population and an expansion of the geographic region they inhabit within the coastal fen ecotype (Figure 3.1, 3.2). Their activities have disturbed vegetation and soils (e.g., Srivastava and Jefferies, 1996; Jefferies et al., 2004; Abraham et al., 2005ab; Jefferies et al., 2006). Knowledge of their effects on coastal ponds within WNP is lacking but important for determining the consequences of this changing wildlife population. Previous limnological studies of waterfowl disturbance in Arctic freshwater ecosystems have relied mainly on single, point-in-time or ‘snapshot’ sampling, or paleolimnological records to characterize their effects on the concentration of major nutrients and phytoplankton biomass (e.g., P, N, chlorophyll *a*; Mallory et al., 2006; Keatley et al., 2009; 2011; Côte et al., 2010; Sun et al., 2013). To date, few, if any, studies have employed multiple sampling over seasonal timescales or C isotope measurements. As we discuss below, C isotope measurements were in fact more informative than standard limnological measurements, because they effectively capture marked differences in C behaviour in the pond affected by LSG activities compared to those with

little to no LSG activity. We also demonstrate that it is important to track seasonal changes in pond hydrology, nutrient concentrations and C isotope behaviour in order to disentangle effects of LSG activity from those caused by seasonally fluctuating meteorological and hydrological changes, because LSG activity exerted the strongest influence on limnological and biogeochemical conditions in mid-summer whereas hydroclimatic controls were more prevalent during June (due to snowmelt) and September (due to late summer rain). Notably, concentrations of major nutrients (TKN, TP, DOC) at WAP 20, the pond with extensive LSG activity, were not outside the range of values measured at the LDCF ponds during the ice-free season of 2010 (except for DOC in September). Instead, LSG activities affected most strongly patterns of change in C cycling, pH and TP concentrations between early-June and late-July, when biological activity increased between ice-off and mid-summer. Thus, a key recommendation is that detection of differences between ponds with and without extensive LSG activity requires a sampling regime that captures temporal variations of both limnological and biogeochemical conditions over the course of the ice-free season.

Carbon Isotope Dynamics

At the 15 ponds with little to no LSG activity, $\delta^{13}\text{C}_{\text{DIC}}$ values increased over the course of the ice-free season (Figure 3.6, part g). As summer progressed, aquatic primary productivity increased, which caused an increase in the $\delta^{13}\text{C}_{\text{DIC}}$ due to preferential use of ^{12}C by algae during photosynthesis (e.g., Quay et al., 1986; Keeley and Sandquist, 1992; Wachinew and Rozanski, 1997). Thus, the increase in $\delta^{13}\text{C}_{\text{DIC}}$ values that occurred between June and July in the LDCF ponds likely reflects an increase in primary productivity under conditions where C supply exceeded C demand. This is supported by the increase in DIC

concentrations that occurred between June and July in the LDCF ponds, which indicate ample supply of DIC to meet demands by photosynthesis. And, it is consistent with the modest rise in phytoplankton biomass in the ponds between June and July, as estimated by pond-water chlorophyll *a* concentration. The source of the DIC to the ponds is not clear, but likely came from decomposition in the pond sediments, which would have been warmer in July compared to June. The import of DIC from the catchment is unlikely as the ponds were drying and no surface inflow was observed at that time. Additionally, C isotope fractionation values were consistently around -20‰ throughout the ice-free season in the LDCF ponds, which are expected when there is sufficient dissolved CO₂ to support aquatic photosynthesis (e.g., Rau, 1978; Herczeg and Fairbanks, 1987; Bade et al., 2004).

In sharp contrast to the rise in $\delta^{13}\text{C}_{\text{DIC}}$ values in the LDCF ponds between June and July, driven by seasonally increasing aquatic productivity under conditions of adequate C supply, $\delta^{13}\text{C}_{\text{DIC}}$ declined sharply between June and July at WAP 20 (Figure 3.6, part g). This feature suggests substantially different behaviour of dissolved C cycling at the pond affected by marked LSG activity. Such deviation from the characteristic seasonal pattern of ¹³C-enrichment of DIC under conditions of increasing productivity can occur in certain situations. For example, elevated supply of soil-derived isotopically-depleted DIC from the catchment can lower $\delta^{13}\text{C}_{\text{DIC}}$ values (Wachinew and Rozanski, 1997). Also, increased net respiration of particulate organic carbon can result in increased DIC concentrations, decreased pH and consequently a decline in $\delta^{13}\text{C}_{\text{DIC}}$ (Quay et al., 1986; Wachinew and Rozanski, 1997). However, elevated supply of soil-derived isotopically-depleted DIC was unlikely at WAP 20, because as stated above, the ponds were drying and no surface inflow was observed at that time. We note that approximately 90% of rainfall in July occurred prior

to July 11 and is unlikely to account for the decline in $\delta^{13}\text{C}_{\text{DIC}}$ as this probably would have influenced all of the ponds. Additionally, because pond water levels were lower in July, they were likely not receiving substantial input from permafrost thaw. Indeed, four of our twenty study ponds desiccated in July. Increased net respiration is also an unlikely explanation as this would result in a corresponding increase in DIC concentration, which was not observed in this pond (Figure 3.6e).

We propose an alternative mechanism to explain the sharp decline in $\delta^{13}\text{C}_{\text{DIC}}$ values between June and July at WAP 20. Under conditions of high algal production, high C demand and high pH, previous studies have identified that strong kinetic C isotope fractionation can occur during CO_2 invasion from the atmosphere, which causes a decline in $\delta^{13}\text{C}_{\text{DIC}}$ (Herczeg and Fairbanks, 1987; Takahashi et al., 1990; Bade et al., 2004). Under these conditions, C isotope fractionation will decline substantially from $\sim 20\text{‰}$ (Rau, 1978; Herczeg and Fairbanks, 1987), as was observed in WAP 20 (13.0‰ ; Figure 3.6, part i). This process, previously termed ‘chemically-enhanced CO_2 invasion’, was initially described by Herczeg and Fairbanks (1987) in their isotope study of Mohonk Lake during a cyanobacterial bloom. This phenomenon has also been observed in other highly productive temperate lakes and ponds (e.g., Emerson, 1975; Takahashi et al., 1990, Bade et al., 2004) and represents a plausible explanation for the $\delta^{13}\text{C}_{\text{DIC}}$ decline that occurred between June and July at WAP 20. We propose that increased photosynthesis due to the LSG activity generated substantial C demand that exceeded dissolved CO_2 availability, which subsequently led to strong kinetic C isotope fractionation during CO_2 invasion. The increased C uptake is likely a consequence of high photosynthetic demand by benthic algae (not measured in our study) rather than phytoplankton, because phytoplankton biomass (as chlorophyll *a* concentration) was similar

in ponds with and without the waterfowl activity and increased only modestly between June and July (see also next section for further details). Also, macrophytes are extremely sparse in WAP 20, and cannot account for the C-demand. This description of C behaviour implies that WAP 20 was a net C sink during mid-summer, which is further supported by low values of CO₂ saturation in July indicative of CO₂ under-saturation (Figure 3.6, part j). In contrast, the majority (9 out of 15) of the LDCF ponds (and their median value) were super-saturated with CO₂ at this time and all of the LDCF ponds had CO₂ saturation values higher than WAP 20. The super-saturated CO₂ values in the LDCF ponds may be a consequence of less intense algal productivity, sediment degassing or higher rates of respiration than in WAP 20. We attribute the rise in $\delta^{13}\text{C}_{\text{DIC}}$ in September at WAP 20 (Figure 3.6, part g) to the reduction in the intensity of this process due to lower C demand as temperatures cooled, which is consistent with the increase in C isotope fractionation (Figure 3.6, part i). High amounts of rainfall and subsequent runoff of comparably isotopically-enriched DIC derived from carbonate dissolution may have also contributed to the rise in $\delta^{13}\text{C}_{\text{DIC}}$ in September at WAP 20 and the LDCF ponds.

Further support for the interpretation of C isotope dynamics from the $\delta^{13}\text{C}_{\text{DIC}}$ patterns is evident in the values of $\delta^{13}\text{C}_{\text{POM}}$ and their seasonal trends (Figure 3.6h). Both WAP 20 and the LDCF ponds depicted similar seasonal patterns of $\delta^{13}\text{C}_{\text{POM}}$, with increases between June and July, and declines between July and September. This pattern, however, was more striking at WAP 20, with both a larger increase between June and July and larger decline between July and September compared to the LDCF ponds. The C isotope composition of particulate organic matter is dependent on the concentration of dissolved CO₂, the degree of productivity within a pond and the source of C (O'Leary, 1981; Allen and Spence, 1981; Keeley and

Sandquist, 1992). In June, $\delta^{13}\text{C}_{\text{POM}}$ values were approximately -25‰ in both WAP 20 and the LDCF ponds, which are typically observed when there is high availability of dissolved CO_2 allowing ample isotopic fractionation to occur during photosynthesis (Keeley and Sanquist, 1992). By July, a large increase in $\delta^{13}\text{C}_{\text{POM}}$ occurred at WAP 20, whereas this value increased only slightly at the LDCF ponds. The larger increase in $\delta^{13}\text{C}_{\text{POM}}$ at WAP 20 can be attributed to higher C demand as evidenced by reduced C isotope fractionation (Figure 3.6i). In contrast, ample supply of dissolved CO_2 at the LDCF ponds resulted in only slight increases in $\delta^{13}\text{C}_{\text{POM}}$. Alternatively, the increase in $\delta^{13}\text{C}_{\text{POM}}$ at WAP 20 between June and July may be due to bicarbonate uptake. Under conditions of low concentrations of DIC and high pH, as was the case for WAP 20, algae may switch from using dissolved CO_2 as their main form of C to bicarbonate (Deuser et al., 1968; Emrich et al., 1970; Allen and Spence, 1981). Bicarbonate is isotopically heavier in C, which would lead to ^{13}C -enrichment of POM. By September, $\delta^{13}\text{C}_{\text{POM}}$ values decreased in WAP 20 likely due to lower C demand, increased inputs of DIC due to large precipitation events, and/or a switch back to uptake of dissolved CO_2 to support photosynthesis.

Pond Hydrology and Nutrient Dynamics

In contrast to the striking differences in the seasonal behaviour of the C isotope composition of dissolved inorganic and particulate organic fractions between the LSG-disturbed pond WAP 20 and LDCF ponds unaffected by LSG population expansion, seasonal patterns of variation in basin hydrology (assessed using $\delta^{18}\text{O}$, $\delta^2\text{H}$) and concentrations of major nutrients (except TP) and phytoplankton biomass (as chlorophyll *a*) were broadly comparable at all ponds. This finding suggests that the changes in basin hydrology are

strongly regulated by a common external driver such as seasonal variations in meteorological conditions, rather than differences in the amount of disturbance by LSG populations. In northern landscapes, intense seasonality of meteorological conditions can exert strong influence on hydrology of tundra ponds, and affect seasonal patterns of change in nutrients and aquatic productivity (Sheath, 1986; Lougheed et al., 2011; White et al., 2014). For example in the HBL, snowmelt in spring increases connectivity of ponds with the surrounding catchment and higher hydrologic inflow increases the transfer of allochthonous materials to ponds (e.g., Macrae et al., 2004; Wolfe et al., 2011; White et al., 2014). As the ice-free season progresses, these allochthonous inputs supplied in spring may lead to higher nutrient concentrations and productivity during summer. Indeed, Macrae (1998) observed that snowmelt runoff supplied nutrients to ponds. Then, hydrologic connectivity may decline as a result of drier conditions that increase evaporation and reduce overland flow (Macrae, 1998; Macrae et al., 2004), which can lead to lake-level drawdown and raise nutrient concentrations and productivity in ponds of the HBL (Macrae et al., 2004; White et al., 2014). Conversely, intense episodes of rain in late summer may result in subsequent dilution of nutrients and ions (Figure 3.3; White et al., 2014). Such seasonal shifts in meteorological conditions appear to have exerted strong influence on pond water balance, nutrient concentrations and phytoplankton biomass in all of the study ponds. For example, increasing pond-water isotope values between June and July indicate strong influence of evaporation (Figure 3.4). These changes were concomitant with increases in concentrations of TKN, DOC and chlorophyll *a* in the water column of all the study ponds (Figure 3.6 a-c), likely due to evaporative concentration and phytoplankton growth. Increases in these variables can also be due to increased allochthonous inputs that occurred in the spring, but there was a low

amount of winter snowfall observed (Figure 3.3). Individual catchment characteristics may result in these processes differing among ponds (Wolfe et al., 2011), and, thus, may account for the wide range of values observed for concentrations of nutrients, DOC and chlorophyll *a* during July in the LDCF ponds. After mid-July, the ponds experienced a decrease in water isotope compositions due to a period of heavy rainfall in August (>double the climate normal; Figure 3.3, 4) and, correspondingly, concentrations of nutrients and chlorophyll *a* were diluted in all ponds (Figure 3.6). Similar seasonal changes in nutrient concentrations in response to hydroclimatic conditions have also been reported for other shallow ponds in the Churchill area (Macrae et al., 2004; White et al., 2014).

In contrast to TKN, DOC and chlorophyll *a*, seasonal variation of TP concentration differed between WAP 20 and the LDCF ponds (Figure 3.6, part d). TP concentrations rose between June and July at the LDCF ponds, but declined at WAP 20 despite modest increase in water-column chlorophyll *a* concentration. A rise in chlorophyll *a* concentration in the water column is typically associated with a coincident increase in TP concentration, because phosphorus is contained within the phytoplankton (Wetzel, 2001). Consequently, the decline in TP concentration at WAP 20 between June and July, when values increased in the LDCF ponds, suggests P demand became greater at WAP 20. As described above, evidence from C isotope measurements and pond-water pH indicates that the substantially greater C demand at WAP 20 in July was likely driven by higher rates of photosynthesis than occurred at the LDCF ponds. The inferred increase in P demand also is likely associated with the elevated rates of photosynthesis that produced the C demand. However, phytoplankton productivity does not appear to explain the greater demand for C and P at WAP 20, because concentrations of chlorophyll *a* in the water column were comparable at WAP 20 and the

LCDF ponds throughout the ice-free season. Instead, we suggest that stimulation of photosynthesis by benthic algae at WAP 20 is a main cause of the increased C and P demand. WAP 20 is very shallow (<0.5m), has sparse macrophytes, and so the luxuriant benthic mat along the pond bottom has potential to contribute a large fraction of the pond's total primary production. We note that lower-than-expected phytoplankton chlorophyll *a* concentrations have been found in other Arctic lakes and ponds and attributed to benthic productivity (e.g., Van Geest et al., 2007; Côté et al., 2010). Moreover, a recent nutrient-enrichment experiment that used microcosms containing water from a nearby coastal fen pond, with and without surficial pond sediments and associated benthic algal mat, demonstrated that these ponds rapidly assimilate additions of dissolved inorganic N (nitrate, ammonia) and P (phosphate) when surficial sediments and associated benthic biofilm are present (Eichel et al., 2014). Phosphate was taken up more rapidly from the water than inorganic N, and benthic algal biomass (as chlorophyll *a* concentration) became elevated when inorganic N and P were co-added to the microcosms, but not when N was added alone. Collectively, results of our study and the experiment by Eichel et al. (2014) suggest that nutrients supplied by waterfowl disturbances (feces, soil erosion) are rapidly taken up by benthic algae, which leads to increased demand for C and P. Measurements of benthic chlorophyll *a* and field-intensive nutrient studies would be needed to test this hypothesis. Stimulation of zooplankton grazing is another process that may explain the low chlorophyll *a* concentrations. In temperate locations, persistent N-limitation as a consequence of waterfowl disturbance has often been reported and has been attributed to the low N:P ratio of bird feces (Manny et al., 1994; Post et al., 1998; Olson et al., 2005). However, in our study the comparable seasonal changes in TKN concentration between WAP 20 and the LCDF ponds suggest that demand for N is

lower than demand for P. Other studies have also found significant alteration of phosphorus dynamics by waterfowl activities in both Arctic (e.g., Keatley et al., 2009; Côté et al., 2010) and temperate locations (e.g., Manny et al., 1994; Post et al., 1998). Consequently, seasonal measurements of TP concentration appear to provide a more effective measure of the effects of the LSG disturbance on coastal fen ponds compared to measurements of TKN or chlorophyll *a* concentrations. However, based on our case study, C-isotope measurements appear to provide the clearest distinction between WAP 20 and the LDCF ponds.

3.6 Concluding Remarks

During the past ~40 years, coastal regions of WNP have witnessed exponential increases in the LSG population and the geographic range of their nesting area. Concerns have been mounting regarding their effects on the abundant shallow ponds (Parks Canada, 2000). We used hydrolimnological and C isotope measurements, as well as seasonal sampling, to evaluate the influence of LSG population on a disturbed pond. We showed that when comparing nutrient concentrations between the highly LSG-disturbed pond WAP 20 and the 15 LDCF ponds, hydrolimnological measurements can identify only small differences which are difficult to attribute conclusively to activities of LSG. In contrast, C isotope measurements reveal distinctive C dynamics over the course of the ice-free season in WAP 20 compared to the LDCF ponds. Our data suggest that increased nutrient supply from the LSG activities at WAP 20 resulted in a shift in C dynamics compared to the LDCF ponds. We propose that ‘chemically-enhanced CO₂ invasion’ occurred at WAP 20 when elevated nutrient supply was quickly assimilated and this stimulated intense mid-summer C demand by benthic algae in the presence of high pH. Consequently, WAP 20 remained as a net sink

of C during mid-summer. In contrast, at the ponds with little to no LSG activity, CO₂ saturation values increased and the majority became net sources of CO₂ to the atmosphere by mid-summer. Knowledge of patterns of seasonal change in this study was important to determine how LSG populations may alter pond ecosystems.

Further studies are required to test whether the unique C behaviour at WAP 20 is evident in other LSG-affected ponds and the persistence of these patterns over multiple years under varying hydroclimatic conditions. Disentangling the roles of hydroclimatic variability and waterfowl disturbance is challenging and future studies should employ methods that include both seasonal sampling and measurements of C isotope composition of both dissolved inorganic and particulate organic fractions. Conventional limnological measurements of nutrient concentrations on a single visit may not capture waterfowl disturbance because of the potential for rapid uptake by the benthic mat. Ongoing contemporary and paleolimnological research throughout WNP aims to further identify linkages among hydrological, limnological and biogeochemical (C isotopic geochemistry and greenhouse gas fluxes) conditions and provide information on the expected trajectories of this dynamic landscape in the context of continued changes in climatic conditions and wildlife populations.

3.7 Acknowledgements

Funding for this study was provided by the Natural Sciences and Engineering Research Council of Canada (Northern Research Chair and Discovery Grants), the Polar Continental Shelf Program, the Northern Scientific Training Program, Parks Canada and the Churchill Northern Studies Centre (Northern Research Fund). We appreciate conversations

with J. Roth that motivated the study. We thank the Churchill Northern Studies Centre, Hudson Bay Helicopters, J. Larkin, E. Light and J. White for assistance with field work, and constructive comments by the reviewers and editors that improved the paper.

3.8 Figures

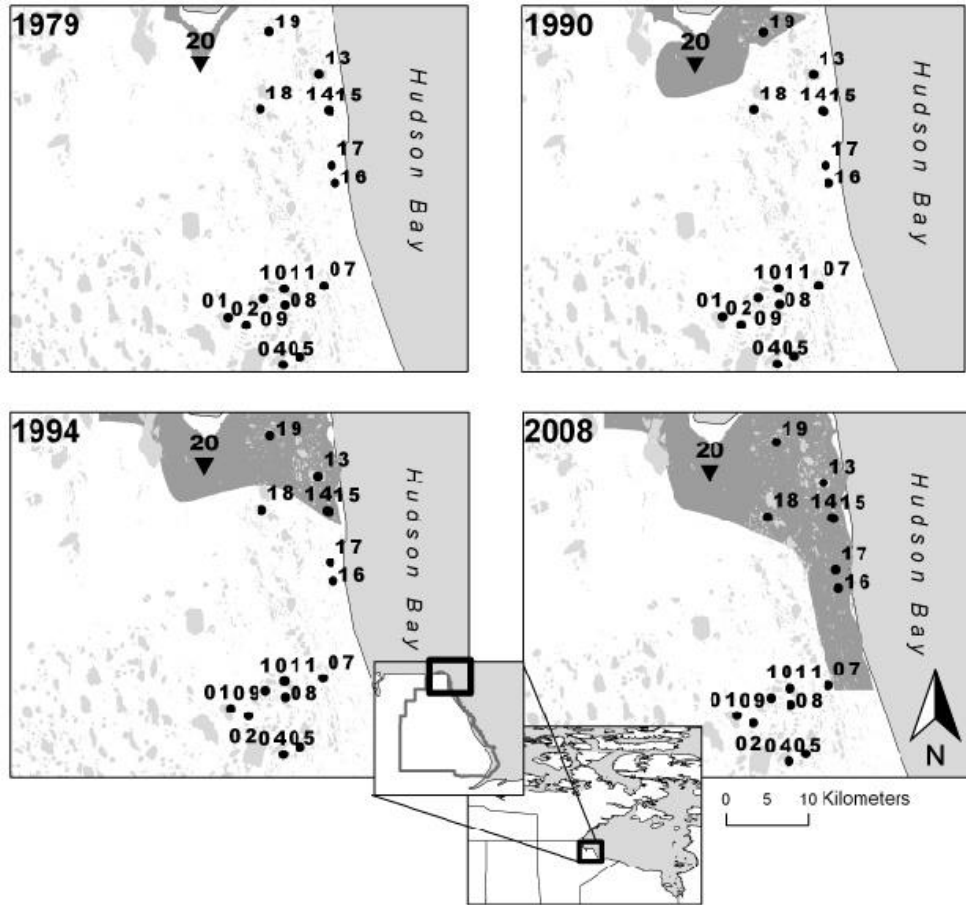


Figure 3.1: Location of Wapusk National Park (Manitoba, Canada) and the distribution of the 16 ponds sampled for this study. Sampled pond ‘20’ (referred to as WAP 20 in the text, 58.6700° N, 93.4437° W) is situated in an area of high disturbance by lesser snow geese (LSG). Gray regions in the four panels on the map depict the geographic limits of the LSG population distribution (data provided by Parks Canada, 2010).

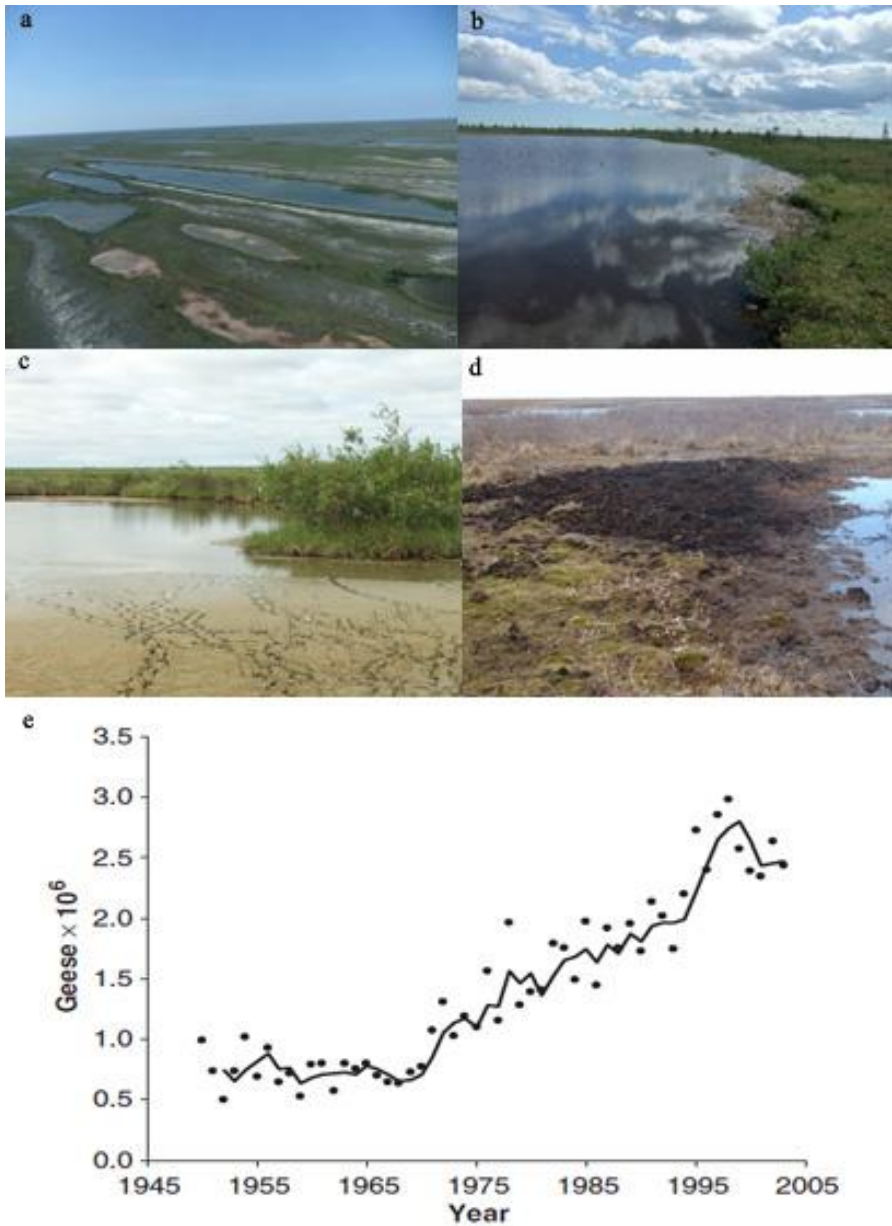


Figure 3.2: Top photographs depict ponds from the coastal fen ecotype of Wapusk National Park with low disturbance from the Lesser Snow Goose population (panels a and b). Bottom photographs are from pond WAP 20 (panels c and d), which has evidence of high disturbance from the LSG population. Graph in panel (e) was taken from data available in Abraham et al. (2005b) on the Mid-Winter Index of Lesser Snow Geese and Ross's geese from 1950-2003. The solid line is a 3-year running average.

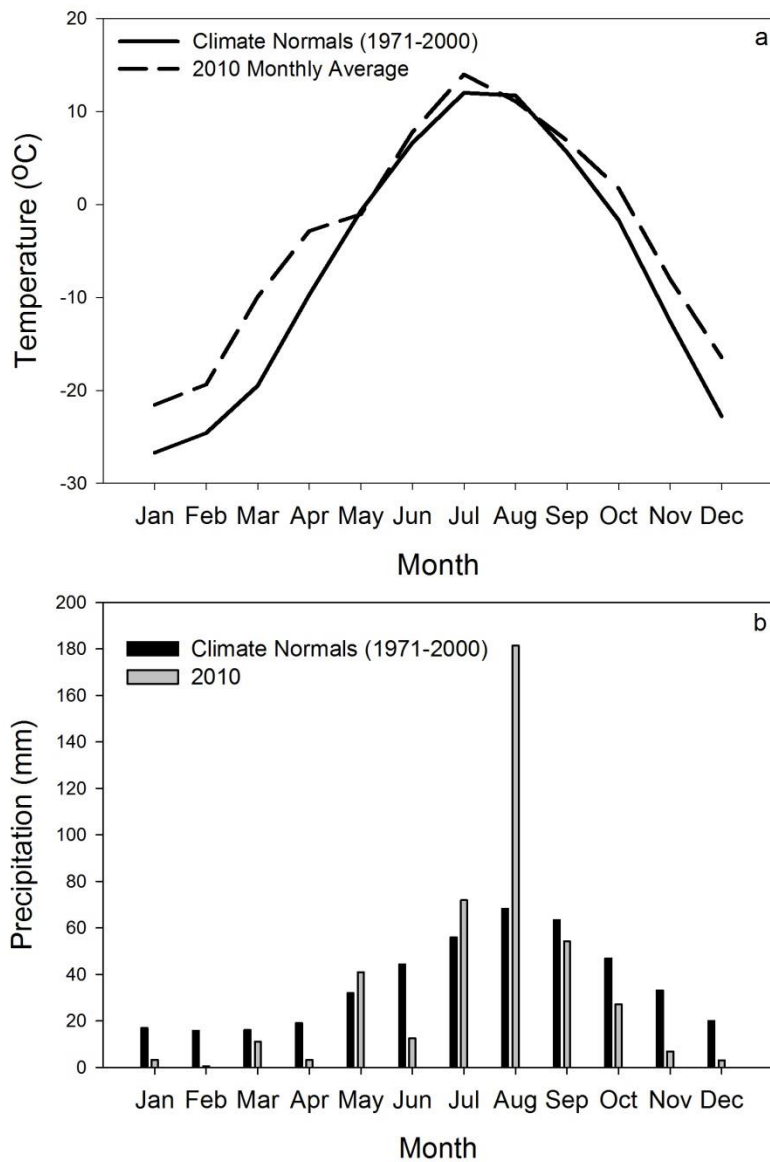


Figure 3.3: Comparison of average monthly (a) temperature and (b) precipitation at Churchill, Manitoba (1971-2000) (Environment Canada, 2010).

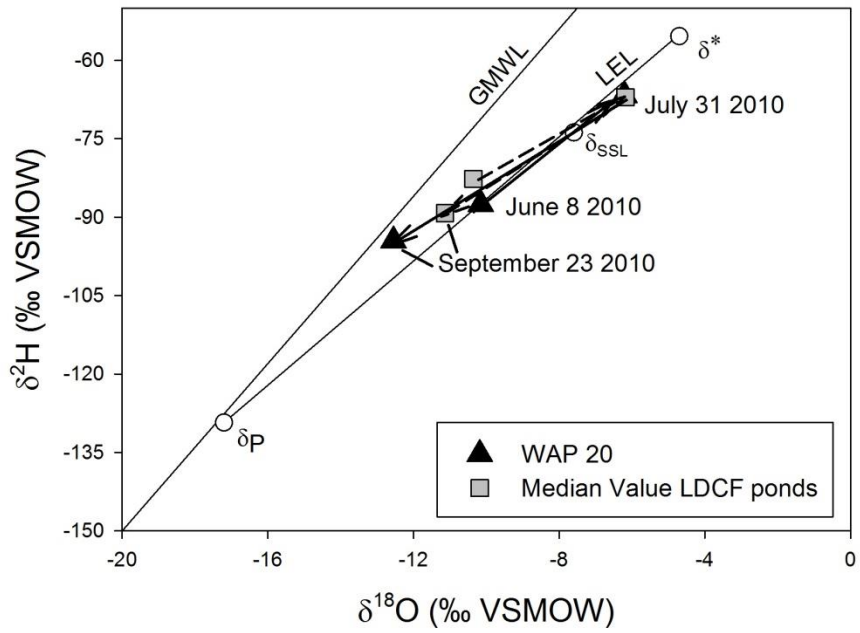


Figure 3.4: $\delta^{18}\text{O}$ - $\delta^2\text{H}$ graph showing the seasonal trajectory of median water isotope compositions for the LDCF ponds (grey squares, dashed line) and WAP 20 (black triangles, solid line) with respect to the Global Meteoric Water Line (GMWL; Craig, 1961) and the Local Evaporation Line for the Churchill region as reported in Wolfe et al. (2011).

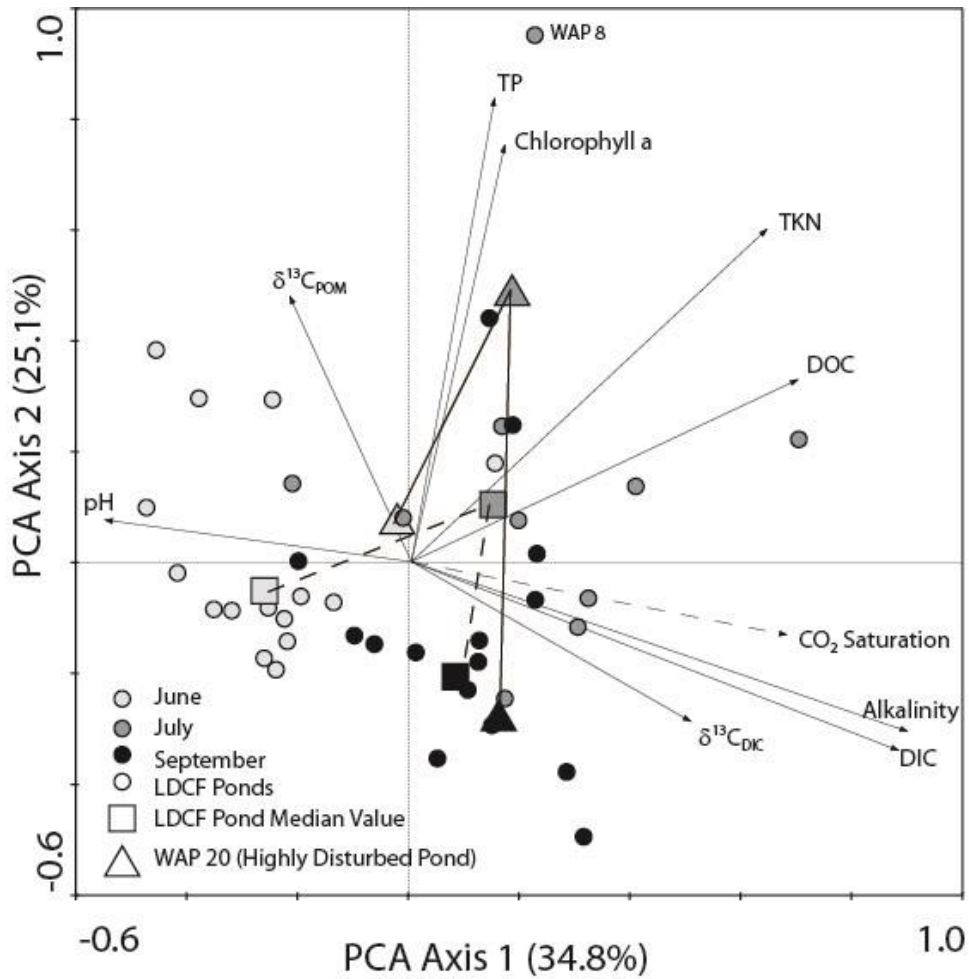


Figure 3.5: Principal components analysis (PCA) ordination biplot to compare limnological and biogeochemical conditions in WAP 20 (triangles) and the LDCF ponds (small circles) from the three sample periods in 2010. Vectors with solid lines represent active variables in the PCA, whereas vectors with dashed lines represent variables added passively. Lines connect sample scores for WAP 20 (triangles and solid line) and the median for the 15 LDCF ponds (squares, dashed lined) to assess seasonal patterns of change in the limnological variables with and without extensive Lesser Snow Goose activity, respectively.

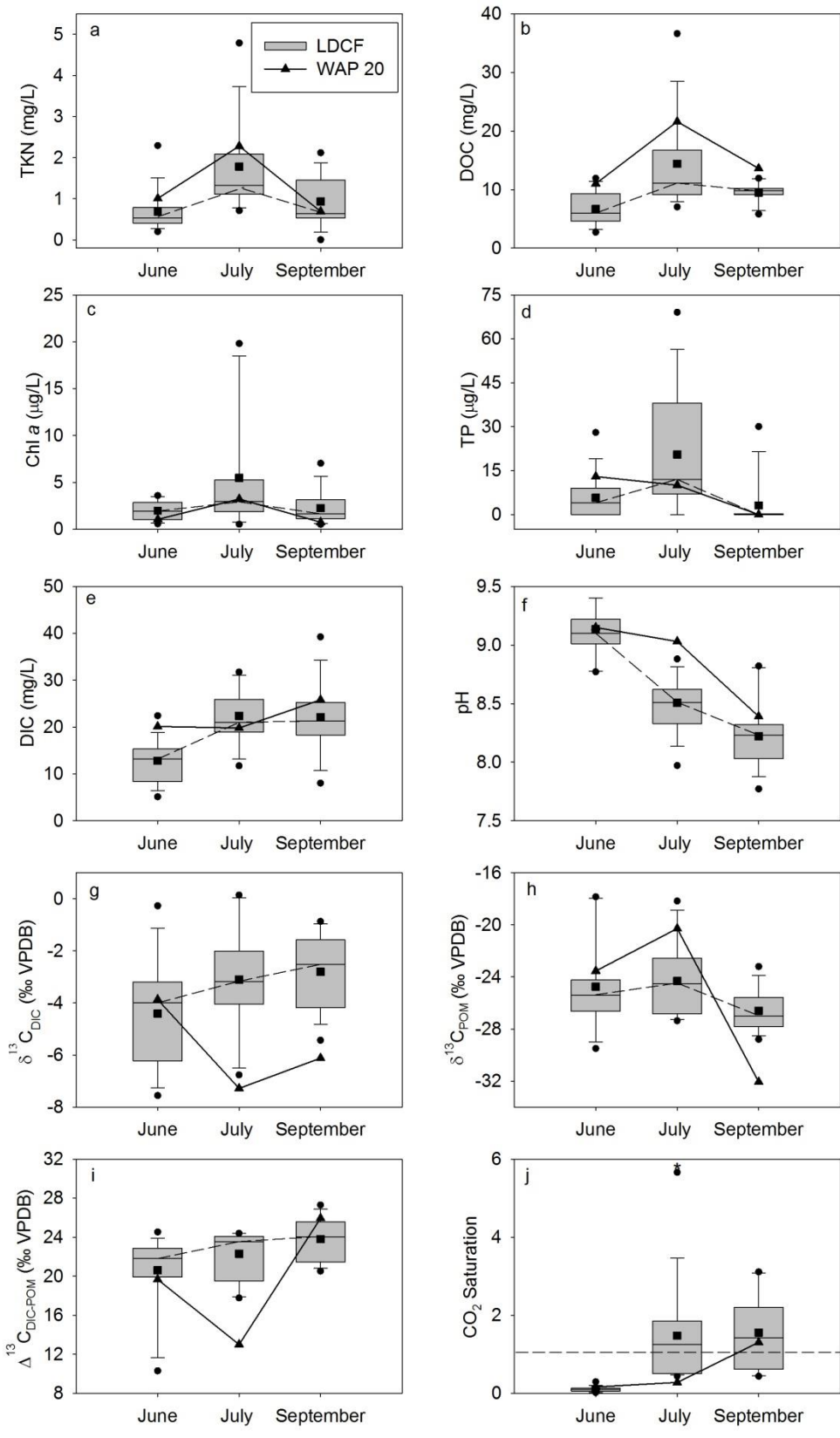


Figure 3.6: Boxplots depicting seasonal changes in (a) TKN concentration, (b) DOC concentration, (c) Chlorophyll *a* concentration, (d) TP concentration, (e) DIC concentration, (f) pH, (g) $\delta^{13}\text{C}_{\text{DIC}}$, (h) $\delta^{13}\text{C}_{\text{POM}}$, (i) $\Delta^{13}\text{C}_{\text{DIC-POM}}$ and (j) CO_2 saturation. The boxes identify the 25th percentile, median value and 75th percentiles for the low disturbance coastal fen (LDCF) ponds. The whisker bars represent the 10th and 90th percentile, the solid black circles represent the maximum and minimum values observed for the LDCF ponds, and asterisks represent outliers. Black squares represent the mean seasonal value for the LDCF ponds. Black triangles joined by the solid line represent the values for WAP 20.

3.9 Tables

Table 3.1: Results of one-sample t-tests which compare the mean value of water chemistry variables from the LDCF ponds with the value obtained at WAP 20. Comparisons are presented for all three sampling episodes (June, July, September).

	June		July		September	
	t-statistic	P value	t-statistic	P value	t-statistic	P value
TKN (mg L ⁻¹)	-2.551	0.023	-1.810	0.092	1.658	0.121
DOC (mg L ⁻¹)	-5.938	3.621x10 ⁻⁵	-3.621	0.003	-9.317	2.228x10 ⁻⁷
Chl <i>a</i> (µg L ⁻¹)	3.513	0.003	1.406	0.181	3.429	0.004
TP (µg L ⁻¹)	-3.797	0.002	2.001	0.065	1.389	0.188
DIC (mg L ⁻¹)	-6.483	1.443x10 ⁻⁵	1.702	0.111	-1.909	0.077
pH	-1.849	0.086	-9.041	3.208x10 ⁻⁷	-1.707	0.11
δ ¹³ C _{DIC} (‰VPDB)	-0.885	0.391	6.979	6.471x10 ⁻⁵	9.055	3.148x10 ⁻⁷
δ ¹³ C _{POM} (‰VPDB)	-1.669	0.117	-4.954	3.343x10 ⁻⁴	13.305	-2.458x10 ⁻⁹
Δ ¹³ C _{DIC-POM} (‰VPDB)	0.899	0.384	12.016	7.614x10 ⁻⁷	-3.908	0.002
CO ₂ Saturation	-3.310	0.05	3.590	0.003	1.108	0.286

Chapter 4: Limnological regime shifts caused by climate warming and Lesser Snow Goose population expansion in the western Hudson Bay Lowlands (Manitoba, Canada)

4.1 Introduction

Shallow lakes and ponds are abundant in Subarctic and Arctic regions and provide important habitat and resources for a variety of wildlife and human populations. Due to their small water volumes and high surface area to volume ratios, they are particularly responsive to multiple environmental stressors, which may lead to limnological regime shifts or rapid transition to a new suite of limnological conditions. Climate warming and changes in avian populations have the potential to influence catchment vegetation, nutrient supply, aquatic productivity and habitat (e.g., Van Geesr et al., 2007; Côté et al., 2010; MacDonald et al., 2014; Luoto et al., 2014). For example, warming has caused reorganization of diatom communities in Arctic lakes by promoting a shift in dominance from benthic species to epiphytic or planktonic species as recorded in sediment cores (e.g., Douglas et al., 1994; Sorvari et al., 2002; Rühland et al., 2003, 2013, 2014; Smol et al., 2005). The influence of avian populations has also been identified as a driver of regime shifts in Subarctic and Arctic lakes and ponds (e.g., Luoto et al., 2014), and they have long been recognized to cause disturbance in other habitats (e.g., terrestrial landscapes, salt marshes; Jefferies et al., 2006; Kotanen and Abraham, 2013). Notably, in Subarctic and Arctic regions experiencing the dual effects of climate warming and changes in avian populations, few studies have comprehensively examined and discriminated limnological responses to these stressors, yet this knowledge is required to assess the status of aquatic resources and to anticipate how they may evolve in the future.

Wapusk National Park (WNP; Manitoba, Canada; Figure 4.1), western Hudson Bay Lowlands, offers opportunity to examine potential limnological regime shifts in response to

changes in climate and avian populations in a Subarctic setting. Shallow lakes and ponds cover ~25 to 40% of the surface area, which provide important habitat for wildlife (Parks Canada, 2008). The climate of the Churchill region has warmed during the past century, and climate models predict that mean annual temperatures will increase by 3.1°C by 2070 (Macrae et al., 2014). Since the ~1970s, a rapid increase in the Lesser Snow Goose (LSG; *Chen caerulescens caerulescens*) population (geometric increase of 5-7% per year; Batt et al., 1997; Jefferies et al., 2006) and spatial extent of breeding grounds in the coastal region of WNP has disturbed the landscape and caused substantial changes in vegetation and habitat in the tidal flats (Figure 4.1, 4.2; e.g., Iacobelli and Jefferies, 1991; Srivastava and Jefferies, 1996; Handa et al., 2002; Jefferies and Rockwell, 2002; Jefferies et al., 2006). With the expansion in breeding grounds, the LSG have moved farther inland, and their activities (grubbing and the removal of grasses, construction and occupation of nests, and deposits of feces) are now evident in catchments of many ponds within the coastal fen ecotype of WNP. Parks Canada (2008) has recognized that climate change and the expanding LSG population are potentially altering the ecological integrity of lakes and ponds within WNP. While prior limnological studies in WNP and in the Churchill area have focused on seasonal and short-term investigations (Macrae et al., 2004; Bos and Pellatt, 2012; Eichel et al., 2014; MacDonald et al., 2014; White et al., 2014), sediments in these ponds contain a rich source of paleoenvironmental information (Wolfe et al., 2011; Bouchard et al., 2013) that has yet to be fully exploited to provide a temporal perspective of shifting limnological conditions.

Here, we integrate paleolimnological analyses, which provide insight into ~250 years of limnological evolution, with three years of water chemistry measurements, to disentangle the limnological responses and identify regime shifts associated with climate warming and

LSG population expansion in WNP. We compare three ponds located within the coastal fen ecotype including 'WAP 20' and 'WAP 21', whose catchments are strongly disturbed by LSG based on recent field observations, and 'WAP 12', which has no visual evidence of recent LSG disturbance. Findings are used to elucidate the influence of warming and increasing LSG population over time through a suite of limnological and paleolimnological indicators that can be used by agencies to monitor the ongoing consequences of these stressors on aquatic ecosystems.

4.2 Materials and Methods

Study Area

The coastal fen ecotype covers ~11% of WNP (Parks Canada, 2000). Here, the terrestrial vegetation consists mainly of graminoids, sedges (*Carex aquatilis*), and rushes (*Scorpidium scorpioides* and *Scirpus caespitosus*). The study ponds WAP 20 and WAP 21 are situated in catchments located within an area of the coastal fen ecotype subjected to the longest observed occupation by LSG (since ~1979; Figure 4.1). Within their catchments, we observed abundant deposits of feces, nests, geese eggs, substantial grubbing, and vegetation loss during sampling campaigns in 2010-2012 (Figure 4.2). In contrast, WAP 12, also located in the coastal fen ecotype, had little to no visual evidence of LSG disturbance, and is positioned outside of the disturbed area identified in 2008 maps developed by Parks Canada (Figure 4.1). WAP 20 and WAP 21 are within 1 km of one another and WAP 12 is located ~29 km from WAP 20 and WAP 21. As all three ponds are located within the same geographic region, we assume they are subject to similar climatic conditions. All three ponds are small (<0.30 km²), shallow (<0.5 m deep), and are situated in low-relief terrain consisting

of sand to stony silt marine/glaciomarine deposits from the former Tyrrell Sea overlain by muskeg (Dredge and Nixon, 1986).

Limnology

Surface water was collected from the ponds during the spring (early-June), summer (late-July), and fall (mid-September) during 2010-2012. Average values for each sampling period (June, July and September) are reported here. All samples were transported to the Churchill Northern Studies Centre (CNSC) via helicopter for on-site processing. In situ measurements for pH and conductivity were taken at approximately 10- to 15-cm water depth using a YSI 600QS multi-parameter probe. Surface water samples collected at each site were passed through an 80- μm mesh to remove large particles and then stored in the dark at 4 °C until they were sub-sampled for subsequent analyses. Samples were measured for a suite of limnological analyses. Here, we report selected variables based on the findings of MacDonald et al. (2014). These include concentration of total Kjeldahl nitrogen (TKN) measured at the Biogeochemistry Lab, University of Waterloo, following standard methods (TKN = Bran Luebbe, Method No. G-189-097; Seal Analytical, Seattle, USA). Carbon isotope composition of dissolved inorganic carbon ($\delta^{13}\text{C}_{\text{DIC}}$) was measured on water samples collected using 125 ml glass serum bottles with rubber stoppers and syringe needles to expel excess air at field sites. These samples were stored at 4 °C until analysis at the University of Waterloo – Environmental Isotope Laboratory (UW-EIL). Samples for the measurement of C isotope composition of particulate organic matter ($\delta^{13}\text{C}_{\text{POM}}$) were collected using a phytoplankton net (mesh size = 25 μm) and multiple horizontal tows. After collection, samples were passed through a 63- μm mesh net to remove zooplankton and other large

particles, filtered onto pre-ashed Whatman® quartz filters (0.45- μm pore size) and dried at 60 °C for 24 hours in an oven. 12N HCl fumes were then used to remove carbonates from the filters following methods of Lorrain et al. (2003). The acidified filters were analysed for $\delta^{13}\text{C}_{\text{POM}}$ at the UW-EIL. Stable C isotope ratios are reported as $\delta^{13}\text{C}$ (‰) relative to the Vienna-PeeDee Belemnite (VPDB) standard. The C isotope fractionation factor was estimated from the difference between $\delta^{13}\text{C}_{\text{DIC}}$ and $\delta^{13}\text{C}_{\text{POM}}$ (i.e., $\Delta^{13}\text{C}_{\text{DIC-POM}}$; Fry, 2006).

Collection of Pond Sediment Cores

Sediment cores were retrieved from the centre of the study ponds using a hand-driven rod attached to an open-barrel corer (Glew et al., 2001) in late July 2010 from WAP 20 (core 2: 13.0-cm long, core 3: 15.0-cm long and core 5: 14.5-cm long) and WAP 21 (33.5-cm long), and in September 2011 from WAP 12 (core 1: 25-cm long; core 2: 22.5-cm long). All cores were transported to the CNSC via helicopter, sectioned into 0.5-cm intervals using a vertical extruder (Glew, 1988) and stored at 4 °C in the dark during shipping and until analysis. Table 4.1 indicates the sampling strategy employed to ensure there was sufficient material for analysis of all parameters for each pond.

Loss-on-Sequential Heating

Sub-samples of $\sim 0.3 \pm 0.05$ g of wet sediment were analysed to determine water content, organic matter content, and carbonate content by conducting weight loss-on-heating (90 °C for 24h), loss-on-ignition (LOI; 550 °C for 1 h), and loss-on-combustion (LOC; 950 °C for 1 h), respectively, following standard methods (Heiri et al., 2001). Mineral matter content was also determined using the residue after LOC.

Sediment Core Chronology

To develop the sediment core chronologies, subsamples of dried sediment were analysed for at least two days for activities of ^{210}Pb , ^{226}Ra (as ^{214}Bi and ^{214}Pb), and ^{137}Cs using an Ortec co-axial HPGe Digital Gamma Ray Spectrometer (Ortec #GWL-120-15) interfaced with Maestro 32 software (version 5.32) at the University of Waterloo Environmental Change Research (WATER) Laboratory. Polypropylene tubes (8 ml; SARSTEDT; product No. 55.524) were used to pack measured masses of freeze-dried sediment, which were then allowed to equilibrate for at least two weeks before analysis. Chronologies were developed using the Constant Rate of Supply (CRS) model (Appleby, 2001). The mean activity of ^{214}Bi and ^{214}Pb were used to estimate background (supported) ^{210}Pb activity. Activity of ^{137}Cs , which often forms a distinctive peak corresponding to maximum atmospheric fallout from above-ground nuclear weapons testing in 1963 (Appleby, 2001), was used as an independent time marker.

Geochemical Analysis of Sediment Cores

Subsamples were prepared for geochemical analysis following standard methods described by Wolfe et al. (2001). Subsamples of wet sediment were treated with 10% HCl to remove carbonates, and subsequently rinsed repeatedly with de-ionized water until a neutral pH was reached. The samples were then freeze-dried, and the fine fraction (<500 μm) was analysed for organic C and N elemental and isotope composition at the UW-EIL. The C to N ratio was calculated using percent dry weight of organic C and N. Stable C and N isotope ratios are reported as $\delta^{13}\text{C}_{\text{org}}$ (‰) units relative to the Vienna-Peedee Belemnite (VPDB)

standard and $\delta^{15}\text{N}$ (‰) units relative to atmospheric N (AIR), respectively. For WAP 20, average reproducibility was $\pm 1.91\%$ and $\pm 0.63\%$ for elemental organic C and N, respectively, and $\pm 0.16\%$ and $\pm 0.10\%$ for $\delta^{13}\text{C}_{\text{org}}$ and $\delta^{15}\text{N}$, respectively. For WAP 21, average reproducibility was $\pm 0.54\%$ and $\pm 0.04\%$ for elemental organic C and N, respectively, and $\pm 0.27\%$ and $\pm 0.08\%$ for $\delta^{13}\text{C}_{\text{org}}$ and $\delta^{15}\text{N}$, respectively. For WAP 12, average reproducibility was $\pm 1.92\%$ and $\pm 0.13\%$ for elemental organic C and N content, respectively, and $\pm 0.01\%$ and $\pm 0.02\%$ for $\delta^{13}\text{C}_{\text{org}}$ and $\delta^{15}\text{N}$, respectively.

Sedimentary Diatom Analysis

For analysis of diatoms, subsamples ($\sim 0.3 \pm 0.05$ g) of wet sediment were treated with 10% HCl for 24 hours to remove carbonates. After allowing sufficient time for diatoms to settle to the bottom of the sample tubes, the supernatant was siphoned off and de-ionized water was added to dilute the acid. This sequence was then repeated several times until a neutral pH was reached. Subsamples were then digested with strong acids (50:50 concentrated sulphuric:nitric acids by volume) to remove organic materials. After allowing sufficient time for diatoms to settle to the bottom of the sample tubes, the supernatant was siphoned off and samples were rinsed with de-ionized water. This sequence was repeated until a neutral pH was obtained. The resulting cleaned diatom slurries were then dispensed onto circular coverslips and allowed to dry before mounting them onto microscope slides using Naphrax mounting medium. For each sample, approximately 300 diatom valves were identified to the lowest possible taxonomic level at 1000x magnification using a Zeiss Axioskop II Plus compound light microscope fitted with differential interference contrast

optics. Diatom identifications were based on the keys of Krammer and Lange-Bertalot (1986-1991) and Lavoie et al. (2008).

Sedimentary Pigment Analysis

Standard methods (Reuss et al., 2010) were used to prepare, extract and analyse pigment concentrations from subsamples ($\sim 0.3 \pm 0.05$ g) of wet sediment at the University of Waterloo WATER Lab. A WATERS 2695 HPLC was used with the reverse-phase high performance liquid chromatography method by Mantoura and Lleywellyn (1983) and modified by Leavitt et al. (1989). Pigments were identified based on their retention times and elution sequence, and comparison of their spectra compared to known standards (Jeffrey et al., 1997). Pigment concentrations are expressed as nanomoles per gram of organic matter.

Stratigraphic Analysis

To assist identifying the timing of regime shifts in the study ponds, we determined breakpoints in stratigraphic profiles individually for each of the physical and geochemical variables via use of generalized linear models with piece-wise linear relationships having a fixed number of breakpoints. The average fitted breakpoint date and relevant standard error for all physical and geochemical variables was calculated, which we present in stratigraphic plots and the text below. The average fitted breakpoint date and relevant standard error of the physical and geochemical variables calculated for each pond were also applied to the biological data. Numerical procedures were conducted with the use of R statistical language v3.1.1 with the rioja and segmented libraries.

4.3 Results and interpretation

Sediment Core Chronologies

Total ^{210}Pb activity declined steadily with depth in the sediment core from WAP 20, from 0.231 Bq g^{-1} at the top to 0.010 Bq g^{-1} at 12.5 cm (Figure 4.3a). The mean activity of ^{226}Ra (0.011 Bq g^{-1}) was used to estimate supported ^{210}Pb . Total ^{210}Pb activity was almost equivalent to the estimated supported ^{210}Pb at 12.5 cm (0.010 Bq g^{-1}), indicating that background was likely reached at this depth. Using the CRS model and linear extrapolation, a basal date of 1467 was determined for the sediment core from WAP 20. Peak concentration in ^{137}Cs (0.186 Bq g^{-1}) at 6 cm occurred at the CRS date of 1963, which corresponds to the expected year of peak fallout. The sedimentation rate fluctuated between $0.013 \text{ g cm}^{-2} \text{ yr}^{-1}$ and $0.016 \text{ g cm}^{-2} \text{ yr}^{-1}$ before 1977, and then increased to a maximum of $0.029 \text{ g cm}^{-2} \text{ yr}^{-1}$ at the top of the core.

In contrast to WAP 20, total ^{210}Pb activity did not decline steadily down-core at WAP 21 (Figure 4.3b). Instead, peak activity (0.164 Bq g^{-1}) occurred at 12.5 cm, and declined at depths above and below. Total ^{210}Pb activity declined to 0.011 Bq g^{-1} at 26.5 cm depth and was near-equivalent to the estimated supported ^{210}Pb at 26.5 cm (0.011 Bq g^{-1}), indicating that background was reached at this depth. A basal date of 1597 was determined for the core. Peak concentration of ^{137}Cs (0.087 Bq g^{-1}) occurred at 14.5 cm and corresponded to a CRS date of 1957, which is close to the expected date of 1963. The sedimentation rate fluctuated between $0.011 \text{ g cm}^{-2} \text{ yr}^{-1}$ and $0.014 \text{ g cm}^{-2} \text{ yr}^{-1}$, before it began a steady increase during 1961-1978 to $0.021 \text{ g cm}^{-2} \text{ yr}^{-1}$. The sedimentation rate then increased exponentially and reached a maximum value of $0.088 \text{ g cm}^{-2} \text{ yr}^{-1}$ at the top of the core.

Total ^{210}Pb activity was relatively constant ($\sim 0.25 \text{ Bq g}^{-1}$) in the upper 5 cm of the core from WAP 12 (Figure 4.3c). Between 5 cm and 17 cm, ^{210}Pb activity declined to 0.008 Bq g^{-1} . Total ^{210}Pb activity at 17 cm was close to the estimated supported ^{210}Pb (0.006 Bq g^{-1}), indicating that background was likely reached at this depth. Using the CRS model, the base of unsupported ^{210}Pb in WAP 12 core 2 was estimated to be 1904. Extrapolation of the age-depth relation to core 1 gave a basal date of 1813. ^{137}Cs activity did not display a clear peak in the core, likely due to the mobile nature of Cs in the highly organic sediments. Sedimentation rates fluctuated between $0.013 \text{ g cm}^{-2} \text{ yr}^{-1}$ and $0.029 \text{ g cm}^{-2} \text{ yr}^{-1}$ throughout the record. Peak sedimentation rates occurred in 1953 and at the top of the core (0.028 and $0.029 \text{ g cm}^{-2} \text{ yr}^{-1}$, respectively). Although sedimentation rate has increased during the past few decades, values remain within the historical range. Near-constant ^{210}Pb activities at the top of the sediment core from WAP 12 are similar to ^{210}Pb profiles in other pond sediment cores in the Churchill region (Wolfe et al., 2011), and are likely due to increase in sedimentation rate, because sediment mixing is unlikely based on fluctuating values of many parameters during this interval (see below and Bouchard et al., 2013).

Limnological Evolution of the Ponds

Stratigraphic profiles for organic matter content (and organic matter flux for WAP 21), mineral matter content, calcium carbonate content, organic C content, N content, C/N, organic C isotope composition and N isotope composition show prominent temporal variations (Figures 4.4-4.6). Stratigraphic profiles shown also include the percent abundance of *Fragilaria pinnata* (Ehrenberg) and *Denticula kuetzingii* (Kützing), which were the two most dominant diatom taxa in sediment cores from all three ponds, and concentrations of

chlorophyll *a* to represent total algal abundance and concentrations of aphanizopyll or canthaxanthin to represent abundance of potentially nitrogen-fixing cyanobacteria (Figures 4.4-4.6). This broad array of paleolimnological measurements allows us to efficiently characterize past limnological conditions and intervals, and identify changes during the past 200-250 years.

Minimal changes occurred in the older strata of all three sediment records, and to provide sufficient temporal context to evaluate the 20th century changes, only results post-1750 (post-1813 for WAP 12) are reported here. Breakpoint analyses on the physical and geochemical variables were used to guide our identification of the timing of major limnological changes. Breakpoint analyses indicated significant changes at ~1900 (± 49 yrs) and ~1975 (± 15 yrs) for WAP 20, ~1893 (± 22 yrs) and ~1983 (± 25 yrs) for WAP 21, and ~1900 (± 31 yrs) for WAP 12. Based on these breakpoints, three phases of different limnological conditions were identified at WAP 20 and WAP 21 and two phases at WAP 12. The phase boundaries coincide with marked changes in composition of diatom communities and abundance of algal pigments.

Phase 1 (pre-1750 to ~1893-1900). During the first phase of the sediment records (pre-1750 to ~1893-1900), values of the physical, geochemical, and biological variables remained relatively constant or displayed gradual trends over time. Despite relatively coarse temporal resolution, subtle trends are apparent in the core from WAP 20 (Figure 4.4). Organic matter content increased gradually (~11 to 18%) throughout this phase, while mineral matter (~69 to 63%) and calcium carbonate content (~45 to 40%) decreased. Organic C content remained around 11% and N content remained around 0.5%. Values of the C/N ratio decreased

gradually during this interval (26 to 20), but were relatively high overall. Values of $\delta^{13}\text{C}_{\text{org}}$ ($\sim -21\text{‰}$) and $\delta^{15}\text{N}$ (-0.25‰) were relatively constant. Diatom community composition and pigment concentrations varied only slightly. Diatom assemblages were dominated by *Fragilaria pinnata* ($\sim 80\%$), and sediments contained relatively low concentrations of chlorophyll *a* (~ 25 to $30 \text{ nmol g}^{-1} \text{ OM}$).

During Phase 1 in the WAP 21 sediment core, gradual changes are evident in several of the parameters (Figure 4.5). Organic matter content increased gradually but substantially (11 to 48%), and mineral matter (69 to 43%) and carbonate content (45 to 20%) decreased correspondingly. Organic C content increased (16 to 32%), and N content increased from ~ 1 to 2%. Values of the C/N ratio were relatively constant and high (15-16). Values of $\delta^{13}\text{C}_{\text{org}}$ increased gradually (-25 to -22‰) and $\delta^{15}\text{N}$ fluctuated around -0.5‰ . Diatom community composition and pigment concentrations varied only slightly. Diatom assemblages were dominated by *Fragilaria pinnata* (80%) and sediments contained relatively moderate concentrations of the pigments aphanizophyll (~ 500 to $700 \text{ nmol g}^{-1} \text{ OM}$) and relatively low concentrations of chlorophyll *a* (~ 200 to $300 \text{ nmol g}^{-1} \text{ OM}$).

In the core from WAP 12, gradual changes are evident from the base of the core (~ 1813) until ~ 1900 (Figure 4.6). Organic matter increased (84 to 90%), while mineral matter (12 to 9%) and calcium carbonate content (8 to 3%) declined. Organic C and N content fluctuated around $\sim 53\%$ and 3.5%, respectively, and C/N ratios were relatively high (14 to 16). Values of $\delta^{13}\text{C}_{\text{org}}$ increased slightly (-25 to -24‰), and $\delta^{15}\text{N}$ remained near 0‰ . Diatoms were not in sufficient abundance or not sufficiently preserved in sediments deposited during this phase to allow enumeration, and concentrations of pigments

canthaxanthin and chlorophyll *a* fluctuated slightly but were relatively low (~4-11 nmol g⁻¹ OM and ~9-16 nmol g⁻¹ OM, respectively).

Overall, results indicate that limnological conditions at WAP 20, WAP 21 and WAP 12 gradually transitioned towards increased aquatic productivity during Phase 1, as indicated by gradual increases in organic matter content, organic C content and $\delta^{13}\text{C}_{\text{org}}$. Increasing algal demand on DIC usually leads to ¹³C-enrichment of DIC and phytoplankton, which is recorded in pond sediments (Meyers and Teranes, 2001; Meyers, 2003). High C/N ratios in the sediment records from all three ponds suggest that aquatic productivity occurred under N-limited conditions. Likewise, all three sediment cores contained $\delta^{15}\text{N}$ values close to 0‰, possibly indicative of fixation of atmospheric N (Talbot, 2001). At WAP 21 and WAP 12, sediments contained measurable concentrations of the pigments aphanizophyll and canthaxanthin, respectively. These pigments are produced by potentially N-fixing taxa (e.g., Leavitt and Hodgson, 2001), a finding that is consistent with N-limited conditions inferred from C/N ratios and $\delta^{15}\text{N}$ values. However, concentrations of these pigments and chlorophyll *a* were relatively low during this phase, suggesting low algal productivity. Low productivity in the ponds is further substantiated by the diatom assemblage data that reveal information about conditions of pond habitat. *Fragilaria pinnata* was the dominant taxon in WAP 20 and WAP 21 during this phase, while diatom abundance was too low in sediments from WAP 12 to allow enumeration. *Fragilaria pinnata* is an epipsammic and alkaliphilic diatom taxon that can live on mineral grains and is considered to indicate low-light availability caused by minerogenic turbidity, which generates poor habitat for epiphytic and planktonic diatom taxa (Rühland and Smol, 2005; Smol et al., 2005). Dominance by *Fragilaria pinnata*, thus, indicates that the epiphytic and plankton habitats did not support considerable growth of

algae. Instead, dominance by *Fragilaria pinnata* suggests that most of the algal growth occurred in benthic (and mainly epipsammic) habitat. For WAP 20 and WAP 21, shoreline erosion of inorganic sediment may have provided the input of material for *Fragilaria pinnata* to grow and flourish. In contrast, WAP 12 was likely not experiencing shoreline erosion during this phase as indicated by the higher organic matter content and higher organic C accumulation in the sediment core. Low input of inorganic matter would have limited the benthic habitat available for *Fragilaria pinnata*.

Phase 2 (~1893-1900 to 1975-1983). Paleolimnological analyses identified marked changes in sediment records from all three ponds around 1893-1900 (Figures 4.4-4.6). At WAP 20, sedimentary content of organic matter increased after ~1900 (~18 to 56%), and content of mineral matter (~64 to 38%) and calcium carbonate declined (~40 to 13% by 1949 and then remained relatively constant). Organic C content (~13 to 26%), N content (~0.6 to 2.0%) and $\delta^{13}\text{C}_{\text{org}}$ (-25 to -22‰) also increased at WAP 20. Values of the C/N ratio continued to decline gradually (20-14), but remained relatively high, and $\delta^{15}\text{N}$ fluctuated around -0.5‰.

Composition of diatom assemblages changed abruptly during this phase from dominance by the epipsammic *Fragilaria pinnata* (from ~80 to ~1 %) to dominance by *Denticula kuetzingii* (1 to 60 %), a taxon commonly found in benthic biofilms in ponds near Churchill, Manitoba (Macrae, 1998; White et al., 2014). The N-fixing cyanobacterial pigment aphanizophyll first appeared in the sediment record in Phase 2 and reached peak concentrations (~197 nmol g⁻¹ OM). Additionally, concentrations of chlorophyll *a* increased (~35 nmol g⁻¹ OM).

At WAP 21, organic matter content initially increased (56 to 63%) after ~1893 until ~1934, then decreased (to 49%). However, the organic matter flux continued to increase

throughout this phase (0.006 to 0.011 g OM cm⁻² yr⁻¹). Mineral matter (37 to 43%) and calcium carbonate (14 to 18%) content increased. Organic C content decreased (32 to 26%) while N content fluctuated around 2%, and C/N values declined slightly (17 to 13) but remained relatively high. $\delta^{13}\text{C}_{\text{org}}$ values fluctuated around -22‰ and $\delta^{15}\text{N}$ fluctuated around 0.5‰. Similar to WAP 20, the diatom community composition changed abruptly (but earlier; ~1880) from dominance by *Fragilaria pinnata* to dominance by *Denticula kuetzingii*, which reached peak abundance of 62% at ~1952. Aphanizophyll content increased to peak concentrations (~1200 nmol g⁻¹ OM) during this phase. Additionally, concentrations of chlorophyll *a* increased to peak concentrations (~800 nmol g⁻¹ OM).

At WAP 12, changes occurred between ~1875 and ~1900. Organic matter content increased to ~90% and then remained constant to the top of the core. Mineral matter content decreased and then fluctuated around 8%. CaCO₃ content decreased and then fluctuated around 3% until 1925, when it increased slightly to 5% and fluctuated around this level to the top of the sediment record. Organic C and N content became more variable during this phase and fluctuated mostly between 37-53% and around 3%, respectively. Values of the C/N ratio were relatively constant after ~1875 and remained at ~15 to the top of the core. $\delta^{13}\text{C}_{\text{org}}$ was relatively constant around -24‰ from ~1875 to 1900, and then increased to -22‰ and remained relatively stable in the upper sediments. $\delta^{15}\text{N}$ showed an initial increase to about 0.3‰ and then fluctuated between -0.8 and 0‰ until the top of the core. Diatoms became sufficiently abundant to allow enumeration at ~1911 and were dominated by *Denticula kuetzingii*, similar to WAP 20 and WAP 21. Concentrations of canthaxanthin increased slightly at ~1875 and fluctuated between 8 and 11 nmol g⁻¹ OM until 2003 when an increase to peak concentrations of 16 nmol g⁻¹ OM occurred in ~2008. Chlorophyll *a* showed larger

fluctuations in concentrations (average 10 nmol g⁻¹ OM) with an increase to 20 nmol g⁻¹ OM at the top of the core.

Together, the stratigraphic records from WAP 20, WAP 21, and WAP 12 suggest a marked change began during the late 1800s and early 1900s, characterized by increased aquatic productivity and associated shifts in limnological conditions and available habitat. The increase in organic matter content (or organic matter flux), pigment concentrations, and shift in dominant diatom taxa can be explained by reduced rates of shoreline erosion and input of inorganic material, leading to less turbid conditions, increased light penetration, and higher aquatic productivity. Higher productivity is also supported by increased values of $\delta^{13}\text{C}_{\text{org}}$. The increase in productivity likely also fostered a high demand for N and continued N limitation based on $\delta^{15}\text{N}$ values close to 0‰, high C/N values, and increased concentrations of cyanobacterial pigments aphanizopyll and canthaxanthin produced by potentially N-fixing taxa. In addition, the shift in diatom community composition to dominance of *Denticula kuetzingii* indicates a change in available habitat in the ponds from mineral grains to benthic biofilm.

Phase 3 (~1975-1983 to 2010). Marked stratigraphic changes in the physical and geochemical variables, although not all in the same direction, are apparent in sediment cores from WAP 20 and WAP 21 beginning in the mid-1970s, but they are notably absent in the core from WAP 12 (Figures 4.4-4.6). At WAP 20, increases in sedimentation rate (Figure 4.3) and continued increases in organic matter content (~56 to 65%) occurred, while mineral matter (~38 to 30%) and calcium carbonate (~14 to 10%) content declined. Organic C (~26 to 33%) and N (2 to 4%) content increased and the C/N ratio declined substantially (14 to 8).

$\delta^{13}\text{C}_{\text{org}}$ increased initially from -22 to -21‰ and then stabilized for the remainder of the core at -20.9‰ after 1998. $\delta^{15}\text{N}$ values increased (-0.5 to 0.2‰). *Denticula kuetzingii* remained the dominant taxon during this phase. Aphanizophyll content declined abruptly to 67 nmol g⁻¹ OM and remained relatively constant until the top 1 cm of the core when an increase to 97 nmol g⁻¹ OM occurred. Chlorophyll *a* concentrations fluctuated around 35 nmol g⁻¹ OM until the top 1 cm of the core when concentrations increased to 94 nmol g⁻¹ OM.

At WAP 21, the sedimentation rate increased exponentially after the mid-1970s (Figure 4.3), which influenced patterns of change in some of the sedimentary variables. Consequently, values of organic matter are more informative when expressed as flux rate than as concentration. During Phase 3, the flux of organic matter increased (0.01 g cm⁻² yr⁻¹ to 0.02 g cm⁻² yr⁻¹), while C/N ratios declined (12 to 10). Calcium carbonate content increased (~18-35%), while C_{org} and N content declined to ~17% and 1.6%, respectively. $\delta^{13}\text{C}_{\text{org}}$ decreased (-22 to -24‰) and $\delta^{15}\text{N}$ increased (-0.5 to 0.7‰) slightly during this phase. *Denticula kuetzingii* decreased in percent abundance around ~1990 to ~17% at the top of the core, while *Fragilaria pinnata* increased to ~52% at the top of the core. Aphanizophyll concentration declined to 350 nmol g⁻¹ OM, then increased in the top sample to ~604 nmol g⁻¹ OM. Chlorophyll *a* concentrations showed no noticeable trend and values fluctuated between 150 and 817 nmol g⁻¹ OM during this phase.

Increasing concentration or flux of organic matter indicates that aquatic productivity continued to increase in WAP 20 and WAP 21 during Phase 3. At WAP 21, the marked increase in calcium carbonate content may be due to calcite precipitation under conditions of high productivity and pH (Wetzel, 2001). This likely accounts for dilution of organic matter, C_{org} and N content, as well as the increase in *Fragilaria pinnata* due to increased inorganic

material for this diatom to grow on. The decrease in C/N ratios, increase in $\delta^{15}\text{N}$ values and the decline in concentration of the pigment aphanizopyll for both WAP 20 and WAP 21 indicate that there was an increase in supply of N to these ponds. As stated above, increasing aquatic productivity often corresponds to increasing $\delta^{13}\text{C}_{\text{org}}$ in lake sediment cores (Meyers and Teranes, 2001; Meyers, 2003). However, $\delta^{13}\text{C}_{\text{org}}$ decreases at WAP 21 and increases only slightly at WAP 20 before attaining constant values after ~1998. Nonetheless, we attribute these patterns to increasing aquatic productivity because such trends can develop when chemically-enhanced CO_2 invasion occurs, which leads to a decline in $\delta^{13}\text{C}_{\text{DIC}}$ (Herczeg and Fairbanks, 1987), as we describe in the following section. Notably, these inferred limnological changes post-1975 are not evident in the sediment record from WAP 12. Additionally, chlorophyll *a* concentrations were generally lowest in WAP 12 and highest in WAP 21, and the difference increased near the top of the core, providing further support for stimulation of aquatic productivity at WAP 20 and WAP 21 in recent years.

Modern limnology. Average values (2010-12) of several water chemistry variables distinguish present-day limnological conditions of WAP 20 and WAP 21 from those at WAP 12, particularly in July (Figure 4.7). Conductivity was much higher at WAP 20 and WAP 21 than at WAP 12. At all three ponds, pH was alkaline but WAP 20 and WAP 21 had much larger increases in pH between June and July than at WAP 12. All three ponds had lower TKN concentrations in June followed by higher values in July and a return to lower values in September. However, TKN concentrations were substantially lower at WAP 20 and WAP 21 in July than at WAP 12. Values of $\delta^{13}\text{C}_{\text{DIC}}$ at WAP 20 and WAP 21 decreased between June and July, whereas $\delta^{13}\text{C}_{\text{DIC}}$ increased throughout the ice-free season at WAP 12. Although

seasonal patterns in $\delta^{13}\text{C}_{\text{POM}}$ were similar among the ponds, C isotope fractionation ($\Delta^{13}\text{C}_{\text{DIC-POM}}$) declined sharply at WAP 20 and WAP 21 in July, whereas values at WAP 12 were similar in July and June.

The above limnological features mainly reflect differences in LSG disturbance and associated nutrient behaviour at WAP 20 and WAP 21 in comparison to WAP 12. Higher conductivity at WAP 20 and WAP 21 compared to WAP 12 is unlikely to have been caused by differences in evaporative concentration, as WAP 12 generally undergoes greater mid-summer pond water isotopic enrichment (data not shown). Instead, higher conductivity at WAP 20 and WAP 21 is likely due to higher erosional input of dissolved ions to the ponds than at WAP 12, caused by removal of catchment vegetation by the LSG population. Lower TKN concentrations at WAP 20 and WAP 21 may be a result of more rapid uptake of nutrients by the benthic biofilm. Experimental nutrient additions by Eichel et al. (2014) demonstrated that the benthic biofilm rapidly assimilates N and P. As discussed in detail by MacDonald et al. (2014), the seasonal increase in $\delta^{13}\text{C}_{\text{DIC}}$ values at WAP 12 is consistent with preferential use of ^{12}C by algae during photosynthesis when C supply exceeds C demand (and which commonly leads to ^{13}C -enrichment in the organic fraction of lake sediment profiles under conditions of increasing productivity), whereas the decline in July $\delta^{13}\text{C}_{\text{DIC}}$ values at WAP 20 and WAP 21 is likely due to chemically-enhanced CO_2 invasion. The latter may occur under conditions of high productivity, high C demand and high pH, resulting in strong kinetic C isotope fractionation as CO_2 enters from the atmosphere and decline of $\delta^{13}\text{C}_{\text{DIC}}$ (Herczeg and Fairbanks, 1987; Takahashi et al., 1990; Bade et al., 2004). Evidently, this signal has been recorded by muted and declining trends in $\delta^{13}\text{C}_{\text{org}}$ in the uppermost stratigraphic intervals of the sediment records from WAP 20 and WAP 21,

respectively (Figures 4.4, 4.5). Further support for the interpretation of higher C demand at WAP 20 and WAP 21 in July, compared to WAP 12, is the decline in $\Delta^{13}\text{C}_{\text{DIC-POM}}$.

4.4 Discussion

Regime shifts in shallow lakes and ponds are rapid changes due to a stressor that cause modifications to the dynamics, organization, and feedbacks of the particular ecosystem resulting in a shift to a different state (e.g., Scheffer and Carpenter, 2003; Anderson et al., 2009). These shifts can be characterized by distinct habitats and life forms, and persistence of the new state for a substantial period of time (e.g., Beisner et al., 2003; Scheffer and Carpenter, 2003). Limnological regime shifts have been identified in a number of different ecosystems, but their documentation has primarily been based on studies of temperate and boreal lakes, and has largely focused on the effects of changing nutrient loads on aquatic vegetation and turbidity (e.g., Scheffer et al., 1993; Bayley and Prather, 2003; Scheffer and Carpenter, 2003; Bayley et al., 2007). Typically, shallow lakes in temperate and boreal locations switch from a clear-water, macrophyte-dominated state under conditions of low nutrient supply, to a turbid state dominated by phytoplankton as nutrient supply increases and exceeds a threshold (Scheffer et al., 1993). Here we show that, based on integrating the results from analyses of sediment records and water chemistry, three phases of limnological conditions during the past ~200-250 years were identified at the ponds located in catchments disturbed by LSG (WAP 20 and WAP 21), whereas only two phases were evident at the non-disturbed pond (WAP 12). As we discuss below, the rapid phase transitions are consistent with aspects of regime shifts that have been documented in shallow temperate and boreal lakes, but we show they occur also in a Subarctic setting. Furthermore, our study distinguishes limnological regime shifts driven, not only by changes in available habitat due

to warming, but also by the transfer of nutrients from the catchments to the ponds in response to waterfowl disturbance (summarized in Figure 4.8 and discussed below).

Limnological Regime Shift Caused by Climate Warming

Prior to the 20th century (Phase 1), pond conditions can generally be characterized by relatively low nutrient availability, low aquatic productivity, and high mineral matter content of the sediment (with the exception of WAP 12, likely due to lower rates of shoreline erosion). These conditions are consistent with the cold, turbid, low-light conditions of the Little Ice Age (LIA; Overpeck et al., 1997), but abrupt stratigraphic changes occurred in all three ponds during the late ~1800s to the early ~1900s (initiation of Phase 2). Limnological conditions during this new state are characterized by clearer water with abundant light available for algal growth associated with the rapid development of a benthic biofilm. In addition to this change in habitat availability, there were also abrupt shifts in nutrient balance. Increases in $\delta^{13}\text{C}_{\text{org}}$ indicate productivity-driven ^{13}C -enrichment of DIC, and geochemical and pigment data suggest higher N demand relative to supply. These conditions have persisted to the present at WAP 12, whereas WAP 20 and WAP 21 underwent additional limnological changes beginning in the mid-1970s. Rapid changes in nutrient dynamics, and the development of new habitat supporting new algal community composition that persisted for decades in all three ponds are characteristics of a limnological regime shift, which we associate with climate warming at the end of the LIA.

Regime shifts in response to late 19th and early 20th century post-LIA warming have been identified at other Arctic lakes, based on paleolimnological studies, and have mainly identified shifts in aquatic habitat (e.g., Sorvari et al., 2002; Rühland et al., 2003; Rühland

and Smol, 2005; Smol et al., 2005). Common to all of these studies is a shift in the dominant diatom taxa from benthic *Fragilaria* species to more diverse communities in response to post-LIA warming and subsequent reduction in seasonal ice-cover. Other studies have suggested that, during the LIA, extensive ice-cover resulted in only a narrow moat of shallow open water forming during the summer which allowed *Fragilaria* species to dominate (e.g., Smol et al., 2005; Smol and Douglas, 2007). Decreasing ice-cover post-LIA resulted in changes to diatom community composition with moss epiphytic taxa dominant in new littoral habitat (Douglas et al., 1994; Antoniadou et al., 2005; Keatley et al., 2006) and *Cyclotella* species dominant in deeper lakes with the development of planktonic habitat (Sovari et al., 2002; Rühland et al., 2003; Rühland and Smol, 2005). We also find that small epipsammic *Fragilaria* species are outcompeted by taxa commonly found in benthic mats at the end of the 19th century, likely due to decreased ice cover and creation of new available habitat. However, our results also document that this limnological regime shift was accompanied by increased aquatic productivity and low N availability. Increased aquatic productivity and nutrient demand likely led to N-limited conditions and stimulated the growth of benthic biofilms with abundant cyanobacteria, which have been found to dominate under these conditions (Vreca and Muri, 2010; White, 2011).

An important exception to the widespread evidence of late 19th and early 20th century warming in Subarctic and Arctic lakes and ponds is the recent study by Rühland et al. (2013), which used stratigraphic changes in diatom assemblages to suggest that the southern HBL region has undergone post-LIA limnological regime shifts associated with warming only since the 1990s. Additional work by Rühland et al. (2014) provided further support of recent diatom assemblage changes. We suggest that the earlier initiation of the effects of 20th

century warming on limnological conditions reported here compared to that reported by Rühland et al. (2013) may be due to the shallow, and thus more climatically-sensitive nature of northwestern HBL ponds compared to the deep and more resilient southern HBL lakes. As relayed by Rühland et al. (2013), observation that these resilient lakes are now also showing limnological consequences of warming indicates that “climate of the HBL has passed a tipping point” (p. 1).

Limnological Regime Shift Caused by Lesser Snow Goose Population Expansion

The LSG-disturbed ponds WAP 20 and WAP 21 both display a third phase in their stratigraphic records beginning in the mid-1970s, which persists to the present but is absent from the undisturbed pond WAP 12. Based on the paleolimnological and water chemistry data, this phase is characterized by increased N availability, but with rapid uptake, increased C demand and increased productivity. Because these rapid changes in limnological conditions only occurred at WAP 20 and WAP 21 ponds, this suggests a site-specific trigger rather than a regional environmental change. This site-specific trigger led to long-lasting changes in nutrient dynamics and community composition of algae and can, therefore, be considered a regime shift. The timing of this limnological regime shift corresponds well with the documented expansion of the LSG population (e.g., Batt et al., 1997; Jefferies et al., 2006; Figure 4.2e), which likely would have provided the source of additional nutrient loading to the disturbed ponds through fecal deposition or indirectly through alteration of catchment vegetation and habitat (e.g., Batt et al., 1997; Handa et al., 2002; Jefferies et al., 2004; Abraham et al., 2005a).

Based on the patterns in $\delta^{13}\text{C}_{\text{org}}$ in the sediment records, WAP 21 appears to have been disturbed longer, or more intensely, by the LSG population than WAP 20. At WAP 21, $\delta^{13}\text{C}_{\text{org}}$ began to decline soon after the LSG population expansion began. We attribute this trend to declining $\delta^{13}\text{C}_{\text{DIC}}$ caused by chemically-enhanced CO_2 invasion, which occurs under conditions of high productivity, high C demand and high pH (Herczeg and Fairbanks, 1987; Takahashi et al., 1990; Bade et al., 2004). Indeed, while Herczeg and Fairbanks (1987) described this process in their study of the present-day carbon balance of Mohonk Lake NY, they speculated that negative excursions in the carbon isotope composition of lake sediments may develop from increasing aquatic productivity when chemically-enhanced CO_2 invasion occurs to meet C demand. Conversely, the $\delta^{13}\text{C}_{\text{org}}$ record at WAP 20 increased after the LSG population began to expand and stabilized at ~1998, suggesting that chemically-enhanced CO_2 invasion is a more recent and less intense phenomenon at this pond.

Limnological regime shifts in response to nutrient enrichment have been identified in the Arctic (Douglas and Smol, 2000; Douglas et al., 2004; Michelutti et al., 2007; Hadley et al., 2010). Many of these studies document nutrient enrichment as a consequence of anthropogenic inputs (e.g., increased sewage inputs from local communities and Thule whaling activities), or other factors in the catchment (Medeiros et al., 2014), rather than directly from activities of wildlife, as inferred from LSG disturbance in our study. While other Arctic paleolimnological and contemporary limnological studies have attributed increases in productivity to disturbance from waterfowl and seabird populations (Michelutti et al., 2009; 2010; Côté et al., 2010; Keatley et al., 2011; Sun et al., 2013; MacDonald et al., 2014), they have not explicitly identified a regime shift. This is likely because contemporary limnological studies alone tend to not have sufficient temporal perspective to document

persistence of a new set of conditions. In addition, analysis of an insufficient suite of variables in both paleolimnological and contemporary limnological studies may hinder recognition of regime shifts in internal nutrient behaviour and habitat.

Implications for Aquatic Ecosystem Monitoring

Based on our analyses, we identify a suite of pond responses (physico-chemical, biological) and key indicators based on contemporary limnological and paleolimnological measurements that most effectively defined limnological regime shifts caused by climate warming and catchment disturbance by the expansion of LSG population. We use this as a basis for identifying effective tools for ongoing monitoring of limnological changes in ponds of WNP and elsewhere in response to these stressors (Table 4.2). In our study, consequences of warming were best identified by paleolimnological indicators; namely, increasing organic matter content and flux that reflect increasing aquatic productivity, change in composition of diatom assemblages (i.e., switch in dominance from *Fragilaria pinnata* to *Denticula kuetzingii*) that document a shift from epipsammic to benthic habitat, and the appearance of cyanobacteria pigments that indicate more intense competition for dissolved inorganic N. In contrast, limnological consequences of the LSG population expansion were identified from both contemporary and paleolimnological data. High values of conductivity and mid-summer carbon isotope measurements reveal disturbance by LSG on pond catchments, and specifically influx of dissolved ions and nutrients that had a discernable influence on pond-water carbon balance as inferred from carbon isotope data ($\delta^{13}\text{C}_{\text{DIC}}$, $\Delta^{13}\text{C}_{\text{DIC-POM}}$). Interestingly, paleolimnological indicators, including pigments and $\delta^{15}\text{N}$, clearly reveal greater nitrogen availability due to increased nutrient supply, but this is not readily detected

by measurements of TKN concentration in pond water, likely due to rapid nutrient uptake by the benthic biofilm (Eichel et al., 2014; MacDonald et al., 2014). Overall, based on our study we recommend a combination of contemporary limnological and paleolimnological methods for future aquatic ecosystem monitoring initiatives to track responses of Arctic and Subarctic ponds to climate warming and expanding wildlife populations. Also, we recommend that research be conducted on a larger number of ponds within Wapusk National Park, both affected and unaffected by LSG disturbance, to further assess the sensitivity of the metrics we identify here and determine if the regime shifts we identified in a small number of ponds can be generalized to ponds across the landscape.

4.5 Acknowledgements

Funding for this study was provided by the Natural Sciences and Engineering Research Council of Canada (Northern Research Chair and Discovery Grants), the Polar Continental Shelf Program, the Northern Scientific Training Program, Parks Canada, the Churchill Northern Studies Centre (Northern Research Fund), Natural Sciences and Engineering Research Council of Canada Canadian Graduate Scholarship, W. Garfield Weston Foundation Northern Research Award and Ontario Graduate Scholarships. We thank the Churchill Northern Studies Centre, Hudson Bay Helicopters, J. Larkin, E. Light, J. White, K. Thomas and H. White for assistance with field work. We thank J. Wiklund for providing help with developing the chronologies for the sediment records. We thank reviewers and editors for constructive comments that improved the paper.

4.6 Figures

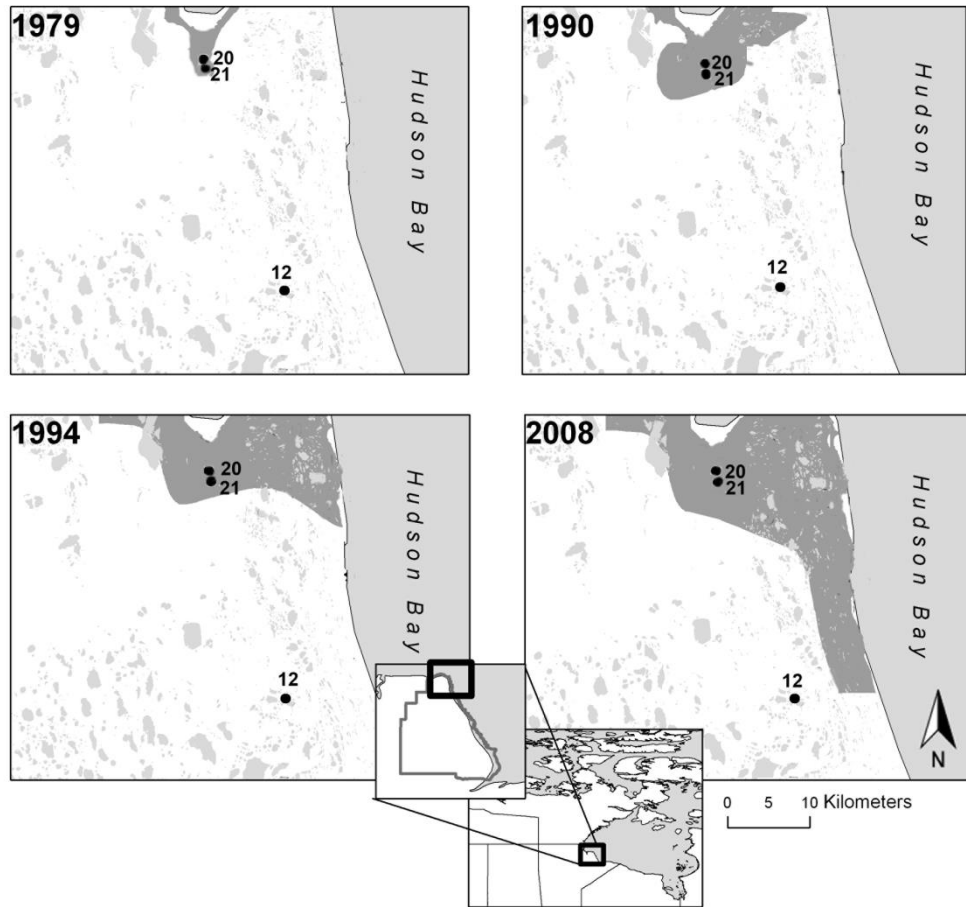


Figure 4.1: Location of Wapusk National Park (Manitoba, Canada) and the three study ponds (WAP 20, WAP 21 and WAP 12). WAP 20 and WAP 21 are situated in an area of high disturbance by LSG since ~1979, whereas WAP 12 is located outside of this area as of 2008. Grey regions depict the geographic limits of the LSG distribution at four time periods (based on data provided by Parks Canada in 2010).

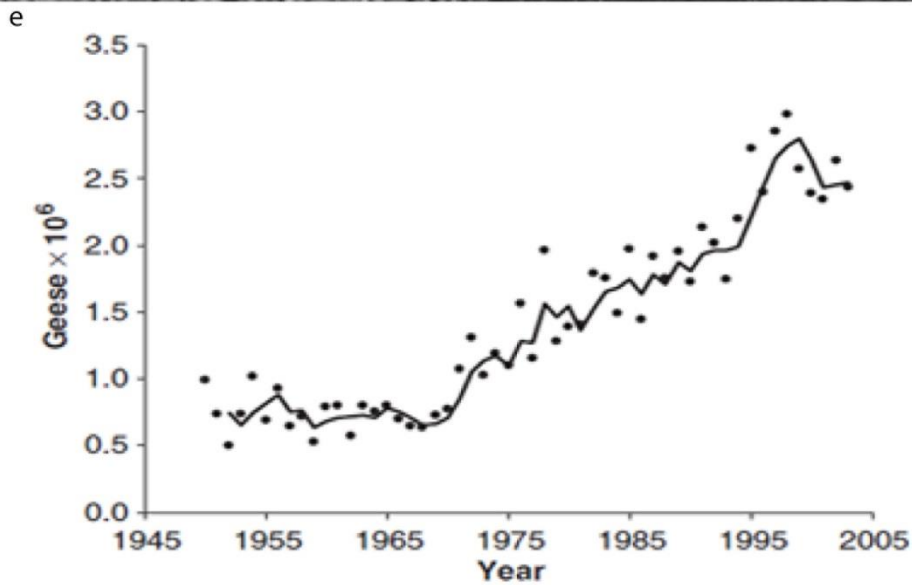
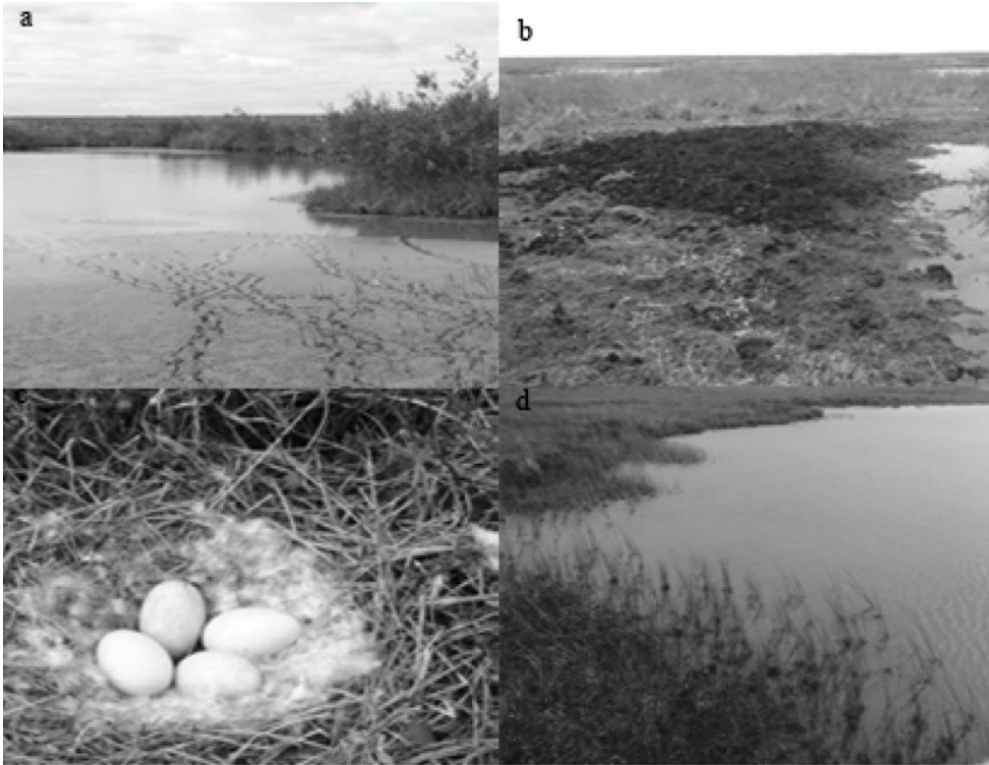


Figure 4.2: Photographs a), b) and c) depict LSG disturbance in and adjacent to ponds WAP 20 and WAP 21. Photograph d) is from WAP 12 and depicts a pond with low disturbance from the LSG population. Graph in panel e) is an estimate of LSG population rise (Abraham et al., 2005b pg. 843). The solid line is a 3-year running average.

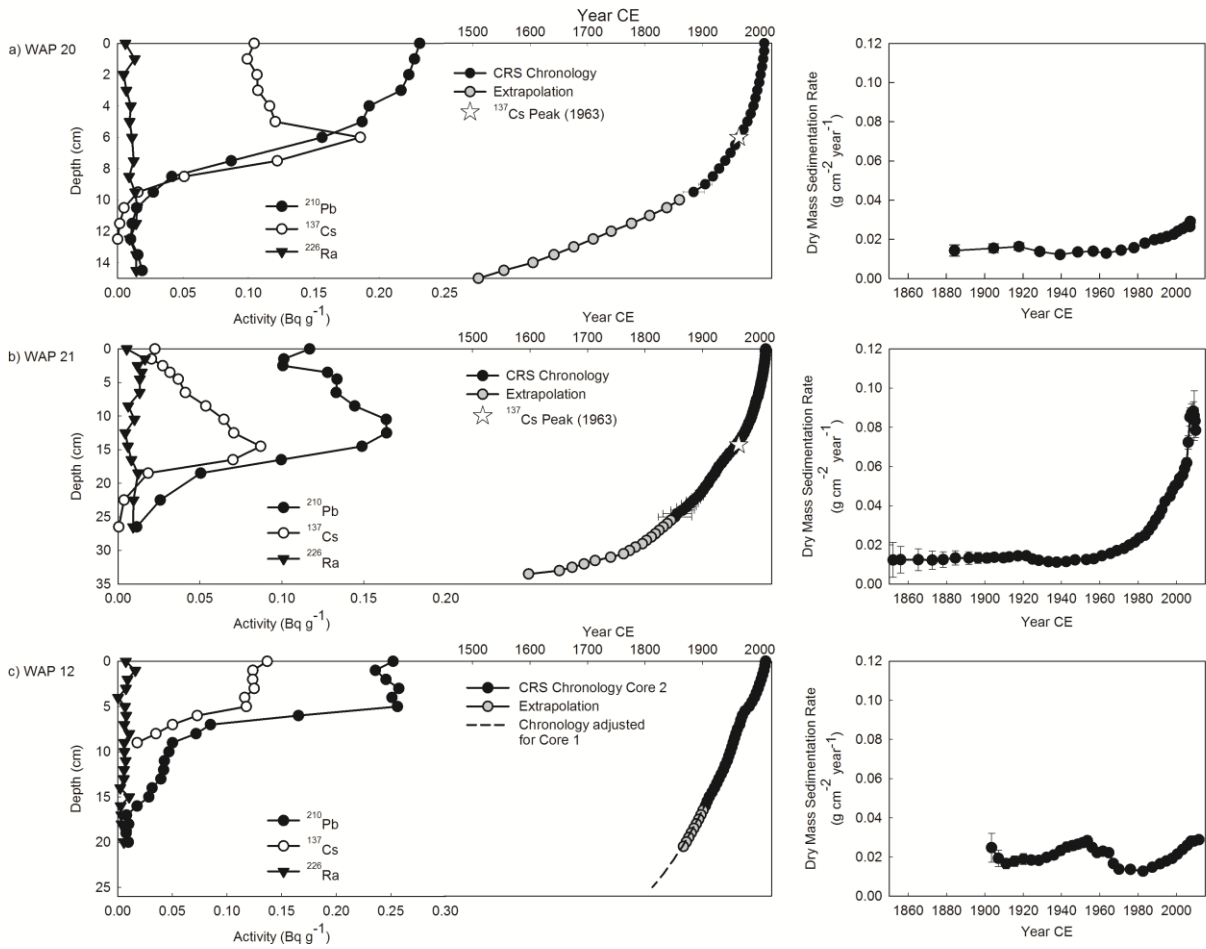


Figure 4.3: Left panels present scatterplots showing activity profiles for the radioisotopes and depth-age profiles for a) WAP 20, b) WAP 21 and c) WAP 12 sediment cores. Right panels present sedimentation rates. Error bars represent standard deviations.

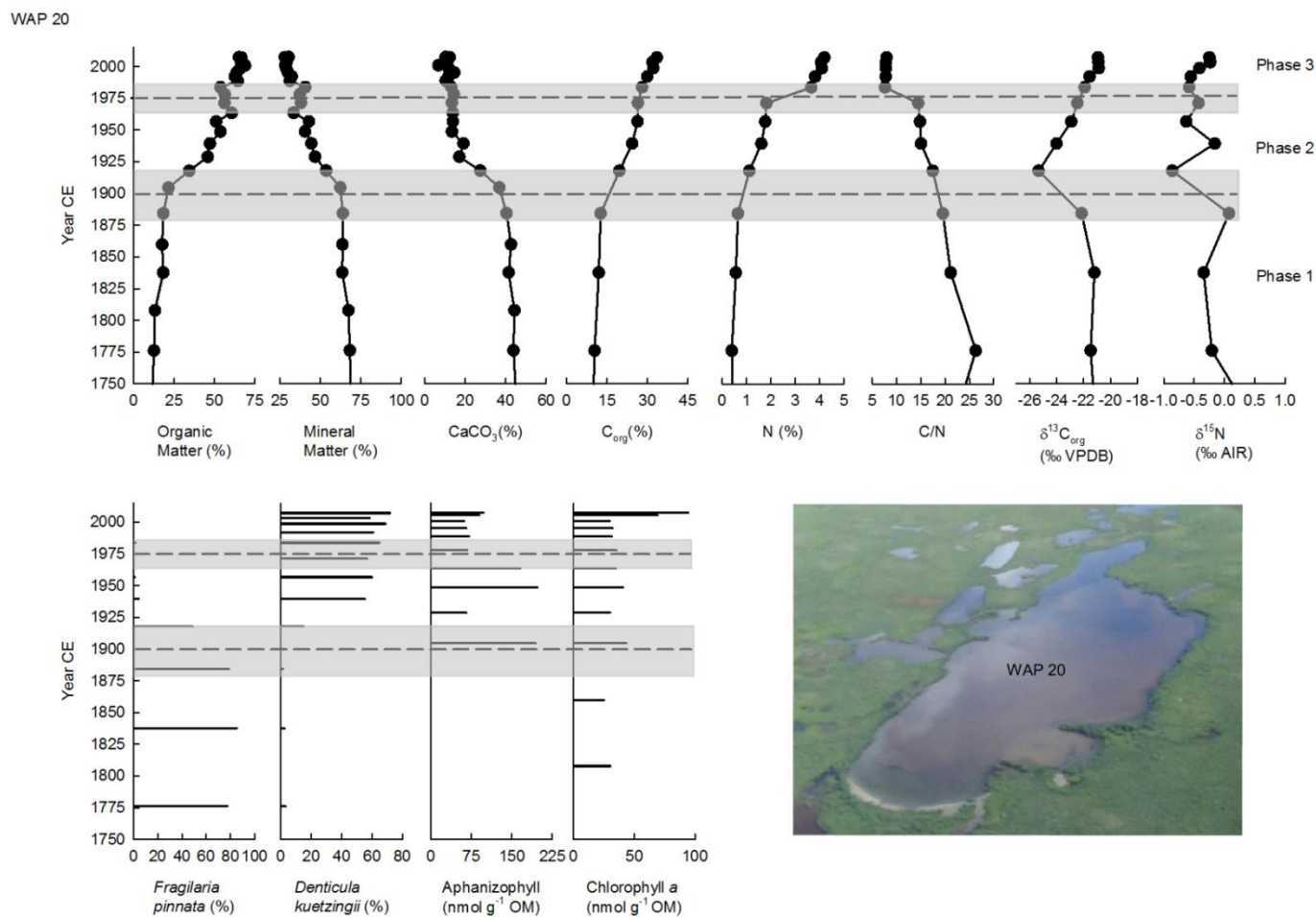


Figure 4.4: Stratigraphic profiles of selected paleolimnological variables for WAP 20. The vertical axis presents the age of the sediment core, as estimated from the ²¹⁰Pb analysis. The average fitted breakpoint date of physical and geochemical variables is shown by a dashed line with the relative error indicated with a gray bar. The breakpoints were also applied to diatom and pigment profiles.

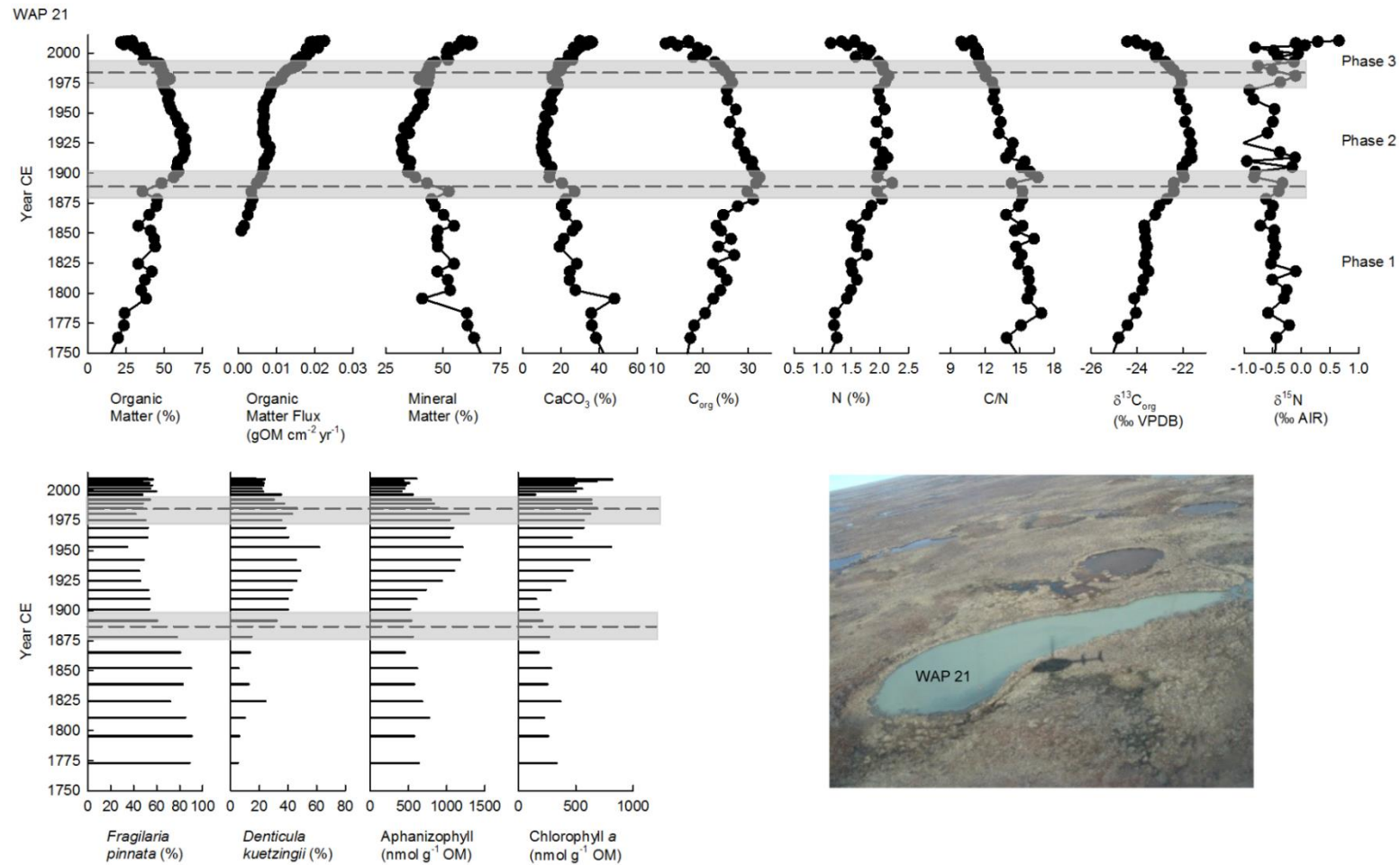


Figure 4.5: Stratigraphic profiles of selected paleolimnological variables for WAP 21. The vertical axis presents the age of the sediment core, as estimated from the ^{210}Pb analysis. The average fitted breakpoint date of physical and geochemical variables is shown by a dashed line with the relative error indicated with a gray bar. The breakpoints were also applied to diatom and pigment profiles.

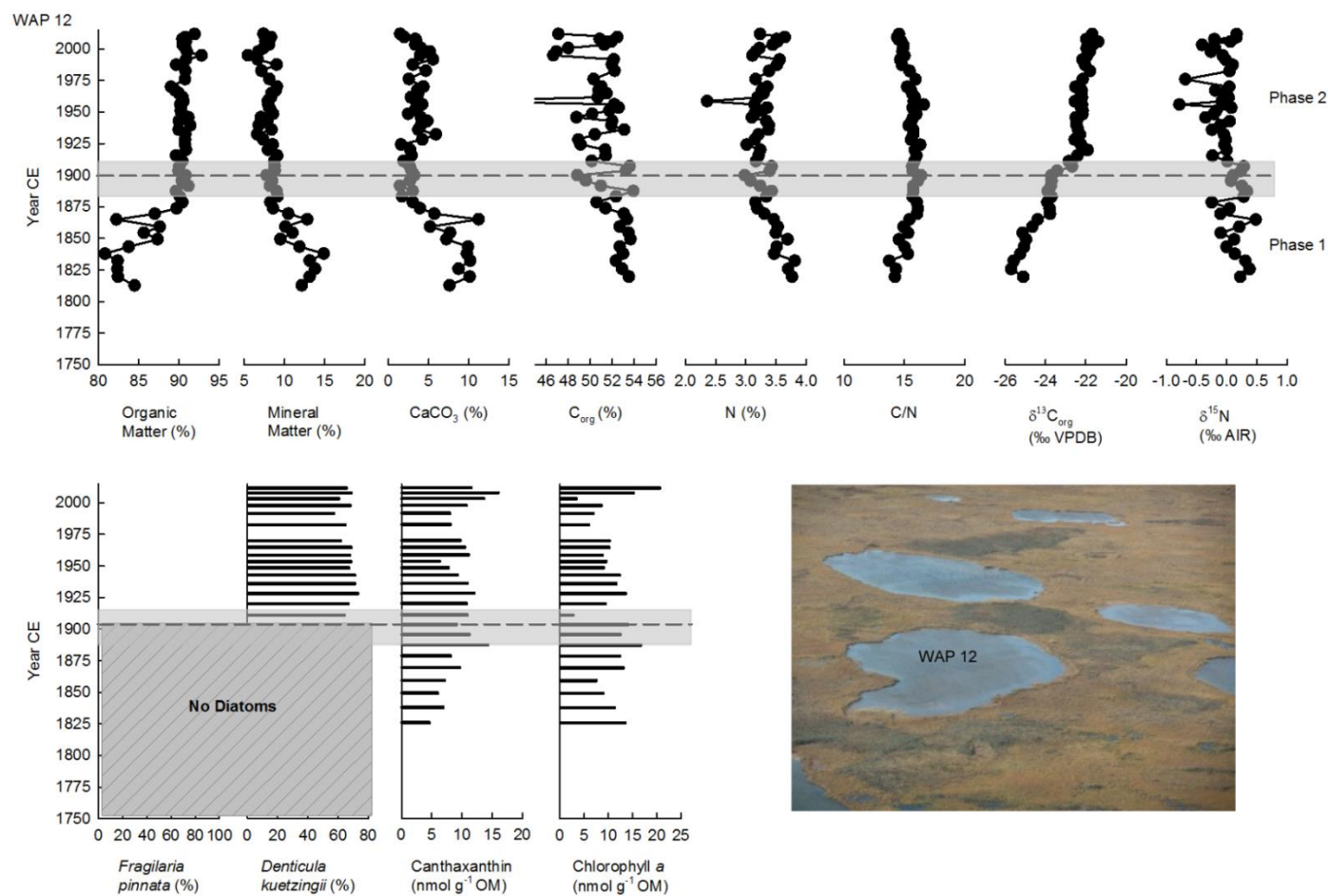


Figure 4.6: Stratigraphic profiles of selected paleolimnological variables for WAP 12. The vertical axis presents the age of the sediment core, as estimated from the ²¹⁰Pb analysis. The average fitted breakpoint date of physical and geochemical variables is shown by a dashed line with the relative error indicated with a gray bar. The breakpoints were also applied to diatom and pigment profiles.

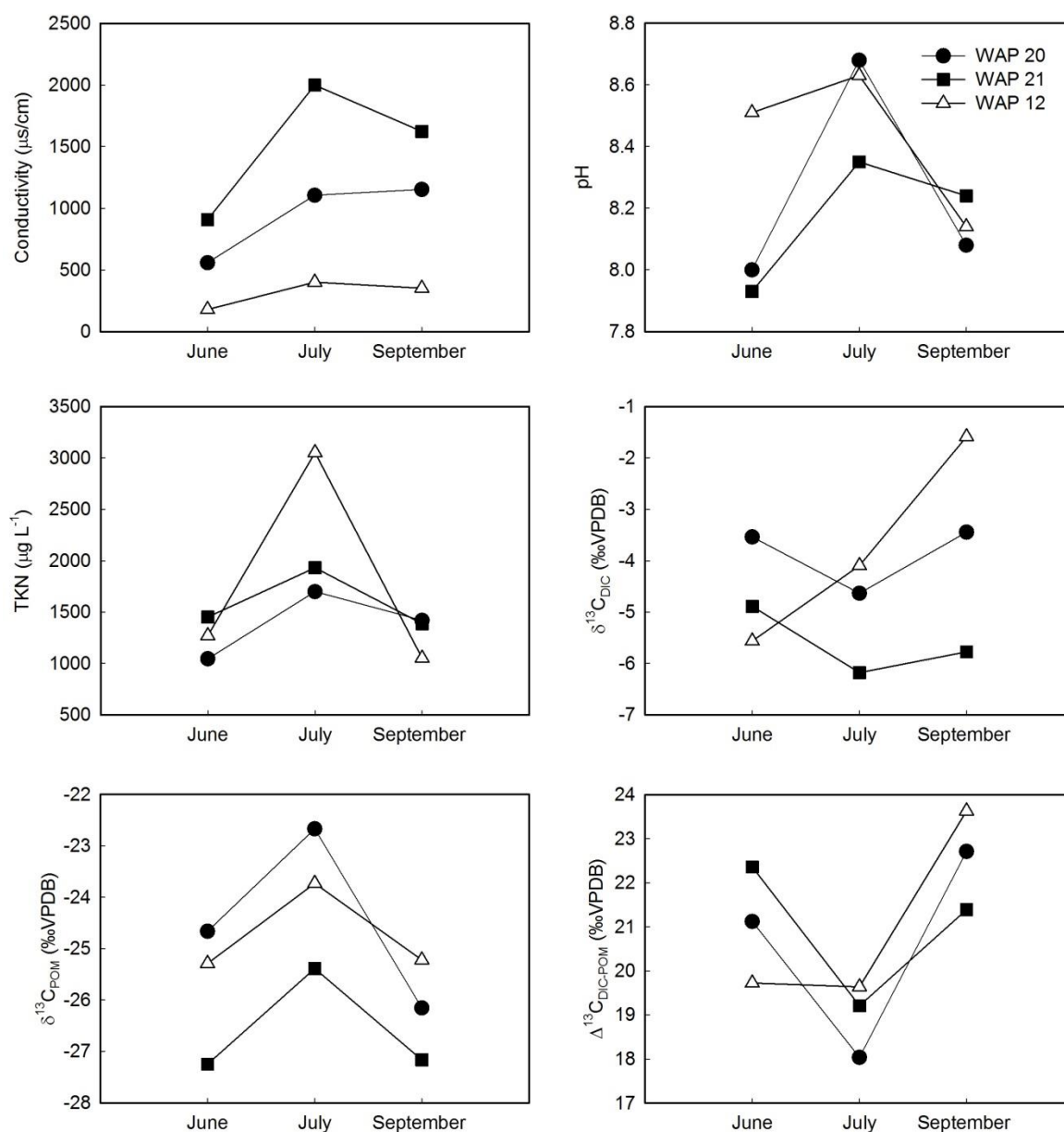


Figure 4.7: Line plots depicting average seasonal values for selected limnological parameters of ponds WAP 20, WAP 21 and WAP 12 based on findings of MacDonald et al. (2014). Values represent the average of samples collected in early June 2010-2012, late July 2010-2012 and mid-September 2010-2012. Values for WAP 12 July do not include July 2010 as the pond desiccated, and thus, samples could not be collected.

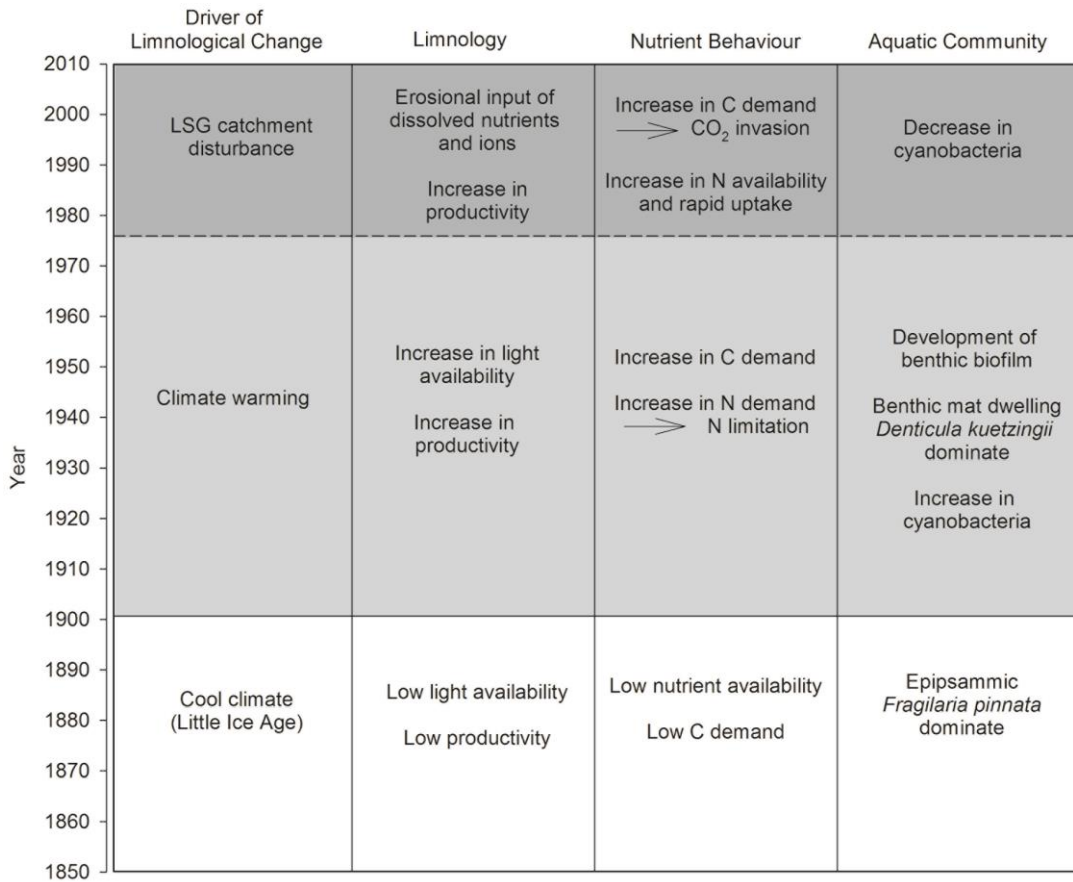


Figure 4.8: Depiction of the inferred evolution of pond limnology, nutrient behaviour, and aquatic community in response to the different drivers of change. The solid horizontal line represents the limnological regime shift that all ponds experienced in response to climate warming and the dashed horizontal line represents the limnological regime shift that only the LSG disturbed ponds (WAP 20 and WAP 21) experienced.

4.7 Tables

Table 4.1: Analytical strategy for the sediment cores.

Analysis	WAP 20	WAP 21	WAP 12
Loss-on-Ignition	Core 2, Core 3, and Core 5 Every 0.5-cm interval	Core 1 Every 0.5-cm interval	Core 1 and Core 2 Every 0.5-cm interval
Chronology	Core 3 Every fourth 0.5-cm interval	Core 1 Every second 0.5- cm interval	Core 2 Every second 0.5- cm interval
Geochemistry	Core 3 Every second 0.5- cm interval	Core 1 0-19 cm: every second 0.5-cm interval 19- bottom: every 0.5-cm interval	Core 1 Every 0.5-cm interval
Diatoms	Core 3 Every second 0.5- cm interval	Core 1 Every second 0.5- cm interval	Core 1 Every second 0.5- cm interval
Pigments	Core 2 Every second 0.5- cm interval	Core 1 Every second 0.5- cm interval	Core 1 Every second 0.5- cm interval

Table 4.2: The most sensitive limnological and paleolimnological parameters for identifying regime shifts from climate warming and LSG population expansion based on this study.

Stressor	Paleolimnology		Limnology	
	Parameter	Interpretation	Parameter	Interpretation
Climate Warming	organic matter content diatoms	<ul style="list-style-type: none"> • Increase reflects increasing productivity • Switch in dominance from episammic to benthic mat-dwelling taxa (e.g., <i>Fragilaria pinnata</i> to <i>Denticula kuetzingii</i>) indicates habitat shift 	n/a	n/a
	pigments	<ul style="list-style-type: none"> • Appearance of cyanobacteria pigments (e.g., aphanizophyll) suggests N-limited conditions 		
Lesser Snow Goose Expansion	$\delta^{15}\text{N}$	<ul style="list-style-type: none"> • Increase from 0‰ suggests increased N availability and increased productivity 	$\delta^{13}\text{C}_{\text{DIC}}$	<ul style="list-style-type: none"> • Mid-summer decline suggests chemically-enhanced CO_2 invasion due to high productivity and high C demand
	pigments	<ul style="list-style-type: none"> • Decrease in cyanobacteria pigment abundance suggests increased N supply 	$\Delta^{13}\text{C}_{\text{DIC-POM}}$	<ul style="list-style-type: none"> • Decrease in values to below 20‰ suggest high C demand
	$\delta^{13}\text{C}_{\text{org}}$	<ul style="list-style-type: none"> • Decrease suggests chemically-enhanced CO_2 invasion due to high productivity and high C demand 	conductivity	<ul style="list-style-type: none"> • High values due to erosional input of dissolved ions

Chapter 5: Paleolimnological assessment of riverine and atmospheric pathways and sources of metal deposition in a floodplain lake (Slave River Delta, Northwest Territories, Canada)

5.1 Introduction

As resource development has increased in northern Canada, so too have concerns regarding effects of associated pollutants on environmental and human health (e.g., Arctic Monitoring and Assessment Programme, 1998; Schindler, 2010). Determining the extent of pollution can be complicated because many contaminants of concern, including organic pollutants, heavy metals and radioactive substances, may come from a variety of industrial sources (CACAR, 2003), and they can be transported to northern communities and ecosystems by multiple pathways including via air and water. Further complexities may arise for those communities and ecosystems that are located near to where natural sources of these contaminants are also present (e.g., Hall et al., 2012). Unfortunately, environmental monitoring programs are often initiated long after resource development has already begun. Without knowledge of baseline, reference conditions, it is difficult or impossible to distinguish industrial-derived pollutants and their pathways from those contaminants that may be supplied from natural sources and processes of transport acting within the watershed (Bowman and Somers, 2005; Hawkins et al., 2010).

The Slave River Delta (SRD), Northwest Territories, is an important floodplain landscape located downstream and downwind of major resource developments (Figure 5.1). Here, concerns of the local community have been growing regarding the potential far-field effects of oil sands mining activities in northern Alberta (Campbell and Spitzer, 2007; Wesche, 2007, 2009). In fact, the region that includes the Slave River and SRD is part of Environment Canada's 'Phase 2' Integrated Monitoring Plan for the Oil Sands in recognition of the possibility for far-field transport and accumulation of oil sands contaminants

(Environment Canada, 2011). These concerns prompted our study. As part of an initiative led by the Slave River and Delta Partnership [<http://www.nwtwaterstewardship.ca/node/74>], we launched a paleolimnological project to assess the nature of polycyclic aromatic compound (PACs; Elmes et al., In Review) and metal (this study) deposition at the SRD, building on the success of similar studies at the Peace-Athabasca Delta (PAD; Hall et al., 2012; Wiklund et al., 2012, 2014). In the absence of direct measurements, paleolimnological investigations offer one of the very few methods to establish pre-development baseline, or reference, conditions for contaminants in aquatic ecosystems, which are necessary to identify pollution from industrial activity (e.g., Kurek et al., 2013). Although paleolimnological results from the PAD suggested that both fluvial and airborne pollution from industrial development of the Alberta oil sands are unlikely to reach the more distant SRD (Hall et al., 2012; Wiklund et al., 2012; 2014), no knowledge exists of baseline conditions of contaminant deposition in the SRD. Nor is there knowledge of whether oil sands and other sources of contaminants derived from *natural processes* occurring upstream along the Athabasca and Peace rivers are present in the delta. Over 100 km of the Athabasca River and its tributaries contain shoreline exposures of the bitumen-rich McMurray Formation. Natural erosion of these strata was identified as the overwhelming source of ‘river-transported bitumen-associated’ PACs that are deposited in floodplain lake sediments of the Athabasca Delta (Hall et al., 2012). And, the Peace River has also been identified as a source of natural, petrogenic PACs supplied to the northern Peace sector of the PAD (Jautzy et al., 2015). During the course of the present study, we also recognized that pollutants from other northern resource developments may be contained in SRD lake sediments, including arsenic (As) from gold smelting emissions at Giant Mine near Yellowknife (Figure 5.1; Hocking et al., 1978).

Deltas are hydrologically-complex landscapes but have the potential to record and archive, in their floodplain lake sediments, contaminants that are derived from multiple pathways. For example, in the PAD, Hall et al. (2012) used lowland floodplain lake sediment records to examine PAC deposition delivered by river floodwaters during high flood frequency intervals before and after onset of oil sands development, and Wiklund et al. (2012) used an upland lake sediment record beyond the reach of river floodwaters to reconstruct temporal changes in atmospheric deposition of metals to the area. Here, we utilize an exceptionally detailed pulse-flood record from a lake in the SRD to improve knowledge of metal deposition via fluvial processes from analysis of sediment intervals deposited during periods of high flood frequency *and* metal deposition by atmospheric transport from analysis of sediment intervals deposited during periods of low flood frequency. We incorporated the approaches described by Wiklund et al. (2014) for accurate interpretations of the extent of pollution, which includes normalizing metal concentrations to Li to account for variations in grain size and mineralogy (Loring, 1991; Kersten and Smedes, 2002) that occur over time and space in deltas and other depositional environments with widely varying energy conditions. We apply this method to establish baseline concentrations of metals, assess temporal patterns of change in relation to depositional processes and pathways, and determine whether there is evidence of pollution from resource development to this remote northern landscape.

5.2 Methods

Study Site

The SRD is a large floodplain landscape (~400 km²) with abundant forests, channels, wetlands and small lakes that span broad hydrological gradients and provide important habitat for a diverse array of wildlife and resources, and which support the traditional lifestyle of the mainly First Nation community of Fort Resolution (English et al., 1997; Brock et al., 2007; Sokal et al., 2008). The SRD has formed in response to deposition of sediment by the Slave River where it enters Great Slave Lake. The Slave River originates north of the PAD where the Peace River and Rivière des Rochers meet in northern Alberta, and its watershed includes the Peace and Athabasca rivers (Figure 5.1). Approximately two-thirds of annual Slave River discharge is derived from the Peace River and the remaining third comes from other north-flowing tributaries in the PAD, including Rivière des Rochers, Revillon Coupé, and Chenal des Quatre Fourches, which carry flow from the Athabasca River and Lake Athabasca (English et al., 1997).

In this study, we utilize the recent (post-1920s) sediment record from lake ‘SD2’ (61°16'56.21"N, 113°34'55.51"W), which is a small (~1.2 km²), shallow (maximum depth ~1.5 m) flood-dominated lake in the SRD (Figure 5.1). SD2 is pivotally located at a sharp bend in the Slave River where it divides into multiple distributary channels, making the lake prone to receive river floodwaters during spring ice-jam events. Prior paleolimnological studies using a diverse set of indicators revealed SD2 contains a very detailed record of 20th century Slave River flood history that corresponds well with temporal patterns evident in river discharge data and with local traditional knowledge of flood events (Brock et al., 2010).

Sediment Core Collection

A 48-cm long sediment core was retrieved from SD2 in September, 2011 using a Glew (1998) gravity corer fitted with a Lucite tube (7.62 cm inner diameter). The core was transported to Deninu School in Fort Resolution and sectioned into 1.0-cm intervals using a vertical extruder (Glew, 1998). All samples were sealed in Whirl-Pak® bags and stored in the dark at 4°C during shipping and until analysis.

Sediment Core Analyses

Chronological (^{137}Cs) and geochemical (organic carbon and nitrogen elemental and isotope composition) results used to reconstruct the lake's flood history to the early 20th century are reported in Elmes et al. (In Review). For metal analyses, subsamples from every 1-cm interval of freeze-dried sediment from the core were analyzed at ALS Canada Ltd (Edmonton) following the method EPA 200.2/6020A and EPA 200.2/245.7 (total Hg). Metals that we report results for include the 13 priority pollutants under the US Environmental Protection Agency's Clean Water Act (Sb, As, Be, Cd, Cr, Cu, Pb, Hg, Ni, Se, Ag, Tl and Zn), as well as V, a key metal of concern associated with the Alberta oil sands development (Jacobs and Filby, 1982; Reynolds et al., 1989; Gosselin et al., 2010). As explained below, we also report Li for the purposes of normalizing metal concentrations to variations in grain size and mineralogy.

Stratigraphic and Numerical Analyses

To assess temporal changes in metal concentrations in the SD2 sediment core, we first explored stratigraphic patterns in relation to intervals of high and low flood frequency,

as defined by Elmes et al. (In Review). Then, we followed normalization approaches using Li outlined by Wiklund et al. (2014) to account for the negative correlation of grain size and metal concentration (Loring, 1991; Kersten and Smedes, 2002) because SD2 is subject to varying energy conditions that result in grain-size variations.

To assess potential for metal pollution in SD2 sediments from the oil sands development, we assumed Slave River floodwaters are the predominant pathway, because evidence indicates atmospheric supply of contaminants has not become elevated at the PAD, which is located ~300 km closer to the mining activity (Hall et al., 2012; Wiklund et al., 2012). First, we developed linear relations for pre-1967 (year commercial oil sands development began; Gosselin et al., 2010) lake sediment metal concentrations relative to Li concentration using samples within high flood frequency intervals (Figure 5.2). And, we established 95% prediction intervals (PI) about this relation to define the natural range of variation in normalized metal concentrations in sediments supplied by the Slave River. Due to the possibility of multiple sources of metals (e.g., eroded from metal-bearing deposits along the Athabasca and Peace rivers), we did not force regressions through the origin, as is commonly done when only one source is expected (e.g., Loring and Rantala, 1992; Wiklund et al., 2014). Second, we evaluated post-1967 sediment metal concentrations for samples within high flood frequency intervals against the baseline constructed from the pre-1967 oil sands development intervals of high flood frequency. We also assessed metal concentrations during low flood frequency intervals against the pre-1967 oil sands development baseline because of the possibility that flood-derived sediment in SD2's catchment may be subsequently mobilized and deposited in the lake by snowmelt and rainfall runoff or by blowing dust. If >2.5% of post-1967 lake sediment samples fall above the upper 95% PI, this

identifies an additional source of the metal (Loring, 1991; Kersten and Smedes, 2002), possibly due to oil sands pollution. Third, we re-expressed these data as time-series plots of residuals about the metal-Li relation, which provides an ability to assess temporal trends of past *and* ongoing monitoring data relative to the baseline (residual = 0) (see Wiklund et al., 2014). In these residual plots, we used linear extrapolation of the widest PI for the pre-1967 samples as a benchmark to assess for pollution, as described in Wiklund et al. (2014).

Atmospheric emissions from the Giant Mine increased rapidly beginning in the 1950s and then decreased rapidly after this decade following implementation of emission control measures (Hocking et al., 1978). To assess potential for As pollution from Giant Mine during the 1950s, we modified the methods described above (and in Figure 5.2) because Giant Mine pollution to the SRD would be primarily by atmospheric pathways and the evidence of pollution would be best captured in the stratigraphic record during times of reduced river flooding rather than in sediments deposited at times of frequent flooding. To do this, we developed baseline As-Li relations and PIs based on pre-1950s and post-1960s samples deposited during periods of low flood frequency. The 1950s was a low flood frequency interval in the SD2 stratigraphic record and As data from this interval were examined against the low flood frequency As-Li baseline, and then subsequently re-expressed as a time-series plot of residuals about the As-Li relation.

5.3 Results

Temporal Patterns of Change

Variations in C/N ratios in the SD2 sediment record are driven by paleohydrological conditions, where high ratios represent intervals of increased allochthonous organic matter

supplied by river floodwaters and low ratios represent intervals of greater autochthonous organic matter from in-lake production (Brock et al., 2010). Based on these data and a sediment chronology linearly extrapolated by depth from the 1963 ^{137}Cs peak at 26.5 cm (Elmes et al., In Review), intervals of high flood frequency include ~1926-1928 (46-45 cm), ~1931 (43 cm), ~1935-1950 (41-33 cm), ~1963-1968 (26-23 cm), ~1974 (20 cm), ~1986-1994 (13-9 cm) and ~1999 (6 cm). Intervals of low flood frequency include ~1924 (47 cm), ~1930 (44 cm), ~1933 (42 cm), ~1952-1961 (32-27 cm), ~1970-1972 (22-21 cm), ~1975-1985 (19-14 cm), ~1996-1998 (8-7 cm) and ~2001-2011 (5-0 cm) (Elmes et al., In Review). These results, and the reconstruction of past variability in flooding, are similar to the previously published record from SD2 (Brock et al., 2010). Notably, the interval from ~1952-1961 has the lowest C/N ratios in the stratigraphic record. Brock et al. (2010) identified that lake levels during this interval were extremely low (5-15 cm) based on the presence of *Sagittaria cuneata* seeds, a consequence of an extended period with minimal influence of Slave River flooding.

The stratigraphic profiles for the 13 priority pollutant metals and V show prominent temporal variations, and are largely mirror images to that of the C/N profile (Figure 5.3). Stratigraphic intervals with high C/N ratios (i.e., high flood frequency) typically have relatively low concentrations of metals and, conversely, stratigraphic intervals with low C/N ratios (i.e., low flood frequency) tend to have relatively high concentrations of metals (Figure 5.3). Peak concentrations for the majority of metals occur during the late 1950s (low C/N ratios, low flood frequency), which is especially evident in the As profile. In contrast, lowest metal concentrations occur during the late 1930s, 1940s and 1990s, which are intervals of high flood frequency. Independent samples t-tests show that concentrations of all metals,

except As, are significantly higher (at $\alpha = 0.05$) in sediments deposited post-oil sands development compared to those deposited pre-development. However, our analyses of the core from SD2 included a greater number of low flood frequency samples after 1967 (16) than before 1967 (9), which confounds the comparison because grain size exerts strong influence on sediment metal concentrations and highlights the need for normalization.

Assessment of Metal Pollution

To evaluate the magnitude of pollution since onset of oil sands development, baseline concentrations normalized to Li were determined from pre-1967 samples within C/N-ratio defined high flood frequency intervals (solid circles in Figure 5.4; See Appendix D Tables D2 and D3). In these samples, all metals show strong linear relations with Li (average $r^2 = 0.801$, not including As; As-Li $r^2 = 0.217$, see below), and reflect the relationship between grain-size variations and metal concentrations. Post-1967 metal concentrations from high flood frequency intervals tightly cluster along the regression lines, overlap with the pre-1967 data, and plot within the 95% PIs established from pre-1967 high flood frequency intervals, with the exception of two analyses (Be, Hg; open circles in Figure 5.4). Metal concentrations from post-1967 low flood frequency intervals show similar distributions, with five values positioned above the 95% PI (Cr, Hg, Se and two for V) and one value positioned right on the 95% PI (Be). Distributions of pre-1967 metal concentrations from low flood frequency intervals tend to be well characterized by the relation established for the pre-1967 high flood frequency intervals, with the notable exception of several As concentrations.

To better visualize the timing of when Li-normalized metal concentrations exceeded the upper 95% PI, the residuals (i.e., the perpendicular distance of metal concentrations from

the metal-Li regression line) were plotted in a temporal sequence (Figure 5.5). During the post-1967 oil sands development era, two analyses from the high flood frequency intervals (Be in 1994 and Hg in 1990) and six analyses from the low flood frequency intervals (Be in 2003, Cr in 1970, Hg in 1977, Se in 2011, V in 1970 and 2009) exceed the upper 95% PI. These eight exceedances represent 2.38% of total metal analyses in samples deposited since onset of oil sands development ($n = 336$), which provides no evidence that they have been enriched by oil sands pollution. On the other hand, it was more common for the residual values of metals to exceed the 95% PI in low flood frequency samples deposited during the 1950s *prior* to the oil sands development era, especially for As (but also Sb, Cr, Se, Tl and V). This observation, combined with prior knowledge that this decade was characterized by extremely low flood frequency (Brock et al., 2010), suggests that a pathway of contaminant transport other than by river flooding may have been important during this pre-oil sands development time period – namely via the atmosphere .

To explore further the high sediment As concentrations during the 1950s, we determined the atmospheric baseline for As-Li from the linear relation and PIs derived from low flood frequency samples deposited pre-1950 and post-1960 (Figure 5.6). Based on this relation, four of the five samples deposited during the 1950s contain unusually high As concentrations (i.e., exceeded the upper PI in 1954, 1955, 1957 and 1959). The As concentrations in these samples are above the Threshold Effects Level (5.9 mg kg^{-1} ; CCME, 2014), which we attribute to far-field emissions from gold smelting at Giant Mine, as further discussed below.

5.4 Discussion

Processes and Pathways of Metal Deposition at SD2

Metal concentrations in the stratigraphic record from lake SD2 show marked fluctuations associated with variations in paleohydrological conditions, yet the apparent relations may seem somewhat unexpected. High sediment metal concentrations are associated with intervals of *low* flood frequency, whereas low concentrations are present in intervals of *high* flood frequency. This inverse relationship contrasts with delivery of ‘river-transported bitumen-associated’ PACs to lakes ‘PAD23’ and ‘PAD31’ in the Athabasca Delta, where flood deposits were enriched in these contaminants compared to lacustrine sediments deposited in the absence of flooding (Hall et al., 2012), but is consistent with variations of ‘river-transported bitumen-associated’ PACs in the SD2 stratigraphic record (Elmes et al., In Review). Evidently, sediment-laden floodwaters from the Slave River that enter SD2 are relatively diluted in metals and organic contaminants in comparison to Athabasca River floodwaters that enter PAD23 and PAD31 at the Athabasca Delta. Although contributions of sediment from the Peace River may account for these differences, SD2 may simply receive a greater proportion of coarser-grained sediment during flood events that has relatively lower concentration per mass of sediment in comparison to finer-grained sediment that enters PAD23 and PAD31 during Athabasca River flood events. Supporting this notion is that SD2 is located immediately adjacent to the Slave River and, thus, likely receives higher-energy flows in comparison to the more ‘off-line’ hydrological settings of PAD23 and PAD31. Relatively higher metal concentrations during low flood frequency intervals in the SD2 sediment record may reflect finer-grained flood-derived sediment with relatively higher metal concentration per unit mass that was stored on the lake’s catchment and re-mobilized

during spring snowmelt or intense rain runoff events. Studies of additional lake sediment core records in the SRD along a gradient of flood intensity are required to further disentangle the influence of hydrological processes on floodplain metal stratigraphy. Clearly, however, these relations demonstrate that knowledge of paleohydrological conditions is crucial to the interpretation of the depositional history of metals at SD2, as has also been demonstrated in the PAD (Hall et al., 2012; Wiklund et al., 2012), and reflects the complex nature of contaminant deposition in lakes of deltas and floodplains. Although most of the variation in metal concentrations in the stratigraphic profile from SD2 can be explained by river floodwaters and their influence on grain size and associated metal content, paleohydrological knowledge was also key to inform that enrichment of some metals, most notably As (but possibly also Sb, Cr, Se, Tl and V), likely occurred via atmospheric pathways during the 1950s.

In the absence of direct measurements, paleolimnological records of contaminant concentrations in locations where there are natural sources of contaminants provide unique opportunity to characterize baseline conditions and inherent, natural variation in the deposition of contaminants. In the pulse flood stratigraphic record of SD2, we utilized high flood frequency intervals to define baseline concentrations of metals delivered by Slave River floodwaters prior to the onset of oil sands development *and* we used low flood frequency data prior to 1950 and after 1960 to define baseline concentrations of metals delivered by atmospheric pathways and detect deposition of metal pollution emitted from the Giant Mine during the 1950s. Paleohydrological knowledge was, thus, also key to applying this novel approach for assessment of pollution from both oil sands development and Giant Mine emissions, as further discussed below.

Assessment of Metal Pollution from the Alberta Oil Sands Industry

Community concerns in the SRD regarding pollution from the Alberta oil sands development have been mounting in response to previous research that has documented evidence of enhanced atmospheric deposition of heavy metals and PACs within a radius of at least 50-km from a defined center of the bitumen-upgrader facilities at the Alberta oil sands (Timoney and Lee, 2009; Kelly et al., 2009; 2010; Kurek et al., 2013; Kirk et al., 2014). Such concerns were the impetus for this study. However, post-oil sands development metal concentrations in both high flood and low flood frequency intervals from lake SD2 align with the determined pre-1967 oil sands development baseline concentrations. Of the 336 post-oil sands development samples measured in the SD2 stratigraphic record, only eight (~2.38%) exceeded the 95% PI. For all metals except As, concentrations in sediments deposited after onset of oil sands development were below the Interim Sediment Quality Guidelines for the Protection of Aquatic Life for those metals where this has been established which include: Cd (0.6 mg kg^{-1}), Cr (37.3 mg kg^{-1}), Cu (35.7 mg kg^{-1}), Pb (35.0 mg kg^{-1}), Hg (0.17 mg kg^{-1}) and Zn (123.0 mg kg^{-1}) (CCME, 2014). Arsenic exceeded the threshold concentration (5.9 mg kg^{-1} ; CCME, 2014) in the majority of samples deposited both before and since onset of oil sands development. Therefore, we conclude that sediment metal concentrations at SD2 have not been enriched by the Alberta oil sands development beyond natural, baseline concentrations. Instead, results indicate that accumulation of metals has occurred at SD2 via natural processes of fluvial transport and deposition for at least the past 90 years.

We note that generally higher metal concentrations post-1967 (except As), evident in both the stratigraphic plots (Figure 5.3) and from independent samples t-tests, clearly point to

the need to normalize metal concentrations to account for variations in grain size, and the need to determine pre-development baseline concentrations. Without such knowledge, it is impossible to evaluate properly time series of sediment metal concentrations for evidence of pollution due to human activities. For example, one might incorrectly associate the apparent rise in bulk metal concentrations in post-1967 samples to pollution from oil sands development, but the difference is simply a function of increased occurrence of finer-grained sediments deposited during intervals of lower flood frequency, which is likely a consequence of climate-driven decline of river discharge (Brock et al., 2010).

While lack of evidence for enhanced metal deposition associated with oil sands development at SD2 is consistent with findings in the PAD, which have assessed both fluvial and atmospheric pathways (Wiklund et al., 2012; 2014), absence of high flood frequency deposits in the most recent strata, which corresponds to a time of accelerated growth in the oil sands industry, does impose some limitations to our findings. Yet, some of the metals contained in the SD2 record delivered by fluvial pathways appear to be derived from elsewhere in the watershed, based on superimposing metal-Li concentrations in post-1967 high flood frequency sediments from SD2 on the baseline metal-Li relations developed by Wiklund et al. (2014) for river sourced-sediment in the Athabasca Delta (Figure 5.7). Li-normalized concentrations for Cd, Cr, Ni, Zn and V in sediments from SD2 consistently plot along unique trajectories at or just above the 95% PIs defined for these metals at the Athabasca Delta, suggesting that SD2 receives metals from sources that are enriched relative to those that supply the Athabasca River. A possible source is the Peace River, which contributes two-thirds of Slave River discharge. Differences in surficial geology of the watersheds of these rivers, including outcrops of coal seams in the Peace watershed identified

as a possible source of PACs that enter the northern Peace sector of the PAD during flood events (Jautzy et al., 2015), likely account for the differences in metal-Li relations in lake sediments at the SRD and PAD. These findings demonstrate that baseline metal concentrations established at one location by paleolimnological methods may not be directly transferrable to other landscapes, but they can be used to detect other potential sources of metal deposition.

Assessment of As Pollution During the 1950s

Although not the original intent of this study, elevated As concentrations identified during the extremely low flood frequency interval of the 1950s at SD2 necessitated further exploration. Assuming deposition via atmospheric pathways, and when plotted against baseline concentrations as determined from low flood frequency intervals pre-1950 and post-1960, four samples had unusually high As concentrations (1954, 1955, 1957 and 1959). After 1959, As concentrations decrease rapidly and return to baseline concentrations. These results indicate an additional source of As was deposited at SD2 during the 1950s.

At this time, the Giant Mine in Yellowknife (NWT) developed rapidly (Hocking et al., 1978; Figure 5.1). The gold deposit at Giant Mine is composed of arsenopyrite ore (AADNC, 2013) and to convert the arsenopyrite to roaster calcine and then to gold, highly toxic As vapour was released as a by-product. Arsenic pollution from Giant Mine has long been a concern for the city of Yellowknife. Consequently, many studies have assessed As in water, sediment, soil, snow, plants and animals in the Yellowknife region and found elevated concentrations (e.g., Hutchinson et al., 1982; Murdoch et al., 1989; Bright et al., 1996; Jackson et al., 1996; Koch et al., 2000; Andrade et al., 2010; Bromstad, 2011). However, to

our knowledge, none have identified As pollution from Giant Mine at more distant locations. Peak sediment As concentrations (19.1 mg kg^{-1}) at SD2 exceeded our defined baseline concentrations, as well as CCMEs Probable Effects Level (17.0 mg kg^{-1}). The timing of the peak is consistent with reported emissions from Giant Mine (Hocking et al., 1978; Figure 5.8). Furthermore, sediments containing the As peak were high in Sb, Ca and Sr concentrations, which are major volatile elements within the mineralogy of the Giant Mine ore deposit (arsenopyrite, stibnite within quartz-carbonate veins; Silke, 2013). In 1958, a two-stage roaster was installed to improve efficiency and recovery of pollutants, and a baghouse was constructed to reduce emission rates (Bromstad, 2011; AADNC, 2013). After these measures were undertaken, As emissions from Giant Mine decreased markedly and this appears to be captured by rapid decline in As concentration to baseline levels in the SD2 sediment record. We note that the timing of maximum As pollution from Giant Mine occurred during very low water levels at SD2. Absence of dilution of sediment-As concentrations by As-poorer sediment from Slave River floodwaters provided the ideal hydrological conditions for atmospheric-transport of pollution to be archived in the stratigraphic profile at this location. Given that Giant Mine is the closest major source of As emissions and the timing of peak sedimentary As concentrations at SD2 coincides with peak emissions from that mine, our findings suggest pollution from Giant Mine extended at least ~140 km to the south of Yellowknife.

Far-field As pollution from Giant Mine may also be evident in the PAD, given that it is likely the closest major point source of As emissions (Figure 5.8). Peak concentrations in residual As have similar timing, despite lower values in lake 'PAD18', an elevated precipitation-fed lake situated ~20 km north of the town of Fort Chipewyan in the Peace

Delta (Wiklund et al., 2012) and ~430 km south of Giant Mine. By the late 1950s, residual As concentrations in PAD18 also decreased, but more gradually than observed in SD2. The gradual decline in PAD18 versus the sharp decline in SD2 may reflect the very different hydrological settings of the two basins. While emissions declined, a return to high flood frequency may have substantially diluted the As concentrations at SD2 with river-transported sediment from unaffected areas, leading to an abrupt decline in the As stratigraphic record. In contrast, PAD18 remained precipitation-fed and perhaps more accurately portrays reduction in atmospheric transport of Giant Mine As emissions.

5.5 Conclusions

Paleohydrological reconstruction based on measurements made on a sediment core from a flood-dominated lake in the Slave River Delta provided necessary context to develop baseline concentrations of metals delivered by fluvial and atmospheric pathways for assessing pollution from regional mining point sources. Since onset of Alberta oil sands development (post-1967), concentrations of metals in both high and low flood frequency intervals, normalized to Li to account for variations in grain size and mineralogy, were within the natural range of variability defined by pre-1967 high flood frequency interval metal concentrations. These results indicate that oil sands development has not yet enriched sediment metal concentrations above natural levels conveyed by Slave River floodwaters to lake SD2. Indeed, our study demonstrates that metals have naturally accumulated in the SRD for at least ~90 years, although greater concentrations are found in finer-grained sediments that are re-deposited from the lake's margins during periods of low flood frequency. Comparison to baseline metal-Li relations developed for the lower Athabasca River reveal

that fluvial-derived metals in SD2 sediments may in fact be derived from other source(s) in addition to the Athabasca River. Erosion of metal-bearing deposits along the Peace River is a likely source because the Peace River supplies two-thirds of the Slave River's flow. Importantly, our analysis revealed elevated As concentrations were captured in the lake sediment record during the 1950s when water levels were extremely low at SD2 and floods were not frequent, suggesting transport from a source of pollution via the atmosphere. Residual As, calculated after defining background Li-normalized As concentrations from pre-1950 and post-1960 low flood frequency intervals, showed strong correspondence with As emission history from Giant Mine, located ~140 km to the north, suggesting a much broader atmospheric pollution footprint during the early phase of mine operation than has previously been recognized. Despite complex hydrological environments of floodplain lakes, their sediments provide a detailed and informative record of pathways and processes of contaminant deposition, as needed to identify sources of pollution.

5.6 Acknowledgements

Research was funded by the Government of the Northwest Territories Cumulative Impacts Monitoring Program and Aboriginal Affairs and Northern Development Canada Northern Scientific Training Program. We thank Erin Kelly and the Slave River and Delta Partnership for providing us with the opportunity to conduct this research, staff at Deninu School in Fort Resolution for providing us with the space to section our sediment cores and the opportunity to share our research with students, and Gaby Lafferty for field assistance.

5.7 Figures

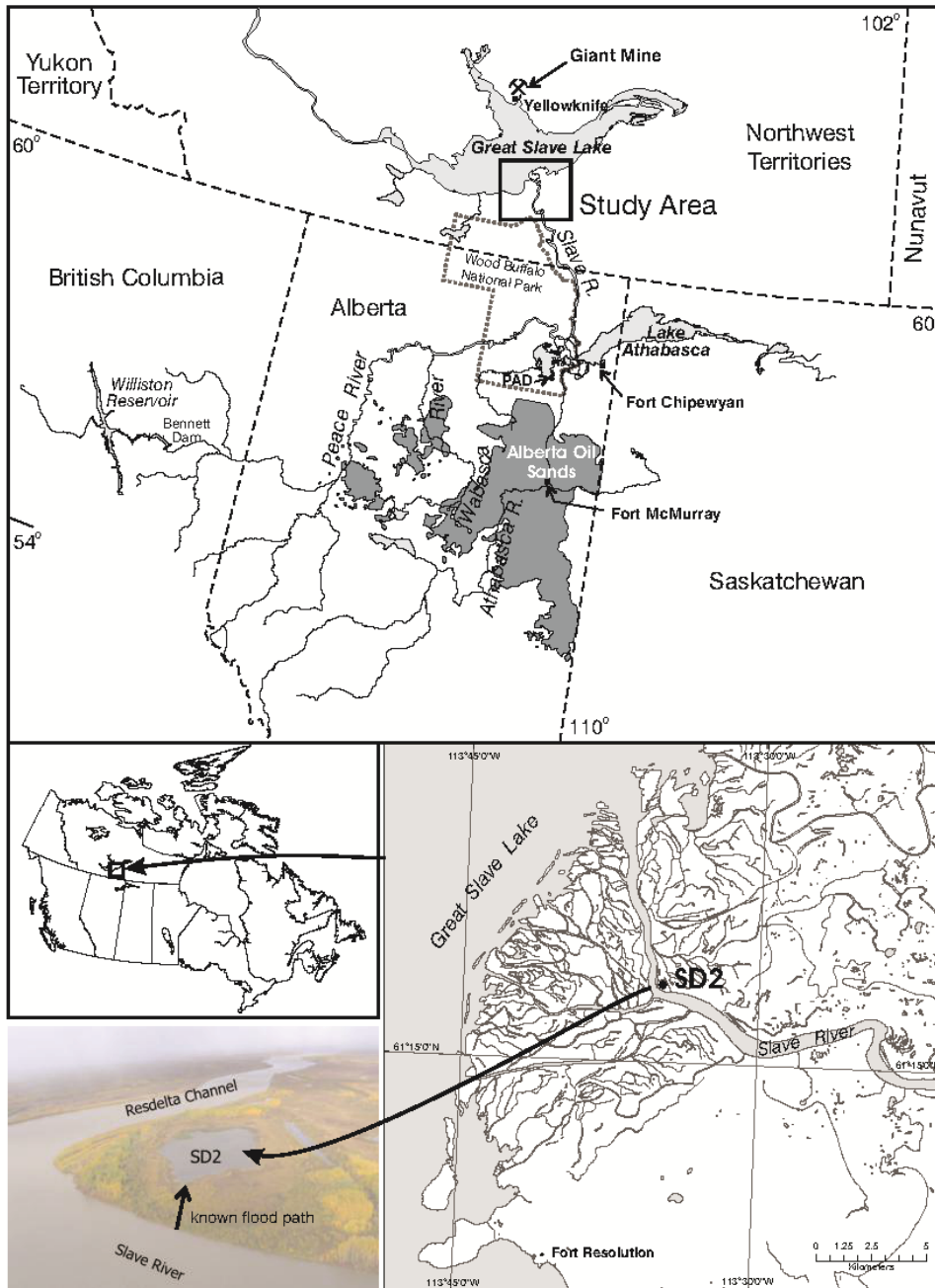


Figure 5.1: Maps and photo showing the Slave River Delta (Northwest Territories, Canada) and the study lake (SD2). The Slave River Delta is located downstream of the Alberta oil sands development and downwind of Giant Mine, a former gold mine near Yellowknife, NWT.

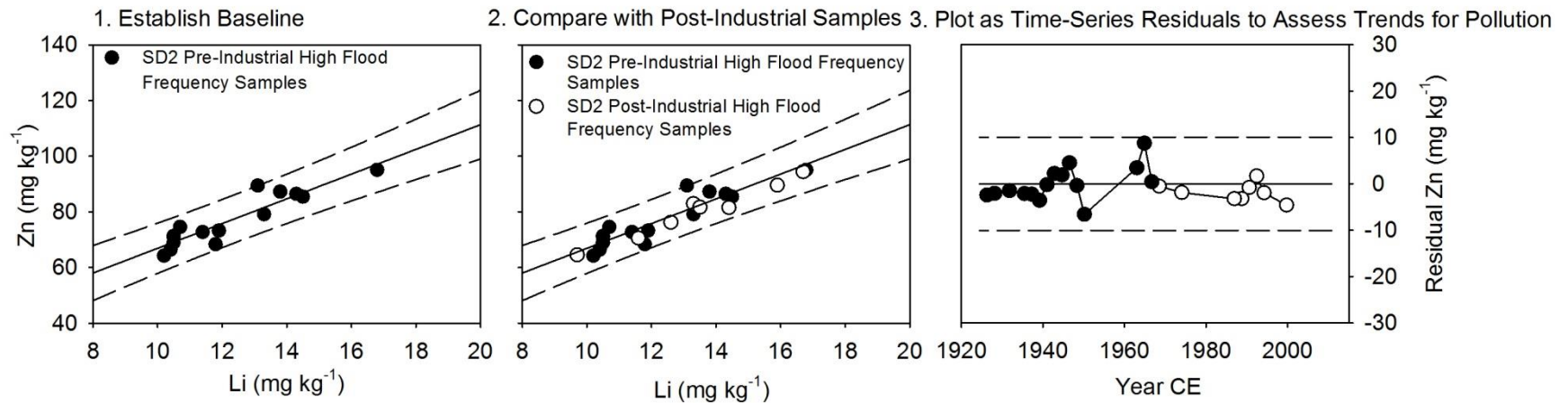


Figure 5.2: Schematic diagram showing the Three-Step approach to assess metal pollution (e.g., zinc) from analyses of pre-development sediments supplied by floodwaters to flood-prone lakes. In the first step, we characterize baseline metal concentrations in river sediment by analyzing metal concentrations in pre-development lake sediments deposited by floodwaters. To do this, we develop linear relations for pre-development lake sediment metal concentrations relative to Li concentration, as is commonly done to normalize for grain-size effects because metals adsorb preferentially to clay-sized sediment and fluctuations in energy of river flow generate grain-size variations (Loring, 1991; Kersten and Smedes, 2002). And, we establish 95% prediction intervals (PIs) about this relation to define the natural range of variation. Second, we evaluate post-development sediment metal concentrations in flood-supplied stratigraphic samples against the pre-development baseline generated in Step 1. If >2.5% of post-development monitoring samples fall above the upper 95% PI, this identifies they have received an additional source of the metal, possibly due to pollution (Loring, 1991; Kersten and Smedes, 2002). Third, we re-express these data as time-series plots of

residuals about the metal-Li relation to assess temporal trends of both past and ongoing monitoring data relative to the baseline (residual = 0), so that individual sample results can be evaluated for pollution immediately upon data acquisition.

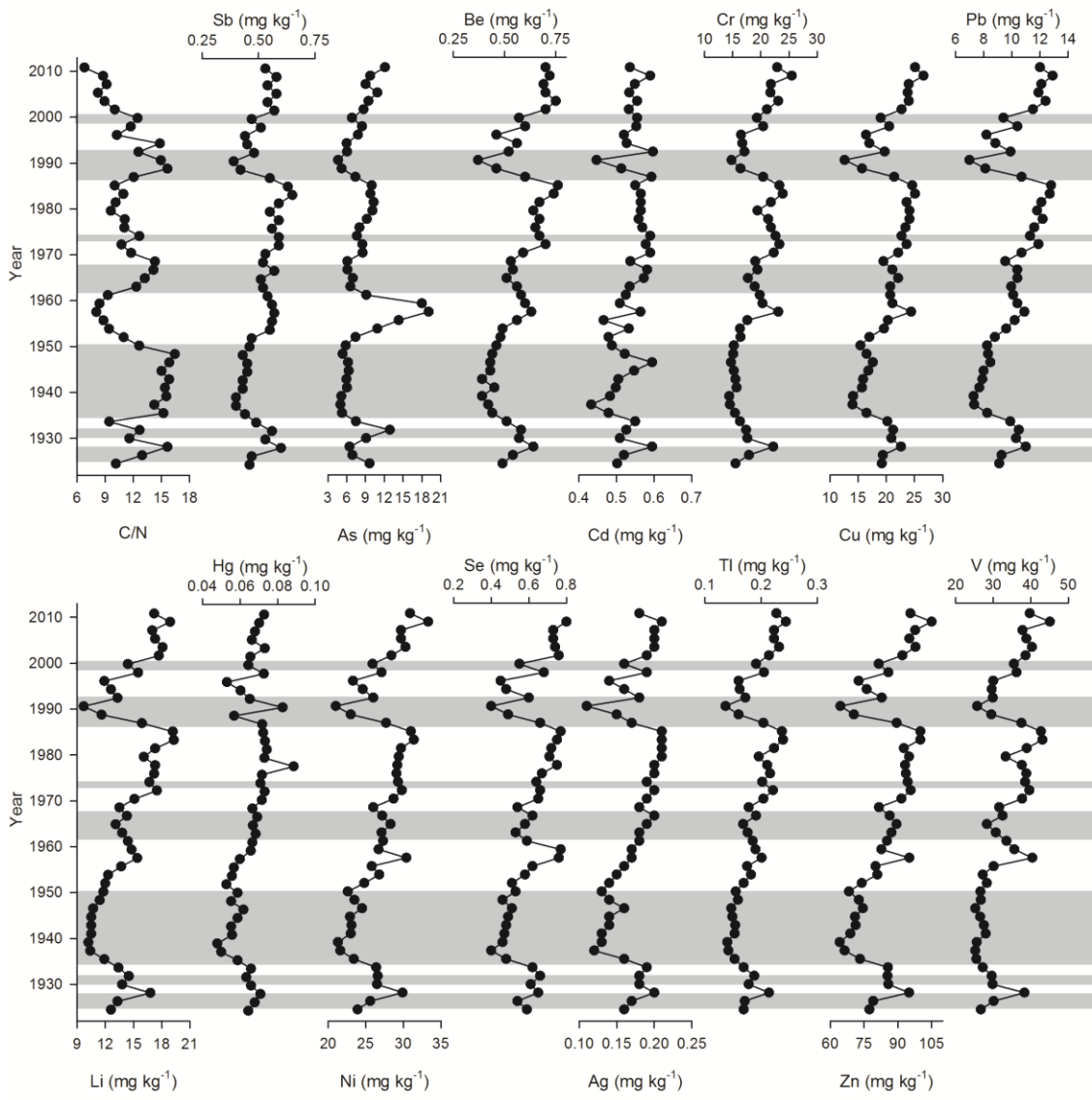


Figure 5.3: Stratigraphic profiles for the ratio of organic carbon-to-nitrogen concentration (C/N) and concentrations of 13 priority pollutant metals, vanadium and lithium. Grey horizontal shading indicates intervals of high flood frequency based on the C/N ratio, whereas absence of shading indicates intervals of low flood frequency (Elmes et al., In Review).

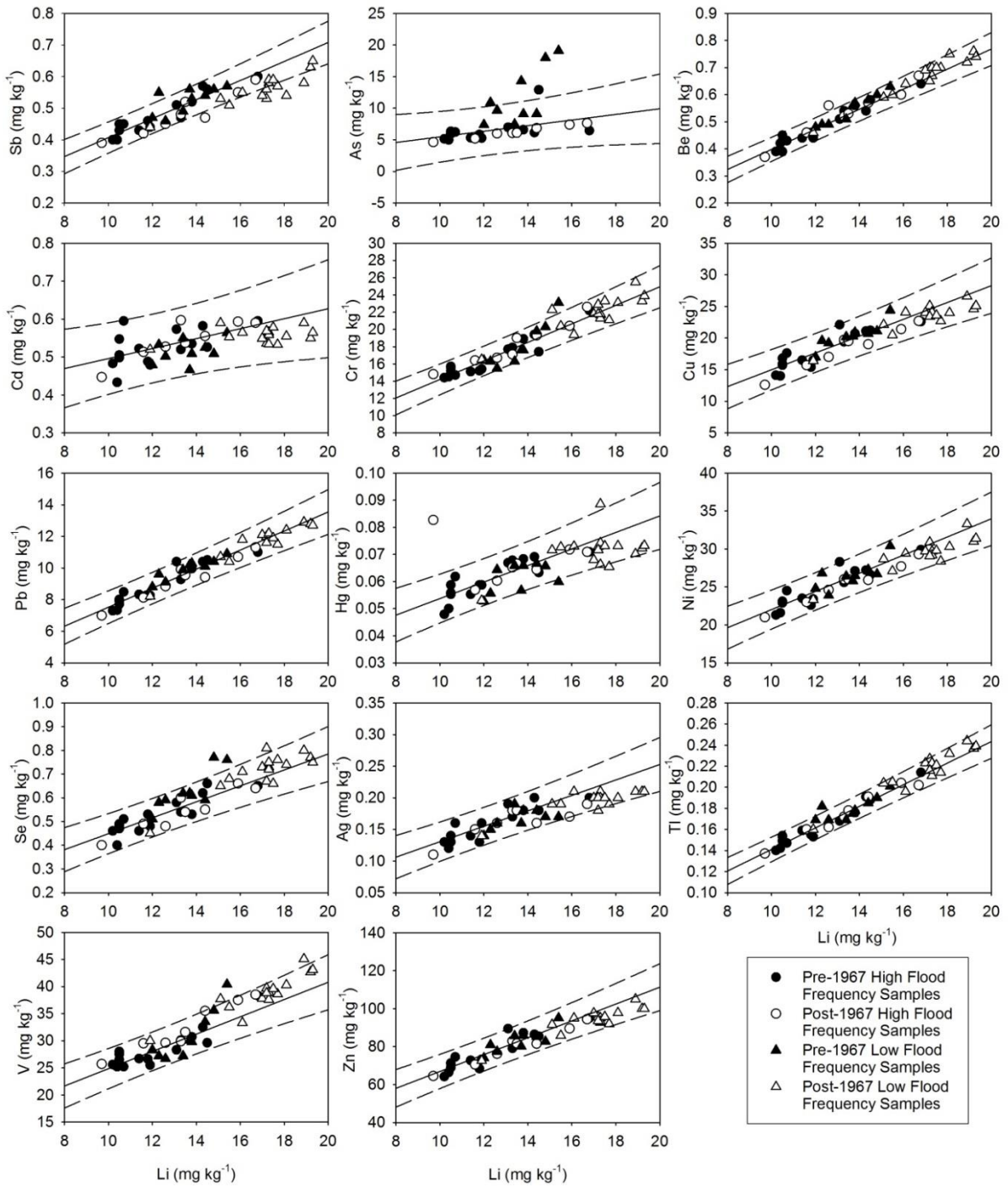


Figure 5.4: Scatterplots showing regressions of metal concentrations versus lithium concentration. Linear regressions (solid lines) and 95% prediction intervals (dashed lines) based on sediments deposited pre-1967 during intervals of high flood frequency.

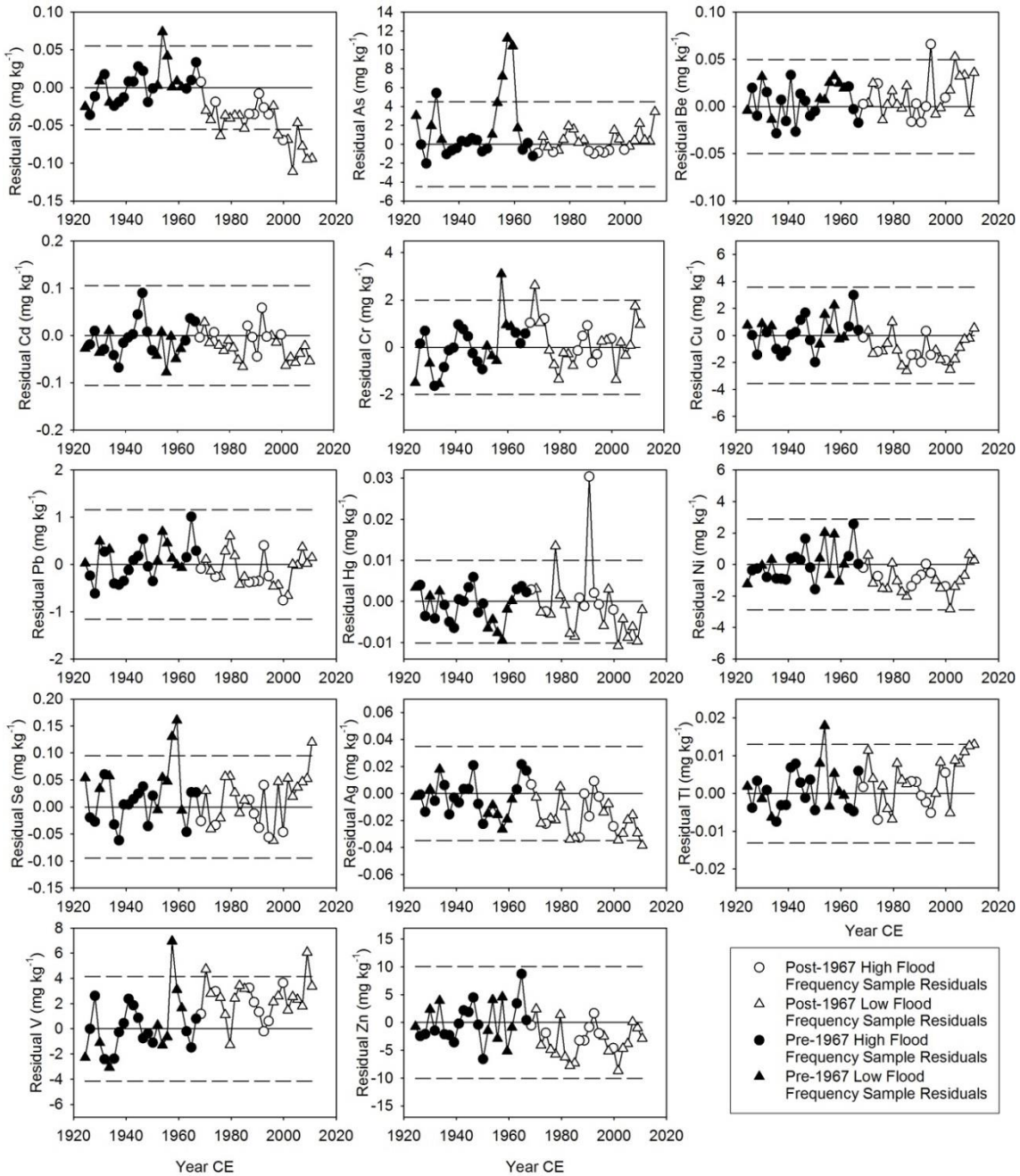


Figure 5.5: Time-series plots showing temporal patterns of change in residual metal concentrations from the Li-normalized pre-1967 baseline based on sediments deposited at lake SD2 during intervals of high flood frequency (horizontal solid line at 0). Dashed lines represent the widest 95% prediction interval from the pre-1967 high flood frequency data.

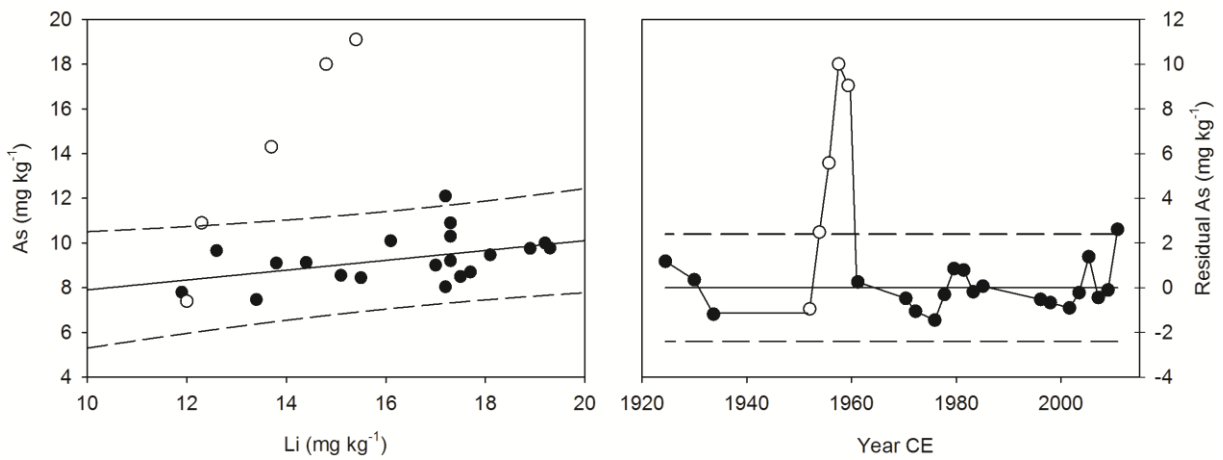


Figure 5.6: Left panel shows a scatterplot of arsenic concentration versus lithium concentration in sediments deposited in lake SD2 during intervals of low flood frequency pre-1950 and post-1960 (black circles). The linear regression (solid line) and 95% prediction intervals (dashed lines) are shown. Open circles are from the low flood frequency interval of the 1950s. Right panel shows a re-expression of these data as time-series plots of residuals about the As-Li relation to assess temporal patterns of arsenic pollution above the pre-1950 and post-1960 low flood frequency baseline (horizontal solid line at 0). Dashed lines represent the widest 95% prediction interval.

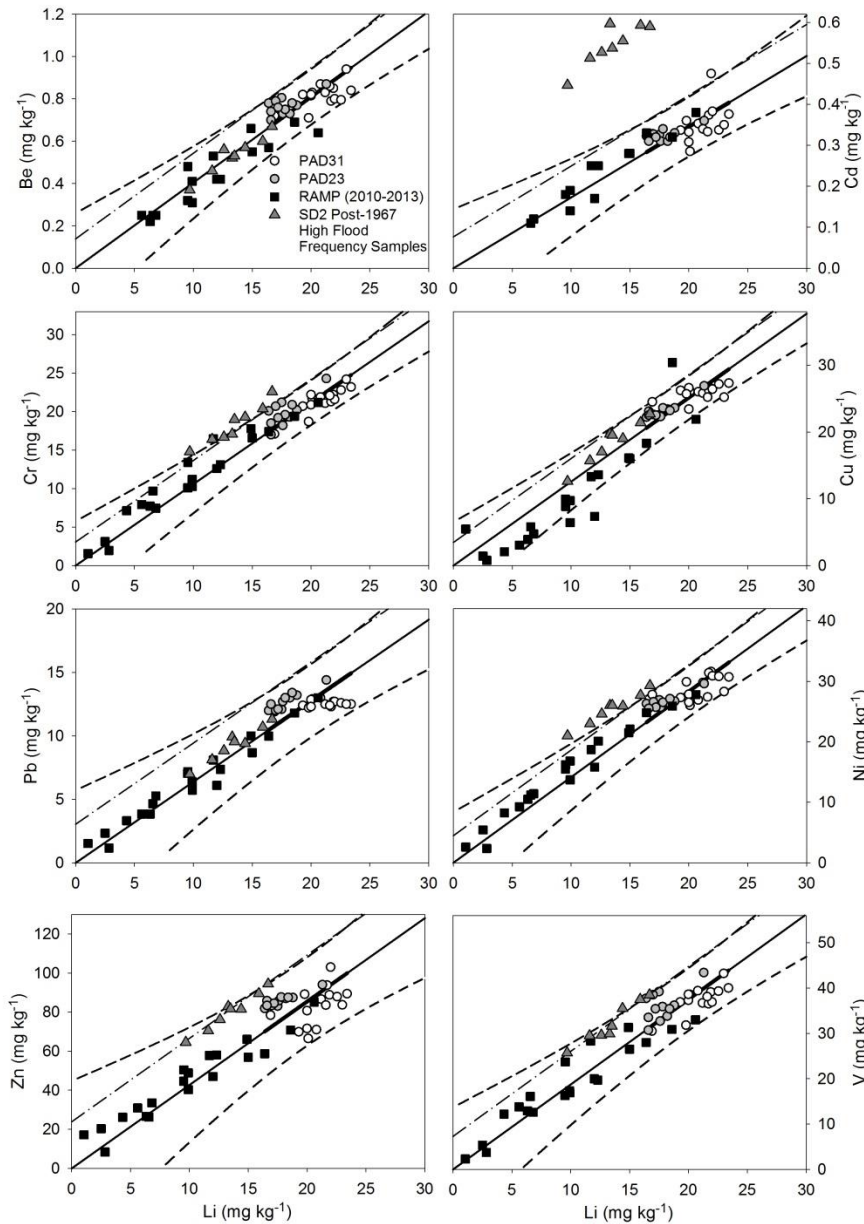


Figure 5.7: Scatterplots showing Li-normalized metal concentrations in sediment samples from lake SD2 deposited post-1967 during intervals of high flood frequency superimposed on pre-development (pre-1920s) baseline (solid lines) and 95% prediction intervals (dashed lines) constructed for the Athabasca Delta from analyses on sediment cores from lakes PAD23 and PAD31 (from Wiklund et al., 2014). Also shown are RAMP (Regional Aquatics Monitoring Program) data from surficial river sediment samples taken from downstream Athabasca River and Delta stations, as reported in Wiklund et al. (2014).

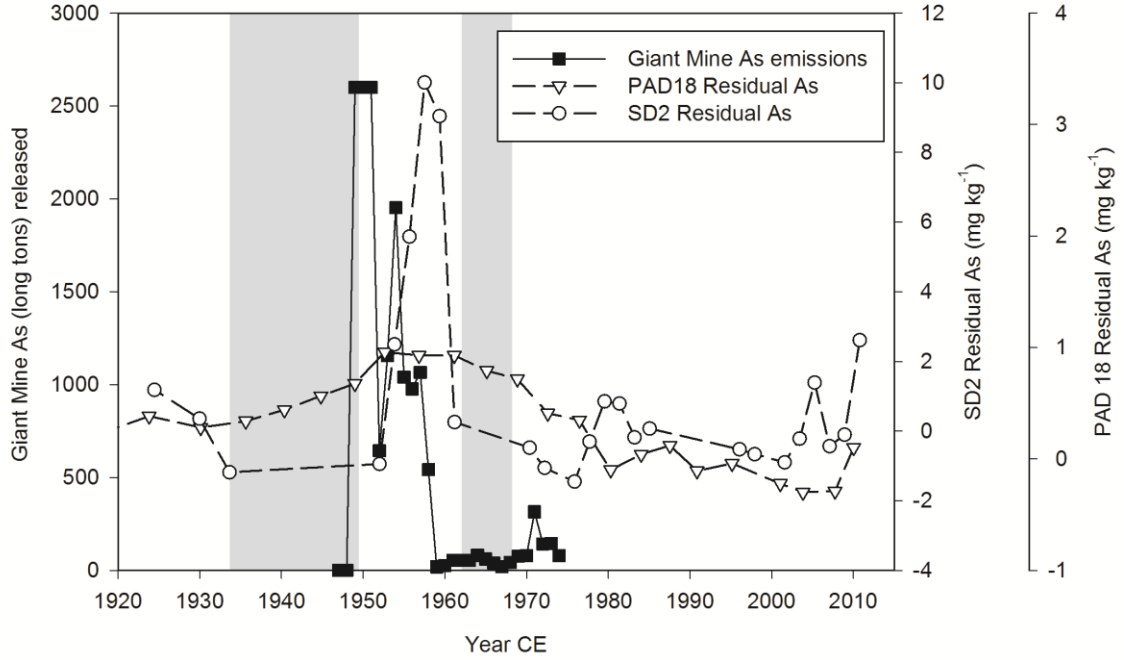


Figure 5.8: Comparison of As emissions from Giant Mine as supplied by the company and by Northwest Region, Environmental Protection Service and reported in Hocking et al. (1978), with the temporal pattern of change in residual As concentration in sediments from lakes SD2 and PAD18 (Wiklund et al., 2012). SD2 residual As concentrations were derived from the As-Li relation of low-frequency flood samples from pre-1950 and post-1960 (Figure 5.6). PAD18 residual As concentrations were derived from the pre-1900 As-organic matter samples. Vertical grey bars represent intervals of high flood frequency at SD2 that bracket the ~1950s.

Chapter 6: Synthesis and Recommendations

Freshwater ecosystems are an abundant and significant feature of northern landscapes, but improved understanding of the observed and predicted effects of environmental stressors is needed in the face of increasing disturbance and change. These water-rich regions are especially vulnerable to climate change, yet remain amongst the least studied and most poorly understood ecosystems, especially with regards to the effects of multiple, potentially-compounding stressors. Within these understudied areas, it is especially crucial that research provides knowledge of pre-disturbance conditions in order to accurately and effectively assess the consequences of stressors that may have been increasing during the past years to decades. Cumulatively, this thesis developed new understanding of both present and past conditions by examining linkages among climate, hydrology and contaminant supply and their effects on the limnology and biogeochemistry of lakes in three relatively understudied areas. This information is crucial to discern the relative roles of multiple stressors, to develop long-term monitoring programs and to provide the required context for anticipating consequences of continued change. Below is a synthesis of the key contributions to research, management implications for government agencies and local communities, and recommendations for ongoing and future research.

6.1 Synthesis of Key Contributions

Characterization of Pre-Disturbance Conditions to Assess Effects of Stressors on Northern Freshwater Ecosystems

Northern freshwater resources are increasingly subjected to disturbances from multiple stressors. Unfortunately, however, environmental monitoring programs are not often

initiated until well after the effects of the stressor have already begun (Schindler and Smol, 2006). This results in a gap of knowledge on the ecosystem's pre-disturbance conditions or baseline and the range of natural variability, which is required to assess the extent of degradation caused by the potential stressors (Smol, 2002). In locations where long-term monitoring data are not available, paleolimnology provides one of the only methods able to quantify the rate and magnitude of environmental change. In this thesis, paleolimnological methods were used in all three landscapes to help address research needs and concerns of local communities and agencies by characterizing the pre-disturbance conditions and evaluating the effects of different stressors.

In the Old Crow Flats (OCF), results from physical, geochemical and biological proxies were used to establish pre-disturbance conditions at Lake OCF48 and assess changes during the past several decades due to climate warming. This complemented information provided by aerial images, and provided new insight into the apparent water-level decline. Four distinct hydroecological phases were identified, including an ~100 year stable period at the start of the sediment record. The stratigraphic changes throughout the core were consistent with a full thermokarst expansion-drainage cycle. By determining the hydrolimnological history of the lake and comparing that with meteorological records, it was determined that the lake-level decline observed in the aerial images was caused by increased precipitation that led to lake drainage. Through this study, methods that could discriminate the cause of water-level declines (thermokarst expansion-drainage cycles vs. lake desiccation) were identified which is important for understanding baseline conditions. Knowledge of increases in lake-desiccation or acceleration of thermokarst-expansion

drainage cycles compared to baselines is important for identifying the effects of climate warming.

At Wapusk National Park (WNP), paleolimnological reconstructions were used to establish baseline hydroecological conditions in three ponds to determine how climate change and waterfowl population expansion have affected freshwater ecosystems, and to distinguish the driver(s) of change. Results identified three phases at ponds located in catchments disturbed by Lesser Snow Geese (LSG) during the past several centuries, whereas only two phases were identified at the non-disturbed pond. All three ponds had baseline conditions that were consistent with a relatively cold, turbid, and low light aquatic environment. Between the late ~1800s and the early ~1900s, all three ponds underwent a limnological regime shift towards increased productivity, which can be attributed to climate warming at the end of the Little Ice Age. While these new conditions persisted to present in the non-disturbed pond, another abrupt shift occurred in the mid-1970s in the two LSG-disturbed ponds, which can be attributed to the LSG population expansion. Additionally, the 15 low disturbance ponds assessed in Chapter 3 provide contemporary baseline information for future studies, as the LSG population is continuously expanding and will likely eventually reach these areas. Overall, the analysis of both multiple contemporary and paleolimnological variables provided information needed to establish baseline conditions, which were then used to distinguish the effects of climate warming and LSG disturbance.

Results from the Slave River Delta (SRD) demonstrated that paleohydrological reconstructions of a flood-dominated lake can be used to effectively inform development of baseline concentrations of metals delivered by both fluvial and atmospheric pathways. These baseline data were then used to assess for heavy metal pollution by industrial sources. To

assess for potential fluvial deposition of contaminants from the Alberta oil sands, baselines were established using only the pre-1967 high flood frequency interval metal concentrations. Natural variations in grain size were accounted for in the baseline by normalizing metal concentrations to Li via linear regression and determining 95% prediction intervals (PI) based on the pre-1967 high flood frequency linear relation. When post-1967 metal concentrations were compared to the baselines, no evidence of enhanced concentrations of metals was identified. Instead, samples were generally within the range of expected variability due to natural processes of supply and deposition from variations in flood-energy conditions. To assess for potential atmospheric contamination from Giant Mine (Yellowknife, NWT), baselines were determined from the pre-1950 and post-1960 low flood frequency interval metal concentrations using the same method as above. The 1950s were tested for pollution, as this is the time period where substantial atmospheric emissions were released from the gold smelting processes at Giant Mine. When metal concentrations from the 1950s were compared to the baseline, unusually high concentrations of As were identified, which suggests far-field atmospheric pollution from Giant Mine reached this site located 150 km to the south.

By using paleolimnological methods in this thesis, pre-disturbance conditions were successfully established in all of the studies. This information was crucial for the accurate determination of the effects of the different stressors in each location. The baselines characterized in this thesis can also provide other researchers, local communities, government agencies and natural resource managers with an effective tool for ongoing monitoring of the freshwater ecosystems. Based on the findings of Chapter 2, predictions were made on the expected stratigraphic profiles or typical baselines for lakes in the OCF

that have experienced water-level decline due to rapid drainage or due to evaporation (Figure 6.1). This template can now be used in the OCF by Parks Canada and other researchers in future studies to help distinguish whether sediment cores from different thermokarst lakes are showing signs of drainage or evaporation. Evidence of accelerated thermokarst expansion-drainage cycles compared to past cycle lengths or evidence of lake-level drawdown from evaporation would likely indicate deviations of the lake away from baseline conditions to a new regime under the influence of climate warming. At WNP, pre-disturbance conditions were established for coastal ponds that had not yet been influenced by climate warming or LSG population expansion. Additionally, new baseline conditions after each regime shift were also established. Based on findings from Chapter 3 and Chapter 4, templates have been made for the expected seasonal profiles of variables in ponds that have experienced climate warming effects and ponds with varying degrees of LSG disturbance (example Figure 6.2). This template can now be used in WNP by Parks Canada and other researchers to improve ability to identify limnological changes from baseline conditions due to these stressors. By developing long-term records, this thesis was also able to identify the best variables for identifying limnological regime shifts away from the baseline conditions (elaborated on in section 6.2). In the SRD, future monitoring programs or studies can use the baselines established in this thesis and the processes outlined in Chapter 5 (example of processes in Figure 6.3) to assess for pollution. Future monitoring programs could collect Slave River sediments or surface sediments from SD2 to compare with the baselines and assess for pollution transported via both the river and atmosphere. If there is a large deviation from the baseline (i.e., if >2.5 % of samples exceed the upper 95% PI), this finding would alert natural resource managers to the fact that concentrations are no longer within the expected range of

natural variability and industrial contamination has reached the SRD. The approaches used in this thesis to characterize baselines in the three different landscapes may be transferrable to other similar landscapes when pre-development data are unavailable.

Methods for Evaluating Effects of Stressors in Northern Freshwater Ecosystems

Another major contribution of this thesis to scientific research was the expansion on methods that have been previously used or are commonly used in northern hydrolimnological studies that assess the consequences of different stressors. In thermokarst landscapes, studies that evaluate lake-level changes have largely relied on remote sensing images (e.g., Smith et al., 2005; Riordan et al., 2006). In Arctic and Subarctic landscapes, limnological studies that assess waterfowl disturbance have traditionally relied on single, point-in-time sampling or sediment records to assess waterfowl effects on concentrations of major nutrients (N, P; e.g., Keatley et al., 2009; 2011; Côté et al., 2010). In northern landscapes facing increased resource development, potential contamination has often been examined by the comparison of metal concentrations upstream and downstream of industry (e.g., Kelly et al., 2010). However, findings from this thesis illustrate that important trends and changes could potentially be missed when relying on these methods alone. Instead, when additional tools in this thesis were used in combination with the more conventional approaches, consequences of stressors in northern freshwater environments were able to be more fully and accurately assessed. For example, research presented in Chapter 2 expanded on previous methods by combining aerial images, which indicated a lake-level decline somewhere within a ~30 year period, with multi-proxy paleolimnological analysis to reconstruct a continuous record of hydrological conditions for a thermokarst lake. Paleolimnology had not been widely used in

thermokarst lakes due to concerns that active thermokarst processes may disrupt the record. The stratigraphic variations in the sediment record and timing from age-depth model based on ^{210}Pb dating corresponded well with the timing of changes in the aerial images, which provided support for the paleolimnological approach in this landscape. The sediment record actually identified an additional hydrologic phase, provided more precise timing of lake-level decline than the aerial images, and allowed the attribution of water-level change to lake drainage. The success of this study confirmed that paleolimnological methods can be applied in thermokarst landscapes to obtain a coherent record of hydrolimnological change, despite their complex sedimentary environments, and provide more information than aerial images alone.

Research presented in Chapter 3 expanded on previous methods by using seasonal instead of single point-in-time sampling of major nutrients, as well as carbon isotope measurements of dissolved inorganic carbon and particulate organic matter instead of just major nutrient concentrations. Results demonstrated that carbon isotope measurements were far more informative than standard limnological measurements alone, as they were able to track the large shift in carbon cycling due to LSG disturbance that were otherwise missed, likely due to rapid nutrient uptake by the benthic mat. The use of seasonal sampling was critical in distinguishing these changes from fluctuating meteorological conditions. Overall, this study showed that carbon isotope tracers can be used effectively to track variations in biogeochemical conditions from waterfowl disturbance, which may be undetectable using conventional limnological measurements alone.

In Chapter 4, the integration of contemporary methods from Chapter 3 with paleolimnological approaches allowed the dual effects of climate warming and LSG

population expansion to be assessed and regime shifts to be identified for each stressor. The understanding of contemporary limnological and biogeochemical conditions in LSG disturbed ponds compared to non-disturbed ponds helped to attribute temporal changes in the sediment record to their appropriate stressors. As well, measuring a wide array of variables (diatoms, pigments, nutrients and physical properties) allowed for better characterization of each phase and the consequence of the stressor than is often possible when only one proxy is examined.

Research presented in Chapter 5 expanded on previous contaminant study methods by assessing changes in metal concentrations while incorporating the hydrological history of the lake, which provided a more accurate assessment of the results. This was found to be particularly important in the delta environment as metal concentrations fluctuated with flood conditions. By normalizing data with Li, natural variations in grain size due to flood conditions were taken into account. This chapter illustrated that knowledge of the flood history and their relationships with metal concentrations were crucial in assessing pollution and determining important vectors and sources. And in contrast, blindly assessing only stratigraphic changes in metal concentration without hydrological information may have led to the incorrect conclusion of pollution from the Alberta oil sands in this study. The success of this study also confirmed that paleolimnological methods can be used in delta lakes to get a clear record of contaminant deposition, despite their complex sedimentary environments.

Together, the use of multi-proxy studies throughout this thesis allowed for an assessment of the best indicators for tracking hydrolimnological responses to different stressors. In Chapter 2 and 4 a wide range of variables in the sediment record were measured including physical (organic matter, mineral matter and calcium carbonate), geochemical

(carbon and nitrogen elemental and isotopic values) and biological (diatom community composition and pigment concentrations) properties, all of which required different amounts of lab work and analysis, personnel expertise and financial costs. These ranged from the relatively quick, easy and cheap measurements of organic matter, mineral matter and calcium carbonate through loss-on-ignition (LOI) methods to the much more time consuming and costly measurements of diatom community composition. In Chapter 2, the simplest of these measurements, physical properties from LOI, were just as clear as the other more costly variables in tracking the different phases and hydrological evolution of the pond and identifying the cause. Thus, for future paleolimnological studies in the OCF that are interested in only assessing water-level changes the use of the simple cost-effective sediment core analyses of LOI may be adequate. LOI and/or aerial images could also be used to pre-screen for water-level declines, and then a subset of samples could be used to confirm and characterize hydrolimnological responses. However, although cost effective for assessing water-level changes, the use of only LOI runs the risk of over-simplifying lake processes. Additionally, it is possible that with very high sedimentation rates from thermokarst activity that the sediment record may become too disturbed to get a clear record. These methods could also be tested and then applied in other thermokarst landscapes where declining water levels are also of concern, such as the thermokarst landscape in the Hudson Bay Lowlands.

In Chapter 4, multiple-proxies were needed to effectively characterize the different limnological regimes, but the most helpful tools for identifying the consequences of climate warming in coastal fen ponds in WNP were LOI, shifts in diatom community composition and appearance of cyanobacteria pigments. In contrast, the most effective variables for identifying the consequences of LSG disturbance took into account both paleolimnological

information (carbon and nitrogen isotopes and pigments) with seasonal changes in contemporary variables developed in Chapter 3 (carbon isotopes tracers and conductivity). However, it is possible that with very high sedimentation rates from increased LSG disturbance that the sediment record may become too disturbed to get a clear record and paleolimnological methods may be ineffective at providing answers. Further testing is needed to assess whether these trends hold true for ponds with a range of LSG disturbance. Additionally, Chapters 3 and 4 only looked at one and two LSG disturbed ponds, respectively, and further testing is needed to determine whether these patterns are accurate at a larger scale (elaborated on in section 6.2). It was also identified that changes in contemporary variables due to waterfowl disturbance were best identified when seasonal patterns were assessed. However, due to logistical constraints, it may not always be possible to sample seasonally, which could make the identification of changes and the use of the patterns described in Chapter 3 and 4 more difficult and could run the risk of oversimplifying pond processes. But, with further testing, it may be possible to sample only mid-summer for carbon isotopes tracers and conductivity to screen for waterfowl disturbance against the patterns and templates already developed. These methods may also be useful in other Arctic and Subarctic landscapes that are facing the dual effects of climate warming and expanding waterfowl populations. However, patterns may not be directly transferable in other locations if key characteristics of the WAP ponds, such as the benthic mat, are not also observed.

Results from Chapter 5 illustrated that the incorporation of floodplain lake sediments and information on paleohydrology in pollutant studies in delta environments offers great potential for accurately examining contaminant deposition over time to address questions and

concerns regarding industrial development. However, Chapter 5 is based on only one lake which is within a large geographic region and riverine system. Further studies should be conducted to confirm trends and should use lakes with a broad range of hydrological conditions (see section 6.2). Additionally, identifying the relationship between grain size and metal concentration with flood conditions was important for accurate conclusions in this study, but the relationship could vary between different delta systems. This emphasizes the need for the addition of comprehensive paleohydrological reconstructions in contaminant studies.

Addressing Community Concerns and Research Needs

Research reported in the ‘data chapters’ of this thesis was stimulated by the information needs and concerns expressed by local communities and agencies (e.g., Parks Canada, Government of NWT) to assess effects of various stressors on northern freshwater ecosystems. By characterizing the pre-disturbance conditions and assessing the effects of stressors, as described above, these issues in each of the landscapes were addressed. In the OCF, the study was designed to address growing concerns of the Vuntut Gwitchin First Nation and the research needs of Parks Canada. The local community was worried that the observed and perceived climate-driven hydrological changes, such as widespread lake-level declines, would increasingly threaten sustainability of wildlife populations and traditional use of the landscape. Many of the concerns were documented in the ABEK Co-op (2007) report, including that “The water in the rivers is low. Everything is drying up”; “I see a lot of landslides and a lot of lakes drying up”, and “The land is drying and the permafrost is melting fast” (Old Crow Citizens, ABEK Co-op, 2007; 2008). Additionally, Parks Canada

mandate states that Vuntut National Park's landscape, located in the OCF, needs to be maintained as a natural system, with assessments of the ecological integrity and how it is changing conducted on a regular basis and reported at least every 10 years in the State of the Park Report (Parks Canada, 2007). In the 2009 Vuntut National Park State of the Park Report, the wetland complex and freshwater of the park were given a good ecological integrity rating, but it was noted that there was a need for improved monitoring methods and long-term data records to assess change (Vuntut National Park Monitoring Plan, 2010). Both Parks Canada and the VGFN have realized that long-term data are required to answer the necessary questions for understanding the OCF as a whole natural system, and for preserving traditional lifestyle of the community. Although community members of the OCF region have reported that the landscape is 'drying', the observed water-level declines could have been a result of thermokarst expansion-drainage cycles or lake-desiccation, both of which may be increasing in frequency due to recent warming, but would have different consequences for the community and landscape as a whole. As described above, remote sensing images have been the most common tool for investigating water-level declines in the North, but these images provide the community and local resource managers only with evidence of which lakes have changed in surface area, not how, when or why the changes occurred. By using the combination of aerial images and paleolimnological methods a comprehensive long-term perspective of lake changes was developed as well as templates for future studies. This information was required to address community concerns and Parks Canada's needs as it identified long-term changes and that lake-drainage, not lake-desiccation, was the cause of the apparent water-level decline at Lake OCF 48. This information can now be used by the Vuntut Gwitchin First Nation, Parks Canada and other

natural resource managers to inform and ensure effective long-term monitoring programs that assess changes in the ecological integrity of the landscape.

Within WNP there has been little research conducted on the ecologically important lakes and ponds. Similarly to Vuntut National Park, Parks Canada's national mandate governs WNP and the landscape needs to be maintained as a natural system with regular monitoring of ecological integrity. Yet, as of the 2011 State of the Park Report for WNP, the freshwater ecosystem had not been included, did not have a systematic and effective monitoring program and was not assessed for ecological integrity and changes. Additionally, within the 2011 State of the Park Report it was identified that “because of the considerable variability in water conditions, and the lack of historical data, it is not currently possible to establish thresholds or trends” (State of the Park Report, 2011). These data are especially important to Parks Canada as the park is under increasing pressure from climate warming and the rapid LSG population expansion which may cause limnological thresholds to be crossed. And, as discussed in the report, long-term data are needed to understand the current state of the lakes and ponds in response to these stressors. By combining contemporary and paleolimnological analyses, this thesis was able to address this need and develop the necessary temporal perspective for identifying limnological regime shifts for ponds in the coastal fen area of the park. However, in order to accurately understand the effects of stressors and determine the current ecological state of the ponds, data in addition to the conventional limnological and paleolimnological tracers (as described above) were required. Overall, this thesis addressed research needs in the coastal fen area of the park by identifying long-term trends and the effects of stressors. Recommendations were also made to Parks Canada on the best

approaches to be used in the very much needed freshwater monitoring programs for WNP (elaborated on in section 6.2).

Concerns have also increased regarding the potential effects of upstream industrial development on environmental and human health in the SRD. In response to increasing community concerns, the Slave River and Delta Partnership, a multi-stakeholder group, was created to ensure that the local community's voices were heard and that they had a role in guiding research directions and monitoring programs. This group identified that the key community concern and research priority was to assess the environmental conditions of the Slave River and SRD. In particular community members were concerned that the Alberta oil sands development was affecting water quality by adding contaminants, reducing river flows by removing water during the extraction processes, harming the aquatic ecosystem by increasing rates of fish abnormalities and negatively influencing human health by causing increased cancer rates (Wesche 2007; 2009; SRDP Workshop, 2011). These concerns prompted the study of Lake SD2 as part of the Slave River and Delta Partnership project to assess for heavy metal pollution from the Alberta oil sands. An important aspect of this project was developing a long-term record (pre-oil sands) of natural variability with which current conditions could be compared. By combining sediment records of past contaminant deposition and paleohydrology, this study was able to directly address community needs by assessing for pollution in lake sediments from the Alberta oil sands and other industrial developments. Since fluvial transport of pollutants from the oil sands was not detected at Lake SD2 it was concluded that for now community concerns should be low. In fact upon further assessment it appeared that many metals in SD2 sediments may be derived from a source other than the Athabasca River. However, there were unusually high concentrations of

As in the 1950s with highest concentrations above the Probable Effects Level (CCME, 2014). The timing of the increased As concentrations corresponds to the known time of substantial atmospheric emissions from gold smelting at Giant Mine. This suggests far-field atmospheric pollution from Giant Mine at much farther distances than previously documented, which may be of concern to the local SRD community. Another important concern of the local community was that there is insufficient monitoring being conducted at the Alberta oil sands to continuously ensure that pollution is not being transported downstream to the SRD. Although, the community may not be able to directly change the monitoring program at the Alberta oil sands, this study has provided the community and local resource managers with a template for which they can conduct their own sampling to ensure metal concentrations do not become elevated in the future. The pre-1967 high flood-frequency normalized metal-Li baselines from the study can be compared to new sediment samples from the Slave River or SD2 during high flood periods. This will allow continuous monitoring of pollution transported by the Slave River. The low-flood frequency normalized metal-Li baselines from this study can be compared to sediment samples from SD2 collected during low flood periods against. This will allow for continuous monitoring of atmospheric pollution or catchment in-wash of pollutants.

6.2 Recommendations for Ongoing and Future Studies

Old Crow Flats

Based on paleolimnological analyses and aerial images from the OCF, Chapter 2 was able to identify lake drainage as the cause of a water-level decline in OCF 48. However, the

OCF is a vast heterogeneous landscape with lakes that span broad hydrological gradients (Turner et al., 2010; 2014). Thus, information is needed to determine whether the knowledge gained from analyses at Lake OCF 48 is representative of other lakes in the OCF, including lakes with different modern-day hydrological conditions. OCF 48 has previously been classified as a lake that oscillates between snowmelt- and rainfall-dominated hydrological categories (Turner et al., 2010), but other lakes exist solely in each of these groups as well as in an evaporation-dominated category (Turner et al., 2010). Consequently, it is important to test whether lake-drainage is the cause of the apparent wide-spread water-level declines in lakes from all hydrological categories (rainfall-, snowmelt- or evaporation-dominated), or if the cause of previous water-level declines is related to the modern day hydrological conditions. This is particularly important as there will be different consequences for the environment and community depending on whether lake-drainage or lake-evaporation is the dominant cause of the wide-spread declines.

To date, the template established in Chapter 2 (Figure 6.1) has been used to assess for water-level declines due to lake-drainage or lake-expansion in six other lakes in the OCF which span a larger hydrologic gradient (Shaker, 2011; Tondu, 2012; Turner, 2013). Lake expansion and drainage cycles were identified for each of the six lakes, but with variable timing. This suggests that each lake has different threshold levels that trigger drainage and independent factors or catchment characteristics (e.g., vegetation) that control the timing and length of each phase. Research by Turner et al. (2014) has also since shown the importance of catchment vegetation in the contemporary hydrology of OCF lakes, thus this factor may in fact play an important role in determining which lakes follow the expansion-drainage template versus which follow the evaporation template, and the timing of these events.

Collecting information from a larger number of lakes spanning the OCF using the quick LOI method would be an efficient and useful way to establish the potential dominance of lake expansion-drainage cycles in the landscape. Records from additional lakes would allow the refinement of baselines developed in this thesis (i.e., length of cycles, or frequency of drainage). Aerial images could also be combined with these studies to help identify lakes that have experienced a water-level decline and narrow down the time frame needed for paleolimnological studies.

Hudson Bay Lowlands

Given that Chapter 3 and Chapter 4 focused on only one and two LSG-disturbed ponds, respectively, it is important to test the results and the suggested protocols from this thesis on a larger data set with more LSG-disturbed ponds and over multiple years with different meteorological conditions. Using the results of Chapter 3 and Chapter 4, I worked with Parks Canada to help design a monitoring program for summers 2014 and 2015 that would help refine approaches with a larger dataset. While setting up this monitoring program in June 2014, the field team spoke with Rocky Rockwell, a waterfowl biologist and LSG expert, about the LSG population expansion. He informed us that in addition to the areas actively used and disturbed by LSG, where LSG disturbed ponds from Chapter 3 and 4 were located, there is an area within the coastal fen that has been so severely degraded that it has been depleted of vegetation to the point of abandonment by the LSG (Figure 6.4). Taking this information into account, I helped to select 15 new ponds for Parks Canada in June 2014 to track the effects of LSG disturbance and test and refine approaches recommended in this thesis (Figure 6.5). We selected five new non-disturbed ponds to act as controls, five actively

LSG disturbed ponds that had a similar visual state to WAP 20 and WAP 21 and five severely disturbed ponds from the area identified by Rocky Rockwell. These severely degraded ponds were added to see if the suggested protocols were also effective in this new class of ponds. Additionally, it would help identify if there is any evidence of recovery to, or towards the pre-disturbance state after the LSG left, or if recovery to this point has been non-existent. Data from this thesis and the 15 new ponds will help test and refine approaches that are planned to be implemented in a new study of ~30 LSG disturbed ponds in July 2015. For this ongoing monitoring program, a suite of key indicators and pond responses that most effectively tracked the effects of the LSG population expansion and disturbance in Chapters 3 and 4 were recommended to Parks Canada (Table 6.1). Emphasis was placed on carbon isotope measurements ($\delta^{13}\text{C}_{\text{DIC}}$ and $\Delta^{13}\text{C}_{\text{DIC-POM}}$), as they were far more informative than the standard limnological variables in capturing differences in between the disturbed and non-disturbed ponds. With ongoing monitoring by Parks Canada, results will continue to help refine approaches and track the effect of stressors on ponds in WNP. These tools may also be applicable in other northern wetlands facing the stress of waterfowl population expansion. Tracking the effects of waterfowl disturbance on carbon cycling in the North is particularly important as these northern wetlands play influential roles in the carbon cycle, and if LSG disturbance in WNP and waterfowl disturbance in other locations continues to grow, there may be potential for large-scale shifts in the carbon cycle and balance.

With continued climate warming, WNP is likely to become increasingly dynamic, which may lead to altered carbon behaviour in this landscape in addition to changes from LSG disturbance in the coastal fen. WNP spans additional vegetation zones (interior peat plateau palsa bog and boreal spruce forest) and lies in regions of both continuous and

discontinuous permafrost (Rouse, 1991). Permafrost is a large carbon store and concerns exist with the effects of continued climate change on permafrost thaw and the consequences of this to the carbon budget (Schuur et al., 2008; Zimov et al., 2008). Additionally, increased thermokarst activity as a result of climate warming may influence carbon dynamics through the transfer of terrestrial carbon to aquatic systems by peat erosion and pond expansion (Kling et al., 1991; 1992; McGuire et al., 2009). Also, increased wetness or dryness of the landscape could occur through pond expansion or pond drainage and desiccation, resulting in increased CH₄ and CO₂ emissions, respectively (Edwards et al., 2009; McGuire et al., 2009; van Huissteden et al., 2011). Chapter 3 and 4 of this thesis have indicated that carbon cycling of ponds is sensitive to LSG disturbance and it would stand to reason that throughout a broad, dynamic park like WNP, there may also be changes in carbon behaviour spatially and in response to different stressors. As carbon cycling is a very important aspect of northern wetlands, future studies should focus on identifying the controls on carbon pathways in WNP ponds at a landscape scale.

To identify controls on carbon pathways in WNP ponds, repeated measurements of the carbon isotope composition of dissolved inorganic carbon ($\delta^{13}\text{C}_{\text{DIC}}$), as well as a range of limnological parameters and water isotope compositions were collected from 36 ponds from the different ecozones of WNP over three years (2010-2012) to assess influence of internal and external factors on carbon behaviour. Preliminary results show that the ponds possessed a very broad range of $\delta^{13}\text{C}_{\text{DIC}}$ values, spanning -29.5‰ to +1.8‰, suggesting that this is a sensitive index of pond carbon balance. Spatial variability was substantial, and exceeded seasonal variability of individual ponds. Coastal fen ponds had the highest $\delta^{13}\text{C}_{\text{DIC}}$ values (range: -12.0 to +1.8‰; mean: -3.4‰), followed by the boreal spruce forest ponds (range: -

18.5 to -2.4‰; mean: -10.8‰) and the interior peat plateau palsa bog ponds which had the lowest mean $\delta^{13}\text{C}_{\text{DIC}}$ value (-13.3‰) but spanned a considerable range (-29.5 to -0.6‰). The high $\delta^{13}\text{C}_{\text{DIC}}$ values in the coastal fen ponds can be attributed to atmospheric CO_2 exchange, which provides a ^{13}C -enriched source of carbon to the ponds. Supporting this interpretation are water isotope data, which indicate that these ponds tend to receive low amounts of snowmelt runoff and likely low supplies of soil-derived ^{13}C -depleted DIC due to catchments with sparse tundra vegetation. Water isotope data and mid-range $\delta^{13}\text{C}_{\text{DIC}}$ values suggest that boreal spruce forest ponds receive greater snowmelt runoff and soil-derived ^{13}C -depleted DIC from their more densely vegetated catchments, but are also likely influenced by productivity-driven ^{13}C -enrichment. The broad range of $\delta^{13}\text{C}_{\text{DIC}}$ values for the interior peat plateau palsa bog ponds appears to be associated with variation in pond size. The large interior peat plateau palsa bog ponds had relatively high $\delta^{13}\text{C}_{\text{DIC}}$ values (range: -8.1 to -0.6‰; mean: -4.2‰), which were similar to coastal fen ponds and may also suggest that atmospheric CO_2 exchange is the dominant pathway that supplies carbon to these ponds. In contrast, the small interior peat plateau palsa bog ponds had low $\delta^{13}\text{C}_{\text{DIC}}$ values (range: -29.5 to -20.0‰; mean: -24.0‰), which can be attributed to the input of soil-derived ^{13}C -depleted DIC and possibly high rates of organic matter respiration in the pond water column. These preliminary findings suggest that external and internal factors (e.g., catchment vegetation, hydrology, productivity, respiration) are drivers of carbon balance in ponds of WNP. How these factors respond to ongoing climate warming will have a strong influence on pond carbon balance.

Slave River Delta

Although research presented in Chapter 5 has shown no evidence of enhanced metal concentrations since onset of oil sands development, studies closer to the facility have shown elevated deposition of metals and PAHs within an approximately 50-km radius of a central point where upgraders are concentrated (e.g., Kelly et al., 2009; 2010). Therefore, future studies are important and should focus on study sites closer to the Alberta oil sands. This thesis and previous research (Chapter 5, Hall et al. 2012, Wiklund et al. 2014) have identified that sediment records contained in floodplain lakes provide a valuable source of information for characterizing pre-development baseline concentrations, and assessing temporal patterns of change for evidence of pollution. However, this thesis also illustrated that knowledge of the flood history of SD2 was crucial in assessing pollution and determining important vectors and sources. Future studies in complex and dynamic depositional environments closer to the Alberta oil sands should ensure they incorporate paleohydrological information. This would allow researchers to quantify the relative importance of natural versus industrial supplies.

Given that Chapter 5 focused on only one lake, SD2, it remains unknown if the findings from SD2 are representative of other lakes in the SRD and best represent the sediment quality of the Slave River. SD2 is a flood-dominated lake, but one that has not flooded frequently since ~2000 when development of oil sands has accelerated. Consequently, it would be important to sample another lake that has had more frequent and recent flooding to confirm that the Slave River is not an important vector for the transport of contaminants from the Alberta oil sands to the SRD. Additionally, given that the SRD is a heterogeneous and dynamic landscape with lakes that span broad hydrological categories (Brock et al., 2007), future studies should focus on sampling lakes in other hydrological

categories to confirm if the trends observed for contamination or lack thereof from the Alberta oil sands and Giant Mine are consistent throughout the landscape, or if they are more localized in origin.

Further sampling of closed-basin or evaporation-dominated lakes would provide a more continuous record of atmospheric deposition of contaminants. This is particularly important for confirming the decline in As concentration that was observed in SD2 in the ~1960s when the lake began to flood again. Additionally, further research is needed to map out the atmospheric deposition pattern of As from Giant Mine, as it has now been shown to be much broader than previously documented. Much work has been done close to the mine site around Yellowknife (NWT) (e.g., Hutchinson et al., 1982; Murdoch et al., 1989; Bright et al., 1996; Jackson et al., 1996; Koch et al., 2000; Andrade et al., 2010; Bromstad, 2011), but results presented in Chapter 5 suggest pollution was much more widespread, potentially even reaching as far south as the PAD. Sediment cores from closed-basin lakes across large transects from Giant Mine would provide a continuous record of atmospheric metal deposition and should be targeted for these studies. Surface sediment sample surveys from a large number of lakes spanning a wide spatial scale are also important for confirming that As has stayed buried in lakes and is not leaching out of soils and causing new contamination concerns.

6.3 Figures

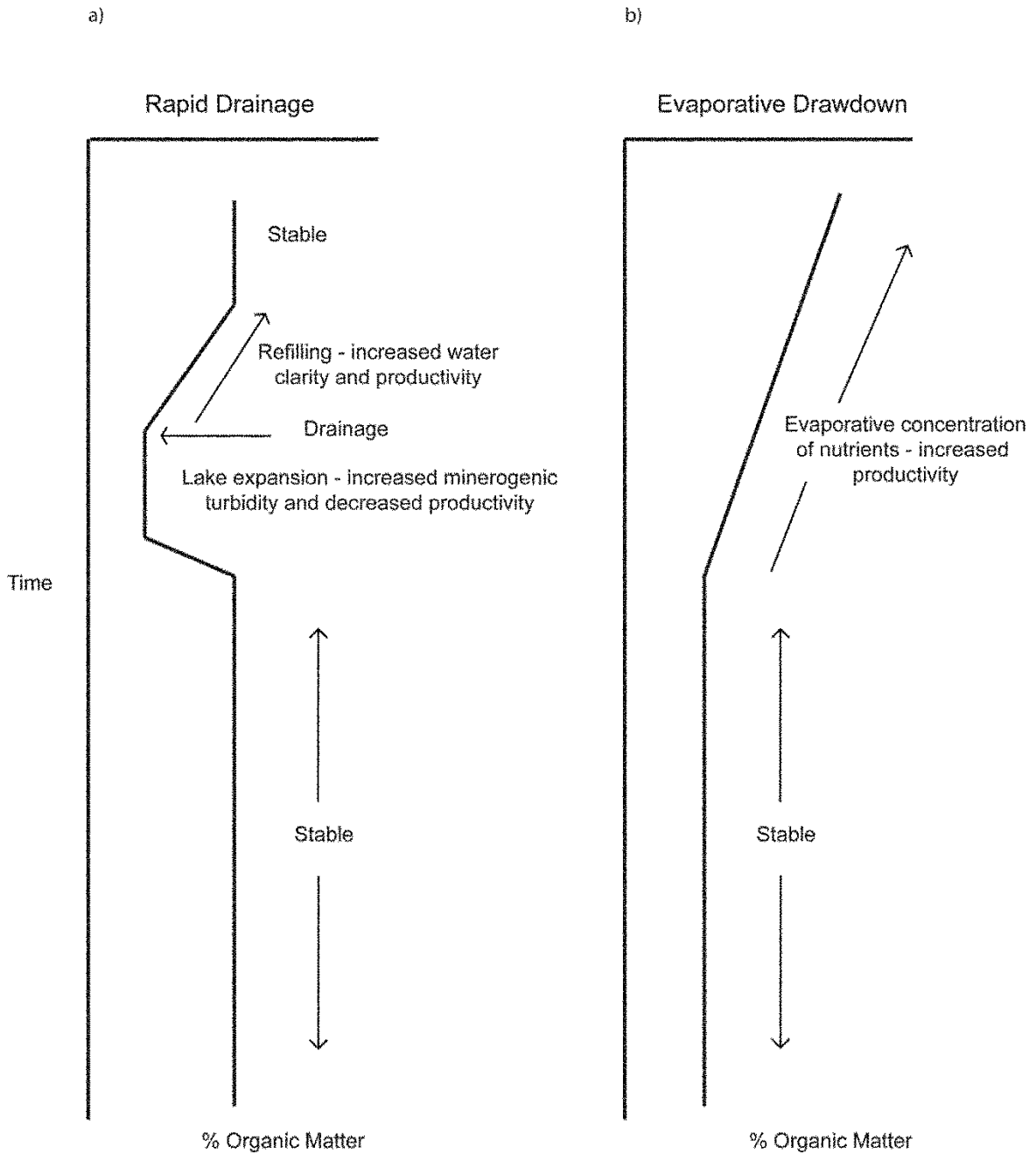


Figure 6.1: Expected sedimentary organic matter content (%) profiles from paleolimnological analysis of lakes experiencing surface area changes from (a) accelerated thermokarst expansion-drainage cycles, and from (b) increased evaporation (from MacDonald et al. 2012).

LESSER SNOW GEESE (LSG) MONITORING

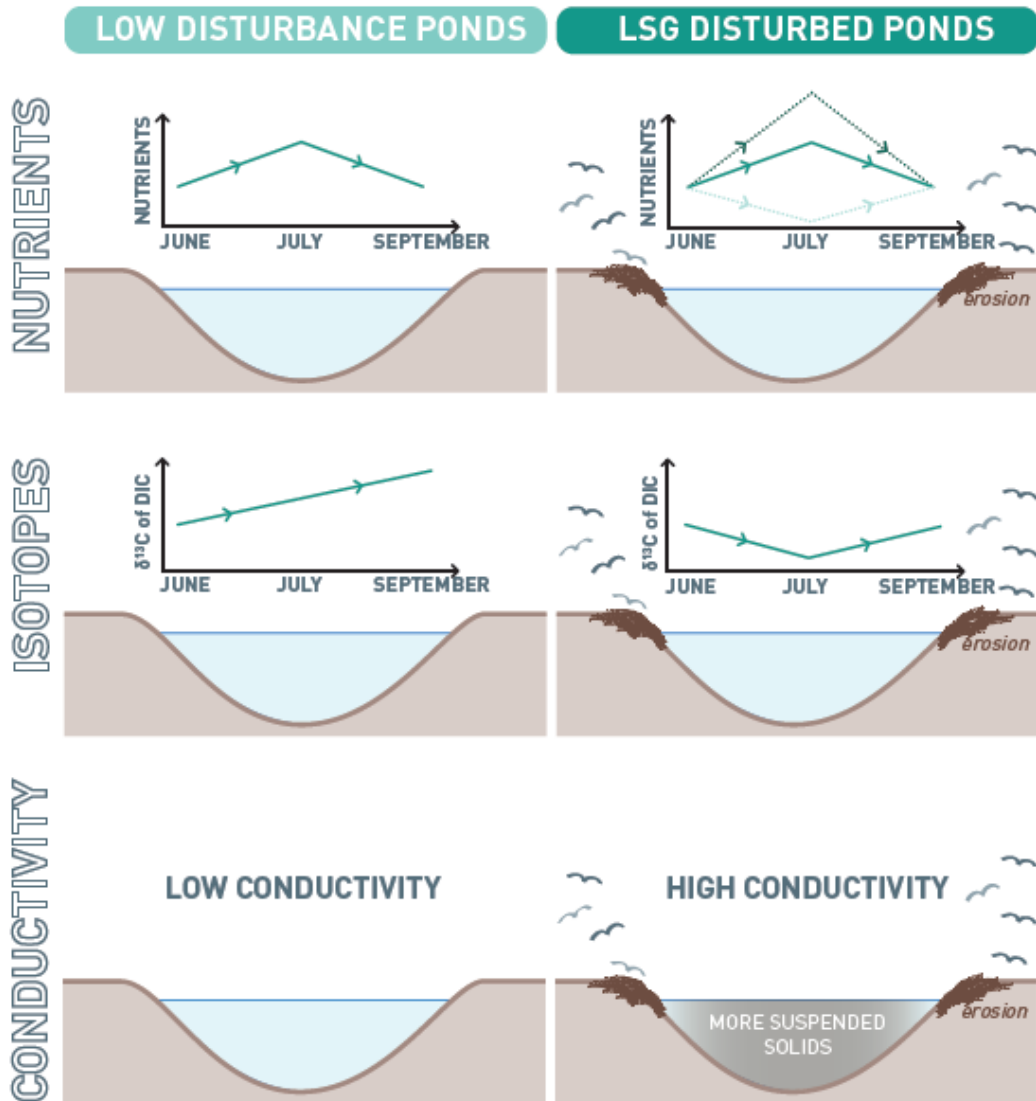


Figure 6.2: Expected seasonal trajectory profiles for nutrients, carbon isotope composition of dissolved inorganic carbon and conductivity for lakes experiencing no disturbance from the LSG population (left side) and lakes that are influenced by LSG disturbed (right side).

Dashed lines represent multiple scenarios that could result depending on the severity of LSG disturbance. Image made by Pieter Aukes.

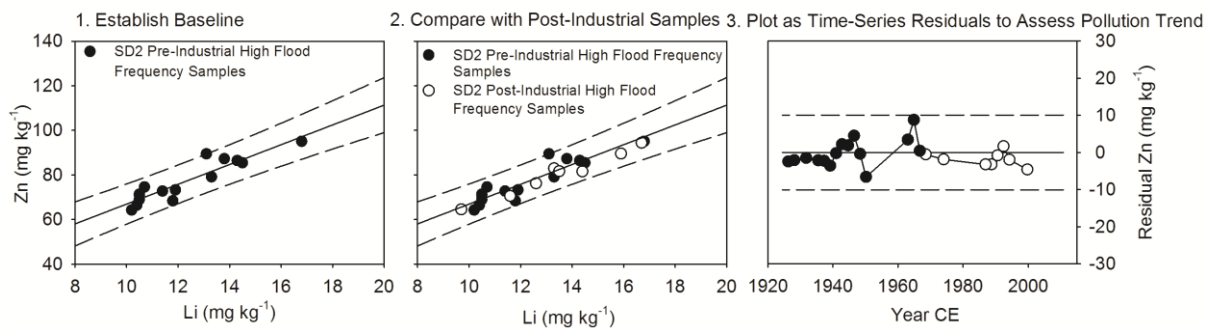


Figure 6.3: Representation of three step approach to assess future pollution in SD2. Left panel shows the establishment of baseline conditions from pre-industrial high flood frequency samples. Centre panel shows the comparison of post-industrial data with the established baseline. Right panel shows the time series that can be used for ongoing risk assessments in the Slave River Delta. Dashed lines represent the 95% prediction intervals based on pre-industrial conditions (left and centre) and the linear extrapolation of the widest 95% prediction interval from pre-industrial conditions (right). Samples that plot within the 95% prediction intervals (centre and right panels) can be interpreted as being within the range of natural variability for the contaminant. In contrast, if >2.5% of post-industrial samples plot above the upper 95% prediction interval, the metal concentration is elevated above baseline possibly due to pollution from human activities.



Figure 6.4: Photo showing a severely degraded pond, with largely absent vegetation and exposed soils used in the 2014-2015 LSG monitoring program by Parks Canada.

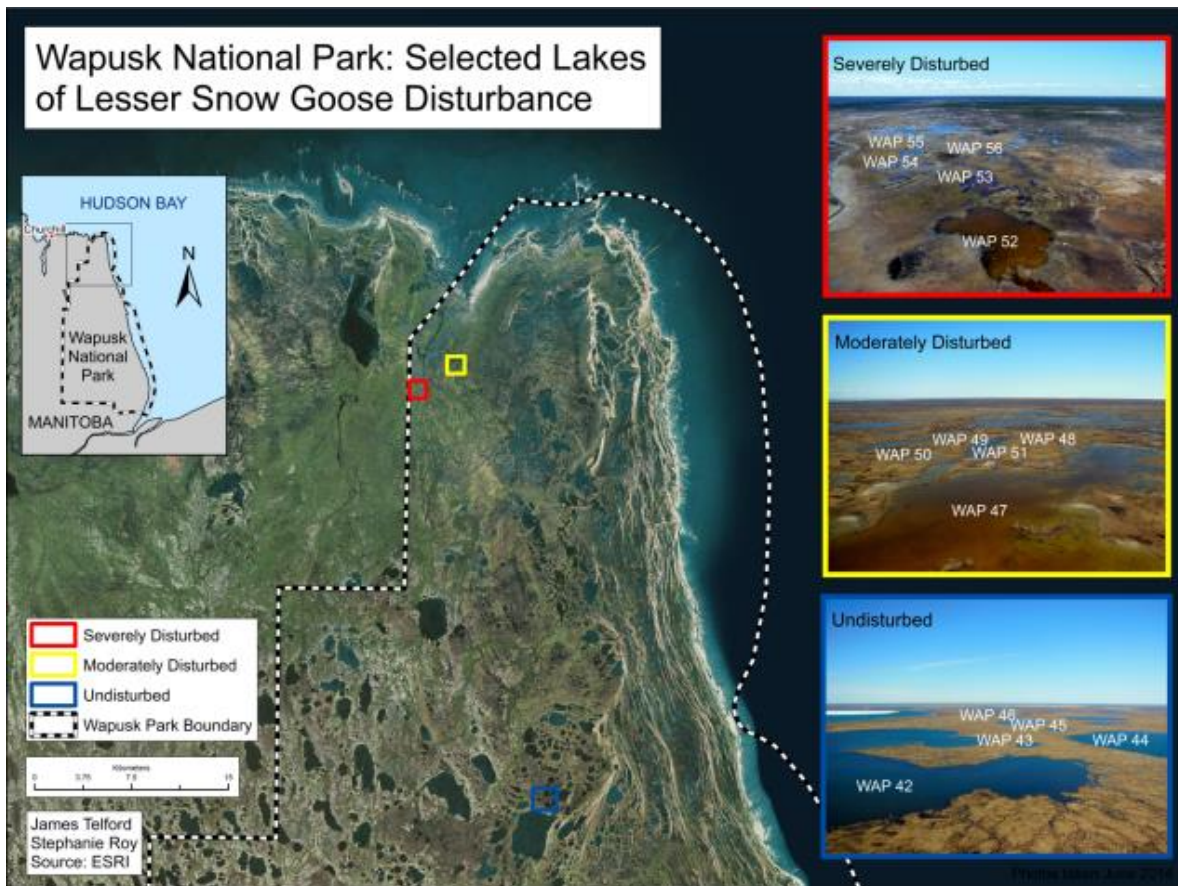


Figure 6.5: Map showing the locations of 15 new ponds used in the 2014-2015 LSG monitoring program by Parks Canada. Map was created by James Telford.

6.4 Tables

Table 6.1: The most sensitive limnological parameters that have been recommended to Parks Canada for monitoring the ongoing effects of LSG disturbance in Wapusk National Park.

These indicators can all be used to track lake water chemistry responses to Lesser Snow Goose disturbance.

Variables	Purpose of Sampling	Basic Interpretations
Nutrient Concentrations: Total Kjeldahl Nitrogen (TKN), Total Phosphorus (TP)	Determine lake nutrient balance	Change in nutrient availability may indicate LSG disturbance.
pH	Determine lake productivity	High and/or stable midsummer values may indicate increased productivity from LSG disturbance
Conductivity	Determine lake catchment erosion	High values may indicate increased erosional inputs from LSG disturbance
Dissolved Inorganic Carbon Concentration (DIC)	Determine lake carbon balance	Similar values between spring and midsummer may indicate increase in C demand
Carbon Isotope Composition of Dissolved Inorganic Carbon ($\delta^{13}\text{C}_{\text{DIC}}$)	Determine lake carbon balance	Decrease in values between spring and midsummer may indicate increase in C demand
Carbon Isotope Fractionation Factor ($\Delta^{13}\text{C}_{\text{DIC-POM}}$)	Determine lake carbon balance	Decrease in values between spring and midsummer may indicate increase in C demand

Copyright Permissions

Three of the chapters of this thesis have been previously published as manuscripts in the journals Hydrological Processes, Arctic, Antarctic and Alpine Research and Ecology and Evolution. Permission to include the manuscripts in this thesis was required from Hydrological Processes and Arctic, Antarctic and Alpine Research. The permission was obtained and included below.

Chapter 2 copyright permissions:


JOHN WILEY AND SONS LICENSE TERMS AND CONDITIONS

Jul 10, 2015



This Agreement between Lauren A MacDonald ("You") and John Wiley and Sons ("John Wiley and Sons") consists of your license details and the terms and conditions provided by John Wiley and Sons and Copyright Clearance Center.

License Number	3665480878193
License date	Jul 10, 2015
Licensed Content Publisher	John Wiley and Sons
Licensed Content Publication	Hydrological Processes
Licensed Content Title	Tracking hydrological responses of a thermokarst lake in the Old Crow Flats (Yukon Territory, Canada) to recent climate variability using aerial photographs and paleolimnological methods
Licensed Content Author	Lauren A. MacDonald, Kevin W. Turner, Ann M. Balasubramaniam, Brent B. Wolfe, Roland I. Hall, Jon N. Sweetman
Licensed Content Date	May 10, 2011
Pages	13
Type of use	Dissertation/Thesis
Requestor type	Author of this Wiley article
Format	Print and electronic
Portion	Full article
Will you be translating?	No
Title of your thesis / dissertation	Integration of paleolimnological and contemporary hydroecological analyses to decipher effects of multiple stressors on water-rich northern landscapes
Expected completion date	Oct 2015
Expected size (number of pages)	250
Requestor Location	Lauren A MacDonald 23 Billington Street Cambridge, ON N1P 0A7 Canada Attn: Lauren A MacDonald
Billing Type	Invoice
Billing Address	Lauren A MacDonald 23 Billington Street Cambridge, ON N1P 0A7 Canada


Chapter 3 copyright permissions:


Inbox: Re: Article Permissions for use in Thesis (5 of 45) 

Mark as: Move | Copy | This message to

[Back to Inbox](#)  

[Delete](#) | [Reply](#) | [Forward](#) | [Redirect](#) | [View Thread](#) | [Blacklist](#) | [Whitelist](#)
[Message Source](#) | [Save as](#) | [Print](#) | [Report as Spam](#) | [Report as Innocent](#)
Headers

Date: Fri, 10 Jul 2015 19:20:49 -0300 (10/07/2015 18:20:49 EDT)
From: Larry Bowlds <Larry.Bowlds@colorado.edu> 
To: l7macdon@uwaterloo.ca <l7macdon@uwaterloo.ca>
Subject: Re: Article Permissions for use in Thesis

 Images have been blocked to protect your privacy. [Show Images?](#) | [Show this HTML in a new window?](#)

Hi Lauren,
You've written to the right person; I handle permissions. You are certainly welcome to use your paper as part of your thesis. Do you need a .pdf?
Best wishes as you finish up your Ph.D.
Larry

Larry Bowlds
Managing Editor
Arctic, Antarctic, and Alpine Research
University of Colorado
<http://aaarjournal.org>

On 7/10/2015 3:32 PM, l7macdon@uwaterloo.ca wrote:

Hello,

I published an article in AAAR in 2014 (46(1): 206-217; Avian-Driven Modification of Seasonal Carbon Cycling at a Tundra Pond in the HBL).
I would like to include that article as part of my PhD thesis. Do I need to obtain permission from AAAR before I include it in my thesis?
How should I go about obtaining that permission?

Thanks for your help,
Lauren

References

- ABEK Co-op (Arctic Borderlands Ecological Knowledge Co-op). 2007. Community reports 2005-2006. <http://www.taiga.net/coop/community/index.html>
- Aboriginal Affairs and Northern Development Canada (AANDC). 2013. History of Giant Mine: Historical Timeline. <http://www.aadnc-aandc.gc.ca/eng/1374760498850/1374760562098>
- Abraham KF, Jefferies RL, Rockwell RF. 2005a. Goose-induced changes in vegetation and land over between 1976 and 1997 in an Arctic coastal marsh. *Arctic, Antarctic and Alpine Research*, 37: 260-275.
- Abraham KF, Jefferies RL, Alisauskas RT. 2005b. The dynamics of landscape change and snow geese in mid-continent North America. *Global Change Biology*, 11: 841-855.
- ACIA. 2005. Arctic Climate Impact Assessment. Cambridge University Press, Cambridge, 1042 pp.
- Allen ED and Spence DHN. 1981. The differential ability of aquatic plants to utilize the inorganic carbon supply in fresh waters. *New Phytologist*, 87: 269-283.
- Anderson T, Carstensen J, Hernandez-Garcia E, Duarte CM. 2009. Ecological thresholds and regime shifts: approaches to identification. *Trends in Ecology and Evolution*, 24: 49-57.
- Andrade CF, Jamieson HE, Kyser TK, Praharaj T, Fortin D. 2010. Biogeochemical redox cycling of arsenic in mine-impacted lake sediments and coexisting pore waters near Giant Mine, Yellowknife Bay, Canada. *Applied Geochemistry* 25(2):199-211.
- Antoniades D, Douglas MSV, Smol, JP. 2005. Quantitative estimates of recent environmental changes in the Canadian High Arctic inferred from diatoms in lake and pond sediments. *Journal of Paleolimnology*, 33: 349-360.
- Appleby PG. 2001. Chronostratigraphic techniques in recent sediments. In *Tracking Environmental Change Using Lake Sediments. Volume 1: Basin Analysis, Coring and Chronological Techniques, Developments in Paleoenvironmental Research*, Last WM, Smol, JP (eds). Kluwer Academic Publishers, Dordrecht: 171-203.
- Arctic Monitoring and Assessment Programme (AMAP). 1998. AMAP Assessment Report: Arctic Pollution Issues. AMPA, Oslo.
- Bade DL, Carpenter SR, Cole JJ, Hanson PC, Hesslein RH. 2004. Controls of $\delta^{13}\text{C}$ -DIC in lakes: Geochemistry, lake metabolism, and morphometry. *Limnology and Oceanography*, 49: 1160-1172.

- Batt BDJ. 1997. Arctic ecosystems in peril: report of the Arctic Goose Habitat Working Group. Arctic Goose Joint Venture Special Publication. U.S. Fish and Wildlife Service, Washington D.C. and Canadian Wildlife Service, Ottawa, Ontario. 120pp.
- Battarbee RW, Jones VJ, Flower RJ, Cameron NG, Bennion H. 2001. Diatoms. In *Tracking Environmental Change Using Lake Sediments: Terrestrial, Algal and Siliceous Indicators*, Vol 3, Smol JP, Birks HJB, Last WM (eds). Kluwer Academic Publishers, Dordrecht: 155-202.
- Bayley SE, Prather CM. 2003. Do wetland lakes exhibit alternative stable states? Submersed aquatic vegetation and chlorophyll in western boreal shallow lakes. *Limnology and Oceanography*, 48: 2335-2345.
- Bayley SE, Creed IF, Sass GZ, Wong AS. 2007. Frequent regime shifts in trophic states in shallow lakes on the boreal plain: alternative “unstable” states? *Limnology and Oceanography*, 52: 2002-2012.
- Beisner BE, Haydon DT, Cuddington K. 2003. Alternative stable states in ecology. *Frontiers in Ecology and Environment*, 1: 376-382.
- Bos DG, Pellatt MG. 2012. The water chemistry of shallow ponds around Wapusk National Park of Canada, Hudson Bay Lowlands. *Canadian Water Resources Journal*, 37: 163-175.
- Bouchard F, Turner KW, MacDonald LA, Deakin C, White H, Farquharson N, Medeiros AS, Wolfe BB, Hall RI, Pienitz R, Edwards TWD. 2013. Vulnerability of shallow subarctic lakes to evaporate and desiccate when snowmelt runoff is low. *Geophysical Research Letters*, 40: 6112-6117.
- Bowman MF and Somers KM. 2005. Considerations when using the reference condition approach for bioassessment of freshwater ecosystems. *Water Quality Research Journal of Canada*, 40(3): 347-360.
- Brewer MC, Carter LD, Glenn R. 1993. Sudden drainage of a thaw lake on the Alaskan Arctic coastal plain. In *Proceedings of the Sixth International Conference on Permafrost*. South China University of Technology Press, Wushan Guangzhou: 48-53.
- Bright DA, Dodd M, Reimer KJ. 1996. As in sub-Arctic lakes influenced by gold mine effluent: the occurrence of organoarsenicals and ‘hidden’ arsenic. *Science of the Total Environment*, 180(2): 165-182.
- Brock BE, Wolfe BB, Edwards TWD. 2007. Characterizing the hydrology of shallow floodplain lakes in the Slave River Delta, NWT, Canada, using water isotope tracers. *Arctic, Antarctic and Alpine Research*, 39(3): 388-401.
- Brock BE, Martin ME, Mongeon CL, Sokal MA, Wesche SD, Armitage D, Wolfe BB, Hall RI, Edwards TWD. 2010. Flood frequency variability during the past 80 years in the Slave

River Delta, NWT, as determined from multi-proxy paleolimnological analysis. *Canadian Water Resources Journal*, 35 (3): 281–300.

Bromstad MJ. 2011. The characterization, persistence, and bioaccessibility of roaster-derived arsenic in surface soils at Giant Mine, Yellowknife, NWT. MSc Thesis. Queen's University, Kingston, Canada. 197 pp.

Canadian Arctic Contaminants Assessment Report II – Highlights (CACAR). 2003. Northern Contaminants Program. Minister of Indian Affairs and Northern Development, Ottawa, 143 pp.

Campbell D and Spitzer A. 2007. High and dry. *Up Here: Explore Canada's Far North*, September 2007.

Canadian Council of Ministers of the Environment (CCME). 2014. www.ccme.ca/publications/ceqg_rcqe.html. (accessed June 16, 2014)

Chapin FS III, Sturm M, Serreze MC, McFadden JP, Key JR, Llyod AH, McGuire AD, Rupp TS, Lynch AH, Schimel JP, Beringer J, Chapman WL, Epstein HE, Euskirchen ES, Hinzman LD, Jia G, Ping C-L, Tape KD, Thompson CDC, Walker DA, Welker JM. 2005. Role of land-surface changes in arctic summer warming. *Science*, 310: 657-660.

Coplen TB. 1996. New guidelines for reporting stable hydrogen, carbon and oxygen isotope ratio data. *Geochimica et Cosmochimica Acta*, 60: 3359-3360.

Côté G, Pienitz R, Velle G, Wang X. 2010. Impact of geese on the limnology of lakes and ponds from Bylot Island (Nunavut, Canada). *International Review of Hydrobiology*, 95, 105-129

Craig H. 1961. Isotopic variations in meteoric waters. *Science*, 133: 1702-1703.

Dean WE. 1974. Determination of carbonate and organic matter in calcareous sediments and sedimentary rocks by loss on ignition: comparison with other methods. *Journal of Sedimentary Petrology*, 44 (1): 242-248.

Deuser WG, Degens ET, Guillard RLL. 1968. Carbon isotope relationships between plankton and sea water. *Geochimica et Cosmochimica Acta*, 32: 657-660.

Douglas MSV, Smol JP, Blake W. 1994. Marked post-18th century environmental change in high-arctic ecosystems. *Science*, 266, 416-419.

Douglas MSV and Smol JP. 1999. Freshwater diatoms as indicators of environmental change in the High Arctic. In *The Diatoms: Applications for the Environmental and Earth Sciences*, Stoermer EF, Smol JP (eds). Cambridge University Press, Cambridge: 227-244.

Douglas MSV and Smol JP. 2000. Eutrophication and recovery in the high arctic: Meretta Lake (Cornwallis Island, Nunavut, Canada) revisited. *Hydrobiologia*, 431: 1932-204.

Douglas MSV, Hamilton PB, Pienitz R, Smol, JP. 2004. Algal indicators of environmental change in arctic and Antarctic lakes and ponds. In: *Long-term Environmental Change in Arctic and Antarctic Lakes* (eds Pienitz R, Douglas MSV, Smol JP) pp. 117-157. Springer. Netherlands.

Dredge LA and Nixon FM. 1986. Surficial geology, Northeastern Manitoba; Geological Survey of Canada, Map 1617A, scale 1:500,000.

Duguay CR and Lafleur PM. 2003. Determining depth and ice thickness of shallow sub-Arctic lakes using space-borne optical and SAR data. *International Journal of Remote Sensing*, 24: 475-489.

Edwards TWD, Wolfe BB, Gibson JJ, Hammarlund D. 2004. Use of water isotope tracers in high latitude hydrology and paleohydrology. In *Long-Term Environmental Change in Arctic and Antarctic Lakes*, Pienitz R, Douglas MSV, and Smol, JP (eds). Springer: Dordrecht, The Netherlands:187-207.

Edwards M, Walterz K, Grosse G, Plug L, Slater L, Valde P. 2009. Arctic thermokarst lakes and the carbon cycle. *Pages News*, 17, 16-18.

Eichel KA, Macrae ML, Hall RI, Fishback L-A, Wolfe B.B. 2014. Nutrient uptake and short-term responses of phytoplankton and benthic communities from a Subarctic pond to experimental nutrient enrichment in microcosms. *Arctic, Antarctic and Alpine Research*, 46: 194-209.

Elmes MC, Wiklund JA, Van Opstal SRV, Wolfe BB, Hall RI. In Review at Environmental Monitoring And Assessment. Characterizing baseline concentrations, proportions and processes controlling deposition of river-transported bitumen-associated polycyclic aromatic compounds in a floodplain lake (Slave River Delta, Northwest Territories, Canada).

Emerson S. 1975. Chemically enhanced CO₂ gas exchange in a eutrophic lake: a general model. *Limnology and Oceanography*, 20: 743-753.

English MC, Hill R, Stone MA, Ormson R. 1997. Geomorphological and botanical change on the outer Slave River Delta, NWT, before and after impoundment of the Peace River. *Hydrological Processes*, 11: 1707-1724.

Emrich K, Ehhalt DH, Vogel JC. 1970. Carbon isotope fractionation during the precipitation of calcium carbonate. *Earth and Planetary Science Letters*, 8: 363-371.

Environment Canada. 1994. *Manual of Analytical Methods: Major Ions and Nutrients, Volume 1*. National Laboratory for Environmental Testing. Canadian Centre for Inland Waters, Burlington, ON.

Environment Canada. 2010. *National Climate Data and Information Archive*. (Accessible at: http://www.climate.weatheroffice.ec.gc.ca/climateData/hourlydata_e.html). (accessed January 2011)

Environment Canada. 2011. Integrated Monitoring Plan for the Oil Sands: Expanded Geographic Extent for Water Quality and Quantity, Aquatic Biodiversity and Effects, and Acid Sensitive Lake Component. Government of Canada.

Epstein S and Mayeda TK. 1953. Variations of ^{18}O contents of waters from natural sources. *Geochimica et Cosmochimica Acta*, 4: 213-224.

Fry B. 2006. *Stable Isotope Ecology*. Springer, New York.

Gagnon A and Gough W. 2005. Climate change scenarios for the Hudson Bay Region: An intermodel comparison. *Climate Change*, 69: 269-297.

Galloway JM, Sanei H, Patterson RT, Mosstarjiri T, Haldlari T, Falck H. 2012. Total arsenic concentrations of lake sediments near the city of Yellowknife, Northwest Territories. Geologic Survey of Canada, Natural Resources Canada. Open File 7037.

Geldsetzer T, van der Sanden JJ. 2010. Lake ice break-up 2009, Old Crow Flats, Yukon, Canada. Natural Resources Canada, Ottawa.

Glew JR. 1988. A portable extruding device for close internal sectioning of unconsolidated core samples. *Journal of Paleolimnology*, 1: 235-239.

Glew JR. 1989. A new trigger mechanism for sediment samples. *Journal of Paleolimnology*, 2: 241-243.

Glew JR, Smol JP, Last WM. 2001. Sediment core collection and extrusion. *In Tracking Environmental Change Using Lake Sediments, Volume 3* (eds Smol JP, Birks HJB, Last WM) pp. 81-98. Kluwer Academic Publishers: Norwell MA.

Gosselin P, Hrudey S, Naeth A, Plourde A, Therrien R, van der Kraar G, and Xue Z. 2010. Environmental and health impacts of Canada's oil sands industry Ottawa: The Royal Society of Canada. pp 414. Available: <http://rscsrc.ca/sites/default/files/pdf/RSC%20Oil%20Sands%20Panel%20Main%20Report%20Oct%202012.pdf>

Gregory-Eaves I, Finney BP, Douglas MSV, Smol JP. 2004. Inferring sockeye salmon (*Oncorhynchus nerka*) population dynamics and water quality changes in a stained nursery lake over the past similar to 500 years. *Canadian Journal of Fisheries and Aquatic Sciences*, 61: 1235-1246.

- Griffis TJ, WR Rouse and JM Waddington. 2000. Interannual variability of net ecosystem CO₂ exchange at a subarctic fen. *Global Biogeochemical Cycles*, 14: 1109-1121
- Hadley KR, Douglas MSV, McGhee R, Blais JM, Smol JP. 2010. Ecological influences of Thule Inuit whalers on high arctic pond ecosystems: a comparative paleolimnological study from Bathurst Island (Nunavut, Canada). *Journal of Paleolimnology*, 44: 85-93.
- Hall RI, Wolfe BB, Wiklund JA, Edwards TWD, Farwell AJ, Dixon DG. 2012. Natural processes dominate the delivery of polycyclic aromatic compounds to the Athabasca Delta downstream of oil sands development. *PLOS ONE*, 7(9): 1-17.
- Handa IT, Harmsen R, Jefferies RL. 2002. Patterns of vegetation change and the recovery potential of degraded areas in a coastal marsh system of the Hudson Bay Lowlands. *Journal of Ecology*, 90: 86-99.
- Hawkins CP, Olson JR, Hill RA. 2010. The reference condition: predicting benchmarks for ecological and water-quality assessments. *Journal of North American Benthological Society*, 29(1): 312-333.
- Herczeg AL and Fairbanks RG. 1987. Anomalous carbon isotope fractionation between atmospheric CO₂ and dissolved inorganic carbon induced by intense photosynthesis. *Geochimica et Cosmochimica Acta*, 51: 895-899.
- Heiri O, Lotter AF, Lemcke G. 2001. Loss on ignition as a method for estimating organic and carbonate content in sediments: reproducibility and comparability of results. *Journal of Paleolimnology*, 25: 101-110.
- Hinkel KM, Jones BM, Eisner WR, Cuomo CJ, Beck RA, Frohn R. 2007. Methods to assess natural and anthropogenic thaw lake drainage on the western arctic coastal plain of northern Alaska. *Journal of Geophysical Research*, 112: F02S16..
- Hocking D, Kuchar P, Plambeck JA, Smith RA. 1978. The impact of gold smelter emissions on vegetation and soils of a sub-arctic forest-tundra transition ecosystem. *Journal of the Air Pollution Control Association*, 28(2): 133-137.
- Hutchinson TC, Aufreiter S, Hancock GV. 1982. Arsenic pollution in the Yellowknife area from gold smelter activities. *Journal of Radioanalytical Chemistry*, 71: 58-73.
- IPCC. 2007. Climate Change 2007: The physical science basis. Contribution from Working Group 1 to the fourth assessment report of the Inter-Governmental Panel on Climate Change, in *IPCC Fourth Assessment Report* edited by Solomon, S., Qin, D., Manning, M., Marquis, M., Averyt, M., Tignor, M., Miller, H.L. Cambridge University Press, Cambridge, U.K.
- Jackson FJ, Lafontaine CN, Klaverkamp J. 1996. Yellowknife – Back Bay Study on Metal and Trace Element Contamination of Water, Sediment and Fish. Joint Report of Indian and Northern Affairs Canada and Fisheries and Oceans Canada. pp 195.

Jacobs FS, Filby RH. 1982. Trace element composition of Athabasca tar sands and extracted bitumen Atomic and nuclear methods in fossil energy research ed Filby RH, Carpenter B S, Ragaini R C (New York, NY: Plenum Press). pp 49-59.

Jautzy JJ, Ahad JME, Hall RI, Wiklund JA, Wolfe BB, Gobeil C, Savard MM. 2015. Source apportionment of background PAHs in the Peace-Athabasca Delta (Alberta, Canada) using molecular level radiocarbon analysis. *Environmental Science and Technology*, 49(15): 9056-9063.

Jefferies RL and Rockwell RF. 2002. Foraging geese, vegetation loss and soil degradation in an Arctic salt marsh. *Applied Vegetation Science*, 5: 7-16.

Jefferies RL, Rockwell RF, Abraham KF. 2003. The embarrassment of riches: agricultural food subsidies, high goose numbers, and loss of Arctic wetlands – a continuing saga. *Environmental Reviews*, 11: 193-232.

Jefferies RL, Rockwell RF, Abraham KF. 2004. Agricultural food subsidies, migratory connectivity and large-scale disturbance in Arctic coastal systems: a case study. *Integrative and Comparative Biology*, 44: 130-139.

Jefferies RL, Jano AP, Abraham KF. 2006. A biotic agent promotes large-scale catastrophic change in the coastal marshes of Hudson Bay. *Journal of Ecology*, 94: 234-242.

Jeffrey SW, Mantoura RFC, Wright SW. 1997. Phytoplankton pigments in oceanography. UNSECO Publishing: Paris.

Kattsov VM, Källén E, Cattle H, Christensen J, Drange H, Hanssen-Bauer I, Jóhannesen T, Karol I, Räisänen J, Svensson G, Vavulin S. 2005. Future climate change: modeling and scenarios for the Arctic. *Arctic Climate Impact Assessment*. Cambridge University Press: Cambridge; 100-146.

Keatley B, Douglas MSV, Smol JP. 2006. Early-20th century environmental changes inferred using diatoms from a small pond on Melville Island, NWT, Canadian High Arctic. *Hydrobiologia*, 553: 15-26.

Keatley BE, Douglas MSV, Blais JM, Mallory ML, Smol JP. 2009. Impacts of seabird-derived nutrients on water quality and diatom assemblages from Cape Vera, Devon Island, Canadian High Arctic. *Hydrobiologia*, 621: 191-205.

Keatley BE, Blais JM, Douglas MSV, Gregory-Eaves I, Mallory ML, Smol JP. 2011. Historical seabird population dynamics and the effects on Arctic pond ecosystems: a multi-proxy paleolimnological study from Cape Vera, Devon Island, Arctic Canada. *Fundamental and Applied Limnology*, 179: 51-66.

Keeley JE and Sandquist DR. 1992. Carbon: Freshwater plants. *Plant, Cell and Environment*, 15: 1021-1035.

Kelly EN, Schindler DW, Hodson PV, Short JW, Ma M, Kwan AK, Fortin BL. 2009. Oil sands development contributes polycyclic aromatic compounds to the Athabasca River and its tributaries. *Proceedings of the National Academy of Sciences*, 106(52): 22346-22351.

Kelly EN, Schindler DW, Hodson PV, Short JW, Radmanovich R, Nielsen CC. 2010. Oil sands development contributes elements toxic at low concentrations to the Athabasca River and its tributaries. *Proceedings of the National Academy of Sciences*, 107(37): 16178-16183.

Kersten M and Smedes F. 2002. Normalization procedures for sediment contaminants in spatial and temporal trend monitoring. *Journal of Environmental Monitoring*, 4: 109-115.

Kirk JL, Muir DCG, Gleason A, Wang X, Lawson G, Frank RA, Lehnerr I, Wrona F. 2014. Atmospheric deposition of mercury and methylmercury to landscapes and waterbodies of the Athabasca Oil Sands Region. *Environmental Science and Technology*, 48: 7374-7383.

Kling GW, Kipphut GW, Miller MC. 1991. Arctic lakes and streams as gas conduits to the atmosphere: implications for tundra carbon budgets. *Science*, 251: 298-301.

Kling GW, Kipphut GW, Miller MC. 1992. The flux of CO₂ and CH₄ from lakes and rivers in Arctic Alaska. *Hydrobiologia*, 240: 23-36.

Klinger LF and Short SK. 1996. Succession in the Hudson Bay Lowland, northern Ontario, Canada. *Arctic and Alpine Research*, 28: 172-183

Koch I, Wang L, Reimer KJ, Cullen WR. 2000. Arsenic species in terrestrial fungi and lichens from Yellowknife, N.W.T., Canada. *Applied Organometallic Chemistry*, 14(5): 245-252.

Kotanen PM, Abraham KF. 2013. Decadal changes in vegetation of a subarctic salt marsh used by lesser snow and Canada geese. *Plant Ecology*, 214: 409-422.

Krammer K, Lange-Bertalot H. 1986-1991. Bacillariophyceae. Süßwasserflora von Mitteleuropa. Band 2 (1-4), vols. 1-4. Gustav Fisher Verlag: Stuttgart.

Kurek J, Kirk JL, Muir DCG, Wang X, Evans MS, Smol JP. 2013. Legacy of a half century of Athabasca oil sands development recorded by lake ecosystems. *Proceedings of the National Academy of Sciences*, 110(5): 1761-1766.

Labrecque S, Lacelle D, Duguay C, Lauriol B, Hawkings J. 2009. Contemporary (1951-2001) evolution of lakes in the Old Crow Basin, northern Yukon, Canada: Remote sensing, numerical modeling and stable isotope analysis. *Arctic*, 62 (2): 225-238.

- Iacobelli A and Jefferies RL. 1991. Inverse salinity gradients in coastal marshes and the death of *Salix*; the effects of grubbing by geese. *Journal of Ecology*, 79: 61-73.
- Lambert A, Courtier N, Sasagawa GS, Klopping F, Winester D, James TS, Liard JO. 2001. New constraints on Laurentide postglacial rebound from absolute gravity measurements. *Geophysical Research Letters*, 28: 2109-2112.
- Lantz TC and Kokelj SV. 2008. Increasing rates of retrogressive thaw slump activity in the Mackenzie Delta region, N.W.T., Canada. *Geophysical Research Letters*, 35: L06502.
- Lauriol B, Duguay CR, Riel A. 2002. Response of the Porcupine and Old Crow rivers in northern Yukon, Canada, to Holocene climatic change. *The Holocene*, 12 (1): 27-34.
- Laurion I, Vincent WF, MacIntyre S, Retamal L, Dupont C, Francus P, Pienitz R. 2010. Variability in greenhouse gas emission from permafrost thaw ponds. *Limnology and Oceanography*, 55: 115-133.
- Lavoie I, Hamilton PB, Campain S, Grenier M, Dillion PJ. 2008. Guide d'identification des diatomees des rivieres de l'Est du Canada. Presses de L'universite du Quebec: Quebec.
- Leavitt PR, Carpenter SR, Kitchell JF. 1989. Whole-lake experiments: The annual record of fossil pigments and zooplankton. *Limnology and Oceanography*, 34 (4): 700-717.
- Leavitt PR, Hodgson DA. 2001. Sedimentary pigments. In *Tracking Environmental Change Using Lake Sediments: Volume 3: Terrestrial, Algal and Siliceous Indicators* (Last W, Smol JP) pp 295-325. Kluwer Academic: Dordrecht.
- Leng M, Lamb A, Heaton T, Marshall J, Wolfe B, Jones M, Holmes J, Arrowsmith C. 2005. Isotopes in lake sediments. In *Isotopes in Paleoenvironmental Research: Developments in Paleoenvironmental Research*, Leng M (eds). Springer: Netherlands: 147-184.
- Light E. 2011. Characterizing the present and past hydrology of shallow ponds in the Churchill area using isotopic methods. Unpublished MSc Thesis, Wilfrid Laurier University, Canada, 175 pp.
- Lim DSS, Douglas MSV, Smol JP. 2005. Limnology of 46 lakes and ponds on Banks Island, N.W.T., Canadian Arctic Archipelago. *Hydrobiologia*, 545: 11-32.
- Loring DH. 1991. Normalization of heavy-metal data from estuarine and coastal sediments. *ICES Journal of Marine Science*, 48: 101-115.
- Loring DH and Rantala RTT. 1992. Manual for the geochemical analyses of marine sediments and suspended particulate matter. *Earth-Science Reviews*, 32: 235-283.

Lorrain A, Savoye N, Chauvaud L, Paulet Y-M, Naulet N. 2003. Decarbonation and preservation method for the analysis of organic C and N contents and stable isotope ratios of low-carbonated suspended particulate material. *Analytica Chimica Acta*, 491: 125-133.

Lotter AF, Pienitz R, Schmidt R. 1999. Diatoms as indicators of environmental change near arctic and alpine treeline. In *The Diatoms: Applications for the Environmental and Earth Sciences*, Stoermer EF and Smol JP (eds). Cambridge University Press: Cambridge; 227-244.

Lougheed VL, Butler MG, McEwen DC, Hobbie JE. 2011. Changes in tundra pond limnology: re-sampling Alaskan ponds after 40 years. *AMBIO*, 40: 589-599.

Luoto TP, Oksman M, Ojala AEK. 2014. Climate change and bird impact as drivers of High Arctic pond deterioration. *Polar Biology*, 38: 357-368.

MacDonald LA, Turner KW, Balasubramaniam AM, Wolfe BB, Hall RI, Sweetman JN. 2012. Tracking hydrological responses of a thermokarst lake in the Old row Flats (Yukon Territory, Canada) to recent climate variability using aerial photographs and paleolimnological methods. *Hydrological Processes*, 26(1): 117-129.

MacDonald LA, Farquharson N, Hall RI, Wolfe BB, Macrae ML, Sweetman JN. 2014. Avian-driven modification of seasonal carbon cycling at a tundra pond in the Hudson Bay Lowlands (northern Manitoba, Canada). *Arctic, Antarctic, and Alpine Research*, 46: 206-217.

MacDonald LA, Farquharson N, Merritt G, Fooks S, Medeiros AS, Hall RI, Wolfe BB, Macrae ML, Sweetman JN. 2015. Limnological regime shifts caused by climate warming and Lesser Snow Goose population expansion in the western Hudson Bay Lowlands (Manitoba, Canada). *Ecology and Evolution*, 5(4): 921-939.

Mackay JR. 1988. Catastrophic lake drainage, Tuktoyaktuk Peninsula area, District of Mackenzie. Current Research, Part D, Geological Survey of Canada, Paper 88-1D, 83-90.

Mackay JR. 1992. Lake stability in an ice-rich permafrost environment: examples from the western Arctic coast. In *Aquatic Ecosystems in Semi-Arid Regions: Implications for Resource Management*, Robarts RD, Bothwell ML (eds). NHRI Symposium Series 7. Environment Canada: Saskatoon, Saskatchewan; 1-26.

Macrae ML. 1998: Variations in organic carbon storage in shallow tundra ponds. MSc Thesis York University, Toronto, Canada.

Macrae ML, Bello RL, Molot LA. 2004. Long-term carbon storage and hydrological control of CO₂ exchange in tundra ponds in the Hudson Bay Lowland. *Hydrological Processes*, 18: 2051-2069.

Macrae ML, Brown L, Duguay CR, Parrott JA, Petrone RM. 2014. Observed and projected climate change in the Churchill region of the Hudson Bay Lowlands and implications for pond sustainability. *Arctic, Antarctic, and Alpine Research*, 46: 272-285.

Mallory ML, Fontaine AJ, Smith PA, Robertson MOW, Gilchrist HG. 2006. Water chemistry of ponds on Southampton Island, Nunavut, Canada: effects of habitat and ornithogenic inputs. *Archiv für Hydrobiologie*, 166: 411-432.

Manny BA, Johnson WC, Wetzel RG. 1994. Nutrient additions by waterfowl to lakes and reservoirs – Predicting their effects on productivity and water quality. *Hydrobiologia*, 280: 121-132.

Mantoura RFC, Llewellyn CA. 1983. The rapid determination of algal chlorophyll and carotenoid pigments and their breakdown products in natural waters by reverse-phase high performance liquid chromatography. *Analytica Chimica Acta*, 151: 297-314.

Marsh P, Neumann NN. 2001. Processes controlling the rapid drainage of two ice-rich permafrost-dammed lakes in NW Canada. *Hydrological Processes*, 15: 3433-3446.

Marsh P, Russell M, Pohl S, Haywood H, Onclin C. 2009. Changes in thaw lake drainage in the Western Canadian Arctic from 1950 to 2000. *Hydrological Processes*, 23: 145-158.

McGuire AD, Anderson LG, Christensen TR, Dallimore S, Guo L, Hayes DJ, Heimann M, Lorenson TD, MacDonald RW. 2009. Sensitivity of the carbon cycle in the Arctic to climate change. *Ecological Monographs*, 79: 523-555.

Medeiros AS, Taylor DJ, Couse M, Hall RI, Quinlan R, Wolfe BB. 2014. Biological and nutrient responses to catchment disturbance and warming in small lakes near the Alaskan tundra-taiga boundary. *Holocene*, 24 (10): 1308-1319.

Meyers PA, Teranes J. 2001 Sediment Organic Matter. In *Tracking Environmental Change Using Lake Sediments: Volume 2: Physical and Geochemical Methods*, Last W, Smol, JP (eds). Kluwer Academic: Dordrecht; 239-269.

Meyers PA. 2003. Applications of organic geochemistry to paleolimnological reconstructions: a summary of examples from the Laurentian Great Lakes. *Organic Geochemistry*, 34: 261-289.

Michelutti N, Hermanson MH, Smol JP, Dillon PJ, Douglas MSV. 2007. Delayed response of diatom assemblages to sewage inputs in an arctic lake. *Aquatic Sciences*, 69: 523-533.

Michelutti N, Keatley BE, Brimble Y, Blais JM, Liu H, Douglas MSV, Mallory M., Macdonald RW, Smol JP. 2009. Seabird-Driven Shifts in Arctic Pond Ecosystems. *Proceedings of the Royal Society: Biological Sciences*, 276: 591-596.

Michelutti N, Brash J, Thienpont J, Blais JM, Kimpe L, Mallory ML, Douglas MSV, Smol JP. 2010. Trophic position influences the efficacy of seabirds as contaminant biovectors. *Proceedings of the National Academy of Science*, 107: 10543-10548.

- Morrison J, Brockwell T, Merren T, Fourel F, Phillips AM. 2001: A new on-line method for high precision stable-hydrogen isotopic analyses on nanolitre water samples. *Analytical Chemistry*, 73: 3570–3575.
- Morrell G and Dietrich JR. 1993. Evaluation of the hydrocarbon prospectivity of the Old Crow Flats area of northern Yukon. *Bulletin of Canadian Petroleum Geology*, 41 (1): 32-45.
- Murdoch A, Joshi SR, Sutherland D, Murdoch P, Dickson KM. 1989. Geochemistry of sediments in the Back Bay and Yellowknife Bay of Great Slave Lake. *Environmental Geology and Water Sciences*, 14(1): 35-42.
- O’Leary MH. 1981. Carbon isotope fractionation in plants. *Phytochemistry*, 20: 553-567.
- Olson MH, Hage MM, Binkley MD, Binder JR. 2005. Impact of migratory snow geese on inputs. *Archiv für Hydrobiologie*, 166: 411-432.
- Overpeck J, Hughen K, Hardy D, Bradley R, Case R, Douglas M. 1997. Arctic environmental change of the last four centuries. *Science*, 278 (5341): 1251-1256.
- Parks Canada. 2000. Background information to the Wapusk Ecological Integrity Statement. Parks Canada, Western Canada Service Centre, Winnipeg Manitoba. 102 pp.
- Parks Canada. 2007. Monitoring and reporting ecological integrity in Canada's national parks. In. Parks Canada Agency Ottawa, pp. 1-115.
- Parks Canada. 2007/2008. Annual Report of Research and Monitoring in Wapusk National Park. 21pp.
- Parks Canada. 2008. Ecological Integrity Monitoring Action Plan for Wapusk National Park of Canada 2008-2013. 88pp.
- Parks Canada. 2009. State of the park report Vuntut National Park. In. Parks Canada Agency Ottawa.
- Parks Canada. 2010. Vuntut National Park Management Plan. In. Parks Canada Agency Ottawa, pp. 1-79.
- Parks Canada. 2011. State of the park report Wapusk National Park. In. Parks Canada Agency Ottawa.
- Parsons TR and Strickland JDH. 1963. Discussion of spectrophotometric determination of marine-plant pigments, with revised equations for ascertaining chlorophylls and carotenoids. *Journal of Marine Research*, 21: 155-163.

- Plug LJ, Walls C, Scott BM. 2008. Tundra lake changes from 1978 to 2001 on the Tuktoyaktuk Peninsula, western Canadian Arctic. *Geophysical Research Letters*, 35: L03502.
- Pohl S, Marsh P, Onclin C, Russell M. 2009. The summer hydrology of a small upland tundra thaw lake: implications to lake drainage. *Hydrological Processes*, 23: 2536-2546. DOI:10.1002/hyp.7238.
- Porter TJ, Pisaric MFJ, DeMontigny P. 2010. The influence of climate on white spruce tree-ring growth in the Old Crow Flats region. Project summary report submitted to the Natural Resources Department of Old Crow, Yukon Territory.
- Post DM, Taylor JP, Kitchell JF, Olson MH, Schindler DE, Herwig BR. 1998. The role of migratory waterfowl as nutrient vectors in a managed wetland. *Conservation Biology*, 12: 910-920.
- Prowse TD, Wrona FJ, Reist JD, Gibson JJ, Hobbie JE, Lévesque LMJ, Vincent WF. 2006. Climate change effects on hydroecology of Arctic freshwater ecosystems. *Ambio*, 35: 347-358.
- Quay PD, Emerson SR, Quay BM, Devol AH. 1986. The carbon cycle for Lake Washington – A stable isotope study. *Limnology and Oceanography*, 31: 596-611.
- Rau G. 1978. Carbon-13 Depletion in a subalpine lake: carbon flow implications. *Science*, 201: 901-902.
- Reynolds JG, Jones EL, Bennett JA, Biggs WR. 1989. Characterization of nickel and vanadium compounds in tar sand bitumen by UV-vis spectroscopy and size exclusion chromatography coupled with element-specific detection. *Fuel Science and Technology International*, 7: 625-642.
- Riordan B, Verbyla D, McGuire AD. 2006. Shrinking ponds in subarctic Alaska based on 1950-2002 remotely sensed images. *Journal of Geophysical Research*, 111. G04002.
- Rowland JC, Jones CE, Altmann G, Bryan R, Crosby BT, Geernaert GL, Hinzman LD, Kane DL, Lawrence DM, Mancino A, Marsh P, McNamara JP, Romanovsky VE, Toniolo H, Travis BJ, Trochim E, Wilson CJ. 2010. Arctic landscapes in transition: responses to thawing permafrost. *EOS, Transactions, American Geophysical Union*, 91 (26): 229-236.
- Rouse WR, Douglas MSV, Hecky RE, Hershey AE, Kling GW, Lesack L, Marsh P, McDonald M, Nicholson BJ, Roulet NT, Smol JP. 1997. Effects of climate change on the freshwaters of Arctic and subarctic North America. *Hydrological Processes*, 11: 873-902.
- Rouse WR. 2000. The energy and water balance of high-latitude wetlands: controls and extrapolation. *Global Change Biology*, 6 (S1): 59-68.

- Reuss N, Leavitt PR, Hall RI, Bigler C, Hammarlund D. 2010. Development and application of sedimentary pigments for assessing effects of climatic and environmental changes on subarctic lakes in northern Sweden. *Journal of Paleolimnology*, 43: 149-169.
- Rouse WR. 1991. Impacts of Hudson Bay on the terrestrial climate of the Hudson Bay Lowlands. *Arctic and Alpine Research*, 23: 24-30.
- Rühland K, Priesnitz A, Smol JP. 2003. Paleolimnological evidence from diatoms for recent environmental changes in 50 lakes across Canadian arctic treeline. *Arctic, Antarctic and Alpine Research*, 35: 110–123.
- Rühland K, Smol JP. 2005. Diatom shifts as evidence for recent subarctic warming in a remote tundra lake, NWT, Canada. *Palaeogeography, Palaeoclimatology, Palaeoecology*, 226: 1-16.
- Rühland KM, Paterson AM, Keller W, Michelutti N, Smol JP. 2013. Global warming triggers the loss of a key Arctic refugium. *Proceedings of the Royal Society Biological Sciences*, 280: 20131887.
- Rühland KM, Hargan KE, Jeziorski A, Paterson AM, Keller W, Smol JP. 2014. A multi-trophic exploratory survey of recent environmental changes using lake sediments in the Hudson Bay Lowlands, Ontario, Canada. *Arctic, Antarctic and Alpine Research*, 46: 139-158.
- Scheffer M, SH Hosper, ML Meijer, B Moss, Jeppesen E. 1993. Alternative equilibria in shallow lakes. *Trends in Ecology and Evolution*, 8: 275-279.
- Schindler D. 2010. Tar sands need solid science. *Nature*, 468: 499-501.
- Scheffer M and Carpenter SR. 2003. Catastrophic regime shifts in ecosystems: linking theory to observations. *Trends in Ecology and Evolution*, 18: 648-656.
- Schindler DW and Smol JP. 2006. Cumulative effects of climate warming and other human activities on freshwaters of Arctic and subarctic North America. *Ambio*, 35, 160-168.
- Schuur EAG, Bockheim J, Canadell JG, Euskirchen E, Field CB, Goryachkin SV, Hagemann S, Kuhry P, Lafleur PM, Lee H, Mazhitova G, Nelson FE, Rinke A, Romanovsky VE, Shiklomanov N, Tarnocai C, Venevsky S, Vogel JG, Zimov SA. 2008. Vulnerability of permafrost carbon to climate change: implications for the global carbon cycle. *BioScience*, 58: 701-714.
- SCOR/UNESCO. 1966: Working group on photosynthetic pigments: monographs on oceanographic methodology. Paris: UNESCO Publishing.

Serreze MC, Walsh JE, Chapin III FS, Osterkamp T, Dyurgerov M, Romanovsky V, Oechel WC, Morison J, Zhang T, Barry RG. 2000. Observational evidence of recent change in the northern high-latitude environment. *Climate Change*, 46: 159-207.

Shaker S. 2011. Multi-proxy paleolimnological analysis of past hydro-ecological changes in a shallow thermokarst lake in the Old Crow Flats, Yukon Territory (Lake OCF 35). BSc Honours Thesis, Biology, University of Waterloo.

Sheath RG. 1986. Seasonality of phytoplankton in northern tundra ponds. *Hydrobiologia*, 138: 75-83.

Silke R. 2013. Giant Mine Milling and Roasting Process, Yellowknife, NWT: A Historical Summary. Giant Mine Remediation Team Directorate, Aboriginal Affairs and Northern Development Canada. Yellowknife, NT.

Smith SL and Burgees MM. 2004. Sensitivity of permafrost to climate warming in Canada. Geological Survey of Canada. *Bulletin*, 579.

Smith LC, Sheng Y, MacDonald GM, Hinzman LD. 2005. Disappearing arctic lakes. *Science*, 308: 1429.

Smol JP. 2008. Pollution of lakes and rivers: A paleoenvironmental perspective, 2nd Edition. Blackwell Publishing. ISBN 13: 978-1-4051-5913-5

Smol JP, Wolfe AP, Birks HJB, Douglas MSV, Jones VJ, Korhola A, Pienitz R, Ruhland K, Sorvari S, Antoniades D, Brooks SJ, Fallu MA, Hughes M, Keatley B, Laing T, Michelutti N, Nazarova L, Nyman M, Paterson AM, Perren B, Quinlan R, Rautio M, Saulnier-Talbot E, Siitonen S, Solovieva N, Weckstrom J, Schindler DW. 2005. Climate-driven regime shifts in the biological communities of Arctic lakes. *Proceedings of the National Academy of Science*, 102: 4397– 4402.

Smol JP and Douglas MSV. 2007a. Crossing the final ecological threshold in high Arctic ponds. *Proceedings of the National Academy of Sciences*, 104: 12395-12397.

Smol JP and Douglas MSV. 2007b. From controversy to consensus: making the case for recent climatic change in the Arctic using lake sediments. *Frontiers in Ecology and the Environment*, 5: 466-474.

Sokal MA, Hall RI, Wolfe BB. 2008. Relationships between hydrological and limnological conditions in lakes of the Slave River Delta (NWT, Canada) and quantification of their roles on sedimentary diatom assemblages. *Journal of Paleolimnology*, 39: 533-550.

Sokal MA, Hall RI, Wolfe BB. 2010. The role of flooding on inter-annual and seasonal variability of lake water chemistry, phytoplankton diatom communities and macrophyte biomass in the Slave River Delta (Northwest Territories, Canada). *Ecohydrology* 3: 41-54.

Sovari S, Korhola A, Thompson R. 2002. Lake diatom responses to recent Arctic warming in Finnish Lapland. *Global Change Biology*, 8: 171-181.

SRDP Workshop. 2011. Our water, our life: building partnerships to assess the health of the Slave River and the Slave River Delta. Aboriginal Affairs and Northern Development Canada and Northwest Territories.

Srivastava DS and Jefferies RL. 1996. A positive feedback: Herbivory, plant growth, salinity and the desertification of an Arctic salt marsh. *Journal of Ecology*, 84: 31-42.

Stumm W and Morgan J. 1981. *Aquatic Chemistry: An Introduction Emphasizing Chemical Equilibria in Natural Waters*. New York, U.S.A. John Wiley and Sons, Inc.

Sun LG, Emslie SD, Huang T, Blais JM, Xie ZQ, Liu XD, Yin XB, Wang YH, Huang W, Hodgson DA, Smol JP. 2013. Vertebrate records in polar sediments: Biological responses to past climate change and human activities. *Earth Science Reviews*, 126: 147-155.

Takahashi K, Yoshioka T, Wada E, Sakamoto M. 1990. Temporal variations in carbon isotope ratio of phytoplankton in a eutrophic lake. *Journal of Plankton Research*, 12: 799-808.

Talbot MR. 2001. Nitrogen isotopes in paleolimnology. In *Tracking Environmental Change Using Lake Sediments. Volume 2: Physical and Chemical Techniques, Developments in Paleoenvironmental Research*, Last WM, Smol JP (eds). Kluwer Academic Publishers: Dordrecht: 401-439.

Tape K, Sturm M, Racine C. 2006. The evidence for shrub expansion in Northern Alaska and the Pan-Arctic. *Global Change Biology*, 12:686–702.

Tetlich R. 2007. Old Crow, Yukon. In: Arctic Borderlands Ecological Knowledge Co-op Community Reports 2005-2006, Gordon AB, Andre M, Kaglik B, Cockney S, Allen M, Snowshoe A, Tetlich R (eds). Arctic Borderlands Ecological Knowledge Society: Whitehorse, Yukon Territory, Canada: 37-39.

ter Braak CJF and Šmilauer P. 2002. CANOCO reference manual and CanoDraw for Windows user's guide: Software for canonical community ordination (version 4.5). Ithaca, New York: Microcomputer Power.

Thomas KE, Hall RI, Scrimgeour GJ. 2013. Evaluating the use of algal pigments to assess the biological condition of streams. *Environmental Assessment and Monitoring*, 185: 7895-7913.

Timoney KP and Lee P. 2009. Does the Alberta tar sands industry pollute? The scientific evidence. *The Open Conservation Biology Journal*, 3: 65-81.

- Tondu JME. 2012. An interdisciplinary approach to monitoring the hydroecology of thermokarst lakes in Old Crow Flats, Yukon Territory, Canada. Masters Thesis, Biology, University of Waterloo.
- Turner KW, Wolfe BB, Edwards TWD. 2010. Characterizing the role of hydrological processes on lake water balances in the Old Crow Flats, Yukon Territory, Canada, using water isotope tracers. *Journal of Hydrology*, 386: 103-117.
- Turner KW. 2013. Investigating the hydrology of a thermokarst landscape (Old Crow Flats, Yukon, Canada) using water isotope tracers. PhD Thesis, Geography, Wilfrid Laurier University.
- Turner KW, Wolfe BW, Edwards TWD, Lantz TC, Hall RI, Larocque G. 2014. Controls on water balance of shallow thermokarst lakes and their relations with catchment characteristics: a multi-year, landscape-scale assessment based on water isotope tracers and remote sensing in Old Crow Flats, Yukon (Canada). *Global Change Biology*, 20: 1585-1603.
- Van Geest GJ, Hessen DO, Spierenburg P, Dahl-Hansen GAP, Christensen G, Faerovig PJ, Brehm M, Loonen MJJE, Van Donk E. 2007. Goose-mediated nutrient enrichment and planktonic grazer control in Arctic freshwater ponds. *Oecologia*, 153: 653-662.
- van Huissteden J, Berrittella C, Parmentier FJW, Mi Y, Maximov TC, Dolman AJ. 2011. Methane emissions from permafrost thaw lakes limited by lake drainage. *Nature Climate Change*, 1: 119-123.
- Vreca P and Muri G. 2010. Sediment organic matter in mountain lakes of north-western Slovenia and its stable isotopic signatures: Records of natural and anthropogenic impacts. *Hydrobiologia*, 648: 35-49.
- Wachniew P and Rózański K. 1997. Carbon budget of a mid-latitude, groundwater-controlled lake: Isotopic evidence for the importance of dissolved inorganic carbon recycling. *Geochimica et Cosmochimica Acta*, 61: 2453-2465.
- Walter KM, Zimov SA, Chanton JP. 2006. Methane bubbling from Siberian thaw lakes as a positive feedback to climate warming. *Nature*, 443: 71-75.
- Wesche S. 2007. Adapting to change in Canada's North: Voices from Fort Resolution, NWT. *Meridian*, Spring/Summer issue: 19-24.
- Wesche S. 2009. Responding to change in a northern aboriginal community: Linking social and ecological perspectives. Ph.D. thesis. Wilfrid Laurier University, Waterloo, Ontario, Canada.
- Wetzel RG. 2001. *Limnology: Lake and River Ecosystems*. Academic Press, New York.

White JE. 2011. Characterizing current and past hydroecological conditions in shallow tundra ponds of the Hudson Bay Lowlands. MSc Thesis. University of Waterloo, Canada.

White JE, Hall RI, Wolfe BB, Light EM, Macrae ML, Fishback L. 2014. Hydrological connectivity and basin morphometry influence seasonal water-chemistry variations in tundra ponds of the northwestern Hudson Bay Lowlands. *Arctic, Antarctic, and Alpine Research*, 46: 218-235.

Wiklund JA, Bozinovski N, Hall RI, Wolfe BB. 2010. Epiphytic diatoms as flood indicators. *Journal of Paleolimnology*, 44: 25-42.

Wiklund JA, Hall RI, Wolfe BB, Edwards TWD, Farwell AJ, Dixon DG. 2012. Has Alberta oil sands development increased far-field delivery of airborne contaminants to the Peace-Athabasca Delta? *Science of the Total Environment*, 433: 379-382.

Wiklund JA, Hall RI, Wolfe BB, Edwards TWD, Farwell AJ, Dixon DG. 2014. Use of pre-industrial floodplain lake sediments to establish baseline river metal concentrations downstream of Alberta oil sands: A new approach for detecting pollution of rivers. *Environmental Research Letters*, 9: 124019.

Wolfe BB, Edwards TWD, Aravena R. 1999. Changes in carbon and nitrogen cycling during tree-line retreated recorded in the isotopic content of lacustrine organic matter, western Taimyr Peninsula, Russia. *The Holocene*, 9 (2): 215-222.

Wolfe BB, Edwards TWD, Elgood RJ, Beuning KRM. 2001. Carbon and oxygen isotope analysis of lake sediment cellulose: methods and applications. In *Tracking Environmental Change Using Lake Sediments: Physical and Chemical Techniques, Developments in Paleoenvironmental Research*, Vol 2, Last WM, Smol JP (eds). Kluwer Academic Publishers: Dordrecht; 373-400.

Wolfe BB, Turner KW. 2008. Near-record precipitation causes rapid drainage of Zelma Lake, Old Crow Flats, Northern Yukon Territory. *Meridian*, Spring: 7-12.

Wolfe BB, Karst-Riddoch TL, Vardy SR, Falcone MD, Hall RI, Edwards TWD. 2005. Impacts of climate and river flooding on the hydro-ecology of a floodplain basin, Peace-Athabasca Delta, Canada since A.D. 1700. *Quaternary Research*, 64: 147-162.

Wolfe BB, Falcone MD, Clogg-Wright KP, Mongeon CL, Yi Y, Brock BE, St. Amour NA, Mark WA, Edwards TWD. 2007. Progress in isotope paleohydrology using lake sediment cellulose. *Journal of Paleolimnology*, 37 (2): 221-231.

Wolfe BB, Hall RI, Edwards TWD, Vardy SR, Falcone MD, Sjunneskog C, Sylvestre F, McGowan S, Leavitt PR, van Driel P. 2008a. Hydroecological responses of the Athabasca Delta, Canada, to changes in river flow and climate during the 20th century. *Ecohydrology*, 1: 131-148.

Wolfe BB, Hall RI, Edwards TWD, Jarvis SR, Sinnatamby RN, Yi Y, Johnston JW. 2008b. Climate-driven shifts in quantity and seasonality of river discharge over the past 1000 years from the hydrographic apex of North America. *Geophysical Research Letters*, 35: L24402.

Wolfe BB, Humphries MM, Pisaric MFJ, Balasubramaniam AM, Burn CR, Chan L, Cooley D, Froese DG, Graupe S, Hall RI, Lantz T, Porter TJ, Roy-Leveillee P, Turner KW, Wesche SD, Williams M. 2011. Environmental change and traditional use of the Old Crow Flats in northern Canada: An IPY opportunity to meet the challenges of the new northern research paradigm. *Arctic*, 64(1): 127-135.

Wolfe BB, Light EM, Macrae ML, Hall RI, Eichel K, Jasechko S, White J, Fishback L, Edwards TWD. 2011. Divergent hydrological responses to 20th century climate change in shallow tundra ponds, western Hudson Bay Lowlands. *Geophysical Research Letters*, 38: L23402.

Yoshikawa K, Hinzman LD. 2003. Shrinking thermokarst ponds and groundwater dynamics in discontinuous permafrost near Council, Alaska. *Permafrost and Periglacial Processes*, 14: 151-160.

Zazula GD, Duk-Rodkin A, Schweger CE, Morlan RE. 2004. Late Pleistocene chronology of glacial Lake Old Crow and the north-west margin of the Laurentide Ice Sheet. In *Quaternary Glaciations – Extent and Chronology, Part II*, Ehlers, J. Gibbard, P.L. (eds.). 347-362.

Zimov SA, Schuur EAG, Chapin FS. 2008. Permafrost and the global carbon budget. *Science*, 312: 1612-1613.

Appendix A – Chapter 2

Table A1: Geochemical data from the core from OCF 48.

Depth (cm)	CRS Year	Organic Matter (%)	Mineral Matter (%)	CaCO ₃ (%)	Sed Rate (g/cm ² /yr)	C _{org} (%)	N (%)	C/N	δ ¹³ C _{org} (‰VPDB)	δ ¹⁵ N (‰AIR)	Cellulose δ ¹⁸ O _{lw} (‰VSMOW)
0	2007.2	17.48	76.07	14.66	0.25	8.13	0.91	8.91	-22.99	2.35	-18.76
0.5	2007	15.04	77.73	16.43	0.31	7.91	0.88	8.97	-23.98	2.53	-22.83
1	2006.7	16.63	78.08	12.01	0.41	7.69	0.86	8.95	-23.00	2.63	-22.01
1.5	2006.5	16.29	76.79	15.73	0.31	7.76	0.86	9.06	-23.04	2.73	-20.30
2	2006.2	16.03	77.91	13.78	0.25	7.64	0.84	9.05	-23.13	2.95	-17.28
2.5	2005.9	16.72	76.28	15.91	0.25	8.10	0.89	9.09	-22.57	2.85	-19.72
3	2005.6	16.26	76.96	15.41	0.24	8.39	0.92	9.15	-22.57	2.92	-24.57
3.5	2005.2	17.61	76.42	13.55	0.26	7.79	0.84	9.26	-22.83	2.84	-20.67
4	2004.5	16.00	77.03	15.85	0.28	7.68	0.84	9.11	-22.69	3.02	-22.20
4.5	2004.1	15.12	81.30	8.14	0.19	7.48	0.82	9.17	-23.08	2.99	-22.06
5	2003.2	15.15	78.53	14.36	0.21	7.63	0.84	9.10	-22.94	2.98	-18.89
5.5	2002.1	17.18	77.03	13.15	0.16	7.46	0.81	9.16	-23.02	3.18	-22.70
6	2001.1	16.37	77.04	14.97	0.21	7.85	0.85	9.23	-22.72	2.89	-21.70
6.5	2000.3	16.53	77.04	14.60	0.19	7.09	0.75	9.39	-23.28	3.00	-22.46
7	1999.3	14.53	80.47	11.36	0.21	7.48	0.79	9.44	-23.27	3.05	-19.99

7.5	1998.2	15.96	79.13	11.15	0.19	7.31	0.80	9.17	-23.79	3.47	-21.92
8	1997.1	17.01	78.91	9.25	0.18	6.99	0.76	9.24	-24.18	3.26	-22.00
8.5	1995.8	14.74	80.15	11.62	0.20	7.08	0.76	9.36	-24.50	3.39	-21.01
9	1994.7	16.19	78.72	11.56	0.23	7.15	0.78	9.18	-24.52	3.13	-20.07
9.5	1993.7	15.70	79.72	10.41	0.27	6.62	0.71	9.37	-25.27	3.30	-21.32
10	1992.8	14.99	80.38	10.53	0.33	6.40	0.68	9.44	-25.37	3.06	-20.27
10.5	1992.2	13.27	84.41	5.29	0.31	5.83	0.60	9.61	-26.34	3.49	-22.02
11	1991.4	12.59	84.09	7.55	0.28	5.08	0.51	9.91	-26.56	3.48	-21.04
11.5	1990.5	14.01	83.69	5.23	0.38	5.09	0.50	10.20	-26.68	3.65	-19.29
12	1989.9	13.67	83.85	5.63	0.60	4.74	0.45	10.54	-26.88	3.52	-19.27
12.5	1989.5	10.23	86.73	6.90	0.36	3.80	0.38	10.10	-26.77	3.44	-18.63
13	1988.6	10.30	87.32	5.41	0.25	4.31	0.42	10.16	-26.31	3.40	-21.40
13.5	1986.9	11.02	86.42	5.81	0.22	4.83	0.47	10.34	-26.34	3.76	-19.76
14	1985.6	11.94	84.82	7.38	0.20	4.84	0.46	10.49	-26.33	3.83	-21.36
14.5	1984.1	12.17	84.97	6.50	0.21	4.62	0.46	10.14	-26.52	4.00	-20.94
15	1982.7	11.47	85.99	5.78	0.21	4.25	0.41	10.38	-26.56	3.98	-18.90
15.5	1981.5	12.21	85.83	4.45	0.22	4.70	0.46	10.15	-26.38	3.76	-21.36
16	1980.6	11.98	85.19	6.43	0.23	4.96	0.48	10.39	-25.96	3.80	-18.53
16.5	1979.6	11.25	85.53	7.32	0.20	4.89	0.47	10.42	-25.60	3.73	-17.80
17	1978.4	11.13	86.48	5.42	0.17	5.01	0.49	10.26	-25.46	3.86	-20.51

17.5	1976.7	11.63	85.27	7.05	0.15	4.89	0.47	10.51	-25.10	3.63	-21.04
18	1975.4	11.52	86.14	5.31	0.13	4.73	0.46	10.28	-25.51	3.81	-19.47
18.5	1973.8	12.12	85.65	5.08	0.18	4.60	0.44	10.41	-25.49	3.97	-20.62
19	1972.4	10.91	86.65	5.54	0.31	4.96	0.48	10.33	-25.33	3.85	-22.02
19.5	1971.6	12.22	85.35	5.51	0.31	5.90	0.57	10.30	-24.36	3.75	-19.42
20	1970.8	12.63	84.49	6.54	0.32	5.96	0.58	10.25	-23.99	3.46	-19.71
20.5	1970.3	12.67	84.46	6.54	0.38	6.16	0.62	10.00	-24.84	3.46	-19.37
21	1969.8	14.14	83.41	5.56	0.47	6.25	0.63	10.00	-24.01	3.33	-20.16
21.5	1969.3	14.44	83.09	5.62	0.62	6.57	0.65	10.07	-23.55	3.18	-19.94
22	1969	12.87	83.62	7.98	0.94	6.64	0.66	10.12	-23.17	3.13	-17.84
22.5	1968.9	13.20	83.79	6.84	0.46	7.00	0.69	10.07	-23.16	3.17	-19.05
23	1968.4	14.42	82.42	7.18	0.30	7.09	0.69	10.33	-22.56	3.25	-16.54
23.5	1967.9	14.65	82.55	6.38	0.32	7.05	0.67	10.45	-22.30	3.11	-20.31
24	1967.3	14.49	82.33	7.22	0.34	8.01	0.75	10.68	-21.29	2.65	-18.05
24.5	1966.8	15.03	81.76	7.31	0.39	8.09	0.77	10.54	-21.43	2.62	-20.49
25	1966.4	16.14	80.24	8.23	0.44	8.31	0.78	10.65	-20.98	2.65	-20.76
25.5	1965.9	16.50	80.34	7.18	0.51	8.40	0.79	10.63	-21.13	2.65	-21.72
26	1965.6	14.77	81.87	7.65	0.60	7.95	0.76	10.53	-21.39	2.56	-19.51
26.5	1965.2	16.41	80.61	6.77	0.46	8.47	0.79	10.69	-20.98	2.58	-19.75
27	1964.8	14.96	81.68	7.63	0.38	7.69	0.73	10.49	-20.77	2.63	-20.09

27.5	1964.3	15.67	81.15	7.23	0.31	7.84	0.75	10.42	-20.95	2.63	-19.70
28	1963.6	16.20	80.85	6.71	0.27	7.83	0.75	10.47	-20.58	2.43	-21.36
28.5	1962.8	16.50	80.87	5.98	0.30	7.94	0.76	10.48	-20.86	2.71	-19.05
29	1962.1	16.49	80.62	6.56	0.35	7.65	0.73	10.51	-20.32	2.46	-21.17
29.5	1961.5	15.17	81.50	7.58	0.42	7.63	0.73	10.50	-20.22	2.36	-21.59
30	1961	16.03	80.88	7.02	0.53	7.71	0.74	10.42	-20.36	2.52	-21.18
30.5	1960.5	15.59	80.92	7.93	0.49	7.63	0.73	10.49	-20.46	2.47	-21.45
31	1960.1	15.13	81.86	6.83	0.44	7.53	0.72	10.44	-20.19	2.43	-23.55
31.5	1959.5	13.60	83.23	7.20	0.41	7.01	0.68	10.29	-20.29	2.48	-19.06
32	1958.7	14.68	82.20	7.07	0.37	7.16	0.69	10.33	-20.19	2.37	-21.49
32.5	1958	15.21	81.81	6.77	0.19	7.80	0.74	10.46	-20.25	2.60	-22.06
33	1956.8	16.32	80.67	6.84	0.13	7.54	0.72	10.44	-20.90	2.46	-21.79
33.5	1955	15.10	81.56	7.58	0.12	7.51	0.72	10.45	-20.26	2.45	-20.90
34	1953.1	15.05	81.49	7.86	0.11	7.61	0.73	10.48	-20.26	2.52	-21.42
34.5	1950.5	15.24	81.15	8.19	0.10	7.32	0.71	10.26	-20.31	2.55	-22.33
35	1948.2	15.83	81.74	5.51	0.09	7.33	0.71	10.30	-19.95	2.47	-21.80
35.5	1945.4	15.16	82.36	5.64	0.09	7.27	0.70	10.37	-20.08	2.47	-23.17
36	1942	15.10	82.34	5.83	0.08	7.40	0.71	10.35	-20.27	2.53	-21.75
36.5	1938.5	15.99	81.02	6.80	0.07	7.66	0.74	10.41	-20.29	2.54	-20.16
37	1934.5	14.49	82.75	6.27	0.07	7.13	0.69	10.33	-20.38	2.40	-23.09

37.5	1931	14.19	82.81	6.83	0.06	7.27	0.71	10.30	-20.04	2.40	-20.98
38	1926.2	15.72	81.36	6.64	0.05	7.81	0.76	10.20	-20.11	2.41	-20.24
38.5	1921	12.94	83.82	7.35	0.04	6.52	0.64	10.13	-19.99	2.53	-21.65
39	1910.1	13.92	83.15	6.66	0.03	6.64	0.66	10.06	-20.13	2.54	-20.34
39.5	1896.8	13.48	83.50	6.86	0.02	6.93	0.68	10.12	-20.09	2.54	-20.91
40	1874.4	12.89	84.05	6.96	0.01	7.25	0.70	10.36	-20.28	2.53	-18.81

Table A2: Diatom data from the core from OCF 48. Data reported from the top of core until years where there were too few diatoms to enumerate.

CRS Year	<i>Fragilaria pinnata</i> (%)	Epiphytic Diatom Taxa (%)
2007.2	64.1075	34.7409
2006.95	63.4483	33.5632
2006.709	59.387	38.3142
2006.495	68.4932	29.2237
2006.228	66.0194	31.4563
2005.922	62.6147	32.5688
2005.552	71.068	26.2136
2005.215	69.4761	28.246
2004.545	68.8488	27.3138
2004.145	78.2313	19.2744
2003.199	77.1845	19.6602
2002.13	79.6253	18.7354
2001.11	75	23.7981
2000.315	70.122	27.7439
1999.302	72.8758	26.4706
1998.162	70.8738	25.5663
1997.078	75.1572	22.327
1995.757	65.0641	30.7692
1994.667	78.0255	19.7452
1993.695	77.8135	18.6495
1992.843	59.4855	39.5498
1992.171	59.9359	35.2564
1991.412	59.292	37.1681
1990.532	77.1429	21.9048
1989.937	0	0
1989.499	0	0
1988.562	0	0
1986.904	0	0

Table A3: Pigment data from the core from OCF 48. Pigment concentrations are reported in nMol/gOM.

CRS Year	Diadinoxanthin	Lutein	β -carotene	Canthaxanthin
2007.2	0	86.5696	16.7909	0
2006.7	6.0288	235.1415	18.0772	16.4334
2006.2	10.8555	252.1352	22.703	45.5377
2005.6	10.6123	304.6341	10.4806	35.1918
2004.5	0	189.5897	19.9528	0
2003.2	9.4433	333.9937	19.0608	73.7498
2001.1	25.9627	114.7892	11.9866	51.272
1999.3	13.7023	577.0461	0	40.2173
1997.1	31.097	236.8758	14.5211	30.3166
1994.7	16.968	643.0473	37.8194	48.1511
1992.8	34.7082	267.1788	25.3889	41.5541
1991.4	9.8379	55.6354	5.617	25.3252
1989.9	9.8934	113.3098	2.6229	0
1988.6	28.0725	190.1965	10.3702	0
1986.9	0	0	0	0
1985.6	10.0652	0	0	0
1982.7	2.0151	0	0	20.9729
1980.6	0	29.4369	0	15.2739
1978.4	0	0	0	23.0772
1975.4	18.5651	0	0	0
1972.4	0	0	0	7.326
1970.3	0	0	0	0
1969.8	0	0	0	5.715
1968.4	23.16	118.8872	0	22.5118
1967.3	54.6802	0	0	0
1966.4	0	228.3049	0	35.2936
1965.6	43.7278	189.2854	13.071	46.5241
1964.8	3.8561	85.1338	6.4484	11.1968
1963.6	0	122.2359	9.1203	15.0359
1962.1	18.321	238.9187	11.9926	36.6162
1961	47.7236	284.378	0	0
1960.1	0	278.3075	0	42.2344
1958.7	14.6357	186.4074	14.9162	12.2993
1956.8	6.6622	133.6582	6.7208	16.0417
1953.1	53.5901	352.6384	15.4886	55.9087
1948.2	2.1921	54.9554	0	0
1942	0	212.4164	15.9971	0
1934.5	20.6903	312.4057	6.5696	50.9883
1926.2	42.7061	264.5836	19.8449	40.1629
1910.1	18.2501	116.2964	5.3757	7.3023
1874.4	0	229.629	16.4859	9.2544

Appendix B – Chapter 3

Table B1: Contemporary hydroecological data from WAP 20 and the 15 LDCF ponds from June 2010.

Pond	$\delta^{18}\text{O}$ (‰VSMOW)	$\delta^2\text{H}$ (‰VSMOW)	Chl a ($\mu\text{g/L}$)	pH	TP ($\mu\text{g/L}$)	TKN ($\mu\text{g/L}$)	DOC (mg/L)	DIC (mg/L)	Alk (mg/L)	CO ₂ Saturation
WAP 1	-12.38	-99.35	1.92	9.1	4	536.2	6	11.1	39.86	0.08
WAP 2	-11.99	-95.21	1.96	9.13	0	790.2	9.5	16.4	67.11	0.12
WAP 4	-9.00	-81.45	2.67	9.13	8	822.2	11.9	13.2	50.64	0.09
WAP 5	-9.44	-80.99	1.66	8.94	10	991.2	9.3	5.1	12.43	0.04
WAP 6	-9.22	-81.35	2.85	9.4	9	2291.2	11.1	22.4	98.85	0.09
WAP 7	-10.14	-82.89	3.58	9.4	28	633.2	4.6	8.1	21.68	0.02
WAP 8	-10.36	-81.01	3.45	9.22	5	528.2	4.7	7.2	21.12	0.03
WAP 9	-9.57	-78.36	1.99	9.38	0	754.2	9.1	16	61.84	0.06
WAP 13	-12.26	-94.53	1.01	8.78	3	495.2	4.1	8.4	32.67	0.13
WAP 14	-10.52	-85.90	1.60	8.77	0	404.2	5.7	15	68.80	0.29
WAP 15	-10.63	-85.81	0.56	9.18	0	439.2	6.2	14.9	66.99	0.10
WAP 16	-15.44	-118.55	2.99	9.1	4	329.2	3.5	15.3	71.43	0.13
WAP 17	-10.59	-81.50	0.98	9.01	13	196.2	2.7	13	63.39	0.15
WAP 18	-10.36	-82.71	1.58	9.02	1	662.2	6.2	13.5	63.34	0.15
WAP 19	-9.49	-77.65	0.74	9.04	0	367.2	5.4	12.3	61.34	0.14
WAP 20	-10.15	-87.56	1.05	9.15	13	1007.2	11	20.1	97.99	0.17

Table B2: Contemporary hydroecological data from WAP 20 and the 15 LDCF ponds from July 2010.

Pond	$\delta^{18}\text{O}$ (‰VSMOW)	$\delta^2\text{H}$ (‰VSMOW)	Chl a ($\mu\text{g/L}$)	pH	TP ($\mu\text{g/L}$)	TKN ($\mu\text{g/L}$)	DOC (mg/L)	DIC (mg/L)	Alk (mg/L)	CO_2 Saturation
WAP 1	-9.99	-90.19	19.80	8.55	38	2088.2	8.5	20	83.70	0.77
WAP 2	-5.69	-67.88	17.65	7.97	44	3031.2	20.5	30.2	157.96	5.66
WAP 4	-2.41	-56.59	2.96	8.88	69	4786.2	36.6	19.9	112.81	0.50
WAP 5	-4.76	-63.35	0.91	8.62	9	1547.2	16	11.7	52.45	0.44
WAP 6	-4.77	-62.44	0.51	8.52	22	2773.2	23.1	31.7	159.32	1.57
WAP 7	-7.36	-72.76	3.27	8.27	22	1257.2	10.5	21	110.92	1.84
WAP 8	-6.49	-70.77	13.90	8.33	48	1797.2	11.1	18	79.38	1.23
WAP 9	-5.08	-63.98	3.38	8.44	6	2047.2	16.7	23.9	119.30	1.42
WAP 13	-7.93	-71.56	3.46	8.58	8	823.2	7	14.1	62.06	0.49
WAP 14	-6.19	-67.08	2.90	8.36	10	1211.2	11.1	30.6	137.92	1.85
WAP 15	-6.91	-67.94	5.24	8.25	12	1118.2	9.1	25	115.78	2.01
WAP 16	-7.93	-77.47	1.85	8.77	12	1106.2	8.8	18.9	99.12	0.50
WAP 17	-6.18	-64.81	1.43	8.34	0	708.2	10.1	25.1	135.49	1.91
WAP 18	-6.11	-64.70	1.86	8.51	0	1324.2	15	25.9	133.64	1.26
WAP 19	-5.98	-61.18	2.88	8.65	7	1096.2	12.4	19.6	105.04	0.71
WAP 20	-6.21	-66.70	3.22	9.03	10	2281.2	21.6	19.8	104.97	0.28

Table B3: Contemporary hydroecological data from WAP 20 and the 15 LDCF ponds from September 2010.

Pond	$\delta^{18}\text{O}$ (‰VSMOW)	$\delta^2\text{H}$ (‰VSMOW)	Chl a ($\mu\text{g/L}$)	pH	TP ($\mu\text{g/L}$)	TKN ($\mu\text{g/L}$)	DOC (mg/L)	DIC (mg/L)	Alk (mg/L)	CO_2 Saturation
WAP 1	-12.17	-94.62	2.21	7.77			9.8	16.7	70.95	3.11
WAP 2	-12.66	-99.99	3.46	7.95	13	2117.2	11.8	19.3	87.38	2.42
WAP 4	-13.17	-100.58	0.84	8.02	0	605.2	11	12.5	49.15	1.21
WAP 5	-12.56	-95.54	1.10	8.24	0	636.2	11.9	8	31.36	0.46
WAP 6	-12.67	-96.14	3.13	8.27	0	1709.2	10.1	21	103.41	1.42
WAP 7	-11.01	-86.22	4.68	8.23	1	1531.2	9.8	24.6	112.83	1.70
WAP 8	-11.14	-89.24	7.02	8.03	30	1459.2	9.5	18.3	80.88	1.94
WAP 9	-11.06	-89.95	1.65	8.23	0	965.2	10.2	20.4	93.26	1.41
WAP 13	-9.87	-82.22	1.95	8.26	0	531.2	7.2	21.3	92.33	1.30
WAP 14	-11.29	-88.71	0.69	8.1	0	641.2	9.2	31	141.72	3.07
WAP 15	-10.31	-83.24	1.24	8.73	0	637.2	9.1	27.3	124.33	0.61
WAP 16	-10.78	-88.61	1.10	8.82	0	483.2	5.8	24.7	109.52	0.44
WAP 17	-11.73	-90.72	0.50	8.32	0	313.2	6.8	39.2	180.07	2.20
WAP 18	-10.99	-87.54	2.68	8.21	0	823.2	10.2	22.7	97.25	1.54
WAP 19	-10.56	-83.64	1.58	8.8	0	599.2	9.6	25.2	116.58	0.49
WAP 20	-12.55	-94.49	0.74	8.39	0	690.2	13.6	25.8	118.17	1.30

Appendix C – Chapter 4

Table C1: Geochemical data from the core from WAP 20.

Depth (cm)	Year	Sed. Rate (g/cm ² /year)	Organic Matter (%)	Mineral Matter (%)	CaCO ₃ (%)	C _{org} (%)	N (%)	C/N	δ ¹³ C _{org} (‰VPDB)	δ ¹⁵ N (‰ AIR)
0.0	2007.3	0.03	65.07	30.41	10.26					
0.5	2007.1	0.03	66.51	28.10	12.24	33.44	4.21	7.95	-20.93	-0.25
1.0	2005.4	0.03	66.40	28.73	11.09					
1.5	2003.4	0.03	66.50	29.16	9.88	31.80	4.07	7.81	-20.91	-0.23
2.0	2000.8	0.02	68.80	28.26	6.70					
2.5	1998.7	0.02	65.92	28.92	11.72	32.09	4.11	7.82	-20.88	-0.41
3.0	1995.2	0.02	63.64	30.00	14.46					
3.5	1992.0	0.02	62.56	32.29	11.72	29.85	3.83	7.80	-21.55	-0.55
4.0	1988.6	0.02	64.40	31.07	10.29					
4.5	1983.7	0.02	53.60	40.67	13.02	27.99	3.66	7.64	-21.92	-0.58
5.0	1978.0	0.02	56.30	37.40	14.32					
5.5	1971.3	0.01	56.12	38.04	13.27	26.39	1.82	14.49	-22.46	-0.42
6.0	1963.5	0.01	60.57	33.40	13.72					
6.5	1956.6	0.01	50.95	42.98	13.79	26.28	1.77	14.83	-22.90	-0.63
7.0	1948.6	0.01	53.58	40.55	13.34					
7.5	1939.3	0.01	47.16	44.48	19.00	24.29	1.61	15.06	-24.00	-0.16
8.0	1928.8	0.01	45.76	46.75	17.01					
8.5	1917.9	0.02	34.35	53.61	27.36	19.53	1.12	17.49	-25.33	-0.86
9.0	1904.6	0.02	21.45	62.37	36.76					
9.5	1884.3	0.01	18.30	63.94	40.36	12.61	0.65	19.54	-22.14	0.08
10.0	1859.7		17.57	63.69	42.59					
10.5	1837.7		18.23	63.54	41.43	11.90	0.56	21.16	-21.20	-0.34
11.0	1807.8		13.14	67.39	44.24					
11.5	1776.3		12.51	68.22	43.79	10.35	0.39	26.32	-21.47	-0.21

Table C2: Biological data from the core from WAP 20.

Year	Aphanizophyll (nmol/gOM)	Chlorophyll <i>a</i> (nmol/gOM)	<i>Fragilaria</i> <i>pinnata</i> (%)	<i>Denticula</i> <i>kuetzingii</i> (%)
2007.3	97.45	94.48		
2007.1			0.00	71.67
2005.4	89.24	69.32		
2003.4			0.00	58.33
2000.8	61.54	29.88		
1998.7			0.00	68.67
1995.2	65.08	31.85		
1992.0			0.00	60.67
1988.6	70.63	31.27		
1983.7			1.67	64.67
1978.0	67.35	35.15		
1971.3			0.33	56.67
1963.5	165.25	34.56		
1956.6			1.00	60.00
1948.6	197.38	40.80		
1939.3			4.33	55.33
1928.8	65.44	30.02		
1917.9			48.67	14.67
1904.6	194.15	43.25		
1884.3			78.67	1.33
1859.7	0.00	24.86		
1837.7			85.00	2.33
1807.8	0.00	30.34		
1776.3			77.33	3.00

Table C3: Geochemical data from the core from WAP 21.

Depth (cm)	Year	Sed. Rate (g/cm ² /year)	Organic Matter (%)	Organic Matter Flux (gOM/cm/yr)	Mineral Matter (%)	CaCO ₃ (%)	C _{org} (%)	N (%)	C/N	$\delta^{13}\text{C}_{\text{org}}$ (‰VPDB)	$\delta^{15}\text{N}$ (‰AIR)
0	2010.0	0.08	28.85	0.02	58.03	29.81	16.95	1.56	10.86	-24.05	0.66
0.5	2009.8	0.08	26.36	0.02	58.17	35.15					
1	2009.3	0.08	23.63	0.02	61.23	34.41	13.24	1.33	9.91	-24.43	0.29
1.5	2008.8	0.09	21.54	0.02	62.50	36.28					
2	2008.0	0.09	22.34	0.02	62.26	35.01	11.97	1.14	10.48	-23.98	-0.10
2.5	2007.1	0.08	23.70	0.02	61.45	33.76					
3	2006.2	0.07	29.08	0.02	57.37	30.79	14.53	1.43	10.15	-23.62	0.06
3.5	2005.4	0.06	30.49	0.02	56.20	30.24					
4	2004.3	0.06	35.76	0.02	52.52	26.64	18.97	1.70	11.18	-23.16	-0.81
4.5	2003.3	0.06	32.36	0.02	55.09	28.53					
5	2001.7	0.05	34.96	0.02	52.95	27.49	20.79	1.83	11.36	-23.08	-0.48
5.5	2000.9	0.05	36.73	0.02	51.62	26.48					
6	1999.3	0.05	36.56	0.02	51.80	26.45	19.99	1.79	11.18	-23.20	-0.06
6.5	1997.9	0.05	37.65	0.02	51.79	24.00					
7	1996.7	0.04	37.19	0.02	51.61	25.44	17.99	1.58	11.40	-23.17	-0.41
7.5	1994.1	0.04	36.41	0.02	52.18	25.93					
8	1992.4	0.04	43.44	0.02	46.58	22.68	22.70	1.98	11.49	-22.76	-0.13
8.5	1991.1	0.03	46.94	0.02	44.71	18.97					
9	1989.2	0.03	47.69	0.02	44.04	18.79	23.91	2.05	11.67	-22.59	-0.76
9.5	1987.4	0.03	47.43	0.01	43.74	20.07					
10	1985.5	0.03	47.16	0.01	44.13	19.80	24.74	2.06	12.03	-22.41	-0.51
10.5	1983.6	0.02	49.44	0.01	42.75	17.74					
11	1980.6	0.02	49.24	0.01	43.94	15.50	25.89	2.15	12.04	-22.10	-0.10
11.5	1978.3	0.02	53.55	0.01	39.57	15.64					
12	1975.4	0.02	48.64	0.01	43.40	18.08	26.44	2.09	12.63	-22.06	-0.37
12.5	1972.6	0.02	49.16	0.01	42.78	18.34					
13	1968.9	0.02	50.54	0.01	42.05	16.84	25.31	1.97	12.82	-22.18	-0.91

13.5	1965.6	0.02	53.40	0.01	40.00	14.99						
14	1961.1	0.01	52.34	0.01	41.14	14.81	25.43	2.00	12.72	-22.11	-0.83	
14.5	1956.8	0.01	53.20	0.01	41.20	12.73						
15	1953.0	0.01	54.26	0.01	39.01	15.30	27.25	2.08	13.08	-21.84	-0.47	
15.5	1947.1	0.01	57.41	0.01	37.50	11.57						
16	1942.4	0.01	58.78	0.01	35.51	12.99	25.98	1.94	13.36	-21.91	-0.50	
16.5	1937.5	0.01	62.23	0.01	32.93	11.01						
17	1933.2	0.01	60.18	0.01	35.24	10.40	28.11	2.13	13.21	-21.72	-0.59	
17.5	1928.2	0.01	63.79	0.01	31.68	10.29						
18	1924.9	0.01	62.47	0.01	32.32	11.83	27.73	1.92	14.41	-21.63	-1.02	
18.5	1921.7	0.01	62.98	0.01	32.69	9.83						
19	1917.2	0.01	63.41	0.01	32.05	10.33	29.11	2.05	14.20	-21.67	-0.38	
19.5	1912.7	0.01	61.82	0.01	32.99	11.81	29.45	2.13	13.82	-21.61	-0.11	
20	1909.7	0.01	59.03	0.01	35.71	11.94	30.81	1.99	15.45	-21.83	-0.95	
20.5	1904.9	0.01	58.20	0.01	35.25	14.90	30.75	2.03	15.13	-22.02	-0.16	
21	1901.0	0.01	59.10	0.01	34.69	14.11	31.36	1.97	15.91	-22.02	-0.80	
21.5	1896.4	0.01	56.07	0.01	37.87	13.79	32.45	1.96	16.60	-21.96	-0.82	
22	1891.6	0.01	48.07	0.00	42.94	20.43	31.68	2.21	14.31	-22.39	-0.33	
22.5	1884.5	0.01	35.60	0.00	52.48	27.08	29.78	1.95	15.26	-22.40	-0.40	
23	1878.2	0.01	45.16	0.00	44.98	22.41	31.03	2.04	15.24	-22.70	-0.62	
23.5	1872.5	0.01	44.64	0.00	46.43	20.29	27.68	1.85	14.93	-23.02	-0.50	
24	1865.2	0.01	40.03	0.00	50.14	22.35	24.53	1.77	13.83	-23.20	-0.54	
24.5	1856.0	0.00	32.91	0.00	54.73	28.09	23.04	1.51	15.27	-23.69	-0.72	
25	1852.0	0.00	40.92	0.00	47.63	26.04	24.02	1.64	14.61	-23.65	-0.47	
25.5	1845.2		43.31		47.27	21.40	26.25	1.61	16.26	-23.64	-0.49	
26	1838.7		43.92		47.64	19.20	23.45	1.60	14.68	-23.56	-0.45	
26.5	1831.7						26.93	1.77	15.20	-23.61	-0.48	
27	1824.5		32.86		54.73	28.21	22.31	1.50	14.91	-23.69	-0.53	
27.5	1818.0		41.72		47.47	24.57	23.91	1.52	15.74	-23.49	-0.10	
28	1810.9		37.27		51.99	24.40	25.26	1.60	15.81	-23.72	-0.51	
28.5	1802.5		34.82		53.06	27.54	23.89	1.50	15.97	-23.77	-0.26	

29	1795.4	38.00	40.89	47.98	22.34	1.43	15.68	-24.12	-0.30
29.5	1783.3	23.94	60.29	35.82	20.56	1.22	16.90	-24.05	-0.58
30	1773.1	23.46	60.64	36.12	18.18	1.20	15.12	-24.42	-0.21
30.5	1762.7	19.68	63.50	38.24	17.34	1.25	13.87	-24.80	-0.43

Table C4: Biological data from the core from WAP 21.

Year	Aphanizopyll (nmol/gOM)	Chlorophyll <i>a</i> (nmol/gOM)	<i>Denticula</i> <i>kuetzingii</i> (%)	<i>Fragilaria</i> <i>pinnata</i> (%)
2010.02	604.83	489.30	17.41	52.22
2009.31	349.44	816.93	23.87	56.77
2007.95	433.39	684.48	21.59	47.30
2006.19	508.50	505.12	22.98	53.42
2004.29	464.57	483.11	22.90	56.13
2001.70	448.01	555.49	21.67	54.49
1999.32	409.88	501.46	22.64	59.75
1996.65	555.24	150.52	35.02	47.63
1992.39	799.49	634.97	30.28	54.26
1989.18	834.70	640.52	37.46	47.94
1985.54	899.42	682.80	46.08	47.65
1980.64	1291.69	627.95	42.90	41.61
1975.41	1039.06	568.29	35.37	50.16
1968.92	1088.15	566.89	38.11	52.44
1961.09	1041.13	465.10	40.19	52.09
1952.96	1207.74	808.30	61.90	34.29
1942.43	1175.98	619.70	45.60	48.86
1933.20	1097.15	472.15	48.56	44.73
1924.86	937.96	409.51	46.03	45.71
1917.23	728.47	281.87	42.67	52.77
1909.69	605.95	151.46	39.94	53.99
1901.01	520.91	177.36	40.06	53.52
1891.58	540.78	210.02	32.29	60.50
1878.19	556.71	267.59	14.60	77.78
1865.19	455.10	179.88	13.61	80.70
1852.04	614.70	286.43	5.54	89.85
1838.74	577.13	254.81	12.62	82.85
1824.46	681.30	364.55	24.37	71.84
1810.95	773.15	224.02	9.91	84.83
1795.44	576.02	257.76	6.13	90.65
1773.14	637.55	333.60	5.08	88.89

Table C5: Geochemical data from the core from WAP 12.

Depth (cm)	Year	Sed. Rate (g/cm ² /year)	Organic Matter (%)	Mineral Matter (%)	CaCO ₃ (%)	C _{org} (%)	N (%)	C/N	δ ¹³ C _{org} (‰VPDB)	δ ¹⁵ N (‰ AIR)
0	2011.74	0.03	91.94	7.42	1.47	47.10	3.24	14.56	-21.68	0.16
0.5	2009.2	0.04	90.78	8.36	1.96	52.47	3.64	14.40	-21.70	0.16
1	2007.7	0.01	90.41	8.12	3.35	50.86	3.51	14.49	-21.98	-0.21
1.5	2005.7	0.03	90.84	7.63	3.47	51.95	3.52	14.76	-21.39	0.06
2	2003.2	0.02	90.44	8.09	3.34	51.27	3.44	14.90	-21.66	-0.41
2.5	2000.5	0.02	90.80	7.42	4.05	48.00	3.22	14.89	-21.96	-0.19
3	1997.8	0.02	90.97	6.77	5.13	46.92	3.16	14.83	-21.80	-0.26
3.5	1994.8	0.02	92.80	5.48	3.93	46.64	3.11	15.00	-21.94	-0.07
4	1991.5	0.01	90.85	6.71	5.54	52.15	3.56	14.66	-22.17	-0.02
4.5	1987.4	0.02	89.63	9.04	3.02	51.97	3.52	14.78	-22.04	0.10
5	1982.6	0.01	90.79	7.16	4.65	52.22	3.38	15.44	-21.79	0.05
5.5	1976	0.01	90.73	8.15	2.55	50.30	3.16	15.91	-22.15	-0.69
6	1970	0.02	89.00	9.09	4.35	51.03	3.35	15.22	-22.52	0.04
6.5	1967.1	0.02	89.50	8.92	3.58	50.75	3.27	15.54	-22.20	-0.19
7	1964.7	0.02	89.98	8.39	3.71	51.49	3.29	15.64	-22.22	-0.06
7.5	1961.6	0.02	90.44	8.33	2.79	50.68	3.19	15.87	-22.19	0.03
8	1958.6	0.02	90.55	7.96	3.39	37.17	2.36	15.76	-22.54	-0.08
8.5	1956	0.02	90.15	8.00	4.20	52.20	3.14	16.60	-22.19	-0.78
9	1953.5	0.02	90.27	8.11	3.69	52.59	3.35	15.69	-22.22	0.08
9.5	1951.1	0.02	90.21	8.35	3.25	51.74	3.27	15.80	-22.16	-0.17
10	1948.5	0.02	90.32	8.60	2.44	50.18	3.14	15.99	-22.16	-0.22
10.5	1945.8	0.02	91.15	7.08	4.02	48.75	3.10	15.73	-22.49	-0.35
11	1942.8	0.02	89.97	7.90	4.84	52.00	3.34	15.57	-22.45	0.05
11.5	1939.5	0.01	91.39	6.82	4.05	51.93	3.38	15.35	-22.46	-0.11
12	1936	0.02	89.95	8.42	3.71	53.10	3.38	15.73	-22.38	-0.25
12.5	1932.2	0.01	90.78	6.63	5.89	50.43	3.21	15.71	-22.29	-0.05
13	1928.2	0.02	90.76	7.39	4.20	48.92	3.15	15.55	-22.56	-0.02
13.5	1924.2	0.01	90.74	8.56	1.58	49.12	3.01	16.30	-22.23	-0.04

14	1920.1	0.01	90.86	7.96	2.68	51.36	3.24	15.86	-21.91	0.00
14.5	1915.5	0.01	89.62	9.11	2.88	51.41	3.21	16.00	-22.42	-0.23
15	1911.1	0.02	90.41	8.77	1.87	50.13	3.17	15.83	-22.85	0.01
15.5	1907	0.02	90.03	8.80	2.67	53.59	3.43	15.64	-22.68	0.28
16	1903.5	0.02	89.92	8.82	2.86	53.24	3.39	15.69	-23.43	0.24
16.5	1899.9	0.02	90.80	7.78	3.22	48.83	2.98	16.38	-23.71	0.11
17	1895.7		90.33	8.49	2.68	49.60	3.08	16.12	-23.70	0.07
17.5	1891.6		91.16	8.21	1.44	50.98	3.24	15.74	-23.73	0.25
18	1887.4		89.63	9.04	3.02	53.93	3.43	15.73	-23.89	0.34
18.5	1883.1		90.10	9.16	1.69	52.35	3.34	15.68	-23.70	0.28
19	1878.6		90.40	8.27	3.03	50.59	3.16	16.01	-23.92	-0.25
19.5	1873.8		89.68	8.60	3.91	51.39	3.19	16.11	-23.79	0.05
20	1869.5		86.99	10.50	5.71	53.06	3.31	16.05	-23.77	-0.10
20.5	1865		82.23	12.85	11.19	53.35	3.46	15.40	-24.39	0.48
21	1859.3		87.60	10.12	5.17	52.68	3.53	14.93	-24.66	0.21
21.5	1854.4		85.62	11.01	7.66	53.48	3.49	15.30	-25.14	-0.10
22	1849.3		87.33	9.50	7.20	53.66	3.69	14.54	-24.96	0.12
22.5	1843.4		83.75	11.90	9.88	52.69	3.51	15.01	-25.06	-0.01
23	1837.9		80.82	14.90	9.74	53.00	3.47	15.28	-25.25	0.13
23.5	1832.3		82.38	13.15	10.15	52.34	3.81	13.74	-25.58	0.31
24	1825.9		82.34	13.83	8.70	52.90	3.70	14.30	-25.70	0.38
24.5	1819.7		82.41	13.15	10.10	53.53	3.77	14.21	-25.10	0.22
25	1812.8		84.48	12.18	7.59					

Table C6: Biological data from the core from WAP 12.

Year	Canthaxanthin (nmol/gOM)	Chlorophyll <i>a</i> (nmol/gOM)	<i>Denticula kuetzingii</i> (%)
2011.74	11.54	20.67	65.79
2007.70	16.03	15.26	69.00
2003.20	13.64	3.44	60.80
1997.80	10.75	8.65	68.11
1991.50	8.06	6.94	57.48
1982.60	8.10	6.02	64.92
1970.00	9.80	10.29	61.97
1964.70	10.53	10.24	68.89
1958.60	11.13	8.78	67.88
1953.50	6.34	9.64	68.67
1948.50	7.81	9.07	67.43
1942.80	9.26	12.37	71.06
1936.00	10.93	11.68	71.33
1928.20	12.09	13.59	73.36
1920.10	10.81	9.42	66.78
1911.10	10.95	2.76	64.26
1903.50	9.17	14.07	0.00
1895.70	11.26	12.56	0.00
1887.40	14.35	16.72	0.00
1878.60	8.17	12.42	0.00
1869.50	9.71	13.18	0.00
1859.30	7.14	7.57	0.00
1849.30	6.04	9.00	0.00
1837.90	6.96	11.29	0.00
1825.90	4.65	13.57	0.00

Table C7: Average seasonal values (2010-2012) for limnological conditions from WAP 20, WAP 21 and WAP 12. Values for WAP 12 do not include July 2010 as the pond desiccated.

Lake	Time	TKN ($\mu\text{g/L}$)	pH	Conductivity ($\mu\text{s/cm}$)	$\delta^{13}\text{C}_{\text{DIC}}$ (‰VPDB)	$\delta^{13}\text{C}_{\text{POM}}$ (‰VPDB)	$\Delta^{13}\text{C}_{\text{DIC-POM}}$ (‰VPDB)
WAP 20	June	1045.07	8.00	559.33	-3.54	-24.66	21.12
WAP 20	July	1700.07	8.68	1106.67	-4.63	-22.67	18.04
WAP 20	Sept.	1420.40	8.08	1152.67	-3.45	-26.16	22.71
WAP 21	June	1452.07	7.93	907.33	-4.89	-27.25	22.36
WAP 21	July	1931.73	8.35	1999.00	-6.18	-25.39	19.21
WAP 21	Sept.	1388.07	8.24	1624.00	-5.77	-27.16	21.39
WAP 12	June	1270.40	8.51	179.67	-5.56	-25.29	19.73
WAP 12	July	3051.50	8.63	401.00	-4.09	-23.73	19.64
WAP 12	Sept.	1051.73	8.14	352.67	-1.59	-25.22	23.63

Appendix D – Chapter 5

Table D1: Metal concentrations (mg/kg) from the core from SD2. 1= presence of condition or influence, 0 = absence of condition or influence.

Depth (cm)	Year	Flood	Oil	Giant Mine	Li	Sb	As	Be	Cd	Cr	Cu	Pb
0	2010.8	0	1	0	17.20	0.53	12.10	0.70	0.54	22.90	25.10	12.00
1	2009.0	0	1	0	18.90	0.58	9.76	0.72	0.59	25.50	26.60	12.90
2	2007.1	0	1	0	17.00	0.54	9.01	0.69	0.55	21.80	24.00	12.10
3	2005.3	0	1	0	17.30	0.58	10.90	0.70	0.53	21.70	23.80	11.90
4	2003.4	0	1	0	18.10	0.54	9.47	0.75	0.56	23.10	24.00	12.40
5	2001.6	0	1	0	17.70	0.57	8.70	0.70	0.53	21.10	22.70	11.50
6	1999.8	1	1	0	14.40	0.47	6.85	0.57	0.56	19.30	19.00	9.41
7	1997.9	0	1	0	15.50	0.51	8.45	0.60	0.55	20.40	20.50	10.40
8	1996.1	0	1	0	11.90	0.44	7.80	0.46	0.52	16.50	16.40	8.20
9	1994.3	1	1	0	12.60	0.45	6.00	0.56	0.53	16.70	17.00	8.84
10	1992.4	1	1	0	13.30	0.48	6.06	0.52	0.60	17.10	19.70	9.91
11	1990.6	1	1	0	9.70	0.39	4.63	0.37	0.45	14.80	12.60	6.99
12	1988.8	1	1	0	11.60	0.42	5.19	0.46	0.51	16.40	15.70	8.12
13	1986.9	1	1	0	15.90	0.55	7.39	0.60	0.59	20.40	21.40	10.70
14	1985.1	0	1	0	19.20	0.63	10.00	0.76	0.55	23.30	24.60	12.80
15	1983.2	0	1	0	19.30	0.65	9.77	0.74	0.57	23.90	25.10	12.70
16	1981.4	0	1	0	17.30	0.59	10.30	0.67	0.57	21.80	23.60	12.10
17	1979.6	0	1	0	16.10	0.55	10.10	0.64	0.57	19.40	24.10	11.80
18	1977.7	0	1	0	17.30	0.59	9.21	0.67	0.56	21.30	24.10	12.20
19	1975.9	0	1	0	17.20	0.56	8.04	0.65	0.57	21.80	23.40	11.60
20	1974.1	1	1	0	16.70	0.59	7.63	0.67	0.59	22.60	22.70	11.30
21	1972.2	0	1	0	17.50	0.59	8.50	0.70	0.58	23.30	23.60	11.90
22	1970.4	0	1	0	15.10	0.53	8.55	0.59	0.59	22.30	22.10	10.70
23	1968.5	1	1	0	13.50	0.52	6.10	0.53	0.54	19.00	19.50	9.54
24	1966.7	1	0	0	14.30	0.57	6.13	0.54	0.58	19.40	21.10	10.40
25	1964.9	1	0	0	13.10	0.51	6.97	0.51	0.57	17.70	22.10	10.40
26	1963.0	1	0	1	13.80	0.52	6.59	0.56	0.54	18.90	20.70	9.96

27	1961.2	0	0	1	14.40	0.54	9.13	0.58	0.53	19.80	20.70	10.10
28	1959.4	0	0	1	14.80	0.56	18.00	0.60	0.51	20.30	21.10	10.40
29	1957.5	0	0	1	15.40	0.57	19.10	0.63	0.56	23.10	24.40	10.90
30	1955.7	0	0	1	13.70	0.56	14.30	0.56	0.47	17.60	20.30	10.20
31	1953.9	0	0	1	12.30	0.55	10.90	0.49	0.53	16.30	19.60	9.60
32	1952.0	0	0	1	12.00	0.47	7.40	0.48	0.48	16.40	17.00	8.80
33	1950.2	1	0	1	11.80	0.46	5.83	0.46	0.49	15.20	15.40	8.25
34	1948.3	1	0	0	11.40	0.43	5.33	0.44	0.52	15.10	16.50	8.32
35	1946.5	1	0	0	10.70	0.45	6.22	0.43	0.60	14.70	17.60	8.48
36	1944.7	1	0	0	10.50	0.45	6.33	0.43	0.55	15.20	16.80	8.00
37	1942.8	1	0	0	10.50	0.43	5.94	0.39	0.51	15.50	15.90	7.91
38	1941.0	1	0	0	10.50	0.43	6.04	0.45	0.50	15.70	15.70	7.70
39	1939.2	1	0	0	10.20	0.40	5.15	0.39	0.48	14.40	14.10	7.29
40	1937.3	1	0	0	10.40	0.40	4.99	0.42	0.43	14.50	14.00	7.33
41	1935.5	1	0	0	11.90	0.44	5.26	0.44	0.48	15.40	16.50	8.26
42	1933.7	0	0	0	13.40	0.49	7.47	0.51	0.55	16.30	20.20	9.89
43	1931.8	1	0	0	14.50	0.56	12.90	0.58	0.53	17.40	21.20	10.50
44	1930.0	0	0	0	13.80	0.53	9.10	0.57	0.51	17.60	20.90	10.30
45	1928.1	1	0	0	16.80	0.60	6.45	0.64	0.60	22.20	22.60	11.00
46	1926.3	1	0	0	13.30	0.47	6.91	0.54	0.52	17.90	19.40	9.27
47	1924.5	0	0	0	12.60	0.46	9.66	0.49	0.50	15.50	19.20	9.11

Table D1 Continued: Metal concentrations (mg/kg) from the core from SD2. 1= presence of condition or influence, 0 = absence of condition or influence.

Depth	Year	Flood	Oil	Giant Mine	Hg	Ni	Se	Ag	Tl	V	Zn
0	2010.8	0	1	0	0.07	30.90	0.81	0.18	0.23	39.70	95.60
1	2009.0	0	1	0	0.07	33.30	0.80	0.21	0.24	45.10	105.00
2	2007.1	0	1	0	0.07	29.70	0.73	0.20	0.22	37.80	97.70
3	2005.3	0	1	0	0.07	29.70	0.73	0.20	0.22	38.80	95.10
4	2003.4	0	1	0	0.07	30.30	0.74	0.20	0.23	40.30	97.80
5	2001.6	0	1	0	0.07	28.40	0.76	0.19	0.21	38.60	92.00
6	1999.8	1	1	0	0.06	25.90	0.55	0.16	0.19	35.50	81.50
7	1997.9	0	1	0	0.07	27.10	0.68	0.19	0.21	36.20	85.80
8	1996.1	0	1	0	0.05	23.30	0.45	0.14	0.16	30.00	72.60
9	1994.3	1	1	0	0.06	24.60	0.48	0.16	0.16	29.60	76.20
10	1992.4	1	1	0	0.07	26.00	0.60	0.18	0.17	29.90	82.90
11	1990.6	1	1	0	0.08	21.00	0.40	0.11	0.14	25.70	64.50
12	1988.8	1	1	0	0.06	23.00	0.49	0.15	0.16	29.50	70.50
13	1986.9	1	1	0	0.07	27.70	0.66	0.17	0.20	37.50	89.50
14	1985.1	0	1	0	0.07	31.00	0.77	0.21	0.24	42.70	100.00
15	1983.2	0	1	0	0.07	31.40	0.75	0.21	0.24	43.10	100.00
16	1981.4	0	1	0	0.07	29.70	0.72	0.21	0.22	38.90	92.70
17	1979.6	0	1	0	0.07	29.40	0.71	0.21	0.20	33.30	95.00
18	1977.7	0	1	0	0.09	29.20	0.75	0.20	0.21	37.60	93.20
19	1975.9	0	1	0	0.07	29.10	0.67	0.20	0.22	38.80	93.60
20	1974.1	1	1	0	0.07	29.30	0.64	0.19	0.20	38.50	94.40
21	1972.2	0	1	0	0.07	29.80	0.66	0.20	0.22	39.60	95.70
22	1970.4	0	1	0	0.07	28.70	0.65	0.19	0.20	37.70	91.60
23	1968.5	1	1	0	0.07	26.00	0.54	0.18	0.18	31.60	81.60
24	1966.7	1	0	0	0.07	27.20	0.62	0.20	0.19	32.50	86.40
25	1964.9	1	0	0	0.07	28.30	0.58	0.19	0.17	28.30	89.40
26	1963.0	1	0	1	0.07	27.10	0.53	0.18	0.18	30.70	87.20
27	1961.2	0	0	1	0.07	27.30	0.59	0.18	0.19	33.50	85.20

28	1959.4	0	0	1	0.07	26.70	0.77	0.17	0.19	35.60	82.70
29	1957.5	0	0	1	0.06	30.40	0.76	0.17	0.20	40.40	95.10
30	1955.7	0	0	1	0.06	25.80	0.62	0.16	0.18	30.10	80.10
31	1953.9	0	0	1	0.06	26.80	0.58	0.15	0.18	27.20	80.90
32	1952.0	0	0	1	0.05	24.80	0.51	0.14	0.17	28.30	74.00
33	1950.2	1	0	1	0.06	22.60	0.53	0.13	0.16	26.60	68.30
34	1948.3	1	0	0	0.06	23.50	0.46	0.14	0.16	26.70	72.70
35	1946.5	1	0	0	0.06	24.50	0.51	0.16	0.15	25.20	74.50
36	1944.7	1	0	0	0.06	22.90	0.49	0.14	0.15	26.50	71.00
37	1942.8	1	0	0	0.06	23.10	0.48	0.14	0.15	27.50	71.30
38	1941.0	1	0	0	0.06	23.00	0.47	0.13	0.15	28.00	68.90
39	1939.2	1	0	0	0.05	21.30	0.46	0.13	0.14	25.60	64.20
40	1937.3	1	0	0	0.05	21.60	0.40	0.12	0.14	25.20	66.40
41	1935.5	1	0	0	0.06	23.40	0.48	0.16	0.15	25.50	73.20
42	1933.7	0	0	0	0.07	26.40	0.62	0.19	0.17	27.20	85.60
43	1931.8	1	0	0	0.06	26.60	0.66	0.18	0.19	29.60	85.40
44	1930.0	0	0	0	0.07	26.50	0.61	0.18	0.18	29.80	85.80
45	1928.1	1	0	0	0.07	29.90	0.65	0.20	0.21	38.30	95.00
46	1926.3	1	0	0	0.07	25.60	0.54	0.17	0.17	30.10	79.10
47	1924.5	0	0	0	0.06	23.90	0.59	0.16	0.17	26.70	77.40

Table D2: 95% Prediction Interval concentrations (mg/kg) for metal-Li relations based on pre-1967 flood samples for use in future monitoring studies from the core from SD2. PIL is the lower 95% prediction interval for the associated Li concentration, PIU is the upper 95% prediction interval for the associated Li concentration.

Li	As 95%PIL	As 95%PIU	Sb 95%PIL	Sb 95%PIU	Be 95%PIL	Be 95%PIU	Cd 95%PIL	Cd 95%PIU	Cr 95%PIL	Cr 95%PIU
14.3	3.3879	11.375	0.4874	0.5855	0.5132	0.6015	0.4586	0.6462	18.8191	17.0438
13.1	2.9682	10.7285	0.4527	0.548	0.4701	0.5558	0.4455	0.6277	17.53	15.8051
13.8	3.224	11.0946	0.4731	0.5698	0.4954	0.5823	0.4534	0.6382	18.282	16.5326
11.8	2.4083	10.1336	0.4138	0.5087	0.4221	0.5075	0.4288	0.6102	16.1335	14.4164
11.4	2.2135	9.973	0.4015	0.4969	0.4071	0.4928	0.4232	0.6054	15.7038	13.9791
10.7	1.8477	9.717	0.3798	0.4765	0.3806	0.4675	0.4127	0.5975	14.9518	13.2027
10.5	1.7375	9.6495	0.3735	0.4707	0.373	0.4604	0.4096	0.5953	14.737	12.9784
10.5	1.7375	9.6495	0.3735	0.4707	0.373	0.4604	0.4096	0.5953	14.737	12.9784
10.5	1.7375	9.6495	0.3735	0.4707	0.373	0.4604	0.4096	0.5953	14.737	12.9784
10.2	1.5675	9.5529	0.364	0.4621	0.3615	0.4497	0.4048	0.5923	14.4147	12.6398
10.4	1.6814	9.6167	0.3704	0.4678	0.3691	0.4568	0.408	0.5943	14.6296	12.8658
11.9	2.4553	10.1754	0.4168	0.5117	0.4259	0.5111	0.4302	0.6115	16.2409	14.525
14.5	3.4492	11.4913	0.4931	0.5919	0.5203	0.6092	0.4606	0.6494	19.034	17.2464
16.8	4.0001	12.9837	0.5565	0.6669	0.6003	0.6995	0.4797	0.6907	21.5047	19.5079
13.3	3.0445	10.8299	0.4585	0.5542	0.4773	0.5633	0.4478	0.6306	17.7449	16.0144

Table D2 continued: 95% Prediction Interval concentrations (mg/kg) for metal-Li relations based on pre-1967 flood samples for use in future monitoring studies from the core from SD2. PIL is the lower 95% prediction interval for the associated Li concentration, PIU is the upper 95% prediction interval for the associated Li concentration.

Li	Cu 95%PIL	Cu 95%PIU	Pb 95%PIL	Pb 95%PIU	Hg 95%PIL	Hg 95%PIU	Ni 95%PIL	Ni 95%PIU	Se 95%PIL	Se 95%PIU
14.3	20.7035	17.5279	9.078	11.1388	0.0579	0.0758	24.6044	29.7216	0.5088	0.6772
13.1	19.108	16.0225	8.3843	10.3866	0.0545	0.0719	23.2415	28.2135	0.4709	0.6345
13.8	20.0387	16.9094	8.7918	10.8225	0.0565	0.0741	24.0435	29.0862	0.4933	0.6592
11.8	17.3794	14.3079	7.6056	9.5989	0.0505	0.0679	21.6976	26.6471	0.4276	0.5904
11.4	16.8476	13.7624	7.3602	9.3623	0.0493	0.0667	21.2081	26.1796	0.4138	0.5773
10.7	15.9168	12.788	6.9243	8.9547	0.047	0.0647	20.3355	25.3773	0.3891	0.555
10.5	15.6509	12.5051	6.7983	8.8398	0.0464	0.0641	20.0826	25.1518	0.3819	0.5487
10.5	15.6509	12.5051	6.7983	8.8398	0.0464	0.0641	20.0826	25.1518	0.3819	0.5487
10.5	15.6509	12.5051	6.7983	8.8398	0.0464	0.0641	20.0826	25.1518	0.3819	0.5487
10.2	15.252	12.0771	6.6081	8.6685	0.0454	0.0633	19.7002	24.8164	0.3711	0.5394
10.4	15.5179	12.3629	6.7351	8.7825	0.046	0.0638	19.9555	25.0396	0.3783	0.5456
11.9	17.5124	14.4429	7.6665	9.6584	0.0509	0.0682	21.8189	26.7651	0.431	0.5937
14.5	20.9695	17.772	9.1914	11.2663	0.0584	0.0765	24.826	29.9785	0.515	0.6845
16.8	24.0276	20.4558	10.4556	12.7735	0.0644	0.0845	27.2758	33.0315	0.5823	0.7717
13.3	19.3739	16.2785	8.5016	10.5103	0.055	0.0725	23.4727	28.4608	0.4773	0.6415

Table D2 continued: 95% Prediction Interval concentrations (mg/kg) for metal-Li relations based on pre-1967 flood samples for use in future monitoring studies from the core from SD2. PIL is the lower 95% prediction interval for the associated Li concentration, PIU is the upper 95% prediction interval for the associated Li concentration.

Li	Ag 95%PIL	Ag 95%PIU	Tl 95%PIL	Tl 95%PIU	V 95%PIL	V 95%PIU	Zn 95%PIL	Zn 95%PIU
14.3	0.1521	0.214	0.1734	0.1966	28.0043	35.3893	77.0247	94.95
13.1	0.1383	0.1985	0.1615	0.184	26.1941	33.3694	71.9489	89.3653
13.8	0.1464	0.2075	0.1685	0.1913	27.2602	34.5376	74.9344	92.5984
11.8	0.1226	0.1825	0.1482	0.1706	24.1357	31.2787	66.2137	83.5516
11.4	0.1176	0.1778	0.1441	0.1666	23.4815	30.6561	64.3985	81.8132
10.7	0.1086	0.1696	0.1368	0.1596	22.3137	29.5898	61.166	78.8271
10.5	0.106	0.1674	0.1346	0.1576	21.9748	29.2904	60.2297	77.9866
10.5	0.106	0.1674	0.1346	0.1576	21.9748	29.2904	60.2297	77.9866
10.5	0.106	0.1674	0.1346	0.1576	21.9748	29.2904	60.2297	77.9866
10.2	0.1021	0.164	0.1315	0.1546	21.4621	28.8455	58.8149	76.7363
10.4	0.1047	0.1662	0.1336	0.1566	21.8045	29.1415	59.7595	77.5685
11.9	0.1238	0.1837	0.1493	0.1716	24.2977	31.4358	66.6638	83.9899
14.5	0.1543	0.2167	0.1754	0.1987	28.2981	35.7339	77.8513	95.9001
16.8	0.1787	0.2484	0.1976	0.2237	31.5333	39.8397	87.0112	107.173
13.3	0.1407	0.201	0.1635	0.1861	26.5017	33.7002	72.8091	90.2818

Table D3: Equation for metal-Li linear relation ($y=mx+b$) for future use in monitoring studies.

Metal	m	b (mg/kg)
As	1.0295	0.4442
Sb	0.1061	0.0301
Be	0.0279	0.037
Cd	0.3645	0.0131
Cr	3.4574	1.0742
Cu	1.6897	1.3296
Pb	1.4933	0.6025
Hg	0.0232	0.003
Ni	10.0564	1.1963
Se	0.1124	0.0336
Ag	0.0086	0.0122
Tl	0.0386	0.0102
V	8.8761	1.5959
Zn	22.4684	4.4419

Table D4: Reported detection limits from ALS Canada Ltd for metals analyzed in the core from SD2.

Metal	Reported Detection Limit	Units
Sb	0.10	mg/kg
As	0.050	mg/kg
Be	0.20	mg/kg
Cd	0.10	mg/kg
Cr	0.50	mg/kg
Cu	0.50	mg/kg
Pb	0.50	mg/kg
Hg	0.0050	mg/kg
Ni	0.50	mg/kg
Se	0.20	mg/kg
Ag	0.10	mg/kg
Tl	0.050	mg/kg
Zn	1.0	mg/kg
V	0.20	mg/kg
Li	1.0	mg/kg